Targeted screen for novel protein-protein interactions and their role in iron deficiency response regulation

Inaugural-Dissertation

zur Erlangung des Doktorgrades
der Mathematisch-Naturwissenschaftlichen Fakultät
der Heinrich-Heine-Universität Düsseldorf

vorgelegt von

Daniela M. Lichtblau
aus Mannheim

Düsseldorf, Juni 2020

aus dem Institut für Botanik
der Heinrich-Heine-Universität Düsseldorf

Gedruckt mit der Genehmigung der
Mathematisch-Naturwissenschaftlichen Fakultät der
Heinrich-Heine-Universität Düsseldorf

Berichterstatter:

1. Prof. Dr. Petra Bauer

2. Prof. Dr. Peter Westhoff

Tag der mündlichen Prüfung: 28.09.2020

Eidesstattliche Erklärung

Ich versichere an Eides Statt, dass die Dissertation von mir selbständig und ohne unzulässige fremde Hilfe unter Beachtung der „Grundsätze zur Sicherung guter wissenschaftlicher Praxis an der Heinrich-Heine-Universität Düsseldorf“ erstellt worden ist.

Ich habe die Dissertation in dieser oder ähnlicher Form bisher keiner anderen Fakultät vorgelegt.

Ich habe bisher keine erfolglosen Promotionsversuche unternommen.

Daniela Lichtblau
Düsseldorf, 17.06.2019

Acknowledgements

My sincerest gratitude goes to Prof. Dr. Petra Bauer for giving me the opportunity to work in her institute and for the freedom to choose some of the projects to work on by myself. Thank you, Petra, for all our discussions, as well as your continuous support and enthusiasm during so many meetings.

I also thank Prof. Dr. Peter Westhoff for being my mentor and supporting me not only during my Bachelor and Master theses but for continuing to do so during my PhD. Furthermore, I thank Karin Meierhoff for being part of my committee meetings, especially in the beginning.

My special thanks goes to the Bauer lab. Without all of you, my time working on the PhD would not have been half as enjoyable. Particularly Birte – I couldn't imagine anyone better to work with, it was such a good collaboration. Thank you for working hand in hand throughout. Thank you Anna, for all our healing evenings after hard days in the lab. It was a great pleasure having you as a good friend, both, in the lab and in my private life. Thanks as well to Ksenia and Moni for our good conversations, the friendship and for, together with Anna, always taking care of my cats. Thanks to Ksenia and Inga for the help with the microscope. Thanks to "my" students Kai, Theresa, Christin, Chris and Jannik. I want to thank Tzvetina, Rumen and Hansi for all their great advice during these years. Ulrike, Ginte and Elke I thank for all the technical support.

Thanks to the friends I made during this time. I enjoyed your company and being able to talk about the good and the bad very much, especially when things were difficult. Meng-Ying, Kumari and Flo it is a great pleasure having you in my life. And Flo, thanks for your help with CRISPR/CAS9. My thanks to all iGRAD plant members

I want to thank Sieglinde for always taking care of me. Thank you for all your mental support, our wonderful conversations and your thousand WhatsApp messages during the time of corona.

Zu guter Letzt möchte ich meiner Familie, meinen Freunden sowie tierischen Wegbegleitern danken, die mich über all die Jahre so sehr unterstützt haben. Vor allem danke an Rigo für den finanziellen Rückhalt während des Studiums. Sanne, dir danke ich ganz herzlich für die vielen Seiten, die du im Laufe der Jahre von mir gelesen hast. Ich hoffe du hattest zumindest ein bisschen Spaß dabei! Dascha und Rasputin, auch wenn ihr manchmal echt nervige Knallköpfe seid, so habt ihr mir doch die letzten 10 Jahre den nötigen Halt gegeben die Sache durchzuziehen und mich über so manch schlechten Tag hinweggetröstet. Danke dafür! Markus, danke für die wunderschönen sieben Tage.

Table of Contents

1 Preface

This PhD thesis is comprised of four major sections, preceded by an English and German summary. In the beginning, the introduction will provide information about iron uptake and distribution in the plant body as well as iron status sensing. There is a particular focus on transcriptional and post-transcriptional regulation of the iron homeostasis. Subsequently, the thesis objectives are summarized. The second and third part include two manuscripts that make up the main chapters:

1. **E3 ligases BTSL1 and BTSL2 interact with small protein FEP3 and bHLH transcription factors regulating iron deficiency responses in Arabidopsis roots**
   Daniela M. Lichtblau[q], Birte Schwarz[q], Christopher Endres, Christin Sieberg, Petra Bauer -*in preparation*- [q]Authors contributed equally

In this study, a comprehensive targeted yeast two-hybrid screen of 33 proteins possibly involved in iron deficiency responses was performed. This screen resulted in the identification of multiple novel protein-protein interactions. Among them we found two E3 ligases, BRUTUS-LIKE1 (BTSL1) and BTSL2, interacting with a specific set of bHLH TFs from subgroup IVc and POPEYE (PYE). Their physical interaction was further studied *in planta*. Additionally, the BTSLs interacted with the small peptide FE-UPTAKE-INDUCING PEPTIDE3 (FEP3). Based on studies of an Arabidopsis *FEP3* over-expression line we hypothesize that FEP3 acts as an inhibitor of both BTSLs. Thus, the novel protein interactome enhances our knowledge of iron deficiency responses and highlights the importance of protein-protein interactions in the regulation process, while at the same time providing ample opportunity for future research projects.

2. **Analysis of the small POPEYE-interacting protein OLIVIA reveals functions in the iron deficiency responses of *Arabidopsis thaliana***
   Daniela M. Lichtblau, Birte Schwarz, Ksenia Trofimov, Petra Bauer -*in preparation*-

In a second study, we characterized the novel protein OLIVIA (OLV) the function of which is unknown. We identified OLV as protein with a highly conserved motif (TGIYY), which is responsive to iron deficiency in Arabidopsis. Furthermore, we could show that OLV interacts with the transcription factor POPEYE (PYE) via its TGIYY motif. This interaction mainly occurs in the nucleus. Based on the analysis of *OLV* over-expressing Arabidopsis lines, we suggest that OLV has a positive effect on PYE function and enhances PYEs ability to repress its target genes.

The fourth section consists of concluding remarks that put the most important and interesting outcomes of both manuscripts into context.

2 Summary

Iron (Fe) is involved in fundamental biological processes in animals and plants. The lack of Fe leads to severe health problems for all organisms. In plants, Fe deficiency often results in developmental disorders and yield loss. However, because of the strong requirement of Fe on one hand and potential Fe toxicity on the other, the regulation of Fe acquisition and homeostasis is crucial for plant survival. In Arabidopsis (*Arabidopsis thaliana*) many Fe deficiency-induced genes are co-expressed. Several of these genes encode transcription factors (TFs) that often undergo protein-protein interactions to fulfill their regulatory function. The Fe acquisition is mostly controlled by the basic helix-loop-helix (bHLH) TF FER-LIKE IRON DEFICIENCY-INDUCED TRANSCRIPTION FACTOR (FIT). Regarding co-expression, FIT target genes build a co-expression sub-network. Whereas FIT-independent genes form another co-expression sub-network containing e.g. Fe distribution genes including the TF POPEYE (PYE) that represses several Fe distribution genes as well as subgroup Ib bHLH TFs. Protein-protein interactions among members of different Fe deficiency co-expression networks, such as between FIT and Ib bHLH TFs, are crucial to regulate the Fe deficiency response.

In order to investigate whether additional, yet unknown protein-protein interactions between co-expressed Fe responsive genes and known key players of the Fe deficiency response occur, we performed a targeted yeast two-hybrid protein interaction screen. This screen resulted in the detection of a network of interacting proteins. Amongst others, the network is comprised of three homologous E3 ligases, BRUTUS (BTS), BTS-LIKE1 (BTSL1) and BTSL2 that are supposed to be Fe sensors negatively regulating the Fe uptake. They were found to interact with some of the same TFs of subgroup IVc, PYE and a small peptide named FE-UPTAKE-INDUCING PEPTIDE3 (FEP3). In this study, their interaction and possible function was further studied *in planta* demonstrating that the BTSLs might perhaps negatively regulate several TFs while FEP3 acts as a potential inhibitor of the BTSLs, thereby, in turn positively influencing the Fe uptake.

Additionally, we detected one interesting protein interaction between PYE and a yet unknown small protein which we named OLIVIA (OLV). We could verify this interaction *in planta* and showed that both co-localize in the nucleus. Based on *OLV* over-expressing Arabidopsis lines, we examined the role of OLV on PYE function. PYE target genes were more repressed when OLV was over-abundant. Our data implies that OLV enhances PYE function on the protein level. Multiple sequence alignment analysis of OLV revealed a conserved motif (TGIYY) and orthologues in several organisms.

Since plants are often the main source of human Fe supply, it is worthwhile studying plants´ Fe acquisition and homeostasis to be able to improve the food quality by increasing the Fe content in edible parts of the plant. This work contributes to a better understanding of the transcriptional regulation, the interplay of different proteins and especially protein interactions that regulate the Fe deficiency response.

3 Zusammenfassung

Eisen ist an fundamentalen biologischen Prozessen in Tieren und Pflanzen beteiligt. Eisenmangel führt bei allen Organismen zu schwerwiegenden Problemen, die sich bei Pflanzen in Entwicklungsstörungen sowie Ernteverlusten äußern. Einerseits wird Eisen essentiell benötigt, andererseits ist es in zu hohen Konzentrationen giftig. Daher ist die Regulation der Eisenaufnahme und –homöostase entscheidend für das pflanzliche Überleben. In Arabidopsis (*Arabidopsis thaliana*) sind viele Eisenmangel-induzierte Gene koexprimiert. Viele dieser Gene kodieren Transkriptionsfaktoren (TFs), die oftmals Protein-Protein Interaktionen eingehen, um ihre regulatorische Funktion auszuüben. Die Eisenaufnahme wird hauptsächlich durch den basic helix-loop-helix (bHLH) TF FER-LIKE IRON DEFICIENCY-INDUCED TRANSCRIPTION FACTOR (FIT) reguliert. FIT-abhängige Gene und FIT-unabhängige Gene bilden jeweils eigene Koexpressions-Netzwerke. Im FIT-unabhängigem Netzwerk befinden sich Gene, die für die Eisenverteilung verantwortlich sind. Darunter zum Beispiel der bHLH TF POPEYE (PYE), der verschiedene Gene der Eisenverteilung reprimiert. In diesem Koexpressions-Netzwerk befinden sich zusätzlich bHLH TFs der Untergruppe Ib, die als Heterodimer mit FIT die Eisenaufnahme positiv regulieren. Protein-Protein Interaktionen zwischen Mitgliedern der einzelnen Koexpressions-Netzwerken, wie im Falle von FIT und Ib bHLH TFs sind von maßgebender Bedeutung zur Regulation der Eisenmangelantwort.

Um zu erforschen, inwiefern weitere bisher unbekannte Protein-Protein Interaktionen zwischen koexprimierten eisenmangelregulierten Genen und anderen bekannten wichtigen Proteinen der Eisenmangelantwort auftreten, wurde in dieser Arbeit mittels diverser Hefe Zwei-Hybrid Experimente nach neuen Protein-Protein-interaktionen gesucht. Aus diesen Daten konnte ein Interaktionsnetzwerk generiert werden. Im Fokus steht hierbei ein Teil des Interaktionsnetzwerkes um drei homologe E3 Ligasen BRUTUS (BTS), BTS-LIKE1 (BTSL1) und BTSL2, welche teilweise mit den gleichen bHLH, einschließlich PYE und einem kleinen Protein namens FE-UPTAKE-INDUCING PEPTIDE3 (FEP3) interagieren. Die BTS(L)s wirken vermutlich als Eisensensoren, die die Eisenaufnahme negativ regulieren, wohingegen FEP3 ein potentielles Phloem-mobiles Signal darstellt. Mit dieser Arbeit konnten wir zeigen, dass FEP3 als möglicher Inhibitor von BTSL1/ BTSL2 fungiert und die Eisenaufnahme auf diese Weise positiv beeinflusst.

Aus unserer Protein-Interaktionsstudie resultierte eine weitere sehr interessante Proteininteraktion zwischen PYE und einem bisher unbekannten kleinen Protein, das wir OLIVIA (OLV) nannten. Diese Interaktion konnte in Pflanzen verifiziert werden. Beide Proteine kolokaliseren im Zellkern. Es wurden Arabidopsis OLV Überexpressionslinien generiert, anhand derer der Einfluss von OLV auf die Funktion von PYE analysiert wurde. Aus diesen ergab sich, dass PYE Zielgene stärker reprimiert werden, wenn mehr OLV Protein vorhanden ist. Unsere Daten weisen darauf hin, dass OLV

die Funktion von PYE auf Proteinebene verstärkt. Multiple Sequenz-alignments von OLV enthüllten ein konserviertes Motiv (TGIYY) und Orthologe in verschiedenen Organismen.

Pflanzen sind die Hauptbezugsquelle der menschlichen Eisenversorgung. Daher ist es erstrebenswert, die pflanzliche Eisenaufnahme sowie Homöostase weiter zu erforschen, um die Nahrungsmittelqualität durch Steigerung des Eisengehaltes in essbaren Pflanzenbestandteilen zu verbessern. Diese Arbeit trägt zu einem besseren Verständnis der Eisenmangelantwort auf transkriptioneller Ebene sowie dem Zusammenspiel von verschiedenen Proteinen bei.

4 Abbreviation List

bHLH	Basic helix-loop-helix
BTS / BTSL	BRUTUS / BRUTUS-LIKE
Fe	Iron
FEP	FE-UPTAKE-INDUCING PEPTIDE
FIT	FER-LIKE IRON DEFICIENCY-INDUCED TRANSCRIPTION FACTOR
HHE	Hemerythrin/HHE cation binding motif
ILR3	IAA-LEUCINE RESISTANT3
IRT1	IRON REGULATED TRANSPORTER1
PYE	POPEYE
TF	Transcription factor

5 Introduction

5.1 Importance of iron for humans and plants

Iron (Fe) is a vital trace element for all living organisms. As a cofactor of various important enzymes, it is needed for central biological processes, such as DNA synthesis, the respiratory chain and photosynthesis (Zhang, 2014; Briat et al., 2015). In humans the majority of Fe is incorporated in hemoglobin, which as an essential component of red blood cells, is required for the oxygen transport through the body (Al-Fartusie and Mohssan, 2017). The Lack of Fe leads to dramatic health consequences such as Fe deficiency anemia, causing tiredness and general exhaustion. Especially pregnant women and children are often affected by this (Casiday and Frey, 1998). Since humans are not able to produce Fe by themselves, a daily supply of 18 mg for pre- and 8 mg for postmenopausal women and men is recommended (Russell, 2001). According to the World Health Organization (WHO) Fe shortage is the most frequent nutrient deficiency, impacting over 2 billion people worldwide. Therefore, especially in areas with general high undernourishment, where not everyone has access to a diverse died, the population is suffering from Fe deficiency (Naranjo-Arcos and Bauer, 2016).

Many people rely on plants as main Fe source (especially staple crops like maize, rice or wheat, which have a rather low Fe content). Biofortification aims to improve the food quality by increasing the amount of Fe or other essential nutrients like trace elements or vitamins, in edible parts of crops. Conventional breeding alone might not be sufficient to achieve this goal. For this reason, biotechnological approaches, for example the over-expression of crucial genes important for Fe uptake, storage and mobilization should be applied to generate nutrient enriched crops. For this, to be successful, a better understanding of plant nutrient uptake and homeostasis under prevailing soil conditions is needed (Santos et al., 2017; Connorton and Balk, 2019).

Chloroplasts, as site of the photosynthesis in plants, are a major Fe sink. Because Fe is essential in chlorophyll biosynthesis and also involved in the electron transport in Photosystem I and II, Fe availability limits photosynthesis and thus the biomass production (Briat et al., 2015). As sessile organisms, plants take up Fe and other essential nutrients from their direct environment. Therefore, they have to be able to adapt rapidly to changing environmental conditions. Fe shortage leads to many morphological and metabolic changes ensuring an enhanced Fe deficiency response. An alteration of the root architecture, including the formation of more root hairs and change of the primary and lateral root length can be observed (Marschner et al., 1989; Li et al., 2016). Fe deficiency additionally induces changes in gene expression of genes involved in Fe uptake and homeostasis (Gao et al., 2019; Schwarz and Bauer, 2020). To ensure optimal conditions for growth and development plants have to take up a sufficient amount of Fe.

5.2 Fe acquisition strategies in plants

Although Fe is the fourth most abundant element in the continental crust, it is mostly present in its poorly soluble ferric oxidation state (Fe^{3+}). The solubility of Fe in the soil can be influenced by different parameters, such as the soil pH, the redox potential or microbial processes which determine the Fe availability for plants (Wedepohl, 1995; Zhang et al., 2019). Plants have developed different strategies to access the Fe present in the rhizosphere. At the moment, two Fe acquisition strategies are known (**Figure 1**). Non-graminaceous plants are using Strategy I, which is based on the reduction of Fe^{3+} to Fe^{2+} (ferrous Fe). Grasses in contrast apply Strategy II that uses the chelation of Fe^{3+} for take-up from the soil (Marschner et al., 1986; Brumbarova et al., 2015).

5.2.1 Strategy I reduction-based Fe uptake

Non-graminaceous monocots and all dicots, such as Arabidopsis (*Arabidopsis thaliana*) apply this three step Fe uptake Strategy I. Several plasma membrane proteins of root epidermis cells are involved in this mechanism (**Figure 1A**). The first step consists of the acidification of the rhizosphere through proton extrusion, via H^+-ATPASE2 (AHA2). This process increases solubility of Fe^{3+}, which is normally tied to negatively charged soil particles (Santi and Schmidt, 2009). Next, solubilized Fe^{3+} is reduced to Fe^{2+} by FERRIC REDUCTION OXIDASE II (FRO2) (Robinson et al., 1999). Subsequently, IRON REGULATED TRANSPORTER1 (IRT1) imports Fe^{2+} into the roots (Eide et al., 1996; Vert et al., 2002). Noteworthy is that IRT1 does not exclusively take up Fe, but also additional other divalent metals like manganese (Mn) or zinc (Zn) (Korshunova et al., 1999). The secretion of phenolic compounds (e.g coumarins like scopoletin) has an additional positive effect on the Fe uptake (Clemens and Weber, 2016; Tsai et al., 2018). In Arabidopsis coumarins are extruded by the ABC transporter PLEIOTROPIC DRUG RESISTANCE9 (PDR9) and act as Fe^{3+} chelators which facilitate the Fe solubility (Fourcroy et al., 2014). The secretion of Fe chelating compounds is not exclusive for Strategy I performing plants. It also appears in Strategy II and thus is a common feature of both with regard to Fe acquisition (Tsai and Schmidt, 2017). The Fe acquisition machinery is transcriptionally activated by a heterodimer of FER-LIKE IRON DEFICIENCY-INDUCED TRANSCRIPTION FACTOR (FIT) and one basic helix-loop-helix (bHLH) transcription factor (TF) of subgroup Ib under Fe deficiency (Colangelo and Guerinot, 2004; Jakoby et al., 2004).

5.2.2 Strategy II chelation-based Fe uptake

Graminaceous monocots, including several important crops like maize (*Zea mays*) or rice (*Oryza sativa*) perform the chelation-based Fe uptake Strategy II (**Figure 2B**). This strategy relies on the production of phytosiderophores of the mugineic acid (MA) family, which are extruded through the TRANSPORTER OF MUGINEIC ACID1 (TOM1) into the rhizosphere. Phytosiderophores chelate Fe^{3+}, which enhances its solubility (Takagi et al., 1984; Nozoye et al., 2011). Hereafter, MA-Fe^{3+} complexes

are imported into the root via the plasma membrane localized YELLOW STRIPE1 (YS1) transporter in maize (Curie et al., 2001). Rice and barley (*Hordeum vulgare*) have homologous transporters, named YELLOW STRIPE1-LIKE transporters (YSLs) (Murata et al., 2006; Inoue et al., 2009). In rice the TF IRON-DEFICIENCY RESPONSIVE ELEMENT BINDING FACTOR1 (OsIDEF1) positively regulates many genes involved in Fe acquisition. Among others OsIDEF1 induces the expression of the central Fe acquisition regulator IRON RELATED TRANSCRIPTION FACTOR2 (OsIRO2) which forms heterodimers with the rice orthologue of FIT, OsFIT/ OsbHLH156 in order to activate Fe uptake genes (Kobayashi and Nishizawa, 2012; Liang et al., 2020; Wang et al., 2020).

Interestingly, rice is not only able to take up Fe as Fe^{3+}, but additionally possesses IRT1 homologues to absorb Fe^{2+} (Ishimaru et al., 2006; Li et al., 2015). The rice homologues OsIRT1 and OsIRT2 for example are predominantly expressed in the roots and induced under Fe deficiency. Since to date no upregulation of a FRO2 homologue could be found in rice under Fe deficiency, rice might have developed a specific IRT1 dependent Fe uptake to adapt under submerged conditions, where predominantly Fe^{2+} is present (Ishimaru et al., 2006). Therefore, it is suggested that rice utilizes a combined Fe uptake strategy, which is also reflected in the presence of further homologues involved in the regulation of Strategy I Fe uptake.

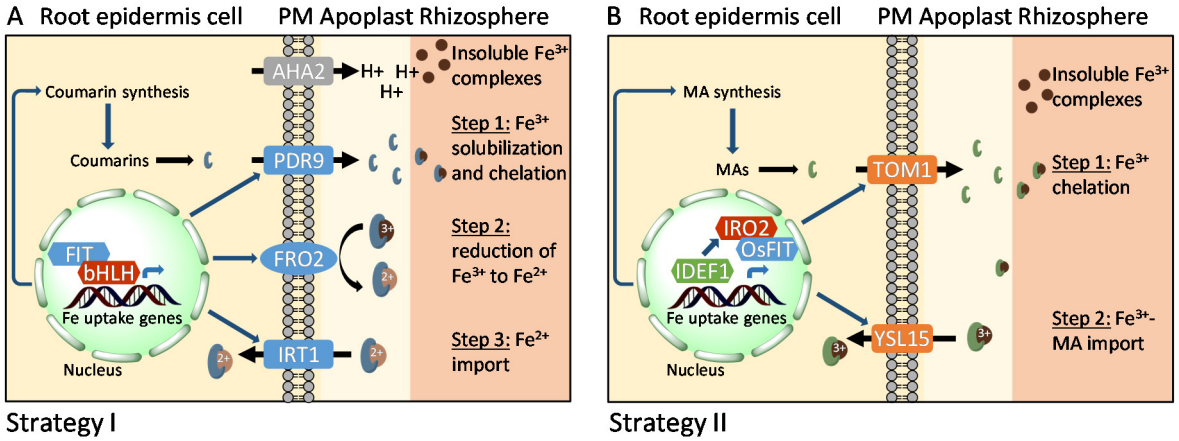

Figure 1: Fe acquisition Strategy I and II. A) Fe acquisition Strategy I in the model plant Arabidopsis. First, the H^+-ATPase AHA2 pumps protons into the rhizosphere, which lowers the soil pH and solubilizes Fe^{3+}. Solubilized Fe^{3+} is chelated by coumarins that are extruded via the ABC transporter PDR9 into the rhizosphere. In a second step, FRO2 reduces chelated Fe^{3+} to Fe^{2+}. The metal transporter IRT1 finally imports Fe^{2+} into the root cells. Genes involved in the Fe uptake are activated by a heterodimer of FIT with one bHLH TF of subgroup Ib. This system is upregulated under Fe deficient conditions. **B)** Fe acquisition Strategy II performed in rice. TOM1 releases phytosiderophores belonging to the MA family into the rhizosphere where they chelate Fe^{3+}. YSL15 transporter imports chelated MA-Fe^{3+} complexes into the roots. The TF IDEF1 induces the expression of Os*IRO2* that forms heterodimers with OsFIT in order to activate Fe acquisition genes. Abbreviations: PM: plasma membrane, AHA2: H^+-ATPASE2, FRO2: FERRIC REDUCTION OXIDASE2, IRT1: IRON REGULATED TRANSPORTER1, PDR9: PLEIOTROPIC DRUG RESISTANCE9, FIT: FER-LIKE IRON DEFICIENCY-INDUCED TRANSCRIPTION FACTOR; IDEF1: IRON-DEFICIENCY RESPONSIVE ELEMENT BINDING FACTOR1, IRO2: IRON RELATED TRANSCRIPTION FACTOR2, MA: mugineic acid. Blue proteins are FIT dependent, red proteins FIT independent. Blue arrows indicate transcriptional induction, black arrows indicate movement or reduction of Fe. Literature: (Kobayashi and Nishizawa, 2012; Brumbarova et al., 2015; Tsai and Schmidt, 2017; Liang et al., 2020; Schwarz and Bauer, 2020; Wang et al., 2020).

5.3 Long distance Fe transport and storage

After Fe has been taken up by roots, it needs to be translocated to sink organs with high Fe demands such as leaves. The root-to-shoot Fe transport takes place via the xylem, driven by the transpiration stream and root pressure (Kobayashi et al., 2019). The transpiration stream is not effective enough to transport Fe to all required organs. Therefore, Fe has to be additionally transported via the phloem into the shoot apex, seeds and root apex. Transport of remobilized Fe from older to younger leaves is likewise carried out by the phloem (Kim and Guerinot, 2007). Soluble Fe^{2+} catalyzes the formation of harmful reactive oxygen species through the Fenton reaction. To prevent cell damage, Fe gets chelated by either citrate in the xylem or nicotianamine (NA) in the phloem and transported as Fe-chelator complex. Thus, modulating cellular Fe availability between roots and shoots and diminishing its cellular toxicity (Durrett et al., 2007; Schuler et al., 2012).

Various transporters participate in Fe translocation processes within the plant body. FERRIC REDUCTASE DEFECTIVE3 (FRD3) functions in loading of citrate to the xylem (Durrett et al., 2007). OLIGOPEPTIDE TRANSPORTER3 (OPT3) in contrast is a phloem specific Fe importer (Stacey et al., 2008). YSL transporters for example in rice play a crucial role in Fe uptake and translocation in the plant. While OsYSL15 is mostly important for Fe uptake from the rhizosphere, other OsYSLs such as OsYSL2, 16 and 18 are suggested to be involved in Fe transport via the phloem and xylem (Kobayashi et al., 2019).

Fe deficiency as well as Fe excess cause severe problems. Thus, plants directly have to translocate absorbed Fe to sink organs or sequester excess Fe. For example the Fe storage protein Ferritin (FER) is transcriptionally induced in response to excess Fe and involved in excess Fe buffering in plastids and mitochondria (Briat et al., 2006; Briat et al., 2009; Vigani et al., 2013). The vacuole is another major Fe storage compartment with special importance for seeds (Kim et al., 2006). Excess Fe can also be stored in the apoplast. Utilization of sequestered Fe is essential to maintain the Fe homeostasis. Fe excess leads to transcriptional induction of genes, such as *FER* and *VITL1*, a vacuole Fe importer, while genes involved in Fe uptake and distribution are repressed. A strict regulation of Fe homeostasis is crucial for plant survival (Kobayashi et al., 2019).

5.4 A network of bHLH transcription factors regulates the Fe uptake and homeostasis

A highly interconnected network of predominantly bHLH TFs controls the Fe deficiency response in Arabidopsis (Lingam et al., 2011; Palmer et al., 2013; Le et al., 2016; Gao et al., 2019). TFs have been shown to be essential in the regulation of all central processes of living beings. They control the expression of their target genes by direct binding to sequence specific *cis* elements in their target promotors. This either leads to the activation or repression of target genes and allows a rapid adaptation to changing conditions (Qu and Zhu, 2006). In Arabidopsis more than 1500 TFs have been

found, covering almost 6 % of the total genes. They belong to different TF families, with bHLH and MYB TFs representing two of the biggest groups (Riechmann et al., 2000).

5.4.1 The bHLH TF family in plants

The Arabidopsis genome comprises over 150 bHLH TFs, more and more of which have been characterized in the last years. Based on their amino acid (aa) sequence and domain structure those bHLH TFs can further be divided into 12 subfamilies (Heim et al., 2003; Gao et al., 2019). Representatives of the same subfamily often participate in similar biological processes, like for example root hair development, stomata differentiation, cell elongation or general stress responses. The bHLH domain consists of about 60 aa that can be subdivided in two functionally different, highly conserved regions. The basic region includes about 13-17 basic residues and is located in the N-terminus, whereas the HLH domain is located more in the C-terminus. The basic region mediates binding to specific DNA 5´ CANNTG 3´ E-box motifs (N = A, T, G or C). The HLH domain on the other hand is necessary for homo- or heterodimerization with other bHLH TFs. bHLH TFs bind their target DNA as dimers. Thus, the formation of homo- or heterodimers is required for specific DNA binding (Heim et al., 2003; Toledo-Ortiz et al., 2003). Because of their importance for Fe deficiency response regulation, bHLH TFs are of particular interest here. The main subgroups involved in the Fe deficiency response are: 1. IIIa bHLH TFs (FIT/ bHLH29), 2. Ib (bHLH38, 39, 100, 101), 3. IVa (bHLH18, 19, 20, 25) 4. IVb (POPEYE (PYE)/ bHLH47, bHLH11, UPSTREAM REGULATOR OF IRT1 (URI)/ bHLH121), 5. IVc (bHLH34, 104, 105/ IAA-LEUCINE RESISTANT3 (ILR3), 115). The formation of heterodimers of bHLH TFs from different subgroups is crucial in the regulation of Fe deficiency responses (Colangelo and Guerinot, 2004; Yuan et al., 2008; Long et al., 2010; Wang et al., 2013; Zhang et al., 2015; Li et al., 2016; Liang et al., 2017; Cui et al., 2018; Gao et al., 2019; Gao et al., 2019; Kim et al., 2019; Tanabe et al., 2019; Schwarz and Bauer, 2020).

5.4.2 The transcriptional regulatory Fe deficiency response cascade in Arabidopsis

Transcriptional regulation allows for the adaptation to changing Fe availability and is mediated by a specific set of TFs. This mechanism is one possible way to regulate the protein level of key players involved in the Fe deficiency response (Zhang et al., 2019).

Fe deficiency leads to the activation of a regulatory cascade regulating the Fe uptake and homeostasis (**Figure 2**). The bHLH TF URI gets phosphorylated under Fe deficiency and acts together with bHLH TFs from subgroup IVc upstream of this cascade. A heterodimer of URI and a bHLH TF of subgroup IVc directly activates several Fe responsive genes including subgroup Ib bHLH TFs and PYE (Gao et al., 2019; Kim et al., 2019). bHLH IVc TFs possess partially redundant functions and form homo- and heterodimers to induce the expression of subgroup Ib *BHLH* genes and *PYE* (Zhang et al., 2015; Li et al., 2016; Liang et al., 2017). PYE is involved in controlling Fe homeostasis and translocation

processes by repressing the expression of Fe homeostasis genes such as *NICOTIANAMINE SYNTHASE4* (*NAS4*), *FRO3* or *ZINC INCUDED FACILITATOR1* (*ZIF1*) (Long et al., 2010).

In contrast, the four functionally redundant bHLH TFs of subgroup Ib have to form heterodimers with FIT to activate the Fe uptake machinery. While subgroup Ib bHLH TFs are expressed in roots and shoots, FIT is exclusively expressed in roots (Jakoby et al., 2004; Yuan et al., 2008; Wang et al., 2013). FIT as a root-specific TF is a key regulator of the Fe uptake and is mandatory for the induction of the root-specific Fe uptake genes *IRT1* and *FRO2* (Colangelo and Guerinot, 2004; Jakoby et al., 2004). In turn, *FIT* expression is at least partially controlled by bHLH39 in a positive feedback loop (Naranjo-Arcos et al., 2017). IVa bHLH TFs in contrast control FIT protein levels negatively (Cui et al., 2018). Another bHLH TF, bHLH11 negatively regulates the FIT-dependent Fe uptake mechanism. In contrast to many other members of the Fe deficiency response cascade, bHLH11 is upregulated under Fe sufficient conditions and downregulated under Fe deprivation. Thus, it influences Arabidopsis Fe levels. bHLH11 interacts with IVc TFs leading to a repression of the transcriptional activation ability of subgroup bHLH IVc TFs. In this way the transcriptional activation of subgroup Ib bHLH TFs will be prevented under Fe sufficient conditions (Tanabe et al., 2019; Li et al., 2020).

As shown in previous examples, transcriptional regulation is not the only mechanism that regulates the Fe deficiency response cascade. To fine-tune this mechanism, protein-protein interactions among several participants of the cascade are crucial. In some cases they also determine the function of a TF. PYE for instance interacts with the IVc bHLH TFs, which are homologues to PYE. But at the moment it is still unclear to what extent and how these interactions play a role in regulating the Fe homeostasis under Fe deficient conditions (Zhang et al., 2015; Li et al., 2016; Gao et al., 2019). The ability to form different heterodimers with varying functions allows for high flexibility in the regulatory system. Recent studies indicate that ILR3 has dual functions as activator or repressor of its target genes, depending on the Fe status and its corresponding interaction partner (Samira et al., 2018; Tissot et al., 2019). By dimerizing with its IVc bHLH homologues, ILR3 acts as activator by inducing Ib *BHLH* gene expression or *PYE* under Fe deficiency (Zhang et al., 2015; Liang et al., 2017). However, by dimerizing with PYE, ILR3 represses the Fe storage proteins *FER* and the Fe distribution genes *NAS4* and *PYE* in a negative regulatory feedback loop (Tissot et al., 2019).

Orthologues of several important components of the Arabidopsis Fe deficiency response are also present in rice. They act in a similar Fe deficiency response cascade as in Arabidopsis. Those will be discussed in more detail in a later section of this introduction.

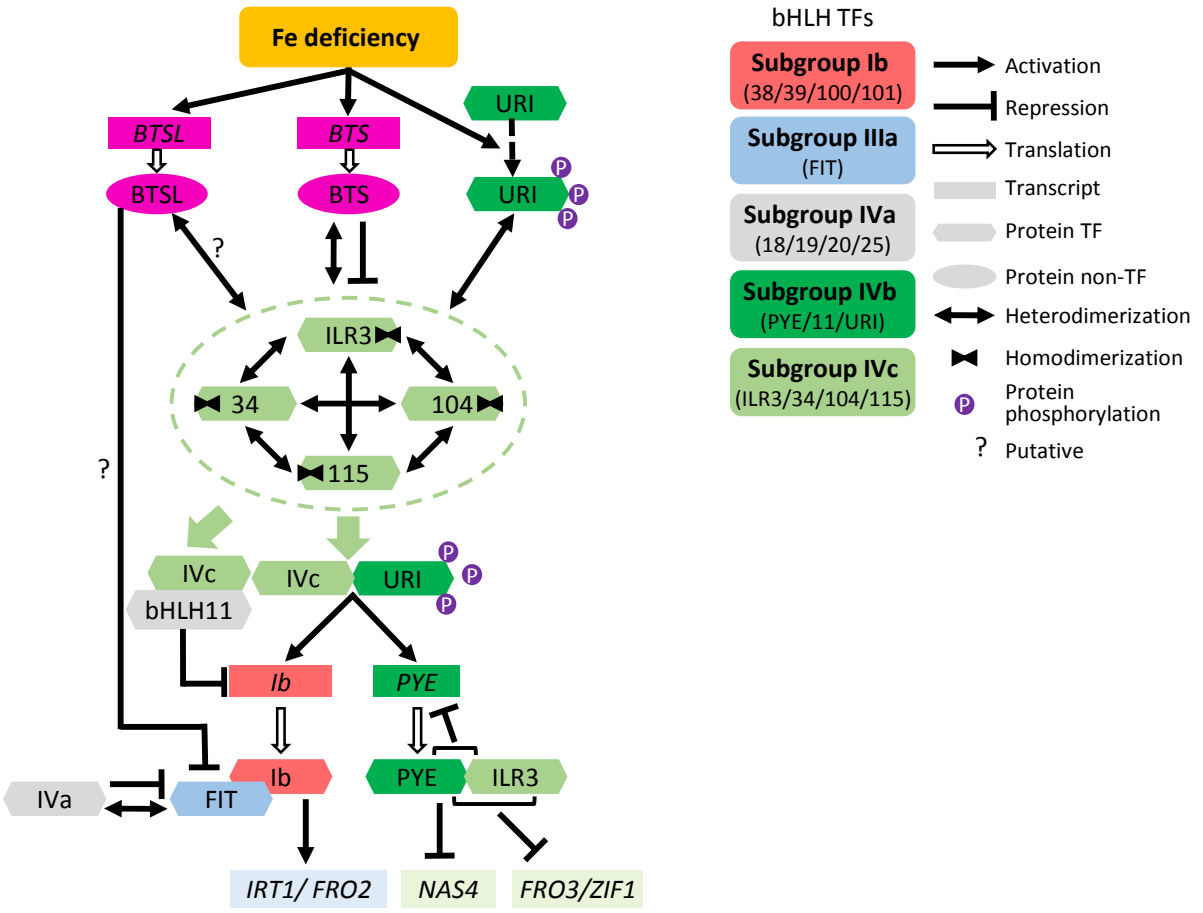

Figure 2: Regulatory network that controls the Fe deficiency response in Arabidopsis. The Fe homeostasis is controlled by a transcriptional regulatory cascade of several bHLH TFs from different subgroups. The TF URI is expressed regardless of the Fe status, but is phosphorylated under Fe deficiency and forms heterodimers with IVc bHLH TFs to activate the expression of several Fe deficiency responsive genes, among them Ib *BHLH* TFs and *PYE*. PYE can form heterodimers with IVc bHLH TFs and represses Fe homeostasis genes: *NAS4*, *FRO3* and *ZIF1*. ILR3 is an activator as heterodimer with other IVc bHLH TFs, and a repressor as heterodimer with PYE. IVc bHLH TFs are partially under the control of the E3 ligase BTS that targets ILR3 and bHLH115 for proteasomal degradation. Ib bHLH TFs interact with FIT to induce the Fe uptake machinery by activating *IRT1* and *FRO2*. While bHLH11 transcriptionally represses the FIT-dependent Fe uptake machinery, IVa bHLH TFs inhibit FIT protein accumulation. FIT protein levels might be controlled by BTSL1/2 (Long et al., 2010; Selote, 2015; Zhang et al., 2015; Cui et al., 2018; Kim et al., 2019; Tanabe et al., 2019; Tissot et al., 2019; Li et al., 2020; Schwarz and Bauer, 2020).

Furthermore, E3 ligases named BRUTUS (BTS) and its paralogous BTS-LIKE1 and 2 (BTSL) act in the Fe deficiency response cascade post-translationally by controlling protein levels of IVc bHLH TFs and possibly FIT. All three are negative regulators of the Fe deficiency response that will be discussed in a later section of this introduction (Selote, 2015; Hindt et al., 2017; Rodríguez-Celma et al., 2019).

5.4.3 Fe deficiency responsive genes form different co-expression networks in Arabidopsis

Fe deprivation leads to rapid alterations of the Arabidopsis root transcriptome. Most of them occur within the first 24 h of Fe deficiency exposure and concern genes involved in Fe uptake, Fe distribution, root morphology or general stress responses (Dinneny et al., 2008; Buckhout et al., 2009). Co-expression analysis based on microarray and RNA-seq data, showed that Fe deficiency-responsive

genes cluster in different co-expression sub-networks. Co-expressed genes are likely regulated by the same factors, act in the same pathway or are members of a protein complex. Therefore, co-expression analysis is a powerful tool to find new potential Fe deficiency response genes and to generate the hypothesis of functional connections between them. Hence, co-expression networks serve as a good starting point to search for novel protein-protein interactions (Ivanov et al., 2012; Schwarz and Bauer, 2020).

Here the ATTED II tool (Obayashi et al., 2018) was used to generate a co-expression network of Fe-deficiency responsive genes in Arabidopsis roots (**Figure 3**). The following Fe deficiency marker genes were used as guides: *IRT1*, *BHLH39*, *PYE* and *IREG2* (Ivanov et al., 2012).

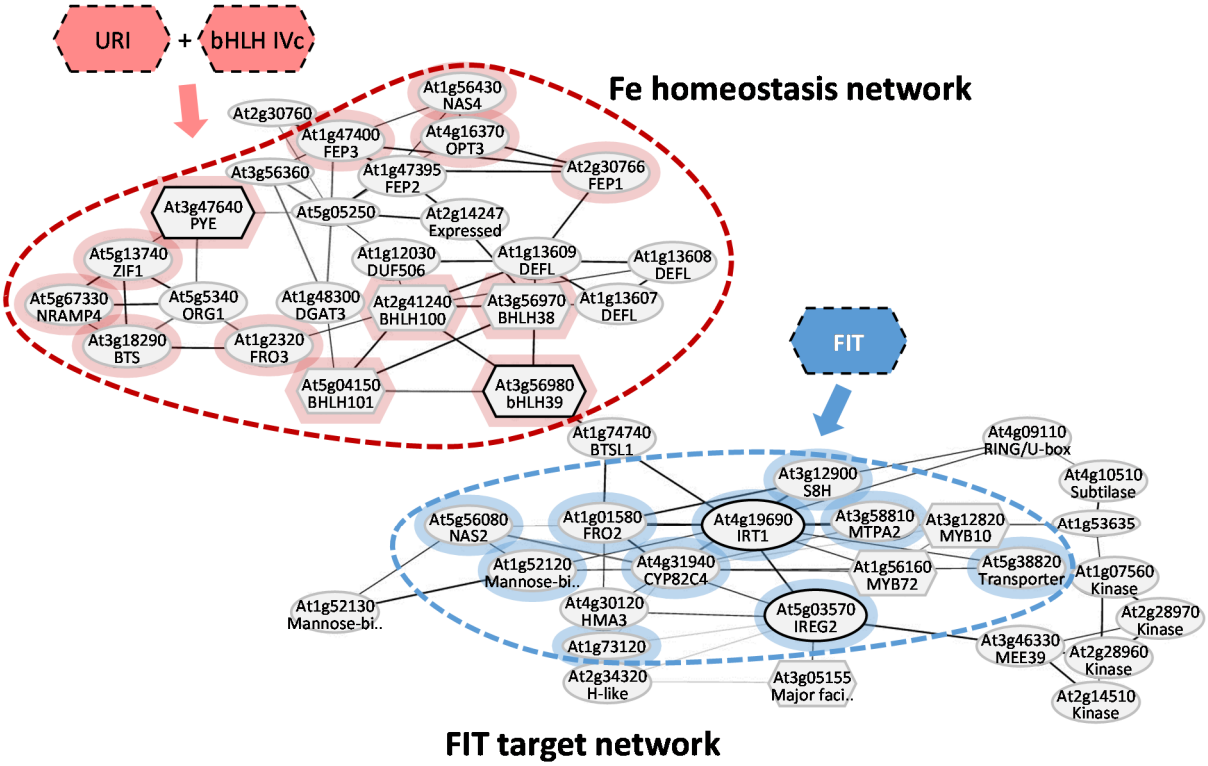

Figure 3: FIT-dependent and FIT-independent sub-clusters of the Fe deficiency co-expression network in Arabidopsis roots. The FIT target network (blue dashed line) contains direct or indirect FIT-dependent genes (highlighted in blue). The Fe homeostasis network (red dashed line) contains FIT-independent genes. URI and bHLH TFs of subgroup IVc directly regulate *PYE* as well as TFs of subgroup Ib and indirectly also other proteins of the Fe homeostasis network (highlighted in red). Hexagons represent TFs, circles represent non-TFs. Proteins that are outside of the co-expression network but involved in regulating members of it, are surrounded by a dashed line. The network was generated using the ATTED II tool (version 9.2) with RNA-sequencing data and the following Fe deficiency marker genes as guides: *IRT1*, *BHLH39*, *PYE* and *IREG2* (shown in light gray). The network is based on (Ivanov et al., 2012; Schwarz and Bauer, 2020). Thickness of the edges correlates with the expression correlation based on the ATTED-II Mutual Rank scoring procedure (Obayashi et al., 2018).

Figure 3 shows the two central Fe deficiency sub-networks. One of them contains FIT-dependent genes (blue dashed line) which are directly or indirectly regulated by FIT (highlighted in blue). The other one is the so called Fe homeostasis network which includes FIT-independent genes (red dashed line) (Schwarz and Bauer, 2020). The Fe homeostasis network is a good example for the fact that co-

expression can indicate regulation by the same factors. The members *PYE a*nd *BHLH38*/*39*/*100*/*101* of subgroup Ib, for example are both transcriptionally regulated by URI and bHLH TFs of subgroup IVc. Additionally, URI and bHLH IVc TFs regulate more genes that are highlighted in red (**Figure 3**). This regulation can either be direct or indirect (Li et al., 2016; Liang et al., 2017; Kim et al., 2019).

5.4.3.1 The FIT target network contains mainly genes involved in the Fe uptake machinery

FIT is a master regulator of the Fe uptake machinery in Strategy I plants. Its homologue FER was first identified in tomato (Ling et al., 2002; Bauer et al., 2007). Both are controlling a similar set of genes. In Arabidopsis in total 448 genes were discovered to be FIT-regulated. Among them 34 were found to be robustly FIT-regulated in seedlings and roots, reflecting the significant role of FIT (Mai et al., 2016). Some very important FIT regulated genes are *FRO2*, *IRT1* and coumarin synthesis genes which are directly involved in the Fe uptake machinery. Likewise *FIT* is mainly expressed in root epidermis cells within the differentiation and elongation zone (Colangelo and Guerinot, 2004; Jakoby et al., 2004; Mai et al., 2016).

5.4.3.2 PYE is a master component in the regulation of the Fe homeostasis network

The Fe homeostasis network on the other hand is comprised of genes that are FIT-independent and mainly involved in Fe distribution processes. The TF PYE belongs to this sub-network and is a key regulator of many components involved in distribution and translocation of Fe throughout the plant. Loss of PYE leads to an impaired Fe deficiency tolerance and disruption of Fe accumulation, including leaf chlorosis, altered/ reduced root growth and decreased amounts of chlorophyll under Fe deprivation. In all, this suggest a positive role of PYE in the Fe deficiency response. However, PYE has been found to negatively regulate the expression of its target genes (Long et al., 2010).

Microarray analysis on roots of the *pye* loss-of-function mutant pye-1 revealed about 70 genes that might be direct PYE targets. Several direct PYE target genes are also members of the Fe homeostasis network, such as *NAS4*, *FRO3* and *ZIF1*, which are studied in more detail. Additionally, OLIGOPEPTIDE TRANSPORTER3 (OPT3) is differentially regulated in *pye-1* (Long et al., 2010; Ivanov et al., 2012). *NAS4* encodes an enzyme responsible for the catalysis of the metal chelator NA, which is mobile in the plant. Therefore, disturbance of NAS4 function leads to severe leaf chlorosis in young leaves as well as sterility (Klatte et al., 2009; Schuler et al., 2012). FRO3 belongs to a family of ferric chelate reductases. While FRO2 is responsible for the reduction of Fe^{3+} at the root plasma membrane, other FRO members are required in the transfer of Fe into subcellular compartments like mitochondria, chloroplasts or vacuoles (Jeong and Connolly, 2009). FRO3 localizes at the mitochondrial membrane of roots and shoots where it is supposed to reduce Fe^{3+} prior to its absorption into mitochondria. Fe is needed in the mitochondria to secure a functioning respiratory chain and Fe-Sulfur (Fe-S) cluster assembly (Jain and Connolly, 2013). The third direct PYE target, ZIF1, is located at the vacuolar

membrane and known to be involved in Zn homeostasis. The PYE mediated repression of *ZIF1* might be crucial for maintaining Zn homeostasis under Fe deprivation (Long et al., 2010). It was recently shown that ZIF1 participates in vacuolar sequestration of NA. The vacuole is an important compartment for cellular Fe storage and detoxification. Thus, it can be crucial in the prevention of Fe toxicity. *ZIF1* repression by PYE might possibly also ensure that no Fe gets transported into the vacuole under Fe deficiency (Haydon et al., 2012).

Additionally, the phloem Fe importer OPT3 is up-regulated in *pye1-1*, showing that it is also negatively regulated by PYE. OPT3 further participates in the regulation of shoot-to-root Fe signaling and translocation (Zhai et al., 2014). Taken together it can be concluded, that PYE plays a major role in the regulation of Fe homeostasis, not only affecting Fe localization and redistribution processes, but possibly also involved in signaling.

5.4.4 Other types of TFs regulating Fe deficiency responses

Besides bHLH proteins, TFs of several families have been identified to play a role in the regulation of the Fe homeostasis. Two MYB TFs, MYB10 and MYB72 for instance, positively regulate *NAS4* expression (Palmer et al., 2013). In addition, MYB72 controls the expression of genes involved in the synthesis of phenolic compounds, needed for Fe mobilization through BGLU42 (BETA-GLUCOSIDASE42) (Zamioudis et al., 2014). Thus, MYB TFs function in Fe acquisition and distribution processes.

Another way to control the Fe deficiency response can be achieved by modulating FIT protein stability. EIN3/EIL1 for example, which are involved in the ethylene signaling pathway can interact with FIT to promote its protein stability. Thus, FIT protein accumulates and enhanced expression of Fe uptake genes is achieved. Therefore, ethylene acts as a signal that triggers Fe deficiency responses (Lingam et al., 2011). The oxidative stress-inducible TF ZAT12, in contrast, interacts with FIT leading to a negative regulation of FIT protein activity, linking oxidative stress response to the negative regulation of prolonged Fe deficiency responses (Le et al., 2016). These two examples demonstrate a regulatory crosstalk between the Fe deficiency response and other signaling pathways or stress responses on the molecular level leading to post-translational regulation of FIT.

5.5 Post-translational regulation is crucial during Fe deficiency response

Post-translational modifications such as phosphorylation or ubiquitination describe a molecular mechanism to regulate protein stability and activity. In contrast to transcriptional regulation this allows a rapid response to changing environmental conditions like for example nutrient availability. Because the Fe uptake machinery is active during Fe deficiency, its proteins like the main Fe importer IRT1 are increasingly present. The poor selectivity of IRT1 results in toxic metal overload if too much IRT1 protein is present over a prolonged time (Barberon et al., 2011). To avoid uptake of Fe

and other metals in toxic amounts, a rapid shut down mechanism of the Fe uptake machinery on protein level is needed. This occurs on different levels (such as FIT/ IRT1/ BTS/BTSL). A recent study of our lab demonstrated that phosphorylation of FIT modulates FIT protein activity. The authors describe a mechanism in which two pools of FIT exist based on their phosphorylation status: active FIT that is phosphorylated and inactive FIT which is not phosphorylated. Phosphorylation of FIT leads to a localization shift of FIT towards the nucleus and allows its interaction with bHLH39 needed to activate downstream Fe uptake genes (Gratz et al., 2019).

Ubiquitination describes the transfer of the small protein ubiquitin to other target proteins. The attachment of a multiple ubiquitin chain usually leads to a rapid degradation of the target protein via the 26S proteasome to regulate protein levels. Monoubiquitination in contrast, commonly affects the location and activity of target proteins. E3 ligases ensure specificity of the ubiquitin-proteasome system. They identify the target protein and mediate the transfer of ubiquitin from an E2 ubiquitin ligase to the substrate (Mazzucotelli et al., 2008; Deshaies and Joazeiro, 2009). The ubiquitin-proteasome system is responsible for the regulation of numerous proteins involved in almost any abiotic stress response process and hormone signaling in plants (Santner and Estelle, 2010). IRT1 itself is supposed to sense excess non-Fe metals in the soil via direct metal binding. This triggers IRT1 phosphorylation followed by ubiquitination and subsequent degradation. Thereby the over-accumulation of non-Fe metals under Fe deficiency is prevented (Dubeaux et al., 2018). The E3 ligase IRT1 DEGRADATION FACTOR1 (IDF1) mediates IRT1 protein turnover and is only one of several examples of E3 ligases regulating Fe deficiency responsive proteins (Barberon et al., 2011; Dubeaux et al., 2018). Additionally, various ubiquitin E3 ligases target Fe deficiency responsive bHLH TFs for proteasomal degradation.

5.5.1 The E3 ligases BTS and its paralogues BTSL1/2 negatively regulate the Fe deficiency response

IVc bHLH TFs are expressed regardless of the Fe availability, implying that their regulation occurs on the protein level (Kim et al., 2019). As previously mentioned, the E3 ligase BTS interacts with IVc bHLH TFs and indeed targets at least two of them (ILR3 and bHLH115) for proteasomal degradation (Selote, 2015). All three BTS, BTSL1 and BTSL2 belong to the E3 Really Interesting New Gene (RING)-type ligases (Hindt et al., 2017). They are up-regulated under Fe deprivation and negatively regulate the Fe deficiency response. When IVc bHLH proteins are degraded, Ib *BHLH* genes are no longer expressed. Consequently, the Fe uptake machinery is no longer activated. BTSL1 and BTSL2 possibly also interact with IVc bHLH TFs. Thus, it remains to be elucidated whether bHLH104 and bHLH34 are targeted for proteasomal degradation by BTS or rather by BTSL1 or BTSL2. Nevertheless, a recent study suggests that at least BTSL2 participates in the Fe deficiency response by targeting FIT for proteasomal degradation, leading to a negative impact on Fe uptake (Rodríguez-Celma et al., 2019). It can be

concluded, that several post-translational mechanisms are crucial in balancing the Fe uptake mechanism.

5.6 Several homologues of Arabidopsis Fe deficiency response key players are also present in rice

Regardless of the differences in the Fe uptake process, the regulatory cascade controlling Fe homeostasis is largely conserved between Arabidopsis and rice. The E3 ubiquitin ligase BTS has two homologues in rice, named HEMERYTHRIN MOTIF-CONTAINING REALLY INTERESTING NEW GENE- AND ZINC-FINGER PROTEINS (OsHRZ1 and OsHRZ2). Likewise, Arabidopsis bHLH IVc TF homologues exist in rice: OsbHLH057, OsbHLH058, OsbHLH059 and OsbHLH060 (also designated bHLH57-59: OsPRI2-4 and OsbHLH60:OsPRI1, POSITIVE REGULATOR OF IRON HOMEOSTASIS). They positively regulate the Fe deficiency response. As in Arabidopsis, in which subgroup IVc bHLH TFs are under the control of BTS, rice IVc homologues are controlled by OsHRZ (Selote, 2015; Kobayashi et al., 2019; Zhang et al., 2020).

The bHLH TF OsIRO2 is homologous to Arabidopsis Ib bHLH38/39/100/101 TFs. OsIRO2 acts as a transcriptional activator of genes involved in Fe uptake under Fe deficiency, including genes involved in MA secretion (e.g. *TOM1*) as well as NA synthesis genes (Ogo et al., 2007). The PYE homologue in rice, OsIRO3 represses a group of genes involved in Fe uptake and translocation. OsIRO3 over-expressing plants are hypersensitive to low Fe. Thus, opposing to PYE, OsIRO3 is suggested to act as a negative regulator of the Fe deficiency response (Zheng et al., 2010). *OsIRO2* and *OsIRO3* are induced under Fe deficiency. This induction is positively controlled by IDEF1 which in turn shows no induction under Fe deficiency, suggesting a role of IDEF1 upstream of the regulatory cascade that controls the Fe deficiency response. OsIRO2 and IDEF1 induce a partially overlapping set of genes responsible for Fe uptake and translocation (**Figure 1B**). However, no homologue is known for IDEF1 in Arabidopsis (Kobayashi et al., 2009; Kobayashi et al., 2012).

Only recently was the rice TF OsbHLH156 identified as FIT orthologue. As in Arabidopsis, OsbHLH156 does not only form homodimers but also physically interacts with OsIRO2 to activate Fe uptake genes. Like FIT in Arabidopsis for bHLH39, OsbHLH156 in rice is involved in controlling the nuclear localization of OsIRO2. In both cases a shift in localization of OsIRO2 and bHLH39 towards the nucleus could be observed in the presence of OsbHLH156 or FIT (Trofimov et al., 2019; Wang et al., 2020). There are even homologues directly involved in Fe uptake, such as the previously mentioned IRT1 homologue OsIRT1 (Ishimaru et al., 2006).

5.7 Fe sensors and signals in plants

While the transcriptional response to Fe deficiency is well studied, little is known about how Fe is sensed and which signals are involved in plants. In bacteria, yeast and animals, the intracellular Fe status is sensed through direct binding of Fe^{2+}, Fe-S clusters or heme to the respective regulatory proteins (Fe sensors). The binding of Fe promotes functional conversions of the sensor that results in

the regulation of the Fe homeostasis. This mechanism creates a link between the actual Fe level and the regulation of the Fe uptake machinery (Kobayashi and Nishizawa, 2014). The mammalian Fe sensor FBXL5 (F-Box and Leucine-rich repeat5) senses Fe via its hemerythrin (HHE) domains, which bind Fe^{2+} which stabilizes the protein. FBXL5 is a component of an E3 ligase complex which regulates the IRON REGULATORY PROTEINS IRP1 and IRP2 and they in turn control many genes involved in Fe homeostasis. Thus, among other mechanisms, Fe homeostasis in mammals is controlled by a process in which FBXL5 targets IRP proteins for degradation in an Fe dependent manner (Salahudeen et al., 2009).

5.7.1 Candidates for Fe sensors in plants

Two possible plant Fe sensors are the focus of current research. One type are the HHE-containing proteins BTS/ BTSL1/ BTSL2 (OsHRZ1/2). Like the mammalian Fe sensor FBXL5, they contain HHE domains that bind Fe^{2+}. While FBXL5 is part of the SCF^{FBXL5} E3-ligase complex, BTS, BTSL1 and 2 (OsHRZ) possess E3 ligase function by themselves and act in a similar way as the SCF^{FBXL5} complex. They therefore could possibly perform multiple functions as Fe sensor combined with the role of an E3 ligase. HRZ and BTS are stabilized upon metal binding as seen in FBXL5 and control the level of their target proteins in a Fe dependent manner (Salahudeen et al., 2009; Kobayashi et al., 2013; Hindt et al., 2017). The molecular interconnection of a sensor, combined with an E3 ligase function also exists, for example, in receptors of hormones and in light signaling pathways, and seems to be a common mechanism in signal transmission processes (Hua and Vierstra, 2011).

The second potential plant Fe sensor, namely IDEF1, was identified in rice. IDEF1 is an important TF in graminaceous plants and regulates genes of both the Fe uptake and utilization machinery (Kobayashi et al., 2007). In contrast to most TFs involved in the Fe deficiency response, the *IDEF1* transcript levels are independent of Fe availability, suggesting a function upstream of other involved TFs, possibly as Fe sensor. Furthermore, IDEF1 comprises histidine-asparagine repeats and proline-rich regions that bind Fe^{2+} and thus, IDEF1 fulfils the characteristics of a possible Fe sensor for transmission and conversion of Fe signals (Kobayashi et al., 2012). However, further research is needed to investigate whether there is a direct link between Fe sensing/ binding and the regulation of Fe deficiency responses.

5.7.2 Potential long distance Fe signaling

While Fe is taken up by roots, many Fe sinks are located in the shoots. Therefore, the Fe deficiency response in roots is not only dependent on a local signal from the rhizosphere, but also on a shoot-derived long distance signal (systemic) that transfers information about the Fe demand in the shoot (Vert et al., 2003; Kumar et al., 2017). Several hormones and signaling molecules such as ethylene, auxin, salicylic acid, nitric oxide or sucrose are increased in Fe deficient roots and seem to influence the Fe acquisition. At the same time, they fail to activate the Fe uptake machinery, when

phloem Fe levels are high, indicating an important role of the phloem and that there must be additional signals regulating the Fe uptake (García et al., 2013; García et al., 2018). The actual long-distance Fe signals are still the focus of current research. Possible candidates are phloem mobile Fe, Fe-NA chelates or other secondary substances such as Heme or Fe-S clusters (Kobayashi and Nishizawa, 2014). The leaf vasculature plays an important role in sensing apoplastic Fe availability in Arabidopsis. It is suggested, that Fe that is transported into upper parts of the plant, is sensed in the xylem and the information about the Fe status there will be forwarded back to the roots via the phloem to regulate the root Fe uptake. It is currently assumed that the phloem Fe levels are essential for systemic Fe sensing by repressing the root Fe uptake under sufficient phloem Fe levels. The phloem Fe importer OPT3 is a key component in this shoot-to-root signaling that prevents Fe overload. If OPT3 is absent in shoots, the negative feedback mechanism that regulates the Fe uptake in roots is not active which consequently leads to an Fe overload (Khan et al., 2018). Regarding the phloem Fe levels, Arabidopsis lines with decreased OPT3 show less phloem Fe, leading to a constant activity of the Fe uptake machinery which additionally indicates an important role of the phloem in Fe signaling (Zhai et al., 2014).

Additionally, it was recently suggested that a family of FE-UPTAKE-INDUCING PEPTIDES (FEPs), also designated IRONMAN (IMA) peptides, positively regulate the Fe uptake machinery, together with the previously described regulatory cascade of bHLH TFs. FEP/ IMA peptides have been proposed to mediate the phloem based shoot-to-root Fe signaling by acting as phloem mobile molecules (Grillet et al., 2018; Hirayama et al., 2018).

5.8 Regulatory small proteins and peptides

Small proteins and peptides are defined as polypeptides with usually less than 100 aa. Many of them possess crucial regulatory functions in various developmental and stress responses including Fe deficiency (Hsu and Benfey, 2018; Takahashi et al., 2019). Peptides are often mobile and act as mediators in long-distance signaling as well as cell-to-cell communication. In this way, plants coordinate stress responses between roots and shoots on the whole plant level (Takahashi and Shinozaki, 2019).

As an example, in Arabidopsis, the nitrogen (N) uptake response is triggered by a root-to-shoot mobile hormone-like peptide, named C-TERMINALLY ENCODED PEPTIDE (CEP) that mediates inter-organ communication. While CEP expression is induced in N-starved roots, CEP peptides travel via the xylem to the shoots where they are recognized by the LRR-receptor kinase CEPR1, leading to an increased production of the phloem-specific CEP DOWNSTREAM1 (CEPD1) and CEPD2 polypeptides in shoots. The shoot derived CEPD1 and CEPD2 polypeptides in turn transmit the signal back to the roots where they are responsible for the upregulation of the nitrate transporter gene *NRT2.1*. This system

allows long-distance signaling from shoot-to-root and vice versa in order to communicate the N status at whole plant level (Tabata et al., 2014; Ohkubo et al., 2017). Recently a shoot phloem-specific mobile shoot-to-root signal, named CEPD-like 2 (CEPDL2) was identified. In contrast to CEPD1 and CEPD2 the expression of CEPDL2 is directly regulated by the shoot N status. Under N deprivation in shoots, CEPDL2 is upregulated in the leaf vasculature and translocated to the roots where it promotes N uptake by upregulating NRT2.1 similar to CEPD1 and CEPD. All three of them are necessary for a balanced regulation of systemic N acquisition (Ota et al., 2020).

A partially similar mechanism is assumed for the Fe uptake regulation. The mobile peptides FEP1 and FEP3 were shown to promote Fe uptake, they are highly expressed under Fe deficiency and located in the phloem. Over-expression of FEP peptides promotes Fe uptake (Grillet et al., 2018; Hirayama et al., 2018). Hirayama et al. 2018 could show, that *fep1* loss-of-function plants had lower shoot Fe levels while root Fe levels were unaffected under sufficient Fe conditions, indicating that the Fe translocation from root-to-shoots is impaired in *fep1* mutants. Nevertheless, it should be mentioned that eight *FEP* genes exist in Arabidopsis that might have similar functions and knock-out of more than one *FEP* gene might be necessary to obtain a severe phenotype (as seen in (Grillet et al., 2018)). In reciprocal grafting experiments using FEP3 over-expressing plants grafted with wildtype (WT), it could be shown that FEP3 might be a phloem-mobile peptide that positively regulates the Fe uptake machinery in roots (Grillet et al., 2018), but the exact mechanism by which FEPs regulate the Fe uptake machinery is still not clear. It is not yet known whether FEPs themselves function as shoot-to-root signal or if they activate another mobile signal that further transmits Fe signals. Additional characterization of FEPs and other signaling candidates will be necessary to fully understand the Fe sensing and signaling process in plants.

Peptides are currently best studied in Arabidopsis. Nevertheless, various evolutionary studies have been performed that revealed that the CEPs as well as FEPs and other peptides are highly conserved in most land plants and likely perform similar functions in signaling processes (Takahashi et al., 2019). They often have a short highly conserved domain near their C-terminus that is important for their function. While the N-terminus of FEPs is often very variable, the C-terminus harbours a highly conserved consensus motif of 17 aa residues, that is necessary for FEP function. While over-expression of FEP3 leads to an enhanced Fe uptake response, over-expression of FEP3 constructs lacking the consensus motif had no effect compared to WT (Grillet et al., 2018).

Several small proteins are involved in the regulation of protein activity. The regulation of protein activity by a small protein can be achieved through the formation of protein-protein interactions between the small protein and its interacting partner to be regulated. Because proteins accomplish their function frequently as part of multi-protein complexes, interaction with a small protein often disturbs the actual protein function by preventing the complex formation needed to enable protein-

activity. Thus, they can play a role as post-translational regulators by forming homotypic dimers with their target proteins (Staudt and Wenkel, 2011).

More and more information has been deciphered regarding Fe homeostasis and especially its transcriptional regulation. Several key players of the Fe deficiency response and their protein-protein interactions have been identified, but still one is just beginning to understand the mechanisms that maintain plant Fe homeostasis. Overall knowledge of the regulatory processes controlling the Fe uptake, distribution, sensing, and signaling remains incomplete. Hence, it is of special importance to further research in this field, for a better understanding that might facilitate the development of genetically modified crops with enhanced Fe bioavailability.

6 Thesis Objectives

The Fe uptake and homeostasis of *Arabidopsis thaliana* is stringently controlled by a regulatory network of mainly transcription factors along with several other proteins of regulatory function. Many genes involved in the Fe deficiency response are co-expressed, indicating a high interplay on the protein level (Schwarz and Bauer, 2020). It has been shown that protein-protein interactions among Fe responsive genes are essential in regulatory processes. This raises the question whether additional, novel protein-protein interactions can be identified (1.) and which role they play within the Fe deficiency response (2. and 3.). In order to tackle these questions the following thesis objectives were formulated:

1. Unravel novel protein-protein interactions within Fe deficiency responsive genes

To further decipher the Fe homeostasis in plants and to investigate the significance of meaningful protein-protein interactions among key players of the Fe deficiency response and members of the Fe deficiency co-expression networks a targeted yeast two-hybrid (Y2H) assay between 33 selected proteins was performed. This screen resulted in a protein interaction network, from which we investigated selected interactors in more detail and analyzed their interplay in the Fe deficiency response.

2. Characterize the interplay between E3 ligases and other Fe deficiency responsive genes

The targeted Y2H interaction screen revealed a network of interacting proteins consisting of E3 ligases, bHLH transcription factors and a small protein. Several members of this interactome were involved in multiple protein-protein interactions. We investigated their interaction potential *in planta* using a targeted bimolecular fluorescence complementation (BiFC) assay together with subcellular localization and co-localization studies. Promotor activities of all involved proteins were compared. We analyzed stable gain- and loss-of-function lines to address the role of these proteins in the Fe deficiency response. Finally, our aim was to identify how these proteins influence each other under Fe deficiency and to generate a model of their function in the Fe deficiency response.

3. Investigate the interaction of the small unknown protein OLIVIA and the transcription factor POPEYE

The interaction of OLIVIA and POPEYE was verified *in planta* as described in the second aim. Additionally, a Förster Resonance Energy Transfer – Acceptor Photo Bleaching (FRET-APB) interaction assay was accomplished. By creating OLIVIA gain-of-function lines the impact of OLIVIA on POPEYE function was investigated. Multiple sequence alignment analysis was used to understand to what extend OLIVIA is conserved and whether a conserved motif is present in the protein, which might provide a hint at the general function of OLIVIA in many species

References

Al-Fartusie FS, Mohssan SN (2017) Essential trace elements and their vital roles in human body. Indian J Adv Chem Sci **5:** 127-136

Barberon M, Zelazny E, Robert S, Conéjéro G, Curie C, Friml J, Vert G (2011) Monoubiquitin-dependent endocytosis of the iron-regulated transporter 1 (IRT1) transporter controls iron uptake in plants. Proceedings of the National Academy of Sciences **108:** E450-E458

Bauer P, Ling HQ, Guerinot ML (2007) FIT, the FER-LIKE IRON DEFICIENCY INDUCED TRANSCRIPTION FACTOR in Arabidopsis. Plant Physiol Biochem **45:** 260-261

Briat J-F, Cellier F, Gaymard F (2006) Ferritins and iron accumulation in plant tissues. *In* Iron nutrition in plants and rhizospheric microorganisms. Springer, pp 341-357

Briat J-F, Dubos C, Gaymard F (2015) Iron nutrition, biomass production, and plant product quality. Trends in Plant Science **20:** 33-40

Briat J-F, Ravet K, Arnaud N, Duc C, Boucherez J, Touraine B, Cellier F, Gaymard F (2009) New insights into ferritin synthesis and function highlight a link between iron homeostasis and oxidative stress in plants. Annals of botany **105:** 811-822

Brumbarova T, Bauer P, Ivanov R (2015) Molecular mechanisms governing Arabidopsis iron uptake. Trends in Plant Science **20:** 124-133

Buckhout TJ, Yang TJ, Schmidt W (2009) Early iron-deficiency-induced transcriptional changes in Arabidopsis roots as revealed by microarray analyses. BMC genomics **10:** 147

Casiday R, Frey R (1998) Iron use and storage in the body: ferritin and molecular representations. Department of Chemistry, Washington University, St. Louis. USA

Clemens S, Weber M (2016) The essential role of coumarin secretion for Fe acquisition from alkaline soil. Plant signaling & behavior **11:** e1114197

Colangelo EP, Guerinot ML (2004) The essential basic helix-loop-helix protein FIT1 is required for the iron deficiency response. The Plant Cell **16:** 3400-3412

Connorton JM, Balk J (2019) Iron biofortification of staple crops: lessons and challenges in plant genetics. Plant and Cell Physiology **60:** 1447-1456

Cui Y, Chen C-L, Cui M, Zhou W-J, Wu H-L, Ling H-Q (2018) Four IVa bHLH transcription factors are novel interactors of FIT and mediate JA inhibition of iron uptake in Arabidopsis. Molecular plant **11:** 1166-1183

Curie C, Panaviene Z, Loulergue C, Dellaporta SL, Briat J-F, Walker EL (2001) Maize yellow stripe1 encodes a membrane protein directly involved in Fe (III) uptake. Nature **409:** 346

Deshaies RJ, Joazeiro CA (2009) RING domain E3 ubiquitin ligases. Annual review of biochemistry **78**

Dinneny JR, Long TA, Wang JY, Jung JW, Mace D, Pointer S, Barron C, Brady SM, Schiefelbein J, Benfey PN (2008) Cell identity mediates the response of Arabidopsis roots to abiotic stress. Science **320:** 942-945

Dubeaux G, Neveu J, Zelazny E, Vert G (2018) Metal sensing by the IRT1 transporter-receptor orchestrates its own degradation and plant metal nutrition. Molecular Cell **69:** 953-964. e955

Durrett TP, Gassmann W, Rogers EE (2007) The FRD3-mediated efflux of citrate into the root vasculature is necessary for efficient iron translocation. Plant physiology **144:** 197-205

Eide D, Broderius M, Fett J, Guerinot ML (1996) A novel iron-regulated metal transporter from plants identified by functional expression in yeast. Proceedings of the National Academy of Sciences **93:** 5624-5628

Fourcroy P, Sisó-Terraza P, Sudre D, Savirón M, Reyt G, Gaymard F, Abadía A, Abadia J, Álvarez-Fernández A, Briat JF (2014) Involvement of the ABCG 37 transporter in secretion of scopoletin and derivatives by Arabidopsis roots in response to iron deficiency. New Phytologist **201:** 155-167

Gao F, Robe K, Bettembourg M, Navarro N, Rofidal V, Santoni V, Gaymard F, Vignols F, Roschzttardtz H, Izquierdo E (2019) The Transcription Factor bHLH121 Interacts with bHLH105 (ILR3) and its Closest Homologs to Regulate Iron Homeostasis in Arabidopsis. The Plant Cell

Gao F, Robe K, Gaymard F, Izquierdo E, Dubos C (2019) The transcriptional control of iron homeostasis in plants: a tale of bHLH transcription factors? Frontiers in plant science **10:** 6

García MJ, Corpas FJ, Lucena C, Alcántara E, Pérez-Vicente R, Zamarreño ÁM, Bacaicoa E, García-Mina JM, Bauer P, Romera FJ (2018) A shoot Fe signaling pathway requiring the OPT3 transporter controls GSNO Reductase and ethylene in Arabidopsis thaliana roots. Frontiers in plant science **9**

García MJ, Romera FJ, Stacey MG, Stacey G, Villar E, Alcántara E, Pérez-Vicente R (2013) Shoot to root communication is necessary to control the expression of iron-acquisition genes in Strategy I plants. Planta **237:** 65-75

Gratz R, Manishankar P, Ivanov R, Köster P, Mohr I, Trofimov K, Steinhorst L, Meiser J, Mai H-J, Drerup M (2019) CIPK11-dependent phosphorylation modulates FIT activity to promote Arabidopsis iron acquisition in response to calcium signaling. Developmental cell **48:** 726-740. e710

Grillet L, Lan P, Li W, Mokkapati G, Schmidt W (2018) IRON MAN is a ubiquitous family of peptides that control iron transport in plants. Nature plants **4:** 953

Haydon MJ, Kawachi M, Wirtz M, Hillmer S, Hell R, Kramer U (2012) Vacuolar nicotianamine has critical and distinct roles under iron deficiency and for zinc sequestration in Arabidopsis. Plant Cell **24:** 724-737

Heim MA, Jakoby M, Werber M, Martin C, Weisshaar B, Bailey PC (2003) The basic helix–loop–helix transcription factor family in plants: a genome-wide study of protein structure and functional diversity. Molecular biology and evolution **20:** 735-747

Hindt MN, Akmakjian GZ, Pivarski KL, Punshon T, Baxter I, Salt DE, Guerinot ML (2017) BRUTUS and its paralogs, BTS LIKE1 and BTS LIKE2, encode important negative regulators of the iron deficiency response in Arabidopsis thaliana. Metallomics **9:** 876-890

Hirayama T, Lei GJ, Yamaji N, Nakagawa N, Ma JF (2018) The putative peptide gene FEP1 regulates iron deficiency response in Arabidopsis. Plant and Cell Physiology **59:** 1739-1752

Hsu PY, Benfey PN (2018) Small but mighty: functional peptides encoded by small ORFs in plants. Proteomics **18:** 1700038

Hua Z, Vierstra RD (2011) The cullin-RING ubiquitin-protein ligases. Annual review of plant biology **62:** 299-334

Inoue H, Kobayashi T, Nozoye T, Takahashi M, Kakei Y, Suzuki K, Nakazono M, Nakanishi H, Mori S, Nishizawa NK (2009) Rice OsYSL15 is an iron-regulated iron (III)-deoxymugineic acid transporter expressed in the roots and is essential for iron uptake in early growth of the seedlings. Journal of Biological Chemistry **284:** 3470-3479

Ishimaru Y, Suzuki M, Tsukamoto T, Suzuki K, Nakazono M, Kobayashi T, Wada Y, Watanabe S, Matsuhashi S, Takahashi M (2006) Rice plants take up iron as an Fe3+-phytosiderophore and as Fe2+. The Plant Journal **45:** 335-346

Ivanov R, Brumbarova T, Bauer P (2012) Fitting into the harsh reality: regulation of iron-deficiency responses in dicotyledonous plants. Mol Plant **5:** 27-42

Jain A, Connolly EL (2013) Mitochondrial iron transport and homeostasis in plants. Frontiers in plant science **4:** 348

Jakoby M, Wang HY, Reidt W, Weisshaar B, Bauer P (2004) FRU (BHLH029) is required for induction of iron mobilization genes in Arabidopsis thaliana. FEBS Lett **577:** 528-534

Jeong J, Connolly EL (2009) Iron uptake mechanisms in plants: functions of the FRO family of ferric reductases. Plant science **176:** 709-714

Khan MA, Castro-Guerrero NA, McInturf SA, Nguyen NT, Dame AN, Wang J, Bindbeutel RK, Joshi T, Jurisson SS, Nusinow DA (2018) Changes in iron availability in Arabidopsis are rapidly sensed in the leaf vasculature and impaired sensing leads to opposite transcriptional programs in leaves and roots. Plant, cell & environment **41:** 2263-2276

Kim SA, Guerinot ML (2007) Mining iron: iron uptake and transport in plants. FEBS letters **581:** 2273-2280

Kim SA, LaCroix IS, Gerber SA, Guerinot ML (2019) The iron deficiency response in Arabidopsis thaliana requires the phosphorylated transcription factor URI. Proceedings of the National Academy of Sciences

Kim SA, Punshon T, Lanzirotti A, Li L, Alonso JM, Ecker JR, Kaplan J, Guerinot ML (2006) Localization of iron in Arabidopsis seed requires the vacuolar membrane transporter VIT1. Science **314:** 1295-1298

Klatte M, Schuler M, Wirtz M, Fink-Straube C, Hell R, Bauer P (2009) The analysis of Arabidopsis nicotianamine synthase mutants reveals functions for nicotianamine in seed iron loading and iron deficiency responses. Plant Physiology **150:** 257-271

Kobayashi T, Itai RN, Aung MS, Senoura T, Nakanishi H, Nishizawa NK (2012) The rice transcription factor IDEF1 directly binds to iron and other divalent metals for sensing cellular iron status. The Plant Journal **69:** 81-91

Kobayashi T, Itai RN, Ogo Y, Kakei Y, Nakanishi H, Takahashi M, Nishizawa NK (2009) The rice transcription factor IDEF1 is essential for the early response to iron deficiency, and induces vegetative expression of late embryogenesis abundant genes. The Plant Journal **60:** 948-961

Kobayashi T, Nagasaka S, Senoura T, Itai RN, Nakanishi H, Nishizawa NK (2013) Iron-binding haemerythrin RING ubiquitin ligases regulate plant iron responses and accumulation. Nature Communications **4:** 2792

Kobayashi T, Nishizawa NK (2012) Iron uptake, translocation, and regulation in higher plants. Annual review of plant biology **63:** 131-152

Kobayashi T, Nishizawa NK (2014) Iron sensors and signals in response to iron deficiency. Plant Science **224:** 36-43

Kobayashi T, Nozoye T, Nishizawa NK (2019) Iron transport and its regulation in plants. Free Radical Biology and Medicine **133:** 11-20

Kobayashi T, Ogo Y, Itai RN, Nakanishi H, Takahashi M, Mori S, Nishizawa NK (2007) The transcription factor IDEF1 regulates the response to and tolerance of iron deficiency in plants. Proceedings of the National Academy of Sciences **104:** 19150-19155

Kobayashi T, Ozu A, Kobayashi S, An G, Jeon J-S, Nishizawa NK (2019) OsbHLH058 and OsbHLH059 transcription factors positively regulate iron deficiency responses in rice. Plant molecular biology **101:** 471-486

Korshunova YO, Eide D, Clark WG, Guerinot ML, Pakrasi HB (1999) The IRT1 protein from Arabidopsis thaliana is a metal transporter with a broad substrate range. Plant molecular biology **40:** 37-44

Kumar RK, Chu H-H, Abundis C, Vasques K, Rodriguez DC, Chia J-C, Huang R, Vatamaniuk OK, Walker EL (2017) Iron-nicotianamine transporters are required for proper long distance iron signaling. Plant physiology **175:** 1254-1268

Le CT, Brumbarova T, Ivanov R, Stoof C, Weber E, Mohrbacher J, Fink-Straube C, Bauer P (2016) ZINC FINGER OF ARABIDOPSIS THALIANA12 (ZAT12) Interacts with FER-LIKE IRON DEFICIENCY-INDUCED TRANSCRIPTION FACTOR (FIT) Linking Iron Deficiency and Oxidative Stress Responses. Plant Physiol **170:** 540-557

Li G, Kronzucker HJ, Shi W (2016) The response of the root apex in plant adaptation to iron heterogeneity in soil. Frontiers in plant science **7:** 344

Li S, Zhou X, Li H, Liu Y, Zhu L, Guo J, Liu X, Fan Y, Chen J, Chen R (2015) Overexpression of ZmIRT1 and ZmZIP3 enhances iron and zinc accumulation in transgenic Arabidopsis. PLoS One **10:** e0136647

Li X, Zhang H, Ai Q, Liang G, Yu D (2016) Two bHLH transcription factors, bHLH34 and bHLH104, regulate iron homeostasis in Arabidopsis thaliana. Plant Physiology **170:** 2478-2493

Li Y, Lei R, Pu M, Cai Y, Lu C, Li Z, Liang G (2020) bHLH11 negatively regulates Fe homeostasis by its EAR motifs recruiting corepressors in Arabidopsis. bioRxiv

Liang G, Zhang H, Li X, Ai Q, Yu D (2017) bHLH transcription factor bHLH115 regulates iron homeostasis in Arabidopsis thaliana. Journal of experimental botany **68:** 1743-1755

Liang G, Zhang H, Li Y, Pu M, Yang Y, Li C, Lu C, Xu P, Yu D (2020) Oryza sativa Fer-like fe deficiency-induced transcription factor (OsFIT/OsbHLH156) interacts with OsIRO2 to regulate iron homeostasis. Journal of Integrative Plant Biology

Ling H-Q, Bauer P, Bereczky Z, Keller B, Ganal M (2002) The tomato fer gene encoding a bHLH protein controls iron-uptake responses in roots. Proceedings of the National Academy of Sciences **99:** 13938-13943

Lingam S, Mohrbacher J, Brumbarova T, Potuschak T, Fink-Straube C, Blondet E, Genschik P, Bauer P (2011) Interaction between the bHLH transcription factor FIT and ETHYLENE INSENSITIVE3/ETHYLENE INSENSITIVE3-LIKE1 reveals molecular linkage between the regulation of iron acquisition and ethylene signaling in Arabidopsis. Plant Cell **23:** 1815-1829

Long TA, Tsukagoshi H, Busch W, Lahner B, Salt DE, Benfey PN (2010) The bHLH transcription factor POPEYE regulates response to iron deficiency in Arabidopsis roots. Plant Cell **22:** 2219-2236

Long TA, Tsukagoshi H, Busch W, Lahner B, Salt DE, Benfey PN (2010) The bHLH transcription factor POPEYE regulates response to iron deficiency in Arabidopsis roots. The Plant Cell **22:** 2219-2236

Mai H-J, Pateyron S, Bauer P (2016) Iron homeostasis in Arabidopsis thaliana: transcriptomic analyses reveal novel FIT-regulated genes, iron deficiency marker genes and functional gene networks. BMC plant biology **16:** 211

Marschner H, Römheld V, Kissel M (1986) Different strategies in higher plants in mobilization and uptake of iron. Journal of plant nutrition **9:** 695-713

Marschner H, Treeby M, Römheld V (1989) Role of root-induced changes in the rhizosphere for iron acquisition in higher plants. Zeitschrift für Pflanzenernährung und Bodenkunde **152:** 197-204

Mazzucotelli E, Mastrangelo AM, Crosatti C, Guerra D, Stanca AM, Cattivelli L (2008) Abiotic stress response in plants: when post-transcriptional and post-translational regulations control transcription. Plant Science **174:** 420-431

Murata Y, Ma JF, Yamaji N, Ueno D, Nomoto K, Iwashita T (2006) A specific transporter for iron (III)–phytosiderophore in barley roots. The Plant Journal **46:** 563-572

Naranjo-Arcos MA, Bauer P (2016) Iron nutrition, oxidative stress, and pathogen defense. Nutritional Deficiency**:** 63-98

Naranjo-Arcos MA, Maurer F, Meiser J, Pateyron S, Fink-Straube C, Bauer P (2017) Dissection of iron signaling and iron accumulation by overexpression of subgroup Ib bHLH039 protein. Scientific reports **7:** 10911

Nozoye T, Nagasaka S, Kobayashi T, Takahashi M, Sato Y, Sato Y, Uozumi N, Nakanishi H, Nishizawa NK (2011) Phytosiderophore efflux transporters are crucial for iron acquisition in graminaceous plants. Journal of Biological Chemistry **286:** 5446-5454

Obayashi T, Aoki Y, Tadaka S, Kagaya Y, Kinoshita K (2018) ATTED-II in 2018: a plant coexpression database based on investigation of the statistical property of the mutual rank index. Plant and Cell Physiology **59:** e3-e3

Ogo Y, Nakanishi Itai R, Nakanishi H, Kobayashi T, Takahashi M, Mori S, Nishizawa NK (2007) The rice bHLH protein OsIRO2 is an essential regulator of the genes involved in Fe uptake under Fe-deficient conditions. The Plant Journal **51:** 366-377

Ohkubo Y, Tanaka M, Tabata R, Ogawa-Ohnishi M, Matsubayashi Y (2017) Shoot-to-root mobile polypeptides involved in systemic regulation of nitrogen acquisition. Nature Plants **3:** 1-6

Ota R, Ohkubo Y, Yamashita Y, Ogawa-Ohnishi M, Matsubayashi Y (2020) Shoot-to-root mobile CEPD-like 2 integrates shoot nitrogen status to systemically regulate nitrate uptake in Arabidopsis. Nature communications **11:** 1-9

Palmer CM, Hindt MN, Schmidt H, Clemens S, Guerinot ML (2013) MYB10 and MYB72 are required for growth under iron-limiting conditions. PLoS Genet **9:** e1003953

Qu L-J, Zhu Y-X (2006) Transcription factor families in Arabidopsis: major progress and outstanding issues for future research. Current opinion in plant biology **9:** 544-549

Riechmann JL, Heard J, Martin G, Reuber L, Jiang C-Z, Keddie J, Adam L, Pineda O, Ratcliffe O, Samaha R (2000) Arabidopsis transcription factors: genome-wide comparative analysis among eukaryotes. Science **290:** 2105-2110

Robinson NJ, Procter CM, Connolly EL, Guerinot ML (1999) A ferric-chelate reductase for iron uptake from soils. Nature **397:** 694

Rodríguez-Celma J, Connorton JM, Kruse I, Green RT, Franceschetti M, Chen Y-T, Cui Y, Ling H-Q, Yeh K-C, Balk J (2019) Arabidopsis BRUTUS-LIKE E3 ligases negatively regulate iron uptake by targeting transcription factor FIT for recycling. Proceedings of the National Academy of Sciences**:** 201907971

Russell RM (2001) New micronutrient dietary reference intakes from the National Academy of Sciences. Nutrition Today **36:** 163-171

Salahudeen AA, Thompson JW, Ruiz JC, Ma H-W, Kinch LN, Li Q, Grishin NV, Bruick RK (2009) An E3 ligase possessing an iron-responsive hemerythrin domain is a regulator of iron homeostasis. Science **326:** 722-726

Samira R, Li B, Kliebenstein D, Li C, Davis E, Gillikin JW, Long TA (2018) The bHLH transcription factor ILR3 modulates multiple stress responses in Arabidopsis. Plant molecular biology **97:** 297-309

Santi S, Schmidt W (2009) Dissecting iron deficiency-induced proton extrusion in Arabidopsis roots. New Phytologist **183:** 1072-1084

Santner A, Estelle M (2010) The ubiquitin-proteasome system regulates plant hormone signaling. The plant journal **61:** 1029-1040

Santos RSd, Araujo Júnior ATd, Pegoraro C, Oliveira ACd (2017) Dealing with iron metabolism in rice: from breeding for stress tolerance to biofortification. Genetics and molecular biology **40:** 312-325

Schuler M, Rellán-Álvarez R, Fink-Straube C, Abadía J, Bauer P (2012) Nicotianamine functions in the phloem-based transport of iron to sink organs, in pollen development and pollen tube growth in Arabidopsis. The Plant Cell **24:** 2380-2400

Schwarz B, Bauer P (2020) FIT, a regulatory hub for iron deficiency and stress signaling in roots, and FIT-dependent and-independent gene signatures. Journal of Experimental Botany

Selote (2015) Iron Binding E3 Ligase Mediates Iron response in Plants by targeting basic helix loop helix transcription factors Plant Physiology

Stacey MG, Patel A, McClain WE, Mathieu M, Remley M, Rogers EE, Gassmann W, Blevins DG, Stacey G (2008) The Arabidopsis AtOPT3 protein functions in metal homeostasis and movement of iron to developing seeds. Plant physiology **146:** 589-601

Staudt AC, Wenkel S (2011) Regulation of protein function by 'microProteins'. EMBO reports **12:** 35-42

Tabata R, Sumida K, Yoshii T, Ohyama K, Shinohara H, Matsubayashi Y (2014) Perception of root-derived peptides by shoot LRR-RKs mediates systemic N-demand signaling. Science **346:** 343-346

Takagi Si, Nomoto K, Takemoto T (1984) Physiological aspect of mugineic acid, a possible phytosiderophore of graminaceous plants. Journal of Plant Nutrition **7:** 469-477

Takahashi F, Hanada K, Kondo T, Shinozaki K (2019) Hormone-like peptides and small coding genes in plant stress signaling and development. Current opinion in plant biology **51:** 88-95

Takahashi F, Shinozaki K (2019) Long-distance signaling in plant stress response. Current opinion in plant biology **47:** 106-111

Tanabe N, Noshi M, Mori D, Nozawa K, Tamoi M, Shigeoka S (2019) The basic helix-loop-helix transcription factor, bHLH11 functions in the iron-uptake system in Arabidopsis thaliana. Journal of plant research **132:** 93-105

Tissot N, Robe K, Gao F, Grant-Grant S, Boucherez J, Bellegarde F, Maghiaoui A, Marcelin R, Izquierdo E, Benhamed M, Martin A, Vignols F, Roschzttardtz H, Gaymard F, Briat JF, Dubos C (2019) Transcriptional integration of the responses to iron availability in Arabidopsis by the bHLH factor ILR3. New Phytol

Toledo-Ortiz G, Huq E, Quail PH (2003) The Arabidopsis basic/helix-loop-helix transcription factor family. The Plant Cell **15:** 1749-1770

Trofimov K, Ivanov R, Eutebach M, Acaroglu B, Mohr I, Bauer P, Brumbarova T (2019) Mobility and localization of the iron deficiency-induced transcription factor bHLH039 change in the presence of FIT. Plant Direct **3:** e00190

Tsai H-H, Rodriguez-Celma J, Lan P, Wu Y-C, Vélez-Bermúdez IC, Schmidt W (2018) Scopoletin 8-hydroxylase-mediated fraxetin production is crucial for iron mobilization. Plant physiology **177:** 194-207

Tsai HH, Schmidt W (2017) Mobilization of iron by plant-borne coumarins. Trends in plant science **22:** 538-548

Vert G, Grotz N, Dedaldechamp F, Gaymard F, Guerinot ML, Briat JF, Curie C (2002) IRT1, an Arabidopsis transporter essential for iron uptake from the soil and for plant growth. Plant Cell **14:** 1223-1233

Vert GA, Briat J-F, Curie C (2003) Dual regulation of the Arabidopsis high-affinity root iron uptake system by local and long-distance signals. Plant Physiology **132:** 796-804

Vigani G, Tarantino D, Murgia I (2013) Mitochondrial ferritin is a functional iron-storage protein in cucumber (Cucumis sativus) roots. Frontiers in plant science **4:** 316

Wang N, Cui Y, Liu Y, Fan H, Du J, Huang Z, Yuan Y, Wu H, Ling H-Q (2013) Requirement and functional redundancy of Ib subgroup bHLH proteins for iron deficiency responses and uptake in Arabidopsis thaliana. Molecular plant **6:** 503-513

Wang S, Li L, Ying Y, Wang J, Shao JF, Yamaji N, Whelan J, Ma JF, Shou H (2020) A transcription factor OsbHLH156 regulates Strategy II iron acquisition through localising IRO2 to the nucleus in rice. New Phytologist **225:** 1247-1260

Wedepohl KH (1995) The composition of the continental crust. Geochimica et cosmochimica Acta **59:** 1217-1232

Yuan Y, Wu H, Wang N, Li J, Zhao W, Du J, Wang D, Ling H-Q (2008) FIT interacts with AtbHLH38 and AtbHLH39 in regulating iron uptake gene expression for iron homeostasis in Arabidopsis. Cell research **18:** 385

Zamioudis C, Hanson J, Pieterse CM (2014) β-Glucosidase BGLU 42 is a MYB 72-dependent key regulator of rhizobacteria-induced systemic resistance and modulates iron deficiency responses in A rabidopsis roots. New Phytologist **204:** 368-379

Zhai Z, Gayomba SR, Jung H-i, Vimalakumari NK, Piñeros M, Craft E, Rutzke MA, Danku J, Lahner B, Punshon T (2014) OPT3 is a phloem-specific iron transporter that is essential for systemic iron signaling and redistribution of iron and cadmium in Arabidopsis. The Plant Cell **26:** 2249-2264

Zhang C (2014) Essential functions of iron-requiring proteins in DNA replication, repair and cell cycle control. Protein & cell **5:** 750-760

Zhang H, Li Y, Pu M, Xu P, Liang G, Yu D (2020) Oryza sativa POSITIVE REGULATOR OF IRON DEFICIENCY RESPONSE 2 (OsPRI2) and OsPRI3 are involved in the maintenance of Fe homeostasis. Plant, cell & environment **43:** 261-274

Zhang J, Liu B, Li M, Feng D, Jin H, Wang P, Liu J, Xiong F, Wang J, Wang H-B (2015) The bHLH transcription factor bHLH104 interacts with IAA-LEUCINE RESISTANT3 and modulates iron homeostasis in Arabidopsis. The Plant Cell **27:** 787-805

Zhang X, Zhang D, Sun W, Wang T (2019) The Adaptive Mechanism of Plants to Iron Deficiency via Iron Uptake, Transport, and Homeostasis. International journal of molecular sciences **20:** 2424

Zheng L, Ying Y, Wang L, Wang F, Whelan J, Shou H (2010) Identification of a novel iron regulated basic helix-loop-helix protein involved in Fe homeostasis in Oryza sativa. BMC plant biology **10:** 166

7 Manuscript 1

E3 ligases BTSL1 and BTSL2 interact with small protein FEP3 and bHLH transcription factors regulating iron deficiency responses in Arabidopsis roots

E3 Ligases BTSL1 and BTSL2 interact with small protein FEP3 and bHLH transcription factors regulating iron deficiency responses in Arabidopsis roots

Daniela M. Lichtblau [1,q], Birte Schwarz [1,q], Christopher Endres[1], Christin Sieberg[1], Petra Bauer[1,2,*]

[1]Institute of Botany, Heinrich Heine University, Düsseldorf 40225, Germany

[2]Cluster of Excellence on Plant Science (CEPLAS), Heinrich Heine University, Düsseldorf 40225, Germany

[q]These authors contributed equally

***Corresponding author:** Petra Bauer, petra.bauer@hhu.de

Funding: This work received funding from the German Research Foundation grant through the DFG International Research Training group 1525 to P.B. and from Germany's Excellence Strategy, EXC 2048/1, Project ID: 390686111.

Author contributions: D.M.L., B.S., C.E., and C.S. performed the experiments and analyzed the data; D.M.L., B.S., and P.B. designed the experiments and supervised the research; D.M.L., B.S., and P.B. conceived the project; B.S. wrote the original draft with contributions of D.M.L. and C.E.; D.M.L completely revised the original draft and extended it with new data. D.M.L., B.S., and P.B. reviewed/edited the article; P.B. acquired funding, agrees to serve as the author responsible for contact and ensures communication.

One sentence summary: A targeted protein-protein interaction screen uncovered novel protein interactions of E3 ligases BTSL1 and BTSL2 with bHLH proteins of subgroup IVc, PYE and with small protein FEP3/ IMA1 to regulate Arabidopsis iron deficiency responses.

Highlights:

- A targeted yeast two-hybrid screen reveals several novel protein-protein interactions with potential function in Arabidopsis Fe deficiency responses
- A regulatory protein interactome emerges containing E3 ligases BTS/BTSL1/BTSL2, bHLH TFs and the small peptide FEP3
- FEP3 acts as inhibitor of BTSL1/BTSL2, acting upstream of ILR3, bHLH104 and PYE

Keywords: Fe deficiency, protein interaction network, regulation, signaling, BTSL1/2, E3 ligase, peptide, bHLH, yeast two-hybrid, Arabidopsis.

Abbreviations:

3AT	3-amino-1,2,4-triazole
aa	Amino acid
AD	Activation domain
BD	Binding domain
bHLH	Basic helix-loop-helix
BiFC	Bimolecular fluorescence complementation
GFP	Green fluorescent protein
GUS	β-Glucuronidase
HHE	Hemerythrin/HHE cation-binding motif
mCherry	Second generation mRFP derivative
mRFP	Monomeric red fluorescent protein
OX	Over-expression
RT-qPCR	Reverse transcription quantitative PCR
SD	Standard deviation (Statistics) / Synthetic defined medium (Y2H)
TF	Transcription factor
WT	Wild type
Y2H	Yeast two-hybrid
YFP	Yellow fluorescent protein

Abstract

Iron (Fe) is an essential micronutrient for plants. Because excess Fe is cytotoxic, plants must carefully balance internal Fe levels. Complex regulatory mechanisms coordinate Fe homeostasis transcriptionally and post-transcriptionally. More than 500 genes are induced upon Fe deficiency in Arabidopsis (*Arabidopsis thaliana*) roots. Many of these genes are strongly co-regulated, but their interplay at the protein level is not well understood. To uncover novel functions and connections between Fe deficiency response proteins, a comprehensive yeast two-hybrid interaction screen was conducted. 24 proteins with either unknown function, putative Fe sensing or signaling function, or regulatory functions during Fe deficiency responses were tested. The screen resulted in the detection of 14 novel and four known interactions. Together they form a root-specific protein interaction network in which we identified BRUTUS-LIKE 1 (BTSL1) as a network hub. BTSL1 interacted with Fe uptake-regulating basic helix-loop-helix (bHLH) transcription factors of subgroup IVc (bHLH104, IAA-LEUCINE RESISTANT3 (ILR3)), with POPEYE (PYE), a key regulator of Fe distribution processes, as well as with small proteins. BTSL1 and its homologues BTS and BTSL2 interacted with some the same proteins. However, only the BTSLs interacted with PYE, indicating the presence of a BTSL specific function. BTS negatively controls Fe uptake by targeting ILR3 for degradation, thus BTSL1/2 presumably have similar functions. By testing several protein deletion mutants, we show that the small protein, FE UPTAKE-INDUCING PEPTIDE3 (FEP3), interacts with BTSL1 at a similar C-terminal region as ILR3 and bHLH104. FEP3 positively regulates Fe uptake. Transgenic Arabidopsis plants over-expressing *FEP3* mimicked the phenotype of *btsl1 btsl2* loss-of-function plants. Together, these results suggest that FEP3 inhibits BTSL protein function, possibly by preventing BTSL-bHLH interaction.

Introduction

In plants, iron (Fe) is a crucial component of chlorophyll synthesis (Tottey et al., 2003), as well as in photosynthetic and respiratory electron transport chains (Nouet et al., 2011). Fe deficiency stress negatively affects plant development and can result in yield loss. Although very abundant in the soil, Fe is often not readily accessible for plants, because at neutral or basic pH it precipitates as insoluble Fe^{3+} oxides (Lindsay, 1988; Wedepohl, 1995). Graminaceaous plants like rice extrude mugineic acids (MAs) as chelating compounds into the rhizosphere to solubilize Fe^{3+} and import Fe^{3+}-MA complexes into the root (Fe acquisition "Strategy II") (Marschner and Römheld, 1994). Non-graminaceaous monocots and dicots, like Arabidopsis, solubilize soil Fe by lowering the local pH through proton extrusion, accompanied by the release of coumarins as chelating compounds. Fe^{3+} is then reduced and imported into the root as Fe^{2+} ("Strategy I") (Marschner and Römheld, 1994; Schmid et al., 2014). Because of its reactivity, free internal Fe^{2+} has to be avoided. Therefore, once it has entered the symplast, Fe is rapidly chelated and transported to local and distant sinks, or sequestered (von Wirén et al., 1999; Hell and Stephan, 2003; Briat et al., 2007; Schuler et al., 2012; Curie and Mari, 2017). To ensure sufficient Fe supply while avoiding cellular Fe content rising to toxic levels, plants need to carefully balance Fe homeostasis. This includes Fe status sensing, signaling of Fe demand, and regulation of internal Fe redistribution and uptake of external Fe. The need to orchestrate different processes is reflected in a complex transcriptomic network of co-regulated genes encoding several transporters, enzymes and transcription factors (TFs) (Ivanov et al., 2012).

In Strategy II, as well as Strategy I, a number of basic helix-loop-helix (bHLH) TFs regulate Fe uptake and distribution genes in the roots (Gao et al., 2019). In Arabidopsis (*Arabidopsis thaliana*), FER-LIKE IRON DEFICIENCY INDUCED TRANSCRIPTION FACTOR (FIT) controls a set of genes co-expressed in roots and acting in Fe acquisition (Colangelo and Guerinot, 2004; Jakoby et al., 2004; Bauer et al., 2007; Sivitz et al., 2012; Mai et al., 2016). Among them for example, *FERRIC REDUCTION OXIDASE2* (*FRO2*), which reduces Fe^{3+} to Fe^{2+} (Robinson et al., 1999), and *IRON-REGULATED TRANSPORTER1* (*IRT1*), which imports Fe^{2+} (Eide et al., 1996; Vert et al., 2002). FIT exerts its function upon heterodimerization with bHLH TFs from group Ib (bHLH38/39/100/101) (Heim et al., 2003; Yuan et al., 2008; Wang et al., 2013). Ib *BHLHs* are transcriptionally induced by bHLH TFs from group IVc (bHLH34/104/105/115) (Zhang et al., 2015; Liang et al., 2017). IVc bHLH TFs have redundant functions and act in a synergistic manner (Li et al., 2016; Liang et al., 2017). bHLH34/104/115 also induce transcription of *POPEYE* (*PYE*) (Zhang et al., 2015; Liang et al., 2017), a group IVb bHLH TF which is considered a direct negative regulator of Fe distribution genes *NICOTIANAMINE SYNTHASE4* (*NAS4*), *FRO3* and *ZINC-INDUCED FACILITATOR1* (*ZIF1*) (Long et al., 2010). IVc bHLH TFs additionally form heterodimers with the bHLH TF UPSTREAM REGULATOR OF IRT1 (URI) belonging to subgroup IVb to activate various Fe responsive genes, including *PYE* and *BHLH* Ib TFs (Gao et al., 2019; Kim et al., 2019). The third member of the IVb bHLH TF family

bHLH11, in contrast, acts as a negative regulator of the Fe uptake machinery (Tanabe et al., 2019; Li et al., 2020).

IVc bHLH protein levels are likely controlled through proteasomal degradation. bHLH105 (ILR3 (IAA-LEUCINE RESISTANT3)) and bHLH115 are targeted by BRUTUS (BTS), an Fe deficiency-induced E3 ligase and negative regulator of Fe uptake (Selote et al., 2015; Matthiadis and Long, 2016). This somewhat paradox situation of *BTS* up-regulation under Fe deficiency, when the protein in turn negatively regulates Fe uptake, was explained by the need to have a rapid shut-down mechanism of Fe uptake (Hindt et al., 2017). Another hypothesis is that BTS ensures a constant turnover of "fresh" IVc bHLH proteins (Selote et al., 2015), a mechanism known from FIT protein activity (Sivitz et al., 2011). BTS, IVc bHLHs, Ib bHLHs and PYE have orthologous counterparts in rice (Kobayashi et al., 2018), indicating that the general mechanism is conserved in both Fe acquisition Strategy I and Strategy II.

Interestingly, BTS´s unique domain composition indicates that it might have Fe sensing functions. BTS has a C-terminal REALLY INTERESTING NEW GENE (RING) domain with E3 ligase activity and N-terminal hemerythrin/HHE cation-binding motif (HHE) domains which can bind Fe^{2+} (Kobayashi et al., 2013; Selote et al., 2015; Matthiadis and Long, 2016). This structure resembles the mammalian Fe sensing E3 ligase complex (Kobayashi et al., 2013), which has the subunit FBXL5, that is stabilized when Fe^{2+} is bound to its HHE domain (Salahudeen et al., 2009). Indeed, BTS protein stability and function was also shown to be directly linked to Fe presence or absence (Selote et al., 2015). Two BTS homologs, BTS-LIKE1 (BTSL1) and BTSL2, have been recently identified and also found to regulate Fe uptake in a negative manner (Hindt et al., 2017). BTS, BTSL1 and BTSL2 have partly redundant functions, but only *BTS* is expressed in roots and shoots, while *BTSL1/2* are root-specific (Hindt et al., 2017). It is assumed that BTSL1/2 work in a similar manner as BTS, but the proteins are not functionally characterized as of yet. However, the BTS orthologues in rice OsHRZ have been shown to control Arabidopsis IVc orthologues (OsbHLH57/58/59/60) in a similar manner as BTS (Kobayashi, 2019).

The root Fe uptake machinery responds to local and systemic Fe deficiency signaling (Vert et al., 2003; Kumar et al., 2017), however, the (chemical) nature of the signals is still unknown. Hormones and small molecules modulate Fe acquisition (Brumbarova et al., 2015), but their activating effect can be overruled by phloem Fe content. Sufficient phloem Fe in shoots seems to be a key factor for the repression of root Fe uptake (Garcia et al., 2013 and references therein; Zhai et al., 2014; Khan et al., 2018). That the shoot vasculature is important for root Fe deficiency responses, implies phloem-localized shoot-to-root signaling (García et al., 2018 and references therein). Recently, phloem-located small peptides conserved in angiosperms, have been suggested as mobile signals that activate root Fe deficiency responses (termed FE UPTAKE-INDUCING PEPTIDE (FEP) or IRON MAN (IMA)) (Grillet et al., 2018; Hirayama et al., 2018). Small peptides in nutrient-related signaling are best described in nitrogen deprivation responses, in which two polypeptides are phloem-mobile shoot-to-root signals that induce

the expression of a root nitrate transporter (Tabata et al., 2014; Ohkubo et al., 2017). Regarding Fe signaling, it is currently unclear if FEPs themselves are a shoot-to-root signal, or if they trigger another kind of mobile signal which ultimately leads to up-regulation of Fe acquisition genes.

In view of the number of Fe deficiency-co-regulated genes in just the roots alone - surprisingly little is known about their interplay at the protein level. This work aims to uncover yet unknown functions and connections between proteins, to improve our mechanistic understanding of Fe deficiency response regulation in Arabidopsis roots.

A comprehensive targeted yeast two-hybrid (Y2H) screen with a set of 24 selected proteins was conducted. Most study candidates were co-expressed under Fe deficiency, and had either unknown functions or a likely function in Fe sensing or signaling, such as BTS, BTSL1 and FEP3. Important transcriptional regulators, such as FIT, bHLH39, PYE and IVc bHLHs were also included. As a result we discovered a protein interaction network, with several novel interactions that deserve thorough follow-up experiments. Here, the focus was on the "BTS(L) interactome", a part of the protein network which connects BTS, BTSL1 and BTSL2 with individual sets of bHLH TFs, and FEP3 (**Figure 1**: highlighted in green). Our work shed light on the multilayered Fe deficiency response regulation and led to the discovery of new players. An emerging mechanism is discussed in which FEP3 inhibits BTSL1/2 E3 ligase activity, thereby de-repressing downstream Fe deficiency responses.

Results

Identifying novel protein-protein interactions in a targeted yeast two-hybrid screen

Because transcriptional co-regulation in many cases has turned out to be a good indicator for protein-protein interaction, we updated the root Fe deficiency co-expression network (based on (Ivanov et al., 2012) and the ATTED-II database (Aoki et al., 2016)). Co-expression networks can be used to study subsets of Fe regulated genes also often linked on protein level (Schwarz and Bauer, 2020). BTS, for example, interacts with ILR3 and bHLH104 (Long et al., 2010; Selote, 2015). All of them belong to the same co-expression cluster. Thus, co-expression networks were used to select candidates for a comprehensive targeted protein-protein interaction screen (**Supplemental Figure S1A**). In the selection process, the focus was on proteins with possible connection to regulation or signaling. Since it is not yet known how exactly Fe deficiency is signaled, criteria for candidates were (i) unknown functions during Fe deficiency responses (at the time the study was initiated; UP1-4, KELCH, S8H, DUF506, FEP3, DGAT3, BTSL1, ORG1, SDI1) and (ii) regulatory functions of Fe homeostasis (TFs: FIT, bHLH39, MYB72, PYE, ILR3, bHLH104; E3 ligase: BTS; 14-3-3 protein: GRF11; enzymes: NAS2, NAS4 (Jakoby et al., 2004; Yuan et al., 2008; Klatte et al., 2009; Long et al., 2010; Palmer et al., 2013; Yang et al., 2013; Selote et al., 2015; Zhang et al., 2015)). In addition, PRS2 and JAL12 were included, because at the time this study was initiated they were suspected to be FIT-dependent, whereas to date they

are no longer considered to be FIT-targets. Known or predicted integral membrane proteins (e.g. transporters) were excluded due to difficulties of investigating such proteins with standard Y2H assays. All 24 candidates are listed in **Table 1**.

Table 1. List of candidates tested in the Y2H screen.

AGI	Short name	Description
FIT-dependent [1, 2]		
AT2G2816	FIT	FER-LIKE IRON DEFICIENCY INDUCED TRANSCRIPTION FACTOR, bHLH29
AT1G34760	GRF11	GENERAL REGULATORY FACTOR 11, 14-3-3 protein
AT1G73120	UP1	unknown protein (109 aa), named OLIVIA in the second study of this thesis
AT3G06890	UP2	unknown protein (128 aa)
AT3G07720	KELCH	galactose oxidase/kelch repeat superfamily protein
AT3G12900	S8H	SCOPOLETIN 8- HYDROXYLASE
AT5G56080	NAS2	NICOTIANAMINE SYNTASE2
FIT-independent [2]		
AT1G12030	DUF506	DOMAIN OF UNKNOWN FUNCTION506
AT1G47400	FEP3	FE-UPTAKE-INDUCING PEPTIDE3, IRONMAN1 (IMA1) (50 aa)
AT1G48300	DGAT3	DIACYLGLYCEROL ACYLTRANSFERASE3, 2Fe-2S cluster protein
AT1G56430	NAS4	NICOTIANAMINE SYNTHASE4
AT1G74770	BTSL1	BRUTUS-LIKE1, RING E3 ligase
AT3G18290	BTS	BRUTUS, RING E3 ligase
AT3G47640	PYE	POPEYE, bHLH TF
AT3G56360	UP3	unknown protein (233 aa)
AT3G56980	bHLH39	bHLH TF
AT5G05250	UP4	unknown protein (239 aa)
AT5G53450	ORG1	OBP3-RESPONSIVE GENE1, predicted protein kinase activity
AT5G48850	SDI1	SULPHUR DEFICIENCY-INDUCED1
Other not co-expressed TFs regulating Fe deficiency responses and other not co-expressed candidates*		
AT3G20770	EIN3	ETHYLENE-INSENSITIVE3
AT4G14410	bHLH104	bHLH TF
AT5G54680	ILR3	IAA-LEUCINE RESISTANT3, bHLH105
AT1G56160	MYB72	MYB TF
AT5G59820	ZAT12	ZINC FINGER OF ARABIDOPSIS THALIANA12
AT1G32380	PRS2	PHOSPHORIBOSYL PYROPHOSPHATE SYNTHASE2
AT1G52120	JAL12	PHOSPHORIBOSYL PYROPHOSPHATE SYNTHASE2

[1](Colangelo and Guerinot, 2004); [2](Mai et al., 2016); *Not co-expressed with the other Fe deficiency response genes (**Supplemental Figure S1**). Short name and description according to The Arabidopsis Information Resource (TAIR), 10.0 genome release. If no short name available, we provided a shortened description version.

Using the Y2H system, all 24 candidates were systematically tested against each other, including themselves (referred to as the "Y2H screen" in this work). Protein pairs were tested reciprocally to capture a majority of interactions (total: 576 tests). To efficiently assay all protein pairs, we transformed bait and prey constructs separately and combined them by yeast mating. Around 6% of all tested interactions were positive (**Supplemental Figure S1B**). Among them, expected/ published interactions were observed (FIT+bHLH39, BTS+ILR3, BTS+bHLH104, PYE+ILR3, ILR3+ILR3) and demonstrated that the targeted Y2H screen worked in general (Yuan et al., 2008; Long et al., 2010; Selote et al., 2015). In addition, 14 novel protein-heterodimer interactions and five homodimers were

found. 11 of the 14 interactions involved BTSL1 or PYE: BTSL1 interacted with PYE, ILR3, MYB72, DUF506, SDI1, PRS2, FEP3 and UP3. Besides with BTSL1, PYE interacted with UP1, UP3 and SDI1. Thus, BTSL1 and PYE emerged as interaction hubs in this Y2H screen (**Figure 1**).

BTS, BTSL1, and BTSL2 interact with individual sets of bHLH TFs and a small peptide

BTS and BTSL1 both interacted with ILR3, but only BTSL1 interacted with PYE. Furthermore, BTSL1 (but not BTS) interacted with the putative mobile peptide FEP3. To validate the results of the Y2H screen, and to test to what extent BTS and BTSL1 have similar interaction partners, a targeted Y2H assays using co-transformation of two potential interactors was conducted. Here, bHLH TFs of subgroup IVc (ILR3, bHLH104), PYE and FEP3 were included. The targeted Y2H assay also included BTSL2, which was not considered in the initial Y2H screen because it did not appear in the Fe deficiency response network by the time the experiments were initialized. Because full-length BD-bHLH104 fusion protein was auto-activating the Y2H system (**Supplemental Figure S3D**), the C-terminal interacting part was cloned and bHLH104-C used for all further experiments (**Supplemental Figure S4A**). The results confirmed that BTS and BTSL1 both interact with ILR3, as well as with bHLH104-C, but BTSL2 did not interact with ILR3. Interestingly, both BTSL1 and BTSL2, but not BTS, interacted with PYE and FEP3 (**Supplemental Figure S4B**). BTS, BTSL1 and BTSL2 did not interact with each other (**Supplemental Figure S4D**), but could interact with themselves in the Y2H screen (BTSL2 not tested). Taken together, BTS, BTSL1 and BTSL2 have partly the same and partly different interaction partners. Together with ILR3, bHLH104, PYE and FEP3, they form a highly interconnected part of the protein interaction network, referred to as the “BTS(L) interactome”, which is subject of the research described in the section below (**Figure 1**).

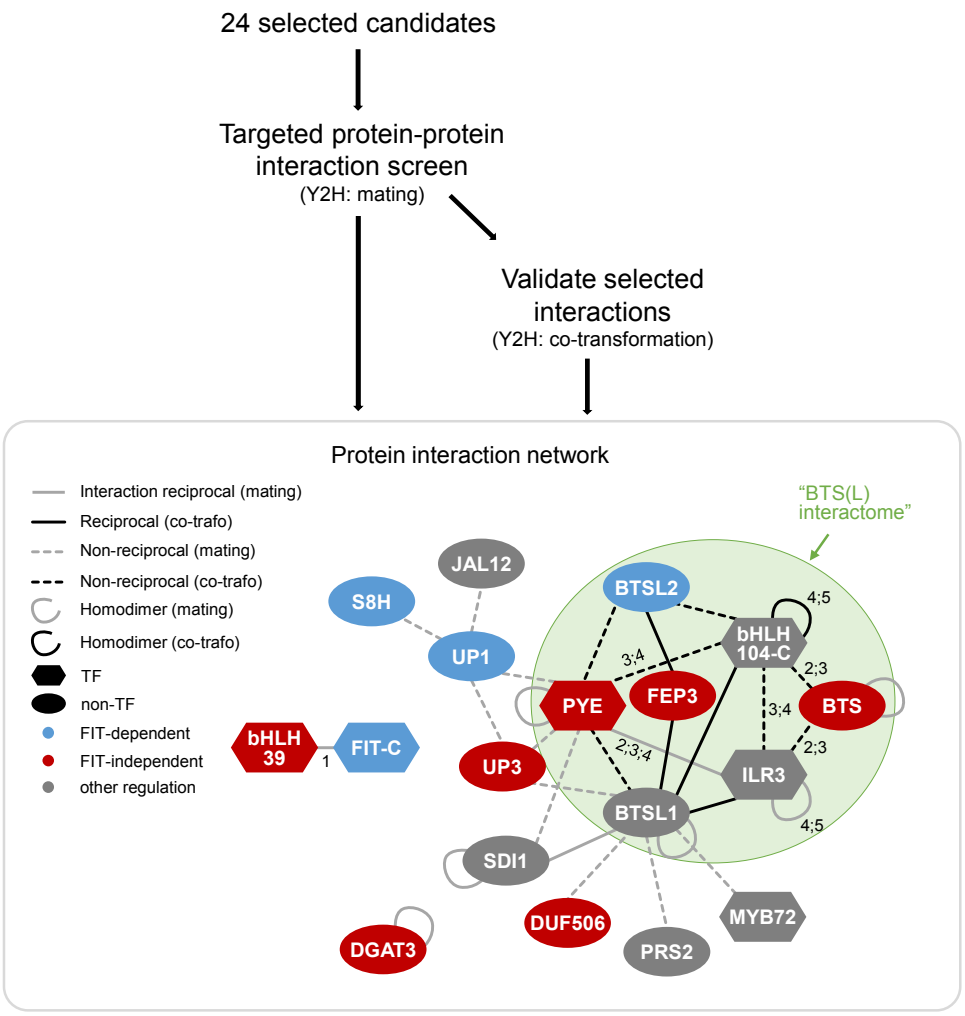

Figure 1. Workflow and protein interaction network based on Y2H data.
Each candidate was tested against all 24 (including itself; total 576 tests). The protein interaction network summarizes all new and known interactions identified with the initial Y2H screen. Seven candidates did not interact with any of the other proteins (GRF11, UP2, UP4, KELCH, NAS2, NAS4 and ORG1). Interactions within the "BTS(L) interactome" (BTS, BTSL1, BTSL2, ILR3, bHLH104, PYE, FEP3) were validated by another round of Y2H experiments, in which yeast was co-transformed with bait and prey ("co-trafo"). BTSL2 was not part of the initial Y2H screen, and tested only against the proteins of the BTS(L) interactome, FIT and bHLH39. BTSL2 was not tested against any of the other proteins or against itself. Solid lines indicate interactions that occurred reciprocally and are more trustworthy than non-reciprocal interactions which are indicated in dashed lines. FIT-dependent genes are marked in blue, FIT-independent in red and other regulation in gray. The 24 candidates are listed in **Table 1**. Overview matrix of Y2H screen interactions and non-interactions: **Supplemental Figure S1B**. Original data of the Y2H screen: **Supplemental Figures 2, 3**. Original data of validated selected interactions and non-interactions: **Supplemental Figures 4, 5**. Literature of known interactions: [1](Yuan et al., 2008); [2](Long et al., 2010); [3](Selote et al., 2015); [4](Zhang et al., 2015); [5](Li et al., 2016), (Schwarz and Bauer, 2020) for classification of FIT-dependent and FIT-independent genes.

Next, it needed to be shown that these proteins also interact in plants. Using bimolecular fluorescence complementation (BiFC) only the interaction between BTSL1 and PYE was detected (**Figure 2C(1)**), but not those between BTSL1 and ILR3, bHLH104 or FEP3, or any of the BTSL2 interactions. One possible explanation is that full-length BTS and BTSL proteins are unstable (Selote et al., 2015; Rodriguez-Celma et al., 2019) and therefore, BTSL1-C was used (C-terminal part of BTSL1; **Figure 2A**). Through Y2H experiments, we showed that BTSL1-C contained the domain needed for the protein-protein interactions (**Figure 2B**), as has been reported for other protein interaction studies

examining BTS (Selote et al., 2015). After switching to BTSL1-C in BiFC experiments the interaction with PYE was still detected, and in addition the interaction with ILR3 (**Figure 2C(2, 3)**), but still none of the other interactions which involve either BTSL1 or BTSL2 were found (negative BiFC data not shown). Interestingly, it was observed that full-length BTSL1 interacted with PYE outside the nucleus, whereas BTSL1-C interacted with PYE and with ILR3 inside the nucleus. As a negative control BTSL1 together with FIT was used. This protein combination was also negative in the Y2H assay. However, surprisingly, other research recently reported that BTSL1 and FIT were shown to be interactors (Rodríguez-Celma et al., 2019). This was never the case in this study.

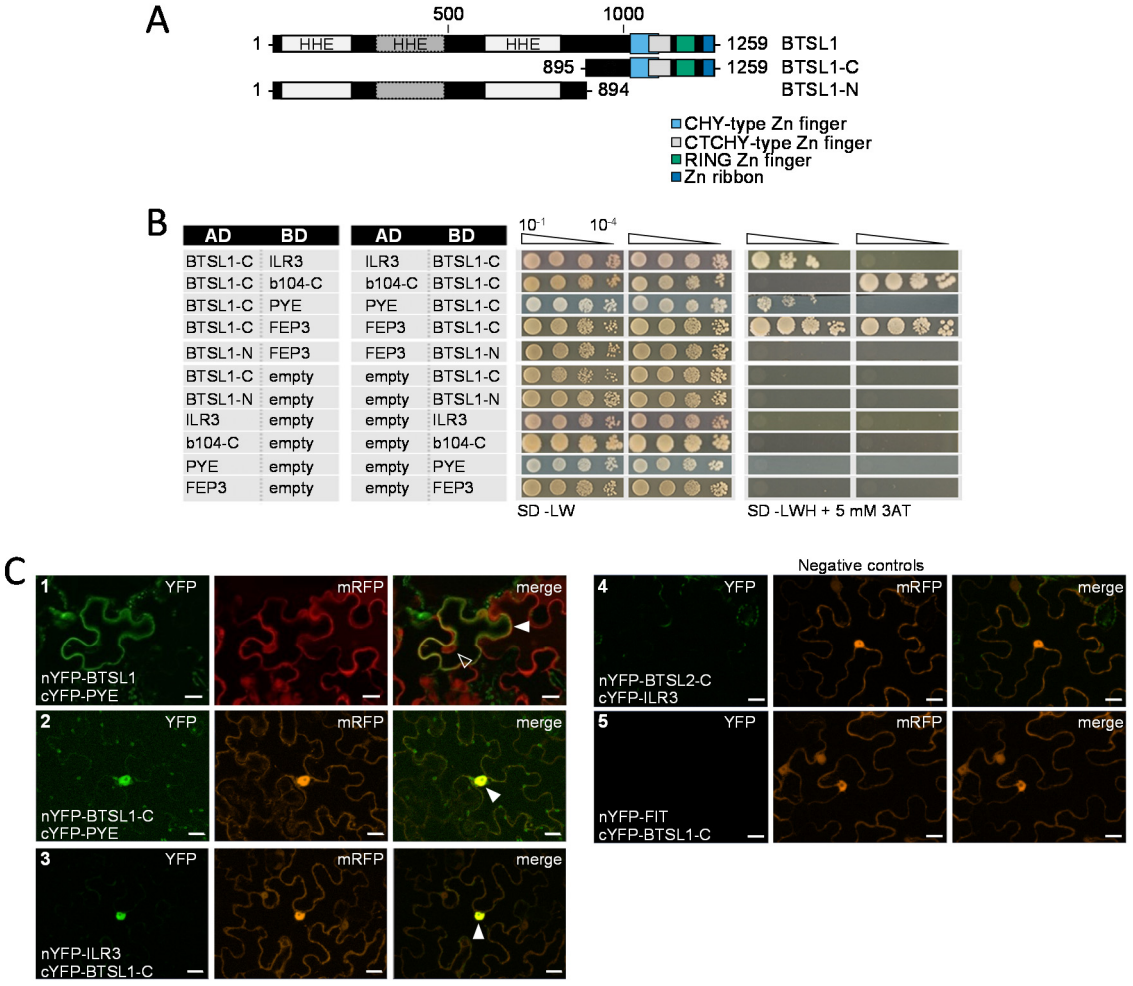

Figure 2. The BTSL1 C-terminus is sufficient for interaction with ILR3, bHLH104-C, PYE and FEP3, and can be used to validate interactions *in planta*.

A: Schematic representation of full-length BTSL1 and the truncated versions BTSL1-C (C-terminal part) and BTSL1-N (N-terminal part). Domain predictions according to (Rodriguez-Celma et al., 2019) (Hemerythrin/HHE cation binding motifs), and InterPro (www.ebi.ac.uk/interpro; C-terminal domains). **B:** Reciprocal targeted Y2H protein interaction assay between BTSL1-C and ILR3, bHLH104-C (C-terminal part of bHLH104; b104-C), PYE, FEP3, and between BTSL1-N and FEP3. Protein pairs were fused to the GAL4 DNA-binding domain (BD) and the GAL4 activation domain (AD), and vice-versa.Yeast co-transformed with the AD and BD combinations were spotted in 10-fold dilution series (A_{600}=10^{-1}-10^{-4})on SD-LW (transformation control) and on SD-LWH supplemented with 5 mM 3AT (selection for protein interaction). Negative controls: empty AD with BD-proteins and empty BD with AD-proteins. **C:** BiFC experiments showing interactions between full-length nYFP-BTSL1 and cYFP-PYE (1), nYFP-BTSL1-C and cYFP-PYE (2), cYFP-BTSL1-C and nYFP-ILR3 (3) in transiently transformed tobacco leaf epidermis cells. Transformation control: mRFP. Non-interacting related proteins were chosen as negative controls: nYFP-BTSL2-C + cYFP-ILR3 (4) for BTSL1-C + ILR3; n-YFP-FIT + cYFP-BTSL1-C (5) for ILR3/PYE + BTSL1-C. The localization shift in (2) compared to (1) additionally validates specificity of BTSL1 + PYE and BTSL1-C + PYE signals. The YFP and mRFP signals were imaged with a fluorescence microscope and an ApoTome for enhanced resolution. Scale bars: 20 µm.

In summary, using Y2H and BiFC, novel protein-protein interactions between several Fe deficiency response proteins were detected. The interactions involving different small proteins (UP1, UP3, FEP3) are of particular interest, especially with regard to Fe deficiency signaling. With the observation of FEP3 being able to specifically interact with BTSL1/2, a novel connection between a small peptide and putative E3 ligases was uncovered. In addition, BTSL1/2 interacted with different bHLH TFs of subgroup IVc and with PYE, which could partially be validated *in planta*. The following part of this article focusses on BTSL1 and BTSL2, and their interactions with FEP3, IVc bHLHs TFs and PYE.

ILR3, bHLH104-C and FEP3 interact with a similar C-terminal region of BTSL1

As shown above, BTSL-C is sufficient for interaction with FEP3, ILR3 and bHLH104-C. BTSL-C lacks the Fe^{2+}-binding HHE domains, but has predicted CHY- and CTCHY-type zinc (Zn) finger domains, a Zn ribbon domain and a RING domain (Kobayashi et al., 2013; Rodriguez-Celma et al., 2019), with putative E3 ligase function (Freemont, 2000; Selote et al., 2015). It was suggested that BTS interacts with its degradation targets ILR3 and bHLH115 via the RING domain (Selote et al., 2015). Y2H was applied to investigate which of the C-terminal domains of BTSL1 interacts with ILR3, bHLH104-C and FEP3. Four BTSL1-C sub-fragments were cloned to allow assessment of each of the domains individually (**Figure 3A, B**).

BTSL1-C.2, which has CHY and CTCHY domains, but lacks the predicted RING domain and the Zn ribbon domain, interacted with ILR3, bHLH104-C and FEP3. This indicates that BTSL1 RING and Zn ribbon are not needed for this interaction. However, the interacting domain must be located close to RING, since a slightly shorter sub-fragment (BTSL1-C.1), lacking the RING-adjacent CTCHY, was no longer able to interact with any of the proteins. Interestingly, CTCHY was also not needed for FEP3 interaction, since BTSL1-C.4 interacted with FEP3. All three deletion constructs interacting with FEP3 (BTSL1-C.2, C.3 and C.4) have one common region of 14 amino acids (aa) (here named M-C site), located between CTCHY and RING (**Figure 3C**, yellow box). In case of ILR3 and bHLH104-C, results were less clear. For interaction with ILR3, CTCHY might also be important (**Figure 3A, B**).

Because BTSL2 and BTS did not interact with ILR3 and FEP3, respectively, we looked for differences in the proposed interacting region of BTSL1. It was found that BTSL1´s region "RTLVEH" containing the evolutionary conserved R and L residues, was different than both the regions of BTSL2 ("RLIVEH") and BTS ("MKLVNH"). We focused on this part of the 14-aa region (named M-C site) because we initially had reason to believe that FEP3 only interacted with BTSL1 and neither BTSL2 nor BTS. Consistent with our later findings that FEP3 interacted with both BTSLs, deleting RTLVEH in BTSL1 (BTSL1-dRH) only slightly reduced interaction with FEP3 (**Figure 3D, F**). Substituting RTLVEH with a sextuple G residue spacer (BTSL1-6G) fully restored the interaction with FEP3. Possibly, the evolutionary conserved aa adjacent to RTLVEH are more important for interaction with FEP3 (**Figure**

3C). However, to our surprise, ILR3 and bHLH104-C could no longer interact with BTSL1-dRH. ILR3 did also not interact with BTSL1-6G, and interaction of bHLH104-C with BTSL1-6G was severely reduced (**Figure 3D, F**). Because FEP3 was still able to interact with BTSL1-dRH the complete MC site was deleted. Interestingly, BTSL1-dMC did not interact with FEP3, indicating that different aa than RTLVEH in the M-C site are involved in the interaction of BTSL1 and FEP3 and that therefore FEP3 interacts at a close, but separate position of BTSL1 than ILR3/ bHLH104-C (**Figure 3E, F**).

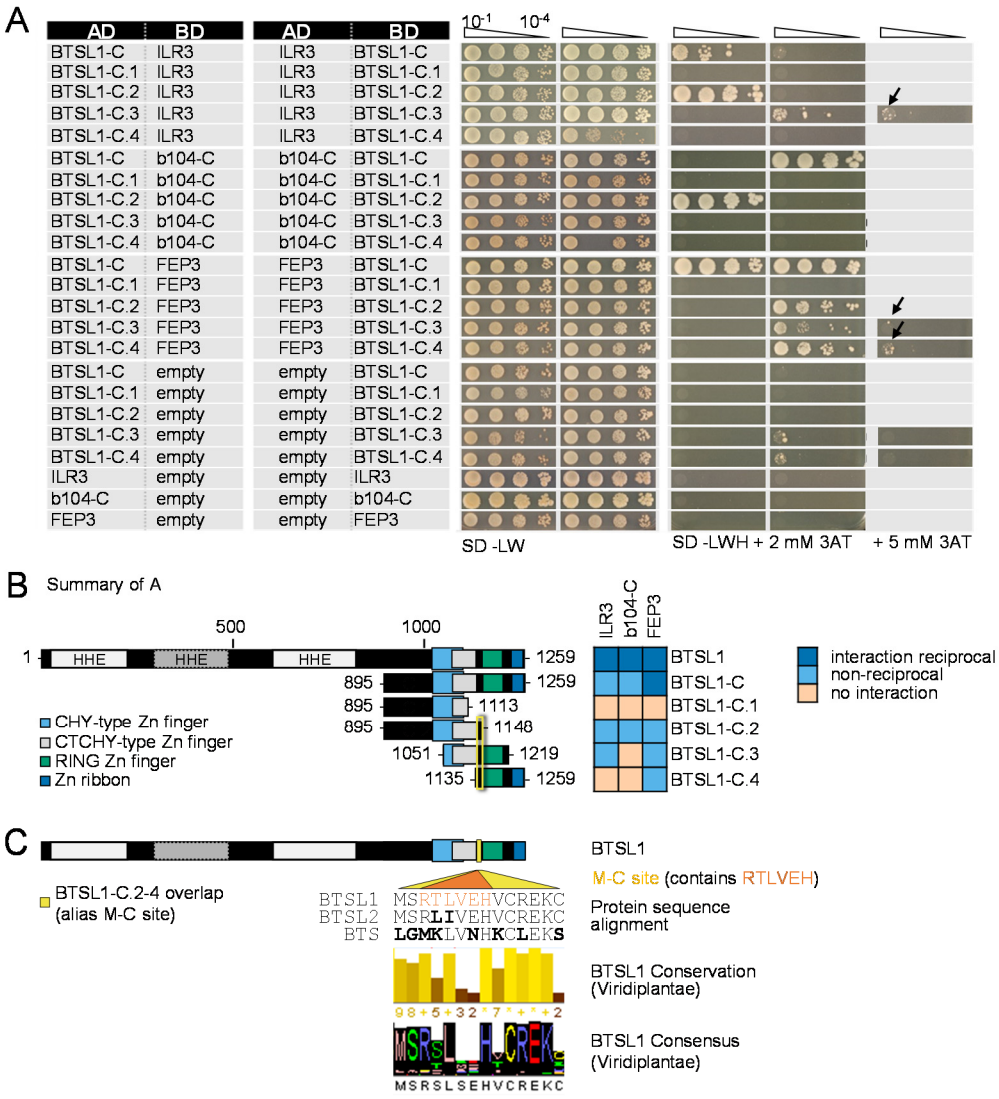

(Figure 3 continued on next page)

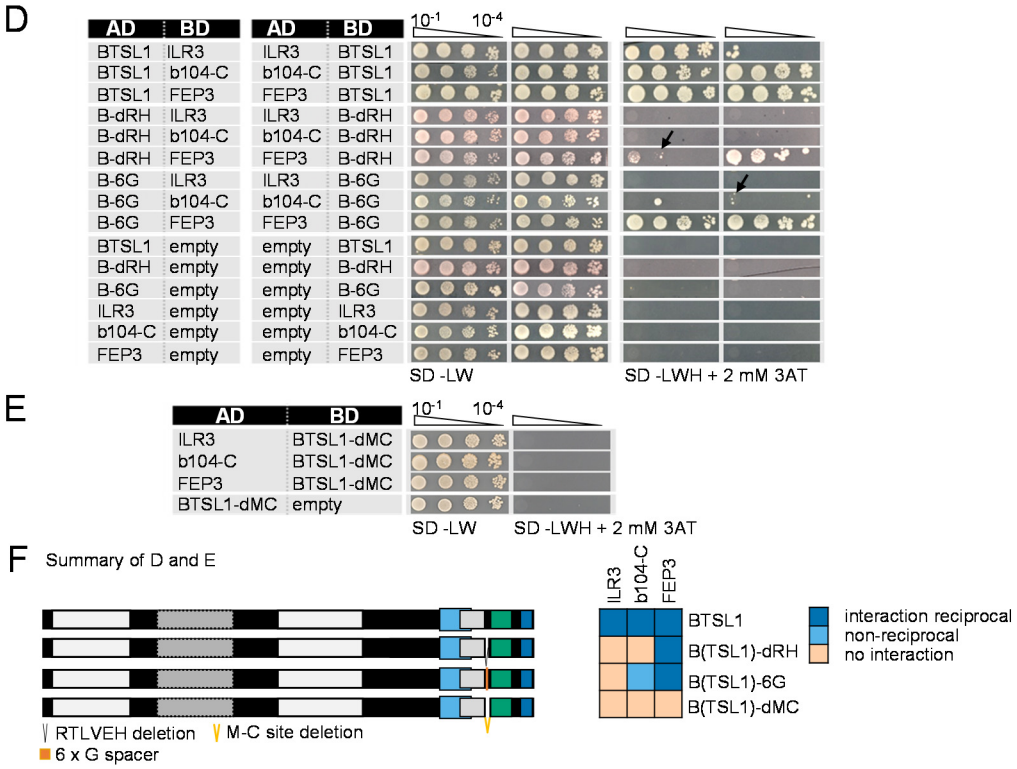

Figure 3. Determining the region in BTSL1 which mediates protein-protein interactions.
A: Reciprocal targeted Y2H protein interaction assay of BTSL1-C and its four sub-fractions (BTSL1-C.1, BTSL1-C.2, BTSL1-C.3, BTSL1-C.4) with ILR3, bHLH104-C (b104-C), PYE, FEP3. Yeast co-transformed with AD and BD combinations were spotted as described in Figure 2. Arrows indicate interaction. **B:** Schematic representation of full-length BTSL1 protein, BTSL1-C and the four sub-fragments of BTSL1-C. Heatmap summarizes the results of A. Sub-fragments interacting with FEP3 (BTSL1-C.2, C.3 and C.4) have one common region (yellow box). **C:** Magnification of the yellow box and alignment of its 14 aa (M-Csite) with BTSL2 and BTS. Bold: aa in BTSL2 and BTS that are different to BTSL1. "RTLVEH" (orange): contains aa that are different between BTSL1 and BTSL2 and between all three proteins (bold letters). "RTLVEH" was chosen for deletion/substitution (see below). Conservation scores of the aa and consensus correspond to a BTSL1 BLAST against the Viridiplantae data base. **D:** Interactions of full-length and deletion forms of BTSL1 with ILR3, bHLH104-C, FEP3. Yeast were co-transformed with full-length BTSL1, a BTSL1 deletion construct lacking RTLVEH (B-dRH), or a BTSL1 deletion-substitution construct in which RTLVEH was substituted with a sextuple glycine spacer (B-6G) in combination with either ILR3, bHLH104-C or FEP3 and spotted as described in Figure 2. Arrows indicate interaction. The single AD-B-6G + BD-b104-C yeast colony growing at A=10^{-2} was not interpreted as reliable interaction. **E:** Y2H interactions of BTSL1-dMC with ILR3, bHLH104-C and FEP3. **F:** Schematic representation of full-length BTSL1, B-dRH,B-6G and BTSL1-dMC proteins. Heatmap summarizes the results of D and E. Full alignment of BTSL1, BTSL2, BTS: **Supplemental Figure S6**.

In summary, the 14-aa M-C site located close to the BTSL1 E3 RING domain which is needed for interaction with FEP3, and possibly also with ILR3 and bHLH104-C was identified. Within this region, RTLVEH is potentially important for interaction with ILR3 and bHLH104-C, but not with FEP3. This indicates that FEP3 and the IVc bHLHs do not bind to the same residues in BTSL1, but to a similar region. However, it should be noted that we cannot rule out that deleting or substituting RTLVEH affects BTSL1 protein folding in a way that only the small FEP3, but not ILR3 or bHLH104-C are able to bind.

FEP3 C-terminal residues are conserved and needed for interaction

Next, it was investigated which domains of FEP3 are important for protein-protein interactions. A BLAST search of the FEP3 protein sequence revealed a single domain consisting of the final 17 aa at the C-terminus (**Supplemental Figure S7**), consistent with findings of (Grillet et al., 2018). This domain

is conserved in dicots as well as monocots with Strategy II Fe acquisition, such as rice, wheat and maize. The N-terminal and a C-terminal half of FEP3 were cloned (termed FEP3-N and FEP3-C, respectively) and not surprisingly, FEP3-C was determined to be the interacting part (**Figure 4A**). Next, two truncated FEP3 versions either lacking the whole conserved domain (FEP3-d17) or lacking the last seven aa (FEP3-d7) were tested (**Figure 4B**). Neither of the two constructs interacted with BTSL1, showing that the last seven aa in FEP3 ("YDYAPAA") are crucial for FEP3 interactions. There is definitely a aa sequence similarity between YDYAPAA and the C-terminus of IVc bHLHs (**Supplemental Figure S8**). As a matter of fact, bHLH104 and FEP3 peptide sequences both end with "PAA". In comparison, Ib bHLH protein C-termini did not align with FEP3 YDYAPAA (data not shown). Therefore, we hypothesized that FEP3 might mimic IVc bHLHs during interaction with BTSL1/2.

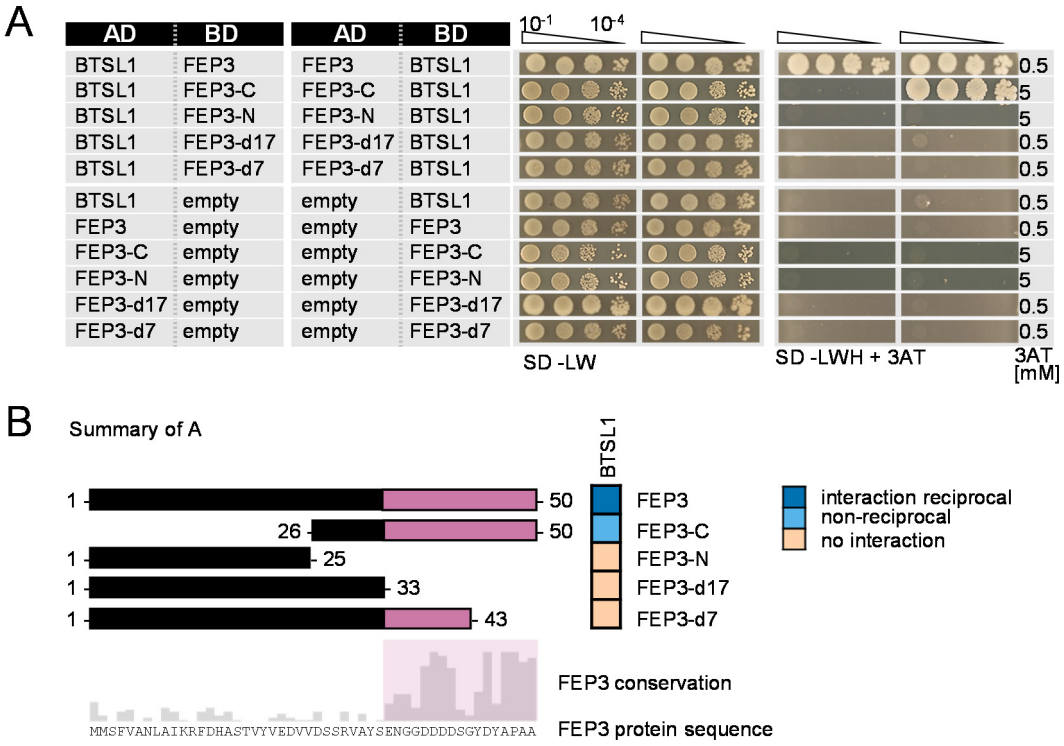

Figure 4. Determining the region in FEP3 needed for protein-protein interaction.
A: Reciprocal targeted Y2H protein interaction assay of full-length FEP3 or four truncated FEP3 versions with BTSL1. Yeast were co-transformed with AD-BTSL1 or BD-BTSL1 combined with BD or AD of FEP3, the C-terminal half of FEP3 (FEP3-C), the N-terminal counterpart (FEP3-N), a version lacking the last 17 aa (FEP3-d17), a version lacking the last 7 aa (FEP3-d7). Yeast were spotted as described in Figure 2. **B:** Schematic representation of FEP3 full-length and truncated versions. The protein sequence and aa conservation in angiosperms is indicated. Heatmap summarizes results of A. Full alignment of FEP3 angiosperm BLAST search results and consensus plot: **Supplemental Figure S7**.

Because bHLH104-C was used in all Y2H experiments, it was already known that the C-terminal part of bHLH104 is sufficient for interaction with BTSL1, BTSL2 and BTS. To test, if the interacting sites lie in the last 25 aa (aligning with FEP3 YDYAPAA), the following constructs were cloned: ILR3-d25 and bHLH104-C-d25 (lacking the last 25 aa) as well as their counterparts ILR3-CC and bHLH104-CC (only the last 25 aa; **Supplemental Figure S9**). Results of the Y2H screen aimed at determining ILR3 and bHLH104 interaction sites were inconclusive, possibly due to limitations of the Y2H method. Other methods

geared to uncover the three dimensional crystal structure of the protein are required to analyze the interaction sites. However, ILR3-d25 and bHLH104-C-d25 still interacted with BTSL1/2 (**Supplemental Figure S9**). Therefore it can be concluded that the C-terminal ends of ILR3 and bHLH104 are not required for interaction, despite their resemblance to FEP3. These results do not support the idea that FEP3 mimics bHLH IVc proteins.

FEP3 and BTSL1/2 are both upstream regulators of Fe deficiency responses and act in an opposite manner

FEP3 is a positive regulator of Fe uptake and a potential mobile signal (Grillet et al., 2018). However, the mechanism by which FEP3 acts is unknown. BTSL1 and BTSL2 are negative regulators of Fe uptake and suspected Fe sensors (Hindt et al., 2017). Because FEP3 physically interacted with BTSL1 and BTSL2, we hypothesized that FEP3 inhibits their function. To investigate this, transgenic Arabidopsis plants over-expressing *FEP3* (FEP3-OX) were compared to *btsl1 btsl2* loss-of-function mutants.

Two independent FEP3-OX lines (FEP3-OX#1, FEP3-OX#3) were generated. Their strong over-expression of *FEP3* in seedlings and roots under Fe sufficient (+Fe) and Fe deficient (-Fe) conditions was verified through reverse transcription quantitative PCR (RT-qPCR) (**Figure 5A**; **Supplemental Figure S10A**). Transcript accumulation was strongest in FEP3-OX#1 (up to 12,000-fold increase compared to the Col-0 wild type (WT) control, in roots of plants grown 14 d at +Fe and then shifted for 3 d to +Fe or -Fe; referred to as 14 + 3d system, **Figure 5A**). *FEP3* was not further up-regulated under -Fe, showing that its expression in FEP3-OX lines was independent from Fe supply. HA_3-FEP3 was detected in whole protein extracts of 6 d-old FEP3-OX#1 seedlings both under +Fe and -Fe (**Supplemental Figure S10B, C**). HA_3-FEP3 protein has a calculated molecular weight of 12.5 kDa, however, a single band of the fusion protein was always found at approximately 20 kDa in SDS protein gels. For very acidic proteins like FEP3 (predicted isoelectric point: 3.83; www.arabidopsis.org) slower migration than expected is a common phenomenon (Graceffa et al., 1992; Peterman et al., 2004). In addition, this behavior could be an indication for post-translational modifications of FEP3 protein. Compared to the amount of transcript over-accumulation, HA_3-FEP3 bands from FEP3-OX#1 protein extracts were very weak. In FEP3-OX#3 protein extracts no HA_3-FEP3 was detectable, which is consistent with the lower transcript over-accumulation compared to FEP3-OX#1. Difficulties to detect HA_3-FEP3 might point towards post-translational control of FEP3 protein levels.

Next, it was assessed at which hierarchical level FEP3 acts within the root Fe deficiency response. Therefore, expression levels of genes that are part of the Fe deficiency regulatory cascade (*FRO2*, *IRT1*, *FIT*, *BHLH38*/*39*, *PYE*, *FRO3*, *NAS4*, *ILR3*, *BHLH104*) were determined in FEP3-OX roots grown in the 14+3 d system. Likewise, their expression level was determined in the *btsl1 btsl2* mutant line and

compared to FEP3-OX (**Figure 5A-N;** verification of *btsl1 btsl2* loss-of-function line see **Supplemental Figure S10D-F**). Fe uptake genes *FRO2* and *IRT1* were up-regulated under +Fe in FEP3-OX#1 compared to the WT control, indicating that the Fe uptake machinery is constantly active irrespective of Fe supply (**Figure 5H, I**). To test if FEP3-OX lines accumulate more Fe, the seed Fe content was measured. Indeed, FEP3-OX#1/#3 seeds contained significantly more Fe than the WT control (**Figure 5O**). However, *FIT* expression levels were not changed in FEP3-OX#1, or even decreased under +Fe in FEP3-OX#3 compared to the WT control (**Figure 5G**). Therefore, enhanced Fe uptake did not seem to be caused by increased *FIT* expression. However, group Ib BHLH38 and BHLH39, which activate *FRO2* and *IRT1* expression as heterodimers with FIT (Yuan et al., 2008), were up-regulated under +Fe and -Fe compared to the WT control (**Figure 5E, F**). This explains the activity of the Fe uptake machinery under +Fe. Up-regulation of *FRO2*, *IRT1*, *BHLH38* and *BHLH39* under +Fe in FEP3-OX lines was also confirmed by others (IMA1c Ox; (Grillet et al., 2018)). It was reported that Ib *BHLH* expression is controlled by IVc bHLHs, which also regulate *PYE* (Zhang et al., 2015). Indeed, *PYE* was also up-regulated under +Fe and -Fe in FEP3-OX#1 (**Figure 5J**). Consequently, *FRO3* and *NAS4*, which are negatively regulated by PYE (Long et al., 2010), were expected to be down-regulated. However, *NAS4* regulation was not changed, and *FRO3* was even up-regulated under +Fe in FEP3-OX#1 compared to the WT control (**Figure 5K, L**), suggesting that other mechanisms in addition to PYE control *NAS4* and *FRO3* expression. Together, this data confirms that FEP3 acts as a positive regulator upstream in the Fe deficiency response cascade.

Fe deficiency response genes were regulated similarly in the *btsl1 btsl2* mutant: *FRO2*, *IRT1*, *BHLH38*/*39*, *PYE* and *FRO3* were up-regulated (even stronger than in FEP3-OX) compared to the WT control, while *FIT* and *NAS4* were not (**Figure 5E-L**). However, *BTS* was up-regulated in *btsl1 btsl2*, but not in FEP3-OX (**Figure 5D**). This might reflect the need to compensate for the missing BTSLs in *btsl1 btsl2* mutant. Unexpectedly, *ILR3* and *BHLH104* were down-regulated in FEP3-OX#1/#3 and *btsl1 btsl2* under +Fe compared to the WT control (**Figure 5M, N**). Thus, *ILR3*/*BHLH104* were transcriptionally regulated in an opposite manner as their putative downstream targets *BHLH38*/*39*/*PYE* and *FRO2*/*IRT1*. This observation was confirmed in an independent experiment using 6 d-old seedlings (**Supplemental Figure S11**).

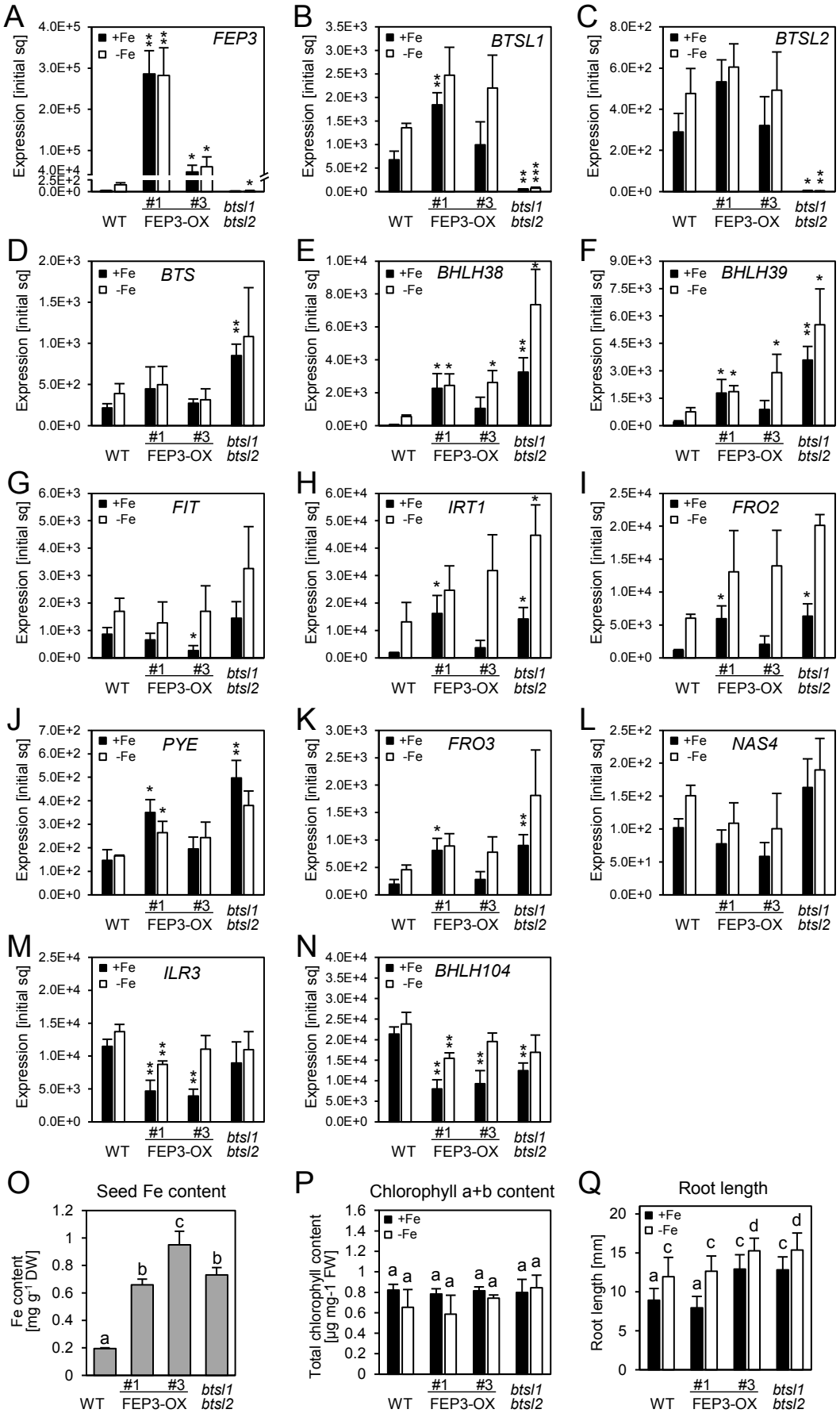

Figure 5. FEP3 and BTSL1/2 oppositely regulate Fe deficiency responses. (*legend continued on next page*)

A-N: Expression analysis (RT-qPCR) of Fe deficiency response genes in roots of two FEP3-OX lines (#1, #3, WT background) and a *btsl1 btsl2* mutant line (see also **Supplemental Figure S10**) in comparison to WT. Expression [initial sq]=Absolute normalized expression [initial starting quantity]. Plants were grown in the 14+3 d system with sufficient (+Fe, black bars) or deficient (-Fe, white bars) Fe supply. Asterisks indicate statistically significant differences to the WT of the same growth condition (n=3) (Student's T-Test, **p*<0.05, ***p*<0.01, ****p*<0.001). **A:** *FEP3*, **B:** *BTSL1*, **C:** *BTSL2*, **D:** *BTS*, **E:** *BHLH38*, **F:** *BHLH39*, **G:** *FIT*, **H:** *IRT1*, **I:** *FRO2*, **J:** *PYE*, **K:** *FRO3*, **L:** *NAS4*, **M:** *ILR3*, **N:** *BHLH104*. **O:** Seed Fe content per dry weight (DW) (n=3). **P:** Chlorophyll a and b content per fresh weight (FW) leaves of WT, FEP3-OX (#1, #3) and *btsl1 btsl2* grown in the 10 d system with +Fe or -Fe supply (n=4). **Q:** Root lengths of WT, FEP3-OX (#1, #3) and *btsl1 btsl2* grown in the 6 d system with +Fe or -Fe supply (n>12). **A-Q:** Data are represented as mean and SD. **O-Q:** Different letters indicate statistically significant differences (one-way ANOVA and Tukey's post-hoc test, *p*<0.05).

In line with the RT-qPCR results, *btsl1 btsl2* seeds also accumulated more Fe than the WT control (**Figure 5O**). Otherwise, both FEP3-OX and *btsl1 btsl2* displayed only weak phenotypic traits. Chlorophyll a and b content in rosette leaves of 10 d-old plants were not changed (**Figure 5P**). The primary root length was also measured. Under our growth conditions, we typically observe longer primary roots in 6 d-old WT plants grown under -Fe compared to +Fe (**Figure 5Q**). This effect was not changed in FEP3-OX and *btsl1 btsl2*, however, FEP3-OX#3 and *btsl1 btsl2* roots were overall significantly longer than the WT. Therefore, FEP3-OX and *btsl1 btsl2* also show weak similarity in their morphological phenotypes.

FEP3 and BTSL1/2 regulate a similar set of genes. To test whether they act consecutively, one being a transcriptional target of the other, or whether they act independently, their transcript levels were measured in the respective mutant. Compared to the WT control, *FEP3* was down-regulated in the *btsl1 btsl2* mutant under -Fe (**Figure 5A**). However, since *FEP3* is Fe deficiency-induced, this relative transcript decrease might be a secondary effect of increased internal Fe in *btsl1 btsl2* plant tissue (Hindt et al., 2017; Rodríguez-Celma et al., 2017). *BTSL2* transcript levels were slightly, but not significantly, increased in FEP3-OX#1 and remained unchanged in FEP3-OX#3, indicating that FEP3 and BTSL2 proteins do not influence each other transcriptionally. On the other hand, *BTSL1* levels were increased in FEP3-OX#1 under +Fe compared to the WT control (**Figure 5B, C**).

Altogether, FEP3-OX plants resemble the phenotype of *btsl1 btsl2* loss-of-function plants, indicating that FEP3 and BTSL1/2 regulate downstream genes in a complementary manner. BTSL1/2 proteins interacted with FEP3, IVc bHLHs and PYE in yeast. We hypothesize that FEP3 may bind and inhibit BTSL function to prevent degradation of their TF targets under -Fe. One prerequisite for protein-protein interactions being relevant *in vivo* is the existing possibility of the proposed interaction partners to meet *in planta*. Therefore, the promoter activities and sub-cellular protein localizations of FEP3, BTSL1, BTS, ILR3, bHLH104 and PYE were determined and compared.

Promoter activities of "BTS(L) interactome" genes

To assess whether the "BTS(L) interactome" genes are expressed in similar plant tissues their promoter activities were studied. Stable Arabidopsis lines expressing the *GUS* (β-glucuronidase) reporter gene under the control of *ILR3*, *BHLH104*, *FEP3*, *PYE*, *BTSL1* and *BTS* promoters were cultivated

under +Fe and -Fe. This experiment is the first in which all above mentioned lines were grown under the same growth conditions. This allows the unique comparison of all their promotor activities. In accordance with previously reported results (Li et al., 2016), GUS activity of *proILR3* and *proBHLH104* was detected in the vasculature of roots, hypocotyl and cotyledons under +Fe and -Fe (**Figure 6A, B, G, H**). *ProFEP3* activity was also detected in root vasculature (mainly in the phloem), hypocotyl and in some plants in the cotyledon vasculature under +Fe and –Fe (**Figure 6C, I, M**). In addition, *proFEP3* was active in true leaves under -Fe (**filled arrowheads**), but not under +Fe. *proPYE* activity was detected mainly outside the root vasculature (**Figure 6D, J**). Whereas *proBTS* activity was found mainly inside the vasculature under +Fe as well as inside and outside the vasculature under -Fe (**Figure 6F, L, O**, **Supplemental Figure S12A**), which is in contrast to other studies, reporting expression mostly or exclusively inside the vasculature (Long et al., 2010; Selote et al., 2015) (**Figure 6F, O**). Also in contrast to reports (Selote et al., 2015), no GUS activity was detected in *proBTS:GUS* cotyledon, while true leaves had small areas of GUS activity under +Fe and -Fe (**Figure 6F, Supplemental Figure 12A; filled arrowheads**). Others have measured *BTS* expression in shoots of 14 d-old plants (Hindt et al., 2017), indicating that 6 d-old seedlings might be too young for proper shoot *GUS* expression. *proPYE* activity was found throughout the length of the entire root under +Fe and -Fe, with highest activity levels in the root meristem. GUS activity was visibly increased in the root differentiation zone under -Fe (**Figure 6D, J**). Because *BTS* and *PYE* promoter regions used were identical to those in (Long et al., 2010; Selote et al., 2015) were used, different cultivation protocols might be a reason for the observed differences. For example, here modified Hoagland medium (Lingam et al., 2011) was used in order to be able to carefully adjust all nutrients. Weak *proBTSL1* activity was detected under +Fe and -Fe in root tissue, mainly outside the vasculature and predominantly in the outer cortex (**Figure 6E, K, N**). Thus, it overlapped with *proPYE* activity. To overlap with *proILR3*, *proBHLH104* and *proFEP3*, *proBTSL1* should be active in the central cylinder. However, GUS activity was either absent from the vasculature, which would be in agreement with other reports (Rodríguez-Celma et al., 2017), or by far not as pronounced as in *proILR3:GUS*, *proBHLH104:GUS*, and *proFEP3:GUS* lines.

Interestingly, *proILR3*, *proPYE*, *proBTSL1*, and *proBTS* activity occurred under +Fe and -Fe in the root tip, possibly around the quiescent center and in the columella (**Figure 6A, D, E, G, J, L**; **Supplemental Figure 12A**; **filled arrowheads**). Noteworthy, while others have measured Fe accumulation in the quiescent center root area, this pattern was disturbed in *bts* mutant roots (Hindt et al., 2017).

In conclusion, *BTSL1* seems to be expressed mainly in the outer root layers, in contrast to its proposed interaction partners *ILR3*, *BHLH104*, and *FEP3*, which are all expressed predominantly in the vascular tissue. Interestingly, the *BTSL1* expression pattern overlaps with the *PYE* expression pattern in the root differentiation zone. However, the location of the gene expression does not necessarily

restrict the protein to the same location. To test if FEP3 protein can move to outer root layers, a *pFEP3:FEP3-GUS* line was generated, but no GUS accumulation could be observed outside the root vascular tissue (**Supplemental Figure S12B**). However, since GUS (68 kDa) is much larger than FEP3 (5.5 kDa), tagged FEP3 itself might behave differently.

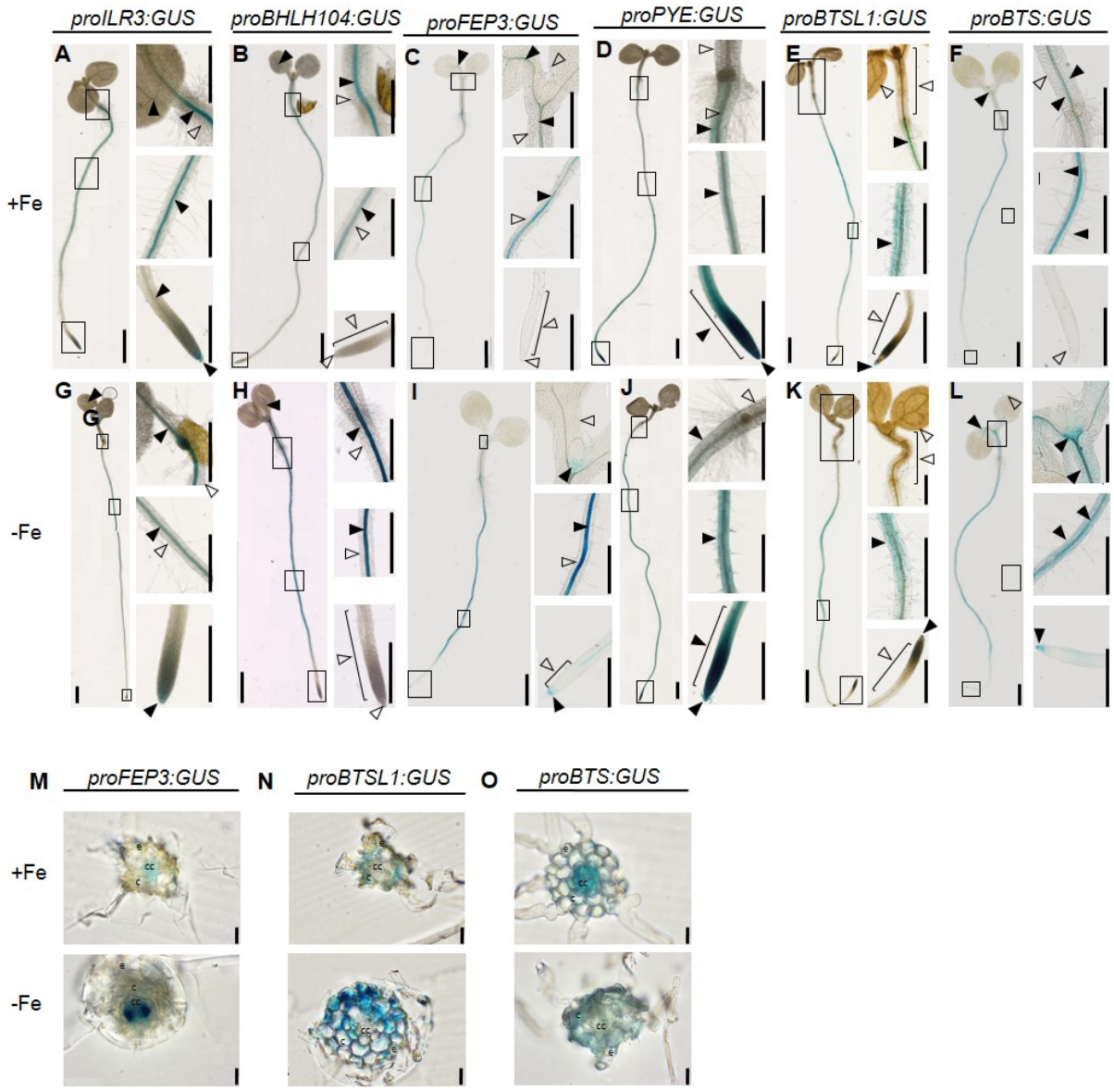

Figure 6. "BTS(L) interactome" genes are partly expressed in the same tissue.
GUS reporter activity, driven by *ILR3, BHLH104, FEP3, PYE, BTSL1*, *BTS* putative promoters. Transgenic Arabidopsis plants with *proILR3:GUS* (**A, G**), *proBHLH104:GUS* (**B, H**), *proFEP3:GUS* (**C, I**), *proPYE:GUS* (**D, J**), *proBTSL1:GUS* (**E, K**), *proBTS:GUS* (**F, L**) in WT background were grown in the 6 d system under sufficient (+Fe, **A-F**) and deficient (-Fe, **G-L**) Fe supply. Reporter gene expression was visualized by using a chemical reaction (GUS) resulting in blue staining of the respective tissues. Plants were imaged with brightfield microscopy. Rectangles in whole-seedling images indicate positions of the enlarged image portions. Filled arrowheads indicate selected areas of GUS activity, un-filled arrowheads indicate selected areas without GUS activity. Vascular tissue is indicated by the arrowhead pointing directly at it, non-vascular tissue is indicated by the arrowhead pointing more to an outside area. Scale bars of whole seedling images: 1 mm; of magnifications: 0.5 mm. Cross sections of *proFEP3:GUS* (**M**), *proBTSL1:GUS* (**N**) and *proBTS:GUS* (**O**). Scale bars: 20 µm. See also **Supplemental Figure S12A**.

Subsequently, our research turned to the subcellular localizations of the proteins. As stated earlier, due to instability, BTS/BTSL proteins are difficult to detect in plant systems. This might be one

reason why, to date, it was not possible to image BTSL1-GFP protein in stable transgenic Arabidopsis lines (data not shown). Therefore, a transient expression system using tobacco leaf epidermis cells was applied.

Subcellular localization and co-localization of "BTS(L) interactome" proteins

BiFC experiments of BTS with ILR3 or bHLH104 have shown that the proteins interact in the nucleus (Selote et al., 2015). This study confirms nuclear localization of fluorophore-tagged BTS, ILR3 and bHLH104 (**Figure 7A (4-6)**). Because BTSL1/2 interacted with ILR3 and/or bHLH104 in Y2H experiments, nuclear localizations similar to those of BTS were expected. Surprisingly, fluorophore-tagged BTSL1 mainly localized to the plasma membrane and only weakly to the nucleus (**Figure 5A (1)**). The fluorophore position (N-/C-terminal) did not affect BTSL1 localization (**Supplemental Figure S13**). Yellow fluorescent protein (YFP)-tagged BTSL2 localized stronger to the nucleus and to the cytoplasm (**Figure 7A (2)**). Remarkably, BTSL1-C-GFP and BTSL2-C-GFP (lacking the HHE domains) localized more to the nucleus and less to the cytoplasm compared to the full-length version (**Figure 7A (8,9)**), raising interesting questions regarding functionality of BTSL1 and the role of the HHE domains. However, additional experiments tacking Z-stacks of the cells that allow quantification of the nuclear to cytoplasmic ratio are needed to confirm this observation.

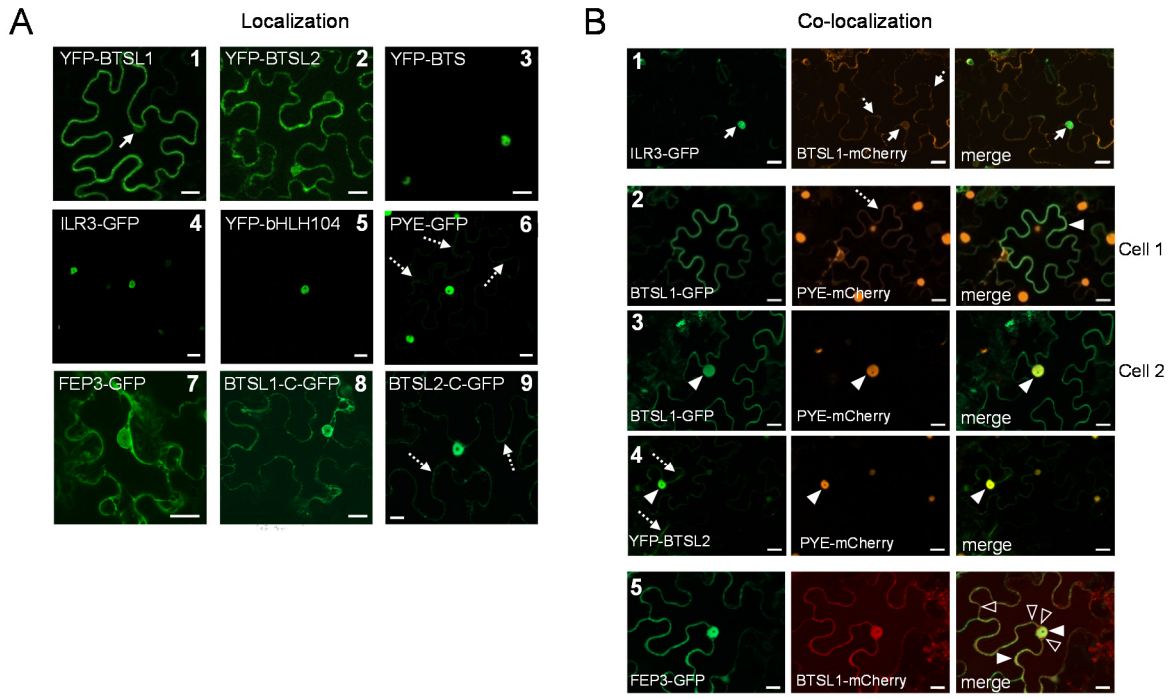

Figure 7. Subcellular localization and co-localization of "BTS(L) interactome" proteins.
A: Subcellular localization of YFP-BTSL1 (1), YFP-BTSL2 (2), YFP-BTS (3), ILR3-GFP (4), YFP-bHLH104 (5), PYE-mCherry (6), FEP3-GFP (7), BTSL1-C-GFP (8), BTSL2-C-GFP (9) in tobacco leaf epidermis cells (see also Supplemental Figure S13). **B:** Co-localization of BTSL1 with ILR3, PYE, FEP3. (1) ILR3-GFP and BTSL1-mCherry, (2, 3) BTSL1-GFP and PYE-mCherry, (4) YFP-BTSL2 and PYE), (5) FEP3-GFP and BTSL1-mCherry. Arrowheads show examples of co-localized GFP and mCherry signals (filled arrowheads) and areas of no co-localization (un-filled arrowheads). **A, B:** Non-dashed arrows indicate nucleus, dashed arrow indicates cytoplasm. The YFP, GFP and mCherry signals were imaged with a fluorescence microscope and an ApoTome for enhanced resolution. Scale bars: 20 µm (except A4, 5, 6). YFP and GFP signals of A4, 5 and 6 were imaged with a laser scanning confocal microscope. Scale bar: 20 µm.

FEP3-GFP and PYE-GFP localized to nucleus and cytoplasm, with a preference of FEP3-GFP for the cytoplasm, and of PYE-GFP for the nucleus (**Figure 7A (6, 7)**). ILR3-GFP and BTSL1-mCherry both localized to the nucleus, but most likely in different areas (**Figure 7B (1)**). BTSL1-GFP and PYE-mCherry co-localized inside the nucleus and possibly also outside the nucleus, although the PYE-mCherry signal at the cell periphery was weak (**Figure 7B (2, 3)**). In support of the peripheral co-localization, BiFC experiments indicated BTSL1 and PYE interaction only outside the nucleus (**Figure 2C (1)**). BTSL2 co-localized with PYE in the nucleus (**Figure 7B (4)**) while no co-localization was observed in the cytoplasm. Full-length BTSL1-mCherry and ILR3-GFP did not co-localize (**Figure 7B (1)**). Interestingly, when BTSL1-mCherry was co-expressed with FEP3-GFP, mCherry was additionally strongly detected inside the nucleus, resembling more the pattern of BTSL1-C. FEP3-GFP and BTSL1-mCherry co-localized in both compartments, except for a small area around the nucleus and small patches at the cell periphery (**Figure 7B (5), un-filled arrowheads**). It remains to be tested whether the mCherry signal corresponds to free fluorophore, to full-length BTSL1-mCherry or to a truncated version of BTSL1-mCherry. In any case, our observations might indicate FEP3-triggered a localization shift of BTSL1. However, Z-stacks of cells co-expressing both are needed for quantification of the nuclear to cytoplasmic ratio.

In summary, these results indicate that some, but not all, of the "BTS(L) interactome" proteins are able to meet *in planta*, when heterologously expressed. The putatively interacting proteins BTSL1/PYE and BTSL1/FEP3 co-localized in different sub-cellular compartments, whereas BTSL1/ILR3 did not co-localize. The same might be true for BTSL1/bHLH104, since bHLH104 and ILR3 single localizations were identical. Single localization experiments further suggest that BTSL2 might co-localize with ILR3 and/or bHLH104, since BTSL2 accumulated more in the nucleus than BTSL1. These co-localization experiments are still in progress.

Discussion

With the help of a comprehensive targeted Y2H screen 24 Fe deficiency response-related proteins, six TFs and 18 non-TFs, were tested for interactions. The screen recovered previously reported interactions (BTS+ILR3/bHLH104, FIT+bHLH39), confirming the suitability of the approach. The Y2H screen revealed a protein interaction network in which BTSL1 and PYE stand out as interaction hubs. Since the Fe sensors BTSL1/2 and the putative mobile signal FEP3 are connected in the network, this might have discovered components of a Fe deficiency sensing system. In this context, we acknowledge the presence of two more small proteins of yet unknown function, linked to BTSL1 and PYE. Noteworthy, FIT did not interact with most of these proteins. The protein interaction network thus rather reflects FIT-independent processes. In conclusion, the Y2H screen was well suited to identify robust protein interactions that are potentially relevant for Fe deficiency responses. The

results are a reliable data source for more detailed additional studies. This study focuses on the highly interconnected "BTS(L) interactome", containing the three homologous RING-type E3 ligases BTS, BTSL1, BTSL2, PYE, bHLH TFs of subgroup IVc (ILR3, bHLH104), and a small peptide (FEP3).

Unique properties of BTS, BTSL1 and BTSL2

Within the "BTS(L) interactome", BTS, BTSL1 and BTSL2 can interact with some of the same proteins, but they additionally seem to have individual sets of interaction partners. It was assumed from studying single, double and triple loss-of-function lines that BTS, BTSL1 and BTSL2 have partly redundant functions as negative Fe uptake regulators during Fe deficiency response (Hindt et al., 2017). Here, *BTS* was significantly up-regulated in the *btsl1 btsl2* mutant, possibly to compensate for lack of BTSL1 and BTSL2. However, *btsl1 btsl2* plants still accumulated more Fe than the WT, indicating that BTS can partly, but not completely, take over BTSL functions.

Apart from this work, experimental data on BTSL1 and BTSL2 is scarce. Other studies reported that *BTS*, *BTSL1* and *BTSL2* are expressed in different and in the same root tissues, and it was suggested that BTSL1/2 and BTS represent different checkpoints to avoid Fe overload during its transport from the rhizosphere into the root vasculature (Rodríguez-Celma et al., 2017). The authors of a recent study present FIT as BTSL1/2 degradation target, because they found increased FIT protein levels in *btsl1 btsl2* mutants and BTSL1/2 interacting with FIT protein *in vitro* (Rodríguez-Celma et al., 2019). Interestingly, in *in vivo* experiments of this study, neither FIT-C which was used in the Y2H screen nor full-length FIT, co-transformed in yeast, did interact with BTS, BTSL1 or BTSL2 (**Supplemental Figure S5**). BTSL1 did only interact with genes of the Fe homeostasis co-expression network or bHLH TFs of subgroup IVc. Thus, it would be unexpected that BTSL1 indeed targets FIT, any gene belonging to the FIT-target network or responsible for Fe acquisition for proteasomal degradation. We also tested BTS and BTSL1 promoter activities and could not confirm a clear expression partitioning in root tissue. Contrary to reports of others, under -Fe *proBTS* activity in this study was detected mostly outside the central cylinder, while *proBTS* activity under +Fe occurred mainly in the central cylinder as was reported before. Thus, it might be possible that *BTS* promotor activity changes under Fe deficiency. At this point it is difficult to further interpret these results, however, different growth media compositions between studies might be a reason for the effect. Noteworthy, the same study reporting vascular *BTS* expression (Long et al., 2010), also reported that *PYE* was expressed only in the vasculature, and that the protein was able to move to outer root layers. However, here *proPYE* activity was detected in all root tissues, indicating that PYE protein does not need to be cell-to-cell mobile in order to act outside the vasculature.

Although this study did not show that BTSL1 and BTS have distinct promoter activities, intriguingly distinct subcellular localizations of BTS, BTSL1 and BTSL2 were determined. BTSL1 was

mostly located at the plasma membrane and only weakly in the nucleus, in contrast to BTS, which was located only in the nucleus. BTSL2 had an intermediate localization pattern (cytoplasm and nucleus). Nuclear BTS localization was reported by others (Selote et al., 2015), but BTSL1 and BTSL2 localizations were not known before. Consistent with our results, the BTS homolog in rice, HRZ1, also localized to the nucleus while HRZ2 localized to nucleus and cytoplasm (Kobayashi et al., 2013). Because BTS, BTSL1 and BTSL2 appear to cover different subcellular compartments, they might target different parts of the Fe deficiency response cascade. For example, both BTS and its degradation target ILR3 localized (result of this study) and interacted in the nucleus (Selote et al., 2015). ILR3 also interacted with BTSL1 in yeast. However, although BTSL1-mCherry and ILR3-GFP were both detected in nuclei of tobacco leaf cells, they localized to mutually exclusive areas. BTSL1-mCherry was localized in the nucleus, but probably only outside of ILR3-GFP-containing areas. This might indicate that BTSL1 does not target ILR3 for proteasomal degradation. However, degradation experiments will be needed to clarify this matter.

BTSL1/2 physically interacted with and might target bHLH104 protein for degradation. bHLH104 is a more likely target of BTSL1/2 than ILR3, since bHLH104 is not targeted by BTS (Selote et al., 2015). *BHLH38*/*39* and *PYE* were expressed at high levels in *btsl1 btsl2* plants, suggesting highly active IVc bHLHs. Since ILR3 and bHLH115 should be degraded by BTS (Selote et al., 2015) in *btsl1 btsl2* plants, the active IVc bHLHs are likely bHLH104 (and/or bHLH34).

BTSL1 and BTSL2, but not BTS, interacted and co-localized with PYE in yeast. In tobacco leaf cells, BTSL1 and PYE co-localized inside and outside the nucleus. In addition, PYE and BTSL1 promoter activities overlapped in outer layers of Arabidopsis roots. BTSL2 in contrast co-localized with PYE only in the nucleus. PYE positively regulates overall Fe deficiency responses, since *pye-1* mutants are chlorotic, and show decreased rhizosphere acidification and reductase activity, both of which are indicators of Fe acquisition when increased. Furthermore, *IRT1* is less expressed under Fe deficient conditions (Long et al., 2010). PYE might therefore be a likely target of BTSL1 (and/or BTSL2).

A localization shift of BTSL?

BTSL1/2 localization changed from peripheral to more cytoplasmic and nuclear when the N-terminal part harboring the HHE domains was cleaved off (BTSL1/2-C). Interestingly, similar experiments with BTS showed the same effect, however in this case the protein shifted from nuclear to cytoplasmic localization (Selote et al., 2015). We conclude that subcellular localizations of full-length BTSL1/2 (and BTS) depend on the N-terminus and possibly on the HHE domains. By binding to HHE domains, Fe^{2+}possibly influences BTS protein stability (Selote et al., 2015) and presumably BTSL1/2 protein is regulated in a similar manner. Because HHE domains and BTSL1/2 localization seem to be linked, it is tempting to speculate that BTSL1/2 protein can exist in two forms, depending on the intracellular Fe status: as full-length protein mostly at the plasma membrane and as truncated version

that moves into the nucleus, perhaps to engage in different regulatory processes. Other E3 ligases are known to move into the nucleus upon stress, such as AtHOS1 (HIGH EXPRESSION OF OSMOTICALLY RESPONSIVE GENES1) moving from the cytoplasm into the nucleus during cold stress (Lee et al., 2001; Dong et al., 2006) or AtRGLG1 (RING domain ligase 1) and AtRGLG2, moving from the plasma membrane into the nucleus upon ABA or salt stress treatment (Cheng et al., 2012, 2016; Belda-Palazon et al., 2019). Because HOS1, RGLG1 and RGLG2 target nuclear proteins for degradation, the nuclear localized E3 ligases could be the active forms during the stress conditions. In this study BiFC experiments showed that full-length BTSL1 and BTSL1-C both interacted with PYE. Both forms of BTSL1 can therefore engage in physical protein-protein interactions *in planta*, but act in different compartments. In contrast, only BTSL1-C, but not full-length BTSL1 interacted with ILR3 in the nucleus. This holds potential for the existence of a mechanism in which BTSL1 switches interaction partners upon truncation. However, it remains speculative whether BTSL1-C is a biologically relevant form of BTSL1. Moreover, since all our tobacco experiments represented a Fe sufficiency situation, it needs yet to be determined if BTSL1 protein structure or localization is altered upon Fe deficiency stress.

Possible function of FEP3-BTSL interaction during Fe acquisition

The small peptide FEP3 is an interesting new player in the Fe deficiency response. Except for being a positive regulator (Grillet et al., 2018), its specific role during Fe deficiency responses is not known. Non-secreted peptides (<100 aa) are one of several classes of short proteins that are encoded by evolutionary conserved small open reading frames (ORFs; (Hsu and Benfey, 2018)). These small ORF-encoded peptides (often termed SEPs (Delcourt et al., 2018)) can act in many ways, for example, as ligands to receptors or by modulating protein-protein interactions (Makarewich and Olson, 2017). As opposed to peptide hormones, another class of short proteins, SEPs do not have to be post-translationally processed in order to become bioactive peptides (Stührwohldt and Schaller, 2019). Although FEPs structurally resemble hormone peptide precursors, this and other studies could not find evidence for FEP3 or FEP1 cleavage and secretion (Grillet et al., 2018; Hirayama et al., 2018), since N-terminally tagged full-length protein was detectable in Arabidopsis stable transgenic lines and protein extracts. Therefore, FEP3 is regarded a SEP. This study shows that FEP3 acts upstream in the Fe deficiency response cascade. That FEP3-OX lines phenocopy the *btsl1 btsl2* mutant indicates that BTSL1/2 function was inhibited in FEP3-OX lines. The molecular phenotype of FEP3-OX was not as pronounced as that of the *btsl1 btsl2* mutant, which probably means that a small amount of BTSL1/2 protein was still functional. Since *BTSL1/2* genes were not down-regulated in FEP3-OX lines, but rather the contrary, the inhibition likely takes place on the protein level. It might be possible that FEP3 acts as direct inhibitor of BTSL1/2, thereby allowing the Fe uptake machinery to be active when Fe levels are low.

To date, there is no reported case of a SEP interacting with an E3 ligase or inhibiting its function in plants. Interestingly, however, SEP-E3 ligase interactions are known from animal systems. For example, the Drosophila SEP *pri* interacts with the E3 ligase Ubr3, facilitating Ubr3 binding to the TF Svb. This changes Svb function (Zanet et al., 2015). From Drosophila as well as mammals, examples are known in which SEPs alter protein localization or bind to enzymes to affect their activity, either by direct competition with the substrate or in an allosteric manner (Cabrera-Quio et al., 2016). Y2H experiments in this research showed that FEP3 and ILR3/bHLH104 interact with adjacent, but not identical residues of BTSL1. Investigations of the BTSL2 interaction site for TFs of subgroup IVc and FEP3 are ongoing, but preliminary results indicate a similar result as for BTSL1 (data not shown). Therefore, it is hypothesized that FEP3 is an allosteric inhibitor, preventing degradation targets of BTSLs from binding. However, protein crystal structure analyses are needed to clarify how BTSL, FEP3 and bHLH proteins interact.

Noteworthy, when BTSL1-mCherry was co-expressed with FEP3-GFP in tobacco, overall stronger mCherry signal and a BTSL1 localization shift more to the nucleus (resembling the pattern of BTSL1-C) were observed. Therefore, FEP3 might trigger BTSL function change by altering the protein structure, stability or localization. However, this hypothesis needs to be confirmed by performing additional co-localization experiments. The plasma membrane localization of BTSL1 might also indicate a ligand-receptor-like relationship of FEP3 and BTSL1. In a hypothetical scenario, FEP3 as mobile signal binds to BTSL1/2 in roots, which leads to de-repression of Fe acquisition. A somewhat comparable principle is known from phosphate (Pi) starvation responses, where a microRNA acts as a shoot-to-root signal, targeting the mRNA of a root E2 conjugase, and thereby de-repressing the function of Pi transporters (Huang et al., 2013).

Several internal layers of control carefully balance Fe deficiency response regulation

These experimental results add to the complexity of the Fe deficiency response regulation cascade both on the transcriptional and on the post-translational level. Next to BTS, BTSL1/2 were added as negative upstream regulators, representing another layer of control for surplus Fe uptake. As stated above FEP3 and BTSL1/2 do not regulate each other transcriptionally, although *BTSL1* was significantly up-regulated in FEP3-OX. bHLH39 possibly induces *BTSL1/2* expression as part of a regulatory feedback loop, because these results match an earlier observation by our group that *BTSL1* (and *BTSL2*) were up-regulated in transgenic plants over-expressing *BHLH39* (39Ox; (Naranjo-Arcos et al., 2017)). 39Ox plants accumulate massive amounts of Fe under +Fe, which represses Fe deficiency-induced genes that are not transcriptionally controlled by bHLH39. For example, *FEP3* itself was down-regulated in 39Ox, therefore up-regulation of *BTSL1* cannot be dependent on FEP3. Increased *BHLH39* expression in FEP3-OX lines used in this study can explain *BTSL1* up-regulation. The feedback loop

between bHLH39 or *BTSL1/2* likely acts as a protective layer to prevent surplus Fe uptake. In comparison, *BTS* transcript levels were not significantly up-regulated in FEP3-OX and 39Ox plants (Naranjo-Arcos et al., 2017), indicating that *BTS* is not regulated by bHLH39.

We initially struggled to explain why *ILR3* and *BHLH104* transcripts were down-regulated in FEP3-OX and *btsl1 btsl2* mutant lines, although all their assumed downstream target genes were highly expressed. IVc *BHLH* transcription in *bts* or *btsl* loss-of-function lines has never been measured by anyone before. This data suggests that ILR3/bHLH104 levels are also controlled transcriptionally, possibly for a case in which the proteins are not sufficiently degraded. This might be an additional layer of control to avoid excessive Fe uptake. This scenario actually could explain why neither *btsl1 btsl2*, nor *btsl1 btsl2 bts-3* triple mutants or - at least in our study design - FEP3-OX plants show signs of severe Fe toxicity under +Fe (Hindt et al., 2017). It was recently reported that PYE represses *ILR3* expression (Samira et al., 2018), hence *ILR3* down-regulation in FEP3-OX and *btsl1 btsl2* can be explained by the elevated *PYE* levels. In another study, ILR3 was shown to dimerize with PYE to repress *PYE* transcription (Tissot et al., 2019). We propose that IVc bHLH proteins in combination with PYE control their own transcription. Overall, though, the regulatory cascade is not fully understood yet. For example, it was expected that PYE and the genes negatively regulated by it (*NAS4/ZIF1/FRO3*; (Long et al., 2010)) have opposite expression patterns. However, although PYE was highly expressed in mutant lines of this study, *NAS4* and *FRO3* were not down-regulated. This aligns with examination results of IVc bHLH gain-of-function lines (Zhang et al., 2015; Li et al., 2016), and indicates that PYE function can be bypassed or that IVc bHLHs and PYE act antagonistically to fine-tune downstream Fe acquisition and distribution genes.

A working model of Fe deficiency response regulation in Arabidopsis roots

Based on these results and the most up-to-date research knowledge on this matter, this study puts forward a hypothetical model of Fe deficiency response regulation in Arabidopsis (**Figure 8A**). BTS, BTSL1 and BTSL2 negatively regulate Fe uptake genes by targeting individual sets of group IVc bHLHs (represented by ILR3 and bHLH104) and PYE for degradation. An interplay of IVc bHLHs and PYE on the protein as well as the transcriptional level impact Fe acquisition and Fe distribution genes both positively and negatively, which ensures carefully balanced Fe uptake and homeostasis. In addition, *BTSL1/2* expression is regulated by bHLH39 in a negative feedback loop. Degradation of group IVc bHLHs and PYE by BTSL1/2 is counteracted by the positive Fe uptake regulator FEP3, which blocks BTSL1/2 function by physically interacting with the proteins (**Figure 8B**). Additionally, FEP3 might be involved in re-localization of BTSL1 through its interactions. The latter hypothesis needs further validation and is therefore not considered in the model.

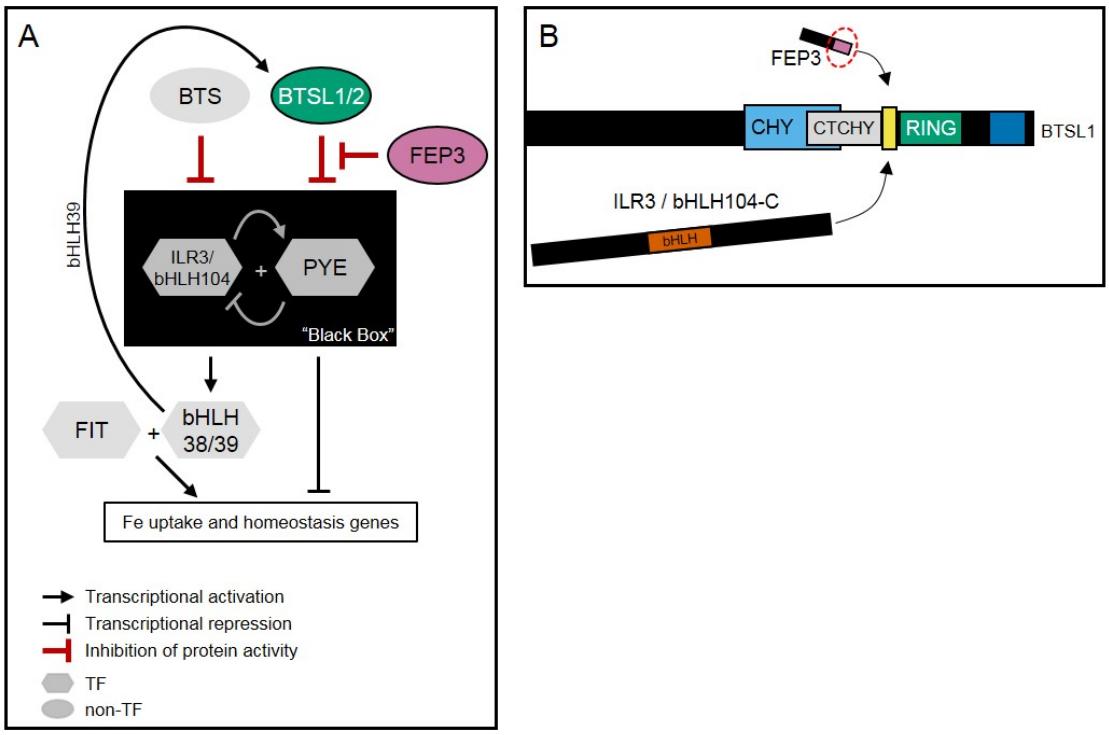

Figure 8. Working hypothesis of BTSL1/2 and FEP3 function, based on expression and protein-protein interaction data.
A: Fe deficiency response data of FEP3-OX and *btsl1 btsl2* lines from this study are incorporated into the current model of the Arabidopsis Fe homeostasis regulatory cascade (Selote et al., 2015; Zhang et al., 2015; Tissot et al., 2019). Going from bottom to top of the model, group Ib bHLHs (represented by bHLH38/39) as dimers with FIT directly induce Fe uptake genes (Yuan et al., 2008; Wang et al., 2013). PYE, possibly as dimer with ILR3, represses Fe homeostasis/distribution genes (*e.g. NAS4*) (Tissot et al., 2019). Group Ib *BHLHs* and *PYE* are transcriptionally up-regulated by group IVc bHLHs (represented by ILR3/bHLH104), which positively regulate Fe acquisition (Zhang et al., 2015; Liang et al., 2017). In turn, PYE represses *ILR3* transcription (Samira et al., 2018). In line with this, *ILR3* and *BHLH104* were down-regulated in our FEP3-OX and *btsl1 btsl2* lines while *PYE* was up-regulated, indicating that PYE might also repress transcription of other IVc *BHLHs* besides *ILR3*. IVc bHLHs and PYE are put in a "Black Box", since data regarding these proteins are not yet fully conclusive. In summary, IVc bHLHs and PYE can homo- and heterodimerize in different combinations, and activate or repress downstream genes, and also each other. BTS/BTSL1/BTSL2 physically interact with different "Black Box" proteins and presumably target some of them for degradation (BTS target: ILR3 (Selote et al., 2015)). This study demonstrated that BTSL1/2 physically interacts with FEP3, a positive regulator of Fe uptake, and FEP3-OX plants phenocopy *btsl1 btsl2* mutant plants. Our model therefore presents FEP3 as inhibitor of BTSL1/2. *BTSL1/2* possibly regulated by bHLH39 (but not FIT) in a negative feedback loop that transcriptionally induces its own upstream negative regulator (data from this study and (Mai et al., 2016; Naranjo-Arcos et al., 2017)). It should be noted that the model does not take into account different cell types. **B:** Proposed mechanistic model of BTSL1 inhibition by FEP3. The model summarizes Y2H data from Figures 3 and 4. FEP3 interacts with BTSL1 in a 14-aa region depicted in yellow (M-C site). The 7 aa at the FEP3 C-terminus are needed for the interaction (red dashed oval). ILR3 and bHLH104-C interact with a similar, but not the same region of BTSL1 within the M-C site. FEP3 might be an allosteric inhibitor, preventing that BTSL1 can bind and target the bHLHs for degradation. Consequently, the Fe acquisition cascade downstream of ILR3/bHLH104 (shown in A) is active and Fe is absorbed.

We hypothesize that BTSL1/2 have specific functions and target PYE for proteasomal degradation. But for this interactions and their impact on the Fe deficiency response regulation further investigation is needed and currently ongoing in our lab to unravel the impact of these protein-protein interactions.

Concluding remarks

We provide evidence that FEP3 over-accumulation phenocopies *btsl1 btsl2* loss-of-function. FEP3 physically interacts with BTSL1 and BTSL2. This study strongly suggests that FEP3 inhibits BTSL1/2 protein function, possibly by outcompeting BTSL1/2 degradation targets. However, additional experiments are needed to confirm that IVc bHLHs and/or PYE are targeted for degradation by BTSL1/2 and that this function is abolished by FEP3. Also, it needs to be clarified how the FEP3-BTSL interaction is disintegrated, once functional BTSLs are needed. Since FEP3 and BTSL1/2 have been attributed with Fe^{2+} binding abilities, we speculate that Fe itself might trigger disruption of the complex. Since the FEP family contains at least three members in Arabidopsis, we propose that BTS is regulated in a similar manner by one of the FEP3 homologs. A mechanism in which small peptides control the function of E3 ligases through direct binding has not been shown in plants yet. Therefore, this study might have uncovered a novel fundamental mechanism of post-translational regulatory control in plants.

Outlook and future perspectives

A complex regulatory cascade is involved in controlling the Fe deficiency response mechanism. With the help of targeted Y2H interaction screen this study contributes to a better knowledge of the key players involved and their interplay at protein level. To date, not all protein-interactions among Fe deficiency response proteins are actually known. Thus, there is great interest into further extending the Y2H interaction screen, especially in regards to the search for novel Fe responsive proteins not known at the inception of this study. Recently, a novel essential TF named URI was reported to be interacting with bHLH TFs of subgroup IVc, thereby regulating several genes including *PYE* and bHLH TFs of subgroup *IB* (Gao et al., 2019; Kim et al., 2019). To determine whether URI itself is also regulated by one of the BTS(L)s on protein level, this is being the case for bHLH TFs of subgroup IVc, a targeted Y2H assay will be performed between the BTS(L)s and URI. Furthermore, bHLH11 will be included in the targeted Y2H screen.

The verification of BTS(L)-protein interactions *in planta* turned out to be extremely complicated. One possible explanation is that BTS/L proteins are very unstable which has also been reported by others (Selote, 2015; Rodríguez-Celma et al., 2019). To validate the Y2H interactions, especially between BTSL1 and FEP3 additional protein-interaction assays, for example co-immunoprecipitation of the BTSL-C-term, should be applied. Localization and co-localization indicates a possible protein-protein interaction. Interacting proteins of our Y2H screen were co-localizing on subcellular level. Nevertheless, more research is ongoing to determine the exact localization of the BTSL proteins inside a cell. To test whether the BTSLs localize at the plasma membrane, they will be co-localized with a plasma membrane marker (for example AHA1) in tobacco leaves. Additionally we are currently analyzing whether co-expression of BTSL1 with FEP3 or BTSL1 with PYE leads to a

localization shift of one of the proteins. Unfortunately this analysis is quite difficult to perform because in many cases of co-transformation only one of the proteins is expressed and can be visualized.

For now, we mostly focused on determing which site of BTSL1 interacts with IVc bHLH TFs and FEP3. The interaction site of BTSL2 with IVc bHLH TFs and FEP3 is also under investigation. The focus is on the M-C site, given that it is very similar to the BTSL1 M-C site. Both proteins share similar protein interactors and it will be analyzed whether the interaction takes place via the same site in both proteins or if there are differences in the interaction site. Finally, Y2H experiments analyzing the interaction between PYE and BTSL1/2 are ongoing.

Through our research we were able to detect a mechanism in which FEP3 positively influences the Fe deficiency response by inhibiting BTSL protein function. The impact of the BTSL interactions with bHLH TFs of subgroup IVc and especially with PYE is still undetermined. Interestingly, PYE does only interact with the BTSLs and not with BTS, in contrast to bHLH TFs of subgroup IVc which interact with BTS and partially with the BTSLs. The interaction of BTS with its target genes leads to their proteasomal degradation (Selote, 2015). Thus, it is plausible that the BTSLs also regulate the Fe deficiency response at protein level by targeting TFs for proteasomal degradation. BTS and the BTSLs might be responsible for the regulation of various target proteins. Therefore, over-expression lines of *PYE*, *BHLH104* and *ILR3* were constructed and will be analyzed. Ultimately, protein-degradation assays have to be performed to analyze the impact of the BTSL1-PYE interaction.

Methods

Plant Material

Arabidopsis (*Arabidopsis thaliana*) ecotype Columbia-0 (Col-0) was used as wild type (WT) and as background for transgenic lines. The *btsl1 btsl2* loss-of-function double mutant was described previously (*btsl1-1 btsl2-2*, crossed SALK_015054 and SALK_048470, (Rodríguez-Celma et al., 2017, bioRxiv)). *btsl1 btsl2* seeds were kindly provided by Dr. Janneke Balk, JIC, Norwich, UK. T-DNA insertion sites were verified with primer pairs LBb1.3/btsl1-1_RP (*btsl1*) and LBb1.3/btsl2-2_RP (*btsl2*) and homozygosity was verified with the primer pairs btsl1-1_LP/btsl1-1_RP and btsl2-2_LP/btsl2-2_RP (all primers are listed in **Supplemental Table S1**). For plant lines ectopically over-expressing triple HA-tagged *FEP3* (FEP3-OX) under the control of a double CaMV 35S promoter, the coding sequence was amplified from cDNA of Fe deficiency treated Arabidopsis WT roots with primers carrying B1 and B2 attachment sites, respectively, transferred into the entry vector pDONR207 (Invitrogen) according to the manufacturer's recommendations (BP reaction, Gateway, Thermo Fisher Scientific) and sequenced. Final constructs were obtained by transferring all candidate genes subsequently into Gateway compatible plant binary destination vector pAlligator2 (N-terminal triple HA fusions=HA_3) (Bensmihen et al., 2004) via LR reactions (Thermo Fisher Scientific), and sequenced. Constructs were

transformed into Agrobacteria (*Rhizobium radiobacter*) strain GV3101 (pMP90) (Koncz and Schell, 1986; Young et al., 2001). Stable transgenic Arabidopsis lines were generated via the Agrobacterium-mediated floral dip method (Clough and Bent, 1998). In brief, inflorescences of 6-7 weeks old Arabidopsis WT plants with removed open flowers and siliques were dipped around 20 s into a suspension (OD_{600}=0.8) of Agrobacteria in 5% (w/v) sucrose supplemented with 0.05% (v/v) Silwet Gold (Spiess-Urania). Positive transformants were selected based on seed GFP expression and genotyping PCR on the transgenic cassette, selfed and propagated to T3 generation. Insertion sites of the transgenic cassettes in FEP3-OX#1 and FEP3-OX#3 were determined by thermal asymmetric interlaced (TAIL) PCR (Liu and Whittier, 1995) with the primers S1_AL2_LB (template: gDNA), S2_AL2_LB (template: S1_AL2_LB amplicon), S3_AL2_LB (template: S2_AL2_LB amplicon), each combined with AD1, AD2, AD3, AD4, AD5, AD6. The insertion sites were verified by genotyping PCR with primer pairs FEP3-OX1_chr5 fw/S3_AL2_LB (FEP3-OX#1), FEP3-OX3_chr1 fw/S3_AL2_LB (FEP3-OX#3). Homozygosity was determined with primer pairs FEP3-OX1_chr5 fw/ FEP3-OX1_chr5 rev (FEP3-OX#1), FEP3-OX3_chr1 fw/FEP3-OX3_chr1 rev (FEP3-OX#3). T3 plants were used for physiological analyses. Promoter sequences of *BTS* (2,994 bp upstream of start codon), *BTSL1* (880 bp upstream of start codon), *PYE* (1,120 bp upstream of start codon) and *FEP3* (1,614 bp upstream of start codon) were amplified from Arabidopsis WT gDNA with primer pairs proBTS_-2994_B1 fw/proBTS_-2994_B2 rev (for *proBTS*), proBTSL1_-880_B1 fw/proBTSL1_-880_B2 rev (for *proBTSL1*), proPYE_-1120_B1 fw/proPYE_-1120_B2 rev (for *proPYE*), proFEP3_-1614_B1 fw/proFEP3_-1614_B2 rev (for *proFEP3*) and proFEP3_-1614_B1 fw/FEP3ns_B2 rev (for *proFEP3:FEP3*), respectively, cloned into the vector pDONR207 (Invitrogen) via the Gateway system (BP reaction, Thermo Fisher Scientific) and sequenced. Sequences were transferred into the Gateway-compatible destination vector pGWB3 (Nakagawa et al., 2007) (kindly provided by Dr. Andreas Weber, HHU, Düsseldorf, Germany) via LR reaction (Thermo Fisher Scientific), generating *proBTS:GUS*, *proBTSL1:GUS*, *proPYE:GUS*, *proFEP3:GUS* and *proFEP3:FEP3-GUS* constructs, followed by sequencing. Constructs were transformed into Arabidopsis WT plants as described above. Positive transformants were selected based on hygromycin resistance and genotyping PCR, selfed and propagated to T2 or T3 generation. *ProILR3:GUS*/WT and *proBHLH104:GUS*/WT Arabidopsis lines were kindly provided by Dr. Diqiu Yu, Chinese Academy of Sciences, Kunming, China. Three to four weeks old tobacco (*Nicotiana benthamiana*) plants were used for subcellular localization and interaction studies.

Plant Growth Conditions

For propagation and seed production, Arabidopsis seeds were surface-sterilized and stratified as described in (Lingam et al., 2011), germinated and cultivated on soil in a climate chamber under long day conditions (16 h light, 8 h dark, 21°C). For phenotypic analyses, physiological or histochemical

assays, mRNA or protein extraction, surface-sterilized seeds were distributed to sterile plates containing modified half-strength Hoagland medium (1.5 mM $Ca(NO_3)_2$, 1.25 mM KNO_3, 0.75 mM $MgSO_4$, 0.5 mM KH_2PO_4, 50 µM KCl, 50 µM H_3BO_3, 10 µM $MnSO_4$, 2 µM $ZnSO_4$, 1.5 µM $CuSO_4$, 0.075 µM $(NH_4)_6Mo_7O_{24}$, 1% (w/v) sucrose, pH 5.8, and 1.4% w/v plant agar (Duchefa)) with (Fe sufficient, +Fe) or without (Fe deficient, -Fe) 50 µM FeNaEDTA. Seeds on plates were stratified at 4°C in the dark for two days and subsequently grown vertically in plant growth chambers (CLF Plant Climatics) under long day conditions. Seeds were germinated and grown for six or ten days directly on +Fe or -Fe medium (6 day (d) system/10 d system). Alternatively, seeds were germinated and grown for 14 days on +Fe medium and then transferred for three days to either +Fe or -Fe medium (14+3 d system). The 6 d system was used for whole-seedling mRNA extraction for RT-qPCR, protein extraction and root length measurements, the 10 d system was used for chlorophyll measurements and the 14+3 d system was used for root mRNA extraction for RT-qPCR.

Yeast Two-Hybrid (Y2H) Assays

Y2H screen: In a targeted manner, all 24 candidate genes were screened for interactions by pair-wise testing each as N-terminal AD and BD fusion proteins in both reciprocal combinations. pACT2-GW:*X* and pGBKT7-GW:*Y* constructs were used, with *X* and *Y* being the coding sequences of the tested gene pair. Coding sequences were amplified from cDNA of Fe deficiency treated Arabidopsis WT roots with primers carrying B1 and B2 attachment sites, respectively, transferred into the entry vector pDONR207 (Invitrogen) according to the manufacturer's recommendations (BP reaction, Gateway, Thermo Fisher Scientific) and sequenced. Final constructs were obtained by transferring all candidate genes subsequently into destination vectors pACT2-GW and pGBKT7-GW (kindly provided by Dr. Yves Jacob, Institut Pasteur, Paris, France) via LR reactions (Thermo Fisher Scientific), and sequenced. Yeast (*Saccharomyces cerevisiae*) strain Y187 was transformed with pACT2-GW:*X* (AD-X) constructs and yeast strain AH109 was transformed with pGBKT7-GW:*Y* (BD-Y) constructs via the lithium acetate (LiAc) method, based on (Gietz and Schiestl, 2007). In brief, 50 ml YPDA liquid culture (1% (w/v) yeast extract, 2% (w/v) Bacto peptone, 2% (w/v) glucose, 30 mg l^{-1} adenine hemisulfate), OD_{600}=0.5, were made competent with 100 mM LiAc. For transformation, 33.3% (w/v) PEG 4000, 0.1 M LiAc, 50 µg denatured Calf Thymus DNA (Invitrogen) and 0.3-0.7 µg of the construct were mixed in a total volume of 360 µl. Heat shock was carried out 20 min at 42°C. Transformants were selected by cultivation for 2 days on minimal synthetic defined (SD) media (Clontech) lacking Leu (pACT2-GW:*X*) or Trp (pGBKT7-GW:*Y*). Yeast expressing both *AD-X* and *BD-Y* were obtained by mating. One fresh colony of each transgenic yeast carrying a pACT2-GW*:X* and a pGBKT7-GW*:Y* construct, respectively, were mixed in YPD (without adenine hemisulfate) liquid medium and cultivated 2-3 d on minimal SD media lacking Leu and Trp to select for diploid yeast cells carrying both constructs. To test for protein-protein interaction, a fresh

diploid colony was resuspended in sterile H_2O to OD_{600}=1 and 10 µl of the suspensions were dropped onto minimal SD media lacking Leu, Trp and His, containing appropriate concentrations of 3-amino-1,2,4-triazole (3AT, suppression of background growth). Plates were cultivated at 30°C for up to 14 days (growth documentation every 2-5 days). Diploid cells expressing each pACT2-GW:*X* construct in combination with an empty pGBKT7-GW and vice versa were used as negative controls. Combination of pGBT9.BS:*CIPK23* and pGAD.GH:*cAKT1* was used as a positive control of the system (Xu et al., 2006).

Targeted Y2H of selected protein pairs: Selected protein pairs of the Y2H screen and mutagenized/truncated protein versions were assayed as N-terminal AD and BD fusion proteins in both reciprocal combinations. Mutagenized *BTSL1* versions *BTSL1-dRH*, *BTSL1-6G and BTSL1-dMC* were created as described in "BTSL1 mutagenesis". Truncated versions *BTSL1-N*, *BTSL1-C*, *BTSL1-C.1*, *BTSL1-C.2*, *BTSL1-C.3*, *BTSL1-C.4*, *FEP3-N*, *FEP3-C*, *FEP3-d7*, *ILR3-d25*, *ILR3-CC*, *bHLH104-C*, *bHLH104-C-d25*, *bHLH104-CC* were amplified with primers listed in **Supplemental Table S1** and cloned into pACT2-GW and pGBKT7-GW as described in the previous section. Yeast strain AH109 was co-transformed with both pACT2-GW:*X* (AD-X) and pGBKT7-GW:*Y* (BD-Y) (including empty vector controls) as described in the previous section. X and Y represent proteins of a tested protein pair. Haploid double transformants were selected on minimal SD media lacking Leu and Trp. To select for protein-protein interaction, overnight liquid cultures were adjusted to OD_{600}=1 with sterile H_2O and dilution series down to OD_{600}=10^{-4} were prepared. 10 µl of the suspensions were dropped onto SD media lacking Leu, Trp and His and containing the appropriate 3-AT concentration and cultivated as described in the previous section.

BTSL1 mutagenesis

Three deletion forms of BTSL1 lacking the region 1137-1142 (RTLVEH) were created: BTSL1-dRH (deletion) and BTSL1-6G (deletion spaced with GGGGGG). An additional deletion form of BTSL1 was lacking the complete M-C site (MSRTLVEHVCREKC). Deletion and 6G substitution were introduced by overlap-extension PCR as described in (Le et al., 2016). Two partially overlapping parts of each sequence were amplified from pDONR207:BTSL1 constructs (see "Plant Material"), using the primer pairs BTSL1_B1 fw/BTSL1_dRH rev, BTSL1_dRH fw/BTSL1_B2 rev (BTSL1-dRH), BTSL1_B1 fw/BTSL1_dRH-G rev, BTSL1_dRH-G fw/BTSL1_B2 rev (BTSL1-6G), BTSL1 B1 fw/ BTSL1_dMC rev, BTSL1_dMC fw/ BTSL1 B2 rev (BTSL1-dMC). Outer primers used to amplify the final construct are underlined. They carry B1 and B2 Gateway attachment sites. Amplicons were transferred into pDONR207, sequenced, subsequently transferred into Y2H destination vectors pACT2-GW and pGBKT7-GW, transformed into yeast and assayed as described in the previous section.

Histochemical β-glucuronidase (GUS) Assay

Arabidopsis lines expressing *proBTS:GUS*, *proBTSL1:GUS, proILR3:GUS, proBHLH104:GUS, proPYE:GUS*, *proFEP3:GUS* and *proFEP3:FEP3-GUS* in WT background (see "Plant Material") were cultivated under Fe sufficient and Fe deficient conditions in the 6 d system (see "Plant Growth Conditions"). From *proBTS:GUS*, *proILR3:GUS, proBHLH104:GUS* and *proPYE:GUS* lines, four to six seedlings were transferred into 1 ml GUS staining solution based on (Jefferson et al., 1987), containing phosphate buffer (50 mM Na_2HPO_4, 50 mM NaH_2PO_4, pH 7.2) and substrate solution (2 mM $K_4[Fe(CN)_6]Fe^{2+}$, 2 mM $K_3[Fe(CN)_6]Fe^{3+}$, 0.2% Triton-X, 2 mM 5-bromo-4-chloro-3-indoyl-b-D-glucuronic acid (X-Gluc)) and incubated at 37°C in the dark for 15 min up to 12 h until blue tissue staining was visible. From *proBTSL1:GUS, proFEP3:GUS* and *proFEP3:FEP3-GUS* lines, four to six seedlings were fixed in ice cold 90% acetone for 1 h and washed in phosphate buffer prior to incubation in the GUS staining solution, which was vacuum infiltrated to obtain better staining. Incubation was performed as described above and stained tissue was fixed in 75% ethanol and 25% acetic acid for 2 h at RT. Chlorophyll of all stained seedlings was removed by incubation in 70% ethanol for 24 h (replaced by fresh ethanol occasionally). Seedlings were imaged with the Axio Imager M2 (Zeiss, 10x objective magnification). The Stitching function of the ZEN 2 BLUE Edition software (Zeiss) was applied to assemble single images to an image of the entire seedling.

Subcellular (co-) localization

To observe subcellular localization, proteins were tagged C-terminally to GFP and/or mCherry fluorophores and/or N-terminally to YFP fluorophore and expressed transiently in tobacco leaf epidermal cells. For N- and C-terminal fusions, coding sequences were amplified with and without the stop codon, respectively, from cDNA of Fe deficiency treated Arabidopsis WT roots with primers carrying B1 and B2 attachment sites, respectively, transferred into the entry vector pDONR207 (Invitrogen) via BP reactions (Gateway, Thermo Fisher Scientific), and sequenced. Final constructs were obtained by transferring all candidate genes subsequently into Gateway-compatible destination vectors pMDC83 (C-terminal GFP fusions) (Curtis and Grossniklaus, 2003), pH7WGY2 (N-terminal YFP) (Karimi et al., 2005), and β-estradiol-inducible pABind-GFP and pABind-mCherry (C-terminal GFP and mCherry fusions, used in co-localization studies) (Bleckmann et al., 2010) via LR reactions, and sequenced. The constructs were transformed into Agrobacteria as described in "Plant Material". A suspension (OD_{600}=0.4) of Agrobacteria carrying the construct of interest in infiltration solution (2 mM NaH_2PO_4, 0.5% (w/v) glucose, 50 mM MES, 100 µM acetosyringone (in DMSO), pH 5.6) was infiltrated into two leaves of the same tobacco plant with the help of a 1 ml syringe pressed to the abaxial leaf side. For co-localization of GFP-tagged and mCherry-tagged fusion proteins, corresponding Agrobacteria suspensions were mixed 1:1 (each to an OD_{600}=0.4) prior to infiltration. For more efficient

expression, Agrobacteria carrying the p19 plasmid were co-infiltrated (suppression of RNA interference) (Voinnet et al., 2003, 2015). Images in **Figure 7** and **Supplemental Figure S13 (3)** were taken with added p19. Transformed plants were kept at RT under long day conditions (16 h light, 8 h dark) and punched-out 0.5 cm leaf discs were imaged after 48-72 h with a LSM 510 meta confocal laser scanning microscope (Zeiss; **Figure 7 (A4, 5, 6), Supplemental Figure S13 (1, 2)**) or an Axio Imager M2 with ApoTome (Zeiss; **Figure 2C**, **Figure 7 (A1**, **2, 3, 7, 8), Supplemental Figure S13 (3)**). GFP and YFP were imaged at an excitation wavelength of 488 nm and emission wavelength of 500 to 530 nm, mCherry was imaged at an excitation wavelength at 563 nm and emission wavelength of 560 to 615 nm. Expression of pABind constructs was induced by spraying β-estradiol mix (20 µM β-estradiol (in DMSO), 0.1% (v/v) Tween20) to the abaxial leaf side 24-48 h post-infiltration. To capture the best moment of expression, which can vary between proteins, leaves were imaged 24 h and 48 h post-induction. The (co-)localization experiments were performed in at least two independent replicates with two infiltrated leaves each. Plasmolysis of cells expressing *BTSL1-GFP* was achieved through treatment of the leaf sample with 1 M mannitol solution for 30 min.

Bimolecular Fluorescence Complementation (BiFC)

Protein-protein interactions *in planta* were explored with BiFC in transiently transformed tobacco epidermal leaf cells. CDS' of gene pairs to be tested were amplified from cDNA of Fe deficiency treated Arabidopsis WT roots. Amplicons generated with primers carrying B3 and B2 attachment sites were transferred into pDONR221-P3P2 (Thermo Fisher Scientific, for nYFP fusion) and amplicons generated with primers carrying B1 and B4 attachment sites were transferred into pDONR221-P1P4 (Thermo Fisher Scientific, for cYFP fusion), respectively, via BP reactions (Gateway, Thermo Fisher Scientific). Primer sequences are listed in **Supplemental Table S1**. Inserts were sequenced. In a multisite Gateway LR reaction, both genes were transferred simultaneously into destination vector pBiFCt-2in1-NN (N-terminal nYFP and cYFP fusions) (Grefen and Blatt, 2012), performed according to the manufacturer's recommendations (Thermo Fisher Scientific), to create pBiFCt-2in1-NN: FEP3:BTSL1, pBiFCt-2in1-NN:PYE-BTSL1, pBiFCt-2in1-NN:PYE-BTSL1-C and pBiFCt-2in1-NN:ILR3-BTSL1-C. The constructs carry a monomeric red fluorescent protein (*mRFP*) as internal transformation control. Construct accuracy was verified by sequencing. Because "empty" split-YFP fusion proteins tend to self-assemble, thereby giving false positive signals (Kudla and Bock, 2016), we used structurally similar proteins known to not interact from previous experiments as negative controls (negative controls: pBiFCt-2in1-NN:ILR3-BTSL2-C, pBiFCt-2in1-NN:FIT-BTSL1-C). Constructs were transformed into Agrobacteria and subsequently infiltrated into tobacco leaves, as described in the previous section. 48 h to 52 h after infiltration, mRFP and YFP signals were detected in punched-out 0.5 cm leaf discs with an Axio Imager M2 (Zeiss). YFP was imaged at an excitation wavelength of 488 nm and emission

wavelength of 500 to 530 nm, mRFP was imaged at an excitation wavelength at 563 nm and emission wavelength of 560 to 615 nm. The BiFC experiments were performed in two independent replicates with two infiltrated leaves each. The vector pBiFCt-2in1-NN was kindly provided by Dr. Christopher Grefen, RUB, Bonn, Germany.

Gene Expression Analysis by RT-qPCR

Gene expression analysis was performed as described previously (Abdallah and Bauer, 2016). In brief, mRNA was extracted from whole seedlings grown in the 6 d system (n>60 per replicate) or from roots grown in the 14+3 d system (n>15 per replicate) (see "Plant Growth Conditions") and used for cDNA synthesis. RT-qPCR was performed using the iTaq™ Universal SYBR® Green Supermix (Bio-Rad) according to the manufacturer's recommendations and the SFX96 Touch™ RealTime PCR Detection System (Bio-Rad). Data was processed with the Bio-Rad SFX Manager™ software (version 3.1). Absolute gene expression values were calculated from a gene specific mass standard dilution series and normalized to the Arabidopsis elongation factor *EF1Bα*. Primers for mass standards and RT-qPCR are listed in **Supplemental Table S1**. The analysis was performed with three biological and two technical replicates.

Immunoblot analysis

Total proteins were extracted from ground plant material (tobacco leaves or Arabidopsis whole seedlings grown in the 6 d system, n=30-60 seedlings) with 2x Laemmli buffer (124 mM Tris-HCl, pH 6.8, 5% (w/v) SDS, 4% (w/v) dithithreitol, 20% (v/v) glycerol, with 0.002% (w/v) bromophenol blue) and denatured at 95°C for 10 min. Equal amounts of total protein (max. volume 15 µl) were separated on SDS-polyacrylamide gels, proteins were transferred to a Protran nitrocellulose membrane and stained with PonceauS as described in (Le et al., 2016). To detect HA_3-tagged FEP3 protein, the nitrocellulose membrane was blocked with 5% (w/v) milk powder solution (Roth) in 1xPBST (137 mM NaCl, 2.7 mM KCl, 10.14 mM Na_2HPO_4, 1.76 mM KH_2PO_4, 0.1% (v/v) Tween® 20, pH 7.4) for 30 min to avoid unspecific antibody (AB) binding, and subsequently incubated 1 h with anti-HA-peroxidase high-affinity monoclonal rat antibody (3F10; Roche [catalog no. 12013819001]) diluted 1:1000 in 2.5% (w/v) milk solution. After three wash steps, each for 15 min in PBST, the nitrocellulose membrane was imaged as described in (Le et al., 2016). Chemiluminescent protein bands were detected with the FluorChem Q system (ProteinSimple) and images were processed with the AlphaView® software (version 3.4.0.0, ProteinSimple).

Root Length Measurement

Arabidopsis WT, FEP3-OX and *btsl1 btsl2* double mutant lines were cultivated in the 6 d system (see "Plant Growth Conditions") and photographed at day six. Length of primary roots of individual seedlings was measured using the JMicroVision software (version 1.2.7, http://www.jmicrovision.com), as described previously (Ivanov et al., 2014). For calculation of mean root lengths and standard deviations, n=13-29 roots per line and condition were measured.

Colorimetric Seed Fe Content Measurement

To determine seed Fe content, 1-3 plants from each line were grown on soil under long day conditions (16 h light, 8 h dark, 21°C). Seeds were harvested, pooled by plant genotype, and dried for 16 h at 100°C. Fe was extracted from ground seed material by incubation in 500 µl 3% (v/v) HNO3 for 16 h at 100°C. Fe^{2+} content in the supernatant was determined as described in (Tamarit et al., 2006). In short, to 400 µl supernatant, 160 µl (38 g l^{-1}) $C_6H_7NaO_6$ (sodium ascorbate) was added to prevent oxidation, 320 µl (1.7 g l^{-1}) bathophenanthrolinedisulfonic acid disodium salt (BPDS, Fe^{2+} chelator) was added and 126 µl of a 33% $C_2H_7NO_2$ (ammonium acetate) solution (1 part saturated solution was diluted with 2 parts H_2O) was added to buffer the system. After an incubation time for 5 min at RT, absorption of the Fe^{2+}-BPDS complex was measured at a wavelength of 535 nm. Total Fe^{2+} content in the sample was calculated with the help of a standard curve (3.125 µM, 6.25 µM, 12.5 µM, 25 µM, 50 µM FeNaEDTA in 3% (v/v) HNO3) and normalized to seed dry weight (typically 1-5 mg). Per seed pool, n=3 samples were measured.

Chlorophyll Content Measurement

Chlorophyll content was measured in leaves of Arabidopsis lines grown in the 10 d system. Chlorophyll a and chlorophyll b were extracted with 100% acetone added to ground leaf material. The supernatant was collected and the washes were repeated until the collected acetone remained colorless. Absorbances of chlorophyll a and b were measured at a wavelength of 662 nm and 645 nm, respectively. Using the absorption coefficients that apply to 100% acetone, chlorophyll a concentration in the measured sample was calculated with $c_{Chl\text{-}a}$ [mg μl^{-1}]=11.75*A_{662}-2.35*A_{645} and chlorophyll b concentration was calculated with $c_{Chl\text{-}b}$ [mg μl^{-1}]=18.61*A_{645}-3.96*A_{662} (Lichtenthaler and Wellburn, 1983), where A is the absorbance at the indicated wavelength in nm. Values were normalized to fresh weight. Four biological replicates were measured, with each biological replicate containing n=5-7 rosettes.

Multiple Sequence alignments and protein sequence conservation

Multiple sequence alignments of BTS/BTSL1/BTSL2, ILR3/bHLH34/104/115/FEP3 and FEP3 orthologs were performed with ClustalX using default settings (Larkin et al., 2007). To determine

conservation scores of aa in BTSL1, the full BTSL1 aa sequence was uploaded to the Basic Local Alignment Search Tool (BLAST, (Altschul et al., 1990); https://blast.ncbi.nlm.nih.gov/) and run against the Viridiplantae database using the standard blastp (protein-protein BLAST) algorithm. The top 100 hits were downloaded, duplicates were removed and the remaining sequences were used for multiple sequence alignment using the Clustal Omega algorithm (Sievers et al., 2011) and visualized with Jalview ((Waterhouse et al., 2009); http://www.jalview.org/). The full aa sequence of FEP3 run against the Viridiplantae database as described above. Hits were only found within the Brassicaceae family, but alignments showed sequence conservation specifically towards the C-terminus. Subsequent blastp of the C-terminal half of FEP3 (25 aa) resulted in several angiosperm hits. FEP3 ortholog sequence hits from exemplary angiosperm orders were downloaded and aligned.

Statistical Analysis

Null hypothesis between normally distributed groups was tested with a two-tailed Student's t-test. Null hypothesis was rejected, when the *p*-value (*p*) was below 0.05. Statistically significantly different groups are indicated by one asterisk for $p<0.05$, two asterisks for $p<0.01$ and three asterisks for $p<0.001$. When comparing more than two groups, null hypotheses were tested with one-way analysis of variance (ANOVA) and a Tukey's post-hoc test. Null hypotheses were rejected when $p<0.05$. Statistically significantly different groups are indicated by different lower-case letters. Number of technical and biological repetitions of the individual experiments are indicated in the respective Methods sections and in the Figure legends.

Accession Numbers

AKT1 (AT2G26650), BHLH34 (AT3G23210), BHLH38 (AT3G56970), BHLH39 (AT3G56980), BHLH100 (AT2G41240), BHLH101 (AT5G04150), BHLH104 (AT4G14410), BTS (AT3G18290), BTSL1 (AT1G74770), BTSL2 (AT1G18910), CIPK23 (AT1G30270), DGAT3 (AT1G48300), DUF506 (AT1G12030), FEP3 (AT1G47400), FIT (AT2G28160), FRO2 (AT1G01580), FRO3 (AT1G23020), GRF11 (AT1G34760), ILR3 (AT5G54680), IRT1 (AT4G19690), JAL12 (AT1G52120), KELCH (AT3G07720), MYB72 (AT1G56160), NAS2 (AT5G56080), NAS4 (AT1G56430), ORG1 (AT5G53450), PRS2 (AT1G32380), PYE (AT3G47640), SDI1 (AT5G48850), S8H (AT3G12900), TCP20 (AT3G27010), UIP1 (AT1G73120), UIP2 (AT3G06890), UIP3 (AT3G56360), UIP4 (AT5G05250)

Supplemental Material

Supplemental Figure S1. Fe deficiency co-expression network and Y2H screen interaction summary.

Supplemental Figure S2. Original Y2H screen images (part 1).

Supplemental Figure S3. Original Y2H screen images (part 2).

Supplemental Figure S4. Verified "BTS(L) interactome" protein-protein interactions and non-interactions.

Supplemental Figure S5. Verified non-interactions between BTS, BTSL1, BTSL2 and different bHLH TFs.

Supplemental Figure S6. BTSL1/BTSL2/BTS multiple sequence alignment, protein domains and regions relevant in this study.

Supplemental Figure S7. FEP3 conserved domain.

Supplemental Figure S8. Multiple sequence alignment of IVc bHLHs and FEP3 to identify potential sequence similarities.

Supplemental Figure S9. The last 25 aa in ILR3 and bHLH104 are not crucial for interaction with BTSL1 or BTSL2.

Supplemental Figure S10. Validation of FEP3-OX and *btsl1 btsl2* mutant lines.

Supplemental Figure S11. Regulation of selected Fe deficiency response genes in whole seedlings of FEP3-OX and *btsl1-btls2*.

Supplemental Figure S12. *ProBTS* activity in two additional Arabidopsis lines, and FEP3-GUS protein localization in Arabidopsis seedlings.

Supplemental Figure S13. Peripheral localization of BTSL1 in tobacco leaf epidermis cells (additional images).

Supplemental Table S1. Primers used in this study.

Acknowledgements

We thank Elke Wieneke and Gintaute Matthäi for excellent technical assistance. We acknowledge the contributions of Sarah Plicht, Theresa Priebe, and Kai Blaeser. We thank Rumen Ivanov, Ksenia Trofimov, Inga Mohr, and Tzvetina Brumbarova for help and advice with microscopy and with the implementation of lab protocols. We thank Ksenia Trofimov for imaging of ILR3-GFP and YFP-bHLH104. D.M.L and B.S. are members of the international graduate school iGRAD-Plant, Düsseldorf. Funding from the German Research Foundation through the DFG International Research Training group 1525 to P.B. is greatly acknowledged. This work received funding from Germany's Excellence Strategy, EXC 2048/1, Project ID: 390686111.

Literature Cited

Abdallah HB, Bauer P (2016) Quantitative reverse transcription-qPCRbased gene expression analysis in plants. Methods Mol Biol **1363:** 9-24

Altschul SF, Gish W, Miller W, Myers EW, Lipman DJ (1990) Basic local alignment search tool. Journal of Molecular Biology **215:** 403-410

Aoki Y, Okamura Y, Tadaka S, Kinoshita K, Obayashi T (2016) ATTED-II in 2016: a plant coexpression database towards lineage-specific coexpression. Plant Cell Physiol **57:** e5

Bauer P (2016) Regulation of iron acquisition responses in plant roots by a transcription factor. Biochemistry and Molecular Biology Education **44:** 438-449

Bauer P, Ling HQ, Guerinot ML (2007) FIT, the FER-LIKE IRON DEFICIENCY INDUCED TRANSCRIPTION FACTOR in Arabidopsis. Plant Physiol Biochem **45:** 260-261

Belda-Palazon B, Julian J, Coego A, Wu Q, Zhang X, Batistic O, Alquraishi SA, Kudla J, An C, Rodriguez PL (2019) ABA inhibits myristoylation and induces shuttling of the RGLG1 E3 ligase to promote nuclear degradation of PP2CA. Plant J

Bensmihen S, To A, Lambert G, Kroj T, Giraudat J, Parcy F (2004) Analysis of an activated ABI5 allele using a new selection method for transgenic Arabidopsis seeds. Febs Letters **561:** 127-131

Bleckmann A, Weidtkamp-Peters S, Seidel CAM, Simon R (2010) Stem cell signaling in Arabidopsis requires CRN to localize CLV2 to the plasma membrane. Plant Physiology **152:** 166-176

Briat JF, Curie C, Gaymard F (2007) Iron utilization and metabolism in plants. Current Opinion in Plant Biology **10:** 276-282

Brumbarova T, Bauer P, Ivanov R (2015) Molecular mechanisms governing Arabidopsis iron uptake. Trends Plant Sci **20:** 124-133

Cabrera-Quio LE, Herberg S, Pauli A (2016) Decoding sORF translation - from small proteins to gene regulation. Rna Biology **13:** 1051-1059

Cheng MC, Hsieh EJ, Chen JH, Chen HY, Lin TP (2012) Arabidopsis RGLG2, functioning as a RING E3 ligase, interacts with AtERF53 and negatively regulates the plant drought stress response. Plant Physiology **158:** 363-375

Cheng MC, Hsieh EJ, Chen JH, Chen HY, Lin TP (2016) CORRECTION. Arabidopsis RGLG2, Functioning as a RING E3 Ligase, Interacts with AtERF53 and Negatively Regulates the Plant Drought Stress Response. Plant Physiology **170:** 1162-1163

Clough SJ, Bent AF (1998) Floral dip: a simplified method for *Agrobacterium*-mediated transformation of *Arabidopsis thaliana*. Plant Journal **16:** 735-743

Colangelo EP, Guerinot ML (2004) The essential basic helix-loop-helix protein FIT1 is required for the iron deficiency response. Plant Cell **16:** 3400-3412

Curie C, Mari S (2017) New routes for plant iron mining. New Phytologist **214:** 521-525

Curtis MD, Grossniklaus U (2003) A gateway cloning vector set for high-throughput functional analysis of genes in planta. Plant Physiology **133:** 462-469

Delcourt V, Staskevicius A, Salzet M, Fournier I, Roucou X (2018) Small proteins encoded by unannotated ORFs are rising stars of the proteome, confirming shortcomings in genome annotations and current vision of an mRNA. Proteomics **18**

Dong CH, Agarwal M, Zhang Y, Xie Q, Zhu JK (2006) The negative regulator of plant cold responses, HOS1, is a RING E3 ligase that mediates the ubiquitination and degradation of ICE1. Proc Natl Acad Sci U S A **103:** 8281-8286

Eide D, Broderius M, Fett J, Guerinot ML (1996) A novel iron-regulated metal transporter from plants identified by functional expression in yeast. Proc Natl Acad Sci U S A **93:** 5624-5628

Freemont PS (2000) Ubiquitination: RING for destruction? Curr Biol **10:** R84-87

Gao F, Robe K, Bettembourg M, Navarro N, Rofidal V, Santoni V, Gaymard F, Vignols F, Roschzttardtz H, Izquierdo E (2019) The Transcription Factor bHLH121 Interacts with bHLH105 (ILR3) and its Closest Homologs to Regulate Iron Homeostasis in Arabidopsis. The Plant Cell

Gao F, Robe K, Gaymard F, Izquierdo E, Dubos C (2019) The transcriptional control of iron homeostasis in plants: a tale of bHLH transcription factors? Frontiers in Plant Science **10**

García MJ, Corpas FJ, Lucena C, Alcántara E, Pérez-Vicente R, Zamarreño Á, Bacaicoa E, García-Mina JM, Bauer P, Romera FJ (2018) A shoot Fe signaling pathway requiring the OPT3 transporter controls GSNO reductase and ethylene in *Arabidopsis thaliana* roots. Front Plant Sci **9:** 1325

Garcia MJ, Romera FJ, Stacey MG, Stacey G, Villar E, Alcantara E, Perez-Vicente R (2013) Shoot to root communication is necessary to control the expression of iron-acquisition genes in Strategy I plants. Planta **237:** 65-75

Gietz RD, Schiestl RH (2007) High-efficiency yeast transformation using the LiAc/SS carrier DNA/PEG method. Nature Protocols **2:** 31-34

Graceffa P, Jancsó A, Mabuchi K (1992) Modification of acidic residues normalizes sodium dodecyl sulfate-polyacrylamide gel electrophoresis of caldesmon and other proteins that migrate anomalously. Archives of Biochemistry and Biophysics **297:** 46-51

Gratz R, Manishankar P, Ivanov R, Köster P, Mohr I, Trofimov K, Steinhorst L, Meiser J, Mai HJ, Drerup M, Arendt S, Holtkamp M, Karst U, Kudla J, Bauer P, Brumbarova T (2019) CIPK11-dependent phosphorylation modulates FIT activity to promote Arabidopsis iron acquisition in response to calcium signaling. Dev Cell

Grefen C, Blatt MR (2012) A 2in1 cloning system enables ratiometric bimolecular fluorescence complementation (rBiFC). Biotechniques **53:** 311-314

Grillet L, Lan P, Li WF, Mokkapati G, Schmidt W (2018) IRON MAN is a ubiquitous family of peptides that control iron transport in plants. Nature Plants **4:** 953-+

Heim MA, Jakoby M, Werber M, Martin C, Weisshaar B, Bailey PC (2003) The basic helix-loop-helix transcription factor family in plants: a genome-wide study of protein structure and functional diversity. Mol Biol Evol **20:** 735-747

Hell R, Stephan UW (2003) Iron uptake, trafficking and homeostasis in plants. Planta **216:** 541-551

Hindt MN, Akmakjian GZ, Pivarski KL, Punshon T, Baxter I, Salt DE, Guerinot ML (2017) BRUTUS and its paralogs, BTS LIKE1 and BTS LIKE2, encode important negative regulators of the iron deficiency response in *Arabidopsis thaliana*. Metallomics **9:** 876-890

Hirayama T, Lei GJ, Yamaji N, Nakagawa N, Ma JF (2018) The putative peptide gene FEP1 regulates iron deficiency response in Arabidopsis. Plant and Cell Physiology **59:** 1739-1752

Hsu PY, Benfey PN (2018) Small but mighty: functional peptides encoded by small ORFs in plants. Proteomics **18:** e1700038

Huang TK, Han CL, Lin SI, Chen YJ, Tsai YC, Chen YR, Chen JW, Lin WY, Chen PM, Liu TY, Chen YS, Sun CM, Chiou TJ (2013) Identification of downstream components of ubiquitin-conjugating enzyme PHOSPHATE2 by quantitative membrane proteomics in Arabidopsis roots. Plant Cell **25:** 4044-4060

Ivanov R, Brumbarova T, Bauer P (2012) Fitting into the harsh reality: regulation of iron-deficiency responses in dicotyledonous plants. Mol Plant **5:** 27-42

Ivanov R, Brumbarova T, Blum A, Jantke AM, Fink-Straube C, Bauer P (2014) SORTING NEXIN1 is required for modulating the trafficking and stability of the Arabidopsis IRON-REGULATED TRANSPORTER1. Plant Cell **26:** 1294-1307

Jakoby M, Wang HY, Reidt W, Weisshaar B, Bauer P (2004) FRU (BHLH029) is required for induction of iron mobilization genes in Arabidopsis thaliana. FEBS Lett **577:** 528-534

Jefferson RA, Kavanagh TA, Bevan MW (1987) GUS fusions: β-glucuronidase as a sensitive and versatile gene fusion marker in higher plants. Embo Journal **6:** 3901-3907

Karimi M, De Meyer B, Hilson P (2005) Modular cloning in plant cells. Trends in Plant Science **10:** 103-105

Khan MA, Castro-Guerrero NA, McInturf SA, Nguyen NT, Dame AN, Wang J, Bindbeutel RK, Joshi T, Jurisson SS, Nusinow DA, Mendoza-Cozatl DG (2018) Changes in iron availability in Arabidopsis are rapidly sensed in the leaf vasculature and impaired sensing leads to opposite transcriptional programs in leaves and roots. Plant Cell Environ

Kim SA, LaCroix IS, Gerber SA, Guerinot ML (2019) The iron deficiency response in Arabidopsis thaliana requires the phosphorylated transcription factor URI. Proceedings of the National Academy of Sciences

Klatte M (2008) Characterisation of the nicotianamine synthase gene family in *Arabidopsis thaliana* in the context of metal homeostasis. Saarländische Universitäts- und Landesbibliothek **[Dissertation]:** doi:10.22028/D22291-22550

Klatte M, Schuler M, Wirtz M, Fink-Straube C, Hell R, Bauer P (2009) The analysis of Arabidopsis nicotianamine synthase mutants reveals functions for nicotianamine in seed iron loading and iron deficiency responses. Plant Physiol **150:** 257-271

Kobayashi T (2019) Understanding the complexity of iron sensing and signaling cascades in plants. Plant and Cell Physiology **60:** 1440-1446

Kobayashi T, Nagasaka S, Senoura T, Itai RN, Nakanishi H, Nishizawa NK (2013) Iron-binding haemerythrin RING ubiquitin ligases regulate plant iron responses and accumulation. Nat Commun **4:** 2792

Kobayashi T, Nozoye T, Nishizawa NK (2018) Iron transport and its regulation in plants. Free Radic Biol Med

Koncz C, Schell J (1986) The promoter of T_L-DNA gene *5* controls the tissue-specific expression of chimeric genes carried by a novel type of Agrobacterium binary vector. Molecular & General Genetics **204:** 383-396

Kudla J, Bock R (2016) Lighting the way to protein-protein interactions: recommendations on best practices for Bimolecular Fluorescence Complementation analyses. Plant Cell **28:** 1002-1008

Kumar RK, Chu HH, Abundis C, Vasques K, Rodriguez DC, Chia JC, Huang R, Vatamaniuk OK, Walker EL (2017) Iron-nicotianamine transporters are required for proper long distance iron signaling. Plant Physiol **175:** 1254-1268

Larkin MA, Blackshields G, Brown NP, Chenna R, McGettigan PA, McWilliam H, Valentin F, Wallace IM, Wilm A, Lopez R, Thompson JD, Gibson TJ, Higgins DG (2007) Clustal W and clustal X version 2.0. Bioinformatics **23:** 2947-2948

Le CTT, Brumbarova T, Ivanov R, Stoof C, Weber E, Mohrbacher J, Fink-Straube C, Bauer P (2016) ZINC FINGER OF ARABIDOPSIS THALIANA12 (ZAT12) interacts with FER-LIKE IRON DEFICIENCY-INDUCED TRANSCRIPTION FACTOR (FIT) linking iron deficiency and oxidative stress responses. Plant Physiology **170:** 540-557

Lee H, Xiong L, Gong Z, Ishitani M, Stevenson B, Zhu JK (2001) The Arabidopsis HOS1 gene negatively regulates cold signal transduction and encodes a RING finger protein that displays cold-regulated nucleo-cytoplasmic partitioning. Genes & development **15:** 912-924

Li X, Zhang H, Ai Q, Liang G, Yu D (2016) Two bHLH transcription factors, bHLH34 and bHLH104, regulate iron homeostasis in *Arabidopsis thaliana*. Plant Physiol **170:** 2478-2493

Li Y, Lei R, Pu M, Cai Y, Lu C, Li Z, Liang G (2020) bHLH11 negatively regulates Fe homeostasis by its EAR motifs recruiting corepressors in Arabidopsis. bioRxiv

Liang G, Zhang H, Li X, Ai Q, Yu D (2017) bHLH transcription factor bHLH115 regulates iron homeostasis in *Arabidopsis thaliana*. J Exp Bot **68:** 1743-1755

Lichtenthaler HK, Wellburn AR (1983) Determinations of total carotenoids and chlorophylls a and b of leaf extracts in different solvents. Biochemical Society Transactions **11:** 591-592

Lindsay WL (1988) Solubility and redox equilibria of iron compounds in soils. *In* S J.W., G B.A., S U., eds, Iron in Soils and Clay Minerals, Vol 217. Springer, Dordrecht, p 894

Lingam S, Mohrbacher J, Brumbarova T, Potuschak T, Fink-Straube C, Blondet E, Genschik P, Bauer P (2011) Interaction between the bHLH transcription factor FIT and ETHYLENE INSENSITIVE3/ETHYLENE INSENSITIVE3-LIKE1 reveals molecular linkage between the regulation of iron acquisition and ethylene signaling in Arabidopsis. Plant Cell **23:** 1815-1829

Liu YG, Mitsukawa N, Oosumi T, Whittier RF (1995) Efficient isolation and mapping of *Arabidopsis thaliana* T-DNA insert junctions by thermal asymmetric interlaced PCR. Plant Journal **8:** 457-463

Liu YG, Whittier RF (1995) Thermal Asymmetric Interlaced PCR: automatable amplification and sequencing of insert end fragments from P1 and YAC clones for chromosome walking. Genomics **25:** 674-681

Long TA, Tsukagoshi H, Busch W, Lahner B, Salt DE, Benfey PN (2010) The bHLH transcription factor POPEYE regulates response to iron deficiency in Arabidopsis roots. Plant Cell **22:** 2219-2236

Mai HJ, Pateyron S, Bauer P (2016) Iron homeostasis in *Arabidopsis thaliana*: transcriptomic analyses reveal novel FIT-regulated genes, iron deficiency marker genes and functional gene networks. BMC Plant Biol **16:** 211

Makarewich CA, Olson EN (2017) Mining for Micropeptides. Trends Cell Biol **27:** 685-696

Marschner H, Römheld V (1994) Strategies of plants for acquisition of iron. Plant and Soil **165:** 261-274

Matthiadis A, Long TA (2016) Further insight into BRUTUS domain composition and functionality. Plant Signal Behav **11:** e1204508

Nakagawa T, Kurose T, Hino T, Tanaka K, Kawamukai M, Niwa Y, Toyooka K, Matsuoka K, Jinbo T, Kimura T (2007) Development of series of gateway binary vectors, pGWBs, for realizing efficient construction of fusion genes for plant transformation. Journal of Bioscience and Bioengineering **104:** 34-41

Naranjo-Arcos MA, Maurer F, Meiser J, Pateyron S, Fink-Straube C, Bauer P (2017) Dissection of iron signaling and iron accumulation by overexpression of subgroup Ib bHLH039 protein. Scientific Reports **7**

Naranjo Arcos MA (2017) Investigating the role of the iron dependent bHLH039 transcription factor in coordinating Fe homeostasis in *Arabidopsis thaliana*. Saarländische Universitäts- und Landesbibliothek **[Dissertation]:** doi:10.22028/D22291-26817

Nouet C, Motte P, Hanikenne M (2011) Chloroplastic and mitochondrial metal homeostasis. Trends Plant Sci **16:** 395-404

Ohkubo Y, Tanaka M, Tabata R, Ogawa-Ohnishi M, Matsubayashi Y (2017) Shoot-to-root mobile polypeptides involved in systemic regulation of nitrogen acquisition. Nat Plants **3:** 17029

Palmer CM, Hindt MN, Schmidt H, Clemens S, Guerinot ML (2013) MYB10 and MYB72 are required for growth under iron-limiting conditions. PLoS Genet **9:** e1003953

Peterman TK, Ohol YM, McReynolds LJ, Luna EJ (2004) Patellin1, a novel Sec14-like protein, localizes to the cell plate and binds phosphoinositides. Plant Physiology **136:** 3080-3094; discussion 3001-3082

Robinson NJ, Procter CM, Connolly EL, Guerinot ML (1999) A ferric-chelate reductase for iron uptake from soils. Nature **397:** 694-697

Rodriguez-Celma J, Chou H, Kobayashi T, Long TA, Balk J (2019) Hemerythrin E3 Ubiquitin Ligases as Negative Regulators of Iron Homeostasis in Plants. Front Plant Sci **10:** 98

Rodríguez-Celma J, Chou H, Kobayashi T, Long TA, Balk J (2019) Hemerythrin E3 ubiquitin ligases as negative regulators of iron homeostasis in plants. Frontiers in plant science **10:** 98

Rodríguez-Celma J, Connorton JM, Kruse I, Green RT, Franceschetti M, Chen Y-T, Cui Y, Ling H-Q, Yeh K-C, Balk J (2019) Arabidopsis BRUTUS-LIKE E3 ligases negatively regulate iron uptake by targeting transcription factor FIT for recycling. Proceedings of the National Academy of Sciences**:** 201907971

Rodríguez-Celma J, Green RT, Connorton JM, Kruse I, Cui Y, Ling HQ, Balk J (2017) BRUTUS-LIKE proteins moderate the transcriptional response to iron deficiency in roots. *bioRxiv* **[Preprint]:** doi.org/10.1101/231365

Salahudeen AA, Thompson JW, Ruiz JC, Ma HW, Kinch LN, Li Q, Grishin NV, Bruick RK (2009) An E3 ligase possessing an iron-responsive hemerythrin domain is a regulator of iron homeostasis. Science **326:** 722-726

Samira R, Li BH, Kliebenstein D, Li CY, Davis E, Gillikin JW, Long TA (2018) The bHLH transcription factor ILR3 modulates multiple stress responses in Arabidopsis. Plant Molecular Biology **97:** 297-309

Schmid NB, Giehl RF, Döll S, Mock HP, Strehmel N, Scheel D, Kong X, Hider RC, von Wirén N (2014) Feruloyl-CoA 6'-Hydroxylase1-dependent coumarins mediate iron acquisition from alkaline substrates in Arabidopsis. Plant Physiol **164:** 160-172

Schuler M (2011) The role of nicotianamine in the metal homeostasis of *Arabidopsis thaliana*. Saarländische Universitäts- und Landesbibliothek **[Dissertation]:** doi:10.22028/D22291-22738

Schuler M, Rellán-Álvarez R, Fink-Straube C, Abadía J, Bauer P (2012) Nicotianamine functions in the phloem-based transport of iron to sink organs, in pollen development and pollen tube growth in Arabidopsis. Plant Cell **24:** 2380-2400

Schwarz B, Bauer P (2020) FIT, a regulatory hub for iron deficiency and stress signaling in roots, and FIT-dependent and-independent gene signatures. Journal of Experimental Botany

Selote (2015) Iron Binding E3 Ligase Mediates Iron response in Plants by targeting basic helix loop helix transcription factors Plant Physiology

Selote D, Samira R, Matthiadis A, Gillikin JW, Long TA (2015) Iron-binding E3 ligase mediates iron response in plants by targeting basic helix-loop-helix transcription factors. Plant Physiol **167:** 273-286

Sievers F, Wilm A, Dineen D, Gibson TJ, Karplus K, Li WZ, Lopez R, McWilliam H, Remmert M, Söding J, Thompson JD, Higgins DG (2011) Fast, scalable generation of high-quality protein multiple sequence alignments using Clustal Omega. Molecular Systems Biology **7**

Sivitz A, Grinvalds C, Barberon M, Curie C, Vert G (2011) Proteasome-mediated turnover of the transcriptional activator FIT is required for plant iron-deficiency responses. Plant Journal **66:** 1044-1052

Sivitz AB, Hermand V, Curie C, Vert G (2012) Arabidopsis bHLH100 and bHLH101 control iron homeostasis via a FIT-independent pathway. PLoS One **7:** e44843

Stührwohldt N, Schaller A (2019) Regulation of plant peptide hormones and growth factors by post-translational modification. Plant Biol (Stuttg) **21 Suppl 1:** 49-63

Tabata R, Sumida K, Yoshii T, Ohyama K, Shinohara H, Matsubayashi Y (2014) Perception of root-derived peptides by shoot LRR-RKs mediates systemic N-demand signaling. Science **346:** 343-346

Tamarit J, Irazusta V, Moreno-Cermeño A, Ros J (2006) Colorimetric assay for the quantitation of iron in yeast. Analytical Biochemistry **351:** 149-151

Tanabe N, Noshi M, Mori D, Nozawa K, Tamoi M, Shigeoka S (2019) The basic helix-loop-helix transcription factor, bHLH11 functions in the iron-uptake system in Arabidopsis thaliana. Journal of plant research **132:** 93-105

Tissot N, Robe K, Gao F, Grant-Grant S, Boucherez J, Bellegarde F, Maghiaoui A, Marcelin R, Izquierdo E, Benhamed M, Martin A, Vignols F, Roschzttardtz H, Gaymard F, Briat JF, Dubos C (2019) Transcriptional integration of the responses to iron availability in Arabidopsis by the bHLH factor ILR3. New Phytol

Tottey S, Block MA, Allen M, Westergren T, Albrieux C, Scheller HV, Merchant S, Jensen PE (2003) Arabidopsis CHL27, located in both envelope and thylakoid membranes, is required for the synthesis of protochlorophyllide. Proc Natl Acad Sci U S A **100:** 16119-16124

Tsugeki R, Kochieva EZ, Fedoroff NV (1996) A transposon insertion in the Arabidopsis SSR16 gene causes an embryo-defective lethal mutation. Plant Journal **10:** 479-489

Vert G, Grotz N, Dedaldechamp F, Gaymard F, Guerinot ML, Briat JF, Curie C (2002) IRT1, an Arabidopsis transporter essential for iron uptake from the soil and for plant growth. Plant Cell **14:** 1223-1233

Vert GA, Briat JF, Curie C (2003) Dual regulation of the Arabidopsis high-affinity root iron uptake system by local and long-distance signals. Plant Physiology **132:** 796-804

Voinnet O, Rivas S, Mestre P, Baulcombe D (2003) An enhanced transient expression system in plants based on suppression of gene silencing by the p19 protein of tomato bushy stunt virus (Retracted article. See vol. 84, pg. 846, 2015). Plant Journal **33:** 949-956

Voinnet O, Rivas S, Mestre P, Baulcombe D (2015) An enhanced transient expression system in plants based on suppression of gene silencing by the p19 protein of tomato bushy stunt virus (Retraction of Vol 33, Pg 949, 2003). Plant Journal **84:** 846-846

von Wirén N, Klair S, Bansal S, Briat JF, Khodr H, Shioiri T, Leigh RA, Hider RC (1999) Nicotianamine chelates both Fe-III and Fe-II. Implications for metal transport in plants. Plant Physiology **119:** 1107-1114

Wang HY, Klatte M, Jakoby M, Bäumlein H, Weisshaar B, Bauer P (2007) Iron deficiency-mediated stress regulation of four subgroup Ib BHLH genes in *Arabidopsis thaliana*. Planta **226:** 897-908

Wang N, Cui Y, Liu Y, Fan H, Du J, Huang Z, Yuan Y, Wu H, Ling HQ (2013) Requirement and functional redundancy of Ib subgroup bHLH proteins for iron deficiency responses and uptake in *Arabidopsis thaliana*. Mol Plant **6:** 503-513

Waterhouse AM, Procter JB, Martin DMA, Clamp M, Barton GJ (2009) Jalview Version 2-a multiple sequence alignment editor and analysis workbench. Bioinformatics **25:** 1189-1191

Wedepohl KH (1995) The composition of the continental crust. Geochimica Et Cosmochimica Acta **59:** 1217-1232

Xu J, Li HD, Chen LQ, Wang Y, Liu LL, He L, Wu WH (2006) A protein kinase, interacting with two calcineurin B-like proteins, regulates K^+ transporter AKT1 in Arabidopsis. Cell **125:** 1347-1360

Yang JL, Chen WW, Chen LQ, Qin C, Jin CW, Shi YZ, Zheng SJ (2013) The 14-3-3 protein GENERAL REGULATORY FACTOR11 (GRF11) acts downstream of nitric oxide to regulate iron acquisition in *Arabidopsis thaliana*. New Phytol **197:** 815-824

Young JM, Kuykendall LD, Martinez-Romero E, Kerr A, Sawada H (2001) A revision of Rhizobium Frank 1889, with an emended description of the genus, and the inclusion of all species of *Agrobacterium* Conn 1942 and *Allorhizobium undicola* de Lajudie *et al.* 1998 as new combinations: *Rhizobium radiobacter*, *R. rhizogenes*, *R. rubi*, *R. undicola* and *R. vitis*. International Journal of Systematic and Evolutionary Microbiology **51:** 89-103

Yuan Y, Wu H, Wang N, Li J, Zhao W, Du J, Wang D, Ling HQ (2008) FIT interacts with AtbHLH38 and AtbHLH39 in regulating iron uptake gene expression for iron homeostasis in Arabidopsis. Cell Res **18:** 385-397

Zanet J, Benrabah E, Li T, Pélissier-Monier A, Chanut-Delalande H, Ronsin B, Bellen HJ, Payre F, Plaza S (2015) Pri sORF peptides induce selective proteasome-mediated protein processing. Science **349:** 1356-1358

Zhai Z, Gayomba SR, Jung HI, Vimalakumari NK, Piñeros M, Craft E, Rutzke MA, Danku J, Lahner B, Punshon T, Guerinot ML, Salt DE, Kochian LV, Vatamaniuk OK (2014) OPT3 is a phloem-specific iron transporter that is essential for systemic iron signaling and redistribution of iron and cadmium in Arabidopsis. Plant Cell **26:** 2249-2264

Zhang J, Liu B, Li M, Feng D, Jin H, Wang P, Liu J, Xiong F, Wang J, Wang HB (2015) The bHLH transcription factor bHLH104 interacts with IAA-LEUCINE RESISTANT3 and modulates iron homeostasis in Arabidopsis. Plant Cell **27:** 787-805

Supplemental Figures and Tables

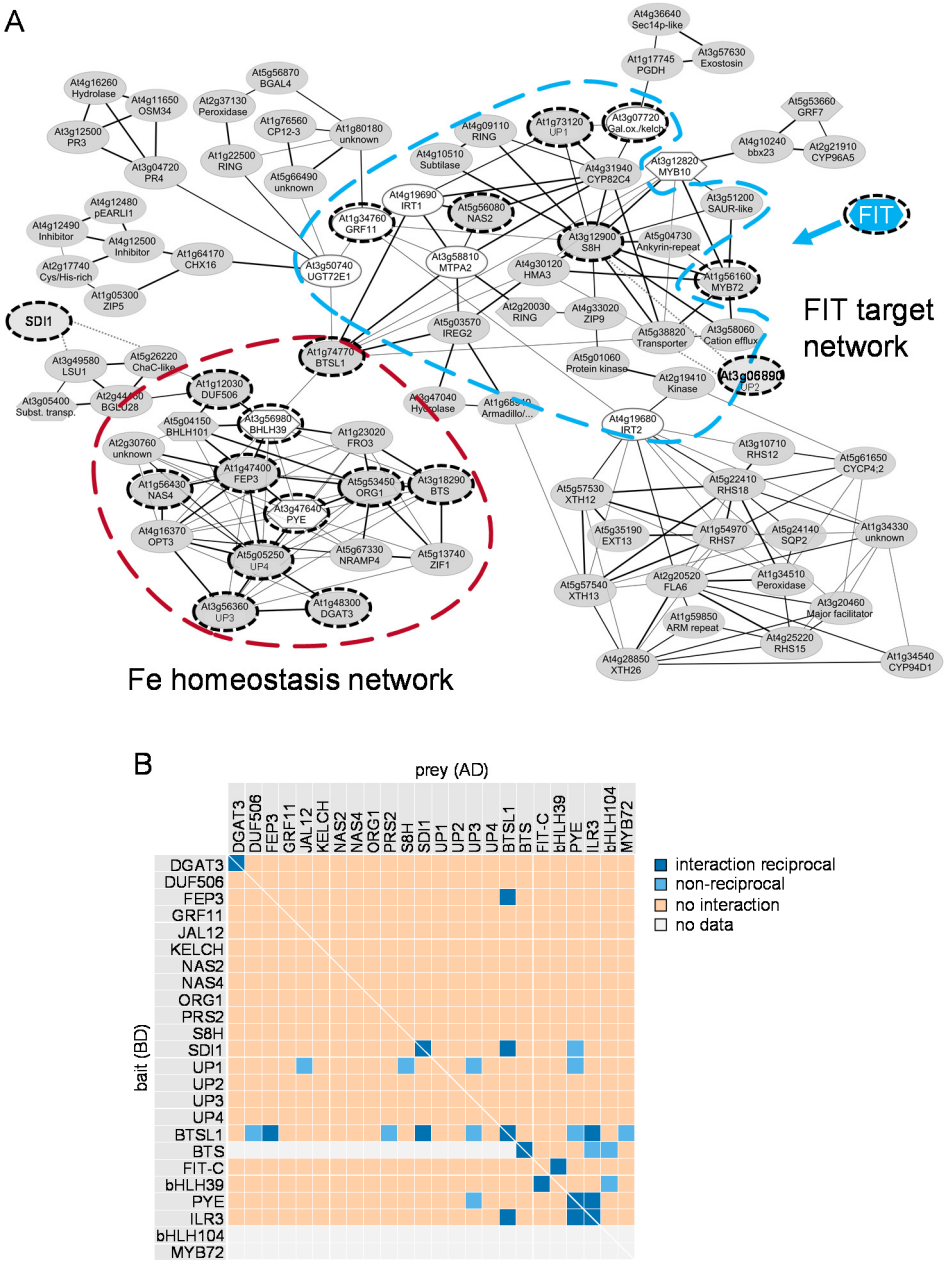

Figure S1. Fe deficiency co-expression network and Y2H screen interaction summary.
A: Genes up-regulated under Fe deficiency stress. Highlighted sub-networks: Root-specific FIT target genes (blue dashed line), root- and shoot-expressed FIT-independent genes (red dashed line). The network was generated with the ATTED-II tool (Ver. 8.0), using the white labeled genes as basis, and visualized with Cytoscape. The network is an updated version of (Ivanov et al., 2012). Candidate genes used in the Y2H screen are highlighted with a dashed border. Candidate genes *ILR3*, *BHLH104*, *PRS2*, *JAL12* do not appear in the network. SDI1 and UP2 appeared in an older ATTED-II (Ver. 7.1) network version, initially used to select candidates.
B: Summary of all protein-protein interactions detected with the Y2H screen. 24 candidates were tested reciprocally in all possible combinations. Bait: protein fused to the GAL4 DNA-binding domain (BD), prey: protein fused to the GAL4 activation domain (AD). The color code distinguishes reciprocal interactions (dark blue), non-reciprocal interactions (light blue), no interactions (light orange). Gray: no data. BD-bHLH104 and BD-MYB72 could not be tested because the proteins auto-activated the Y2H system. Original images and negative controls: **Supplemental Figures S2, S3**.

Figure S2. Original Y2H screen images (part 1).

Targeted Y2H screen between 17 candidates (all non-TFs except BTS) in all pair-wise combinations including homodimerization. Yeast containing both AD- and BD-plasmids were obtained by mating of single transformants and spotted as A_{600}=1 on SD-LW (mating control) and SD-LWH supplemented with different concentrations of 3AT (selection for protein interaction). Positive control (+ control): CIPK23/cAKT1 (Xu et al., 2006); negative controls (empty): AD-protein/empty and BD-protein/empty. Rows should be read in pairs: Each upper row tests interaction between an AD-protein and the protein shown in column header (as BD-fusion). Each lower row tests the reciprocal interaction. All protein pairs appear twice in the matrix, except homodimerization (black x). Protein names in rows appear in same order as in **Supplemental Figure S1B**. Protein names in column header appear in different order (order in which yeast transformants were spotted during the experiment).

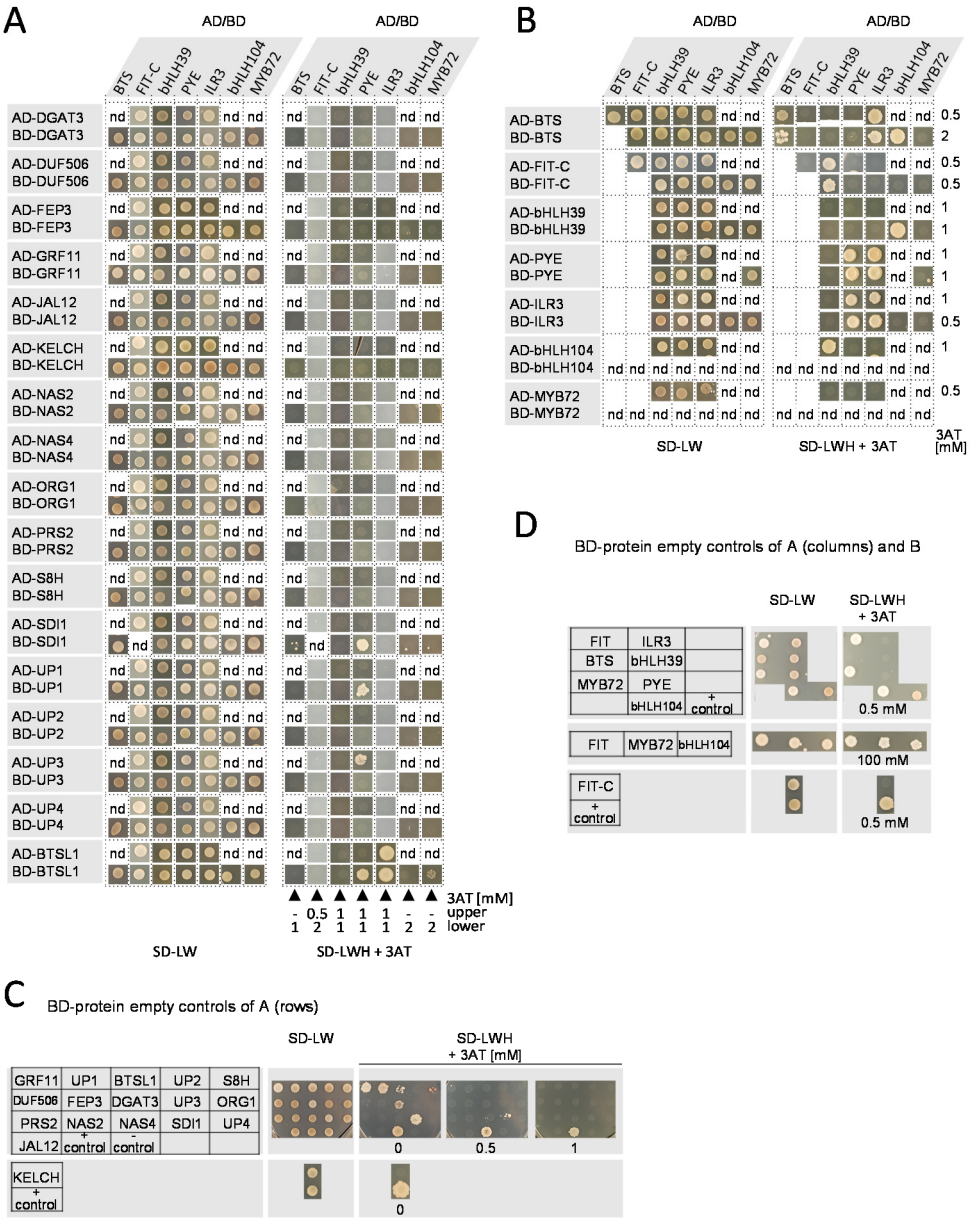

Figure S3. Original Y2H screen images (part 2).

A: Targeted Y2H screen between the 17 candidates shown in part 1 (rows) (**Supplemental Figure S2**) and the 7 remaining candidates (columns) (6 TFs and BTS).

B: Targeted Y2H screen between 6 TFs and BTS in all pair-wise combinations, including homodimerization. Except BTS and FIT-C, all protein pairs appear twice in the matrix. Interaction between AD-bHLH104/BD-bHLH39 could not be verified (see **Supplemental Figure S5B**).

C: Determining the 3AT concentration necessary to suppress background activity induced by the 17 non-TF BD-fusions (= BD-protein/empty negative controls). Positions of protein names in the table correspond to yeast spot positions in the images. Negative controls correspond to the 17 BD-proteins in A (rows). Positive control (+ control): CIPK23/cAKT1 (Xu et al., 2006); negative control of the Y2H system (- control): empty/empty.

D: Determining necessary 3AT concentration for TFs and BTS BD-fusions. Negative controls correspond to the 7 BD-proteins in A (columns) and in B (rows and columns), and of full-length FIT (see also Supplemental Figure S5). Control as described in C.

A, B: Yeast containing both AD- and BD-plasmids were obtained by mating of single transformants and spotted as described in **Supplemental Figure S2**. Rows should be read in pairs: Each upper row tests interaction between an AD-protein and the protein shown in column header (as BD-fusion). Each lower row tests the reciprocal interaction. FIT-C: C-terminal part of FIT. nd: no data. BD-bHLH104 and BD-MYB could not be tested because the proteins auto-activated the Y2H system.

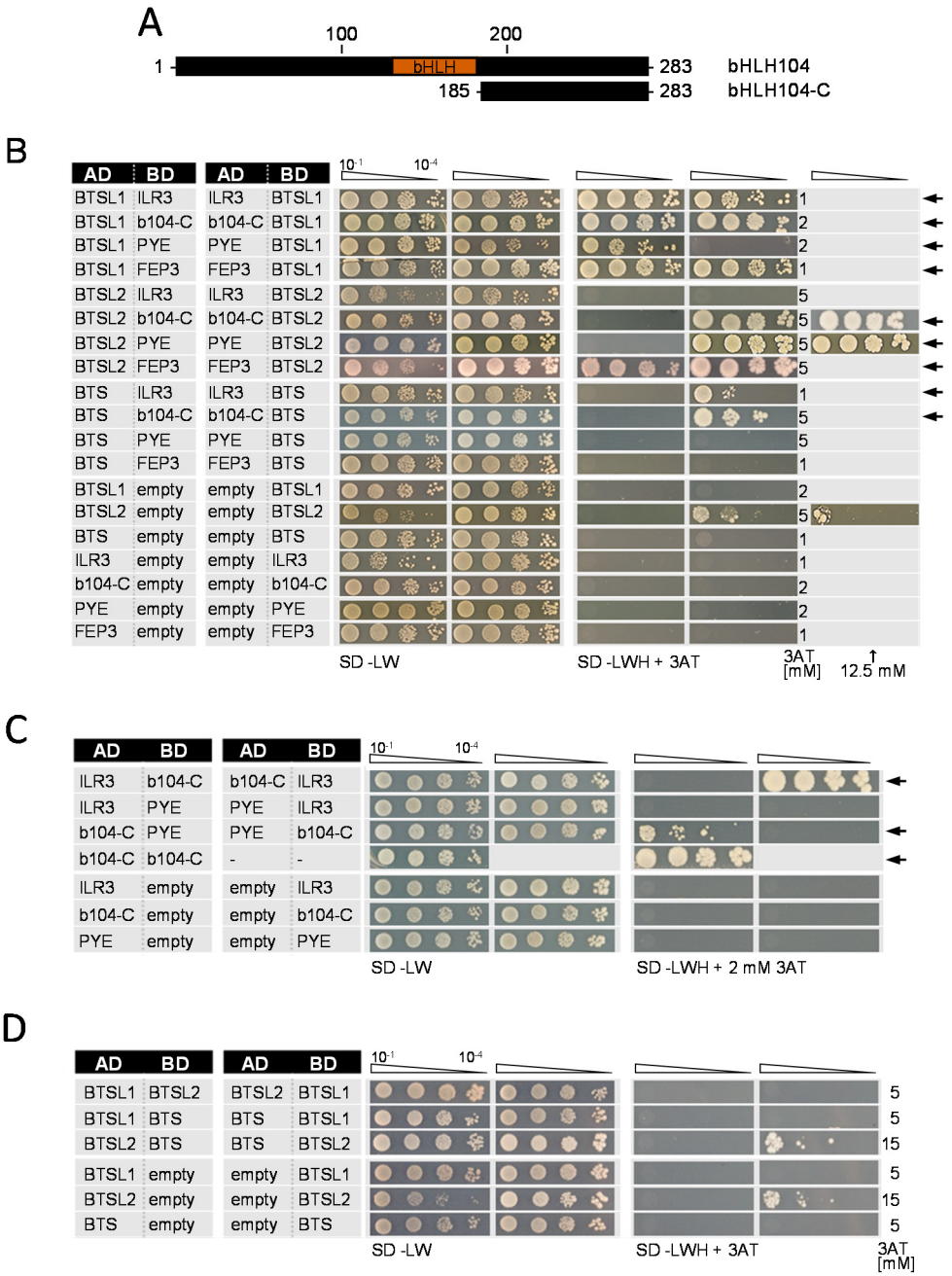

Figure S4. Verified "BTS(L) interactome" protein-protein interactions and non-interactions.
A: Schematic representation of full-length bHLH104 and its C-terminal part lacking the DNA binding domain (bHLH104-C). Because BD-bHLH104 was auto-activating the Y2H system (see **Supplemental Figure S3D**) bHLH104-C was used in all Y2H except the Y2H screen. Protein domain structure based on information deposited on UniProt (www.uniprot.org).
B-D: Reciprocal targeted Y2H protein interaction assays between different combinations of "BTS(L) interactome" proteins. Yeast co-transformed with the AD and BD combinations were spotted in 10-fold dilution series (A_{600}=10^{-1}-10^{-4}) on SD-LW (transformation control) and SD-LWH supplemented with different concentrations of 3AT (selection for protein intraction). Negative controls: empty AD/BD-proteins and empty BD/AD proteins. Arrows indicate interaction.
B: Interactions of BTSL1, BTSL2, BTS with ILR3, bHLH104-C (b104-C), PYE, FEP3. BD-BTSL2 was spotted additionally on higher 3AT concentrations to better distinguish interaction and auto-activation.
C: Interactions of ILR3, bHLH104-C, PYE amongst each other and homodimerization of bHLH104-C.
D: Interactions of BTSL1, BTSL2, BTS amongst each other.

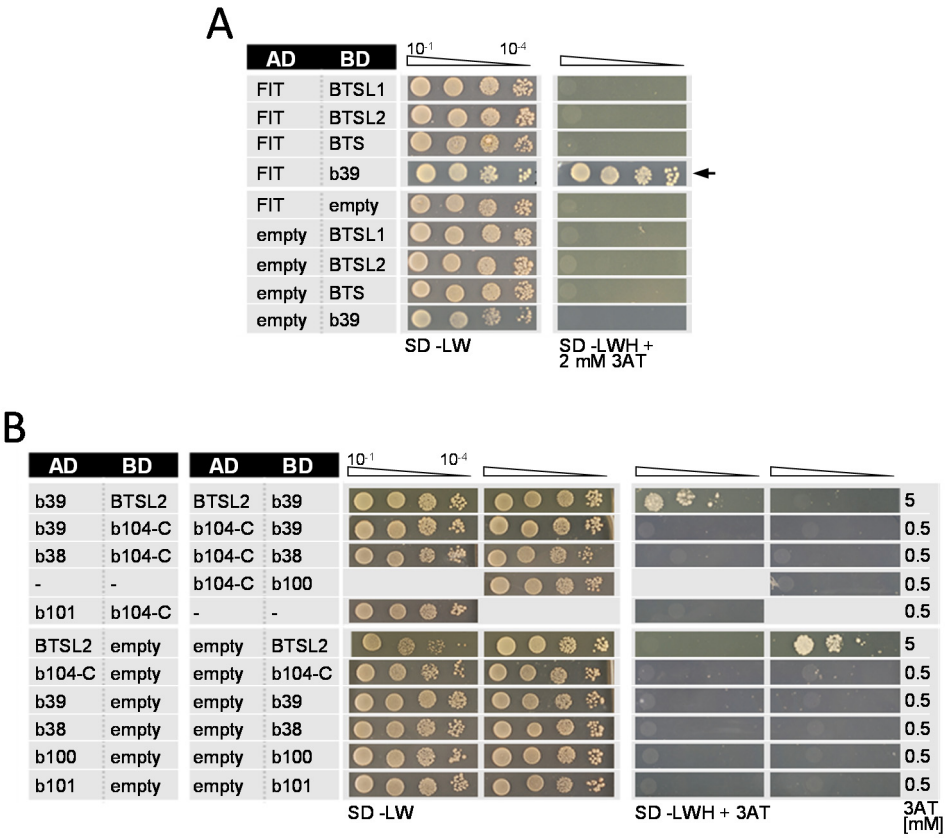

Figure S5. Verified non-interactions between BTS, BTSL1, BTSL2 and different bHLH TFs.
A: Full-length AD-FIT does not interact with BD-BTSL1, BD-BTSL2, BD-BTS in yeast. The known interaction between FIT and b39 (bHLH39) served as positive control (arrow). BD-FIT was not tested because it auto-activates the Y2H system (see **Supplemental Figure S3D**).
B: BTSL2 does not interact with b39. Tested for sake of completeness because BTSL2 was missing in the Y2H screen. b104-C (bHLH104-C) does not interact with b38, b39, b100, b101. Combinations were tested to verify the expected non-interactions (reported as negative in (Zhang et al., 2015)).
A, B: Yeast co-transformed with the AD and BD combinations were spotted as described in **Supplemental Figure S4**.

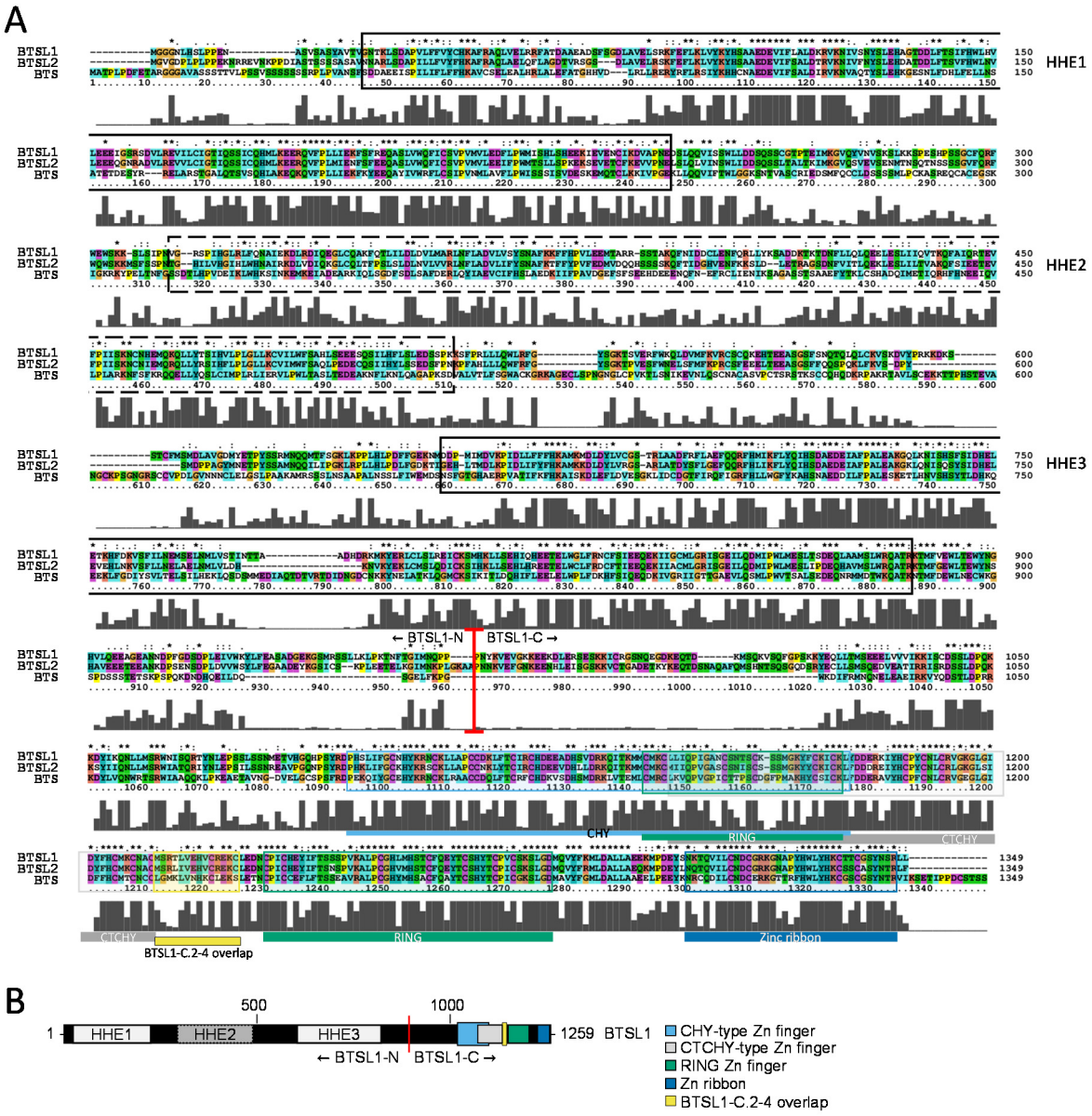

Figure S6. BTSL1/BTSL2/BTS multiple sequence alignment, protein domains and regions relevant in this study.
A: Multiple sequence alignment of BTSL1, BTSL2 and BTS protein sequences. Predicted HHE domains (Rodriguez-Celma et al., 2019) and C-terminal domains (InterPro; (Mitchell et al., 2019)) are indicated. Putative interacting region in BTSL1 indicated in yellow (BTSL1-C.2-4 overlap) (see also **Figure 3**).
B: Schematic representation of BTSL1 protein structure, including all features shown in A.

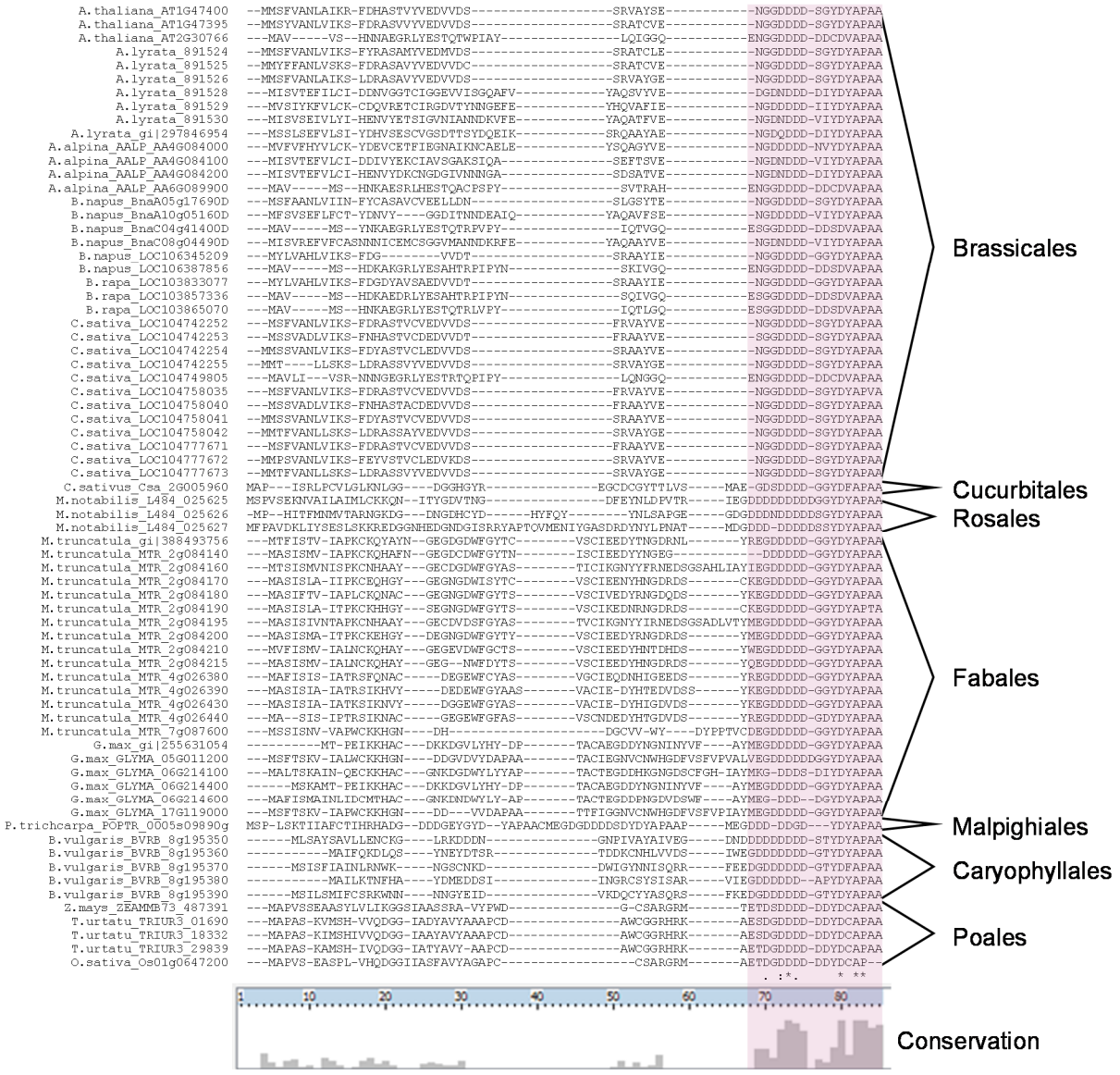

Figure S7. FEP3 conserved domain.
Multiple sequence alignment of FEP3 (AT1G47400) protein sequence and BLAST search hits of selected angiosperm species. Example orders within the angiosperm phylogeny are shown. Corresponds to **Figure 4**.

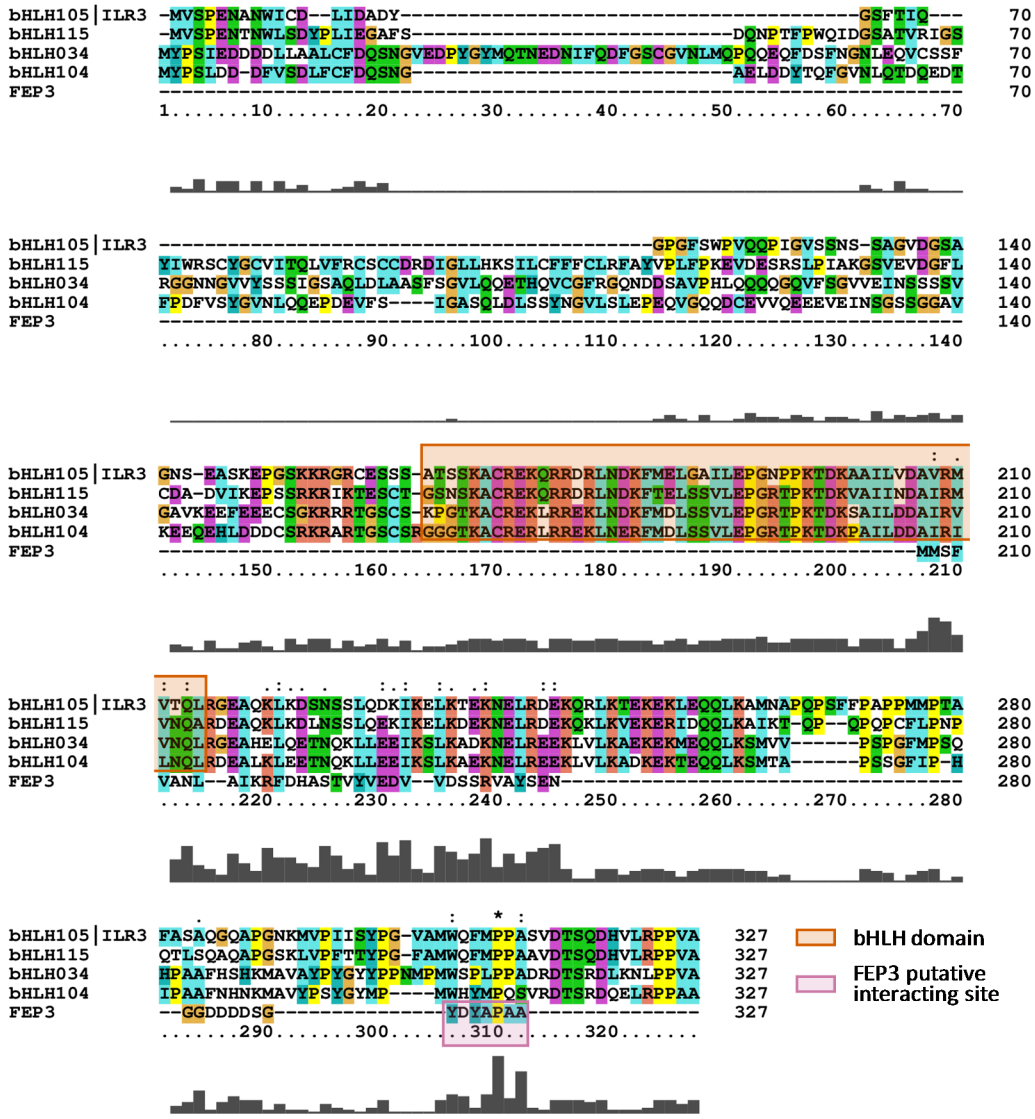

Figure S8. Multiple sequence alignment of IVc bHLHs and FEP3 to identify potential sequence similarities.
Multiple sequence alignment of IVc bHLHs (ILR3/bHLH115/34/104) and FEP3 protein sequences. Indicated regions: bHLH domain (orange) and the seven C-terminal amino acids of FEP3 needed for protein-protein interaction (see **Figure 4**) (pink). bHLH domain annotation based on information deposited on UniProt (www.uniprot.org).

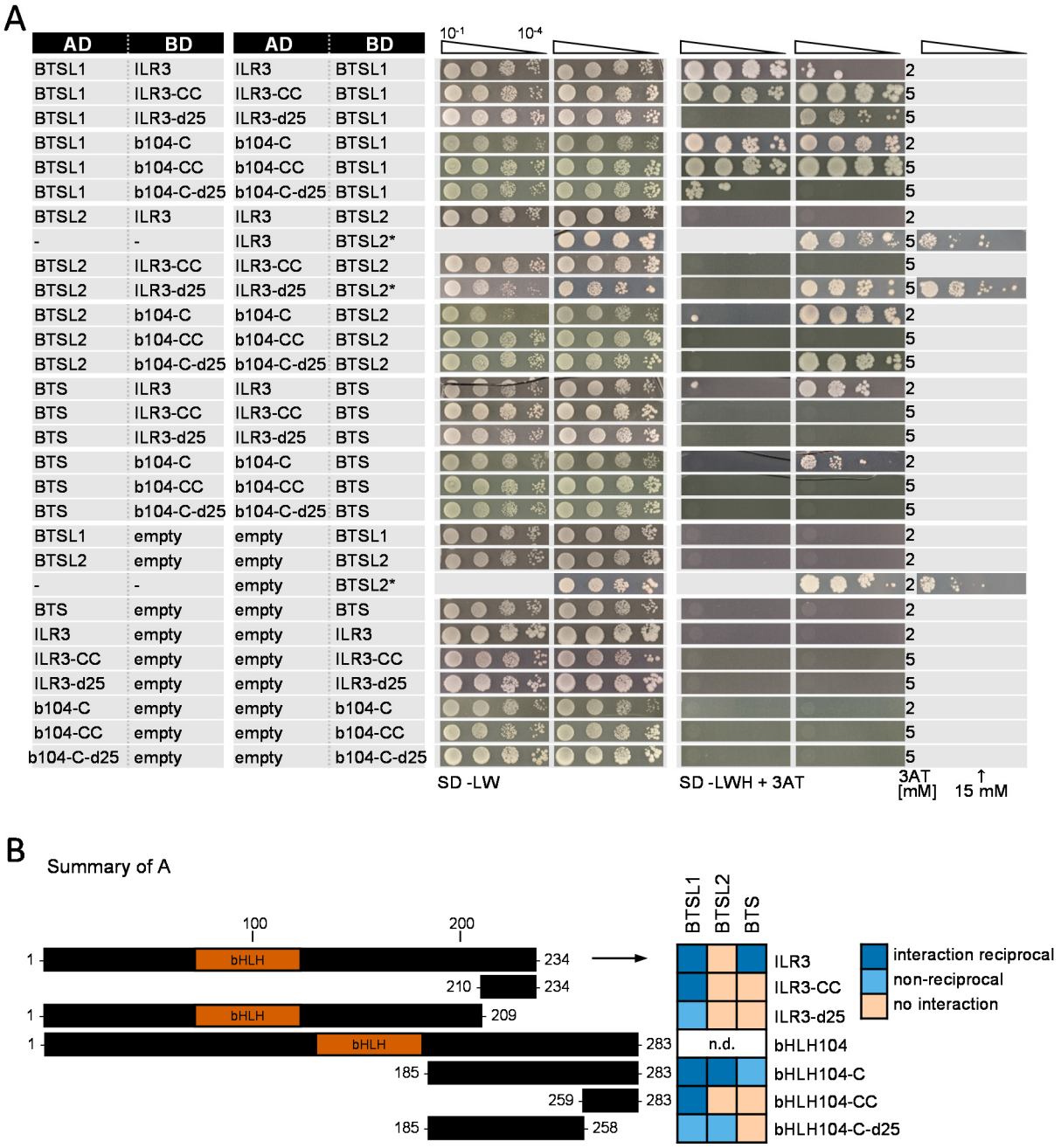

AD	BD	AD	BD	3AT [mM]
BTSL1	ILR3	ILR3	BTSL1	2
BTSL1	ILR3-CC	ILR3-CC	BTSL1	5
BTSL1	ILR3-d25	ILR3-d25	BTSL1	5
BTSL1	b104-C	b104-C	BTSL1	2
BTSL1	b104-CC	b104-CC	BTSL1	5
BTSL1	b104-C-d25	b104-C-d25	BTSL1	5
BTSL2	ILR3	ILR3	BTSL2	2
-	-	ILR3	BTSL2*	5
BTSL2	ILR3-CC	ILR3-CC	BTSL2	5
BTSL2	ILR3-d25	ILR3-d25	BTSL2*	5
BTSL2	b104-C	b104-C	BTSL2	2
BTSL2	b104-CC	b104-CC	BTSL2	5
BTSL2	b104-C-d25	b104-C-d25	BTSL2	5
BTS	ILR3	ILR3	BTS	2
BTS	ILR3-CC	ILR3-CC	BTS	5
BTS	ILR3-d25	ILR3-d25	BTS	5
BTS	b104-C	b104-C	BTS	2
BTS	b104-CC	b104-CC	BTS	5
BTS	b104-C-d25	b104-C-d25	BTS	5
BTSL1	empty	empty	BTSL1	2
BTSL2	empty	empty	BTSL2	2
-	-	empty	BTSL2*	2
BTS	empty	empty	BTS	2
ILR3	empty	empty	ILR3	2
ILR3-CC	empty	empty	ILR3-CC	5
ILR3-d25	empty	empty	ILR3-d25	5
b104-C	empty	empty	b104-C	2
b104-CC	empty	empty	b104-CC	5
b104-C-d25	empty	empty	b104-C-d25	5

Figure S9. The last 25 aa in ILR3 and bHLH104 are not crucial for interaction with BTSL1 or BTSL2.
A: Reciprocal targeted Y2H protein interaction assay testing different truncated versions of ILR3, bHLH104. Full-length ILR3 or b104-C (bHLH104-C) (=positive controls), truncated versions consisting of the last 25 aa (ILR3-CC, b104-CC) and the respective counterparts, lacking the last 25 aa (ILR3-d25, b104-C-d25) were co-transformed with BTSL1, BTSL2, BTS into yeast. Yeast containing the AD and BD combinations were spotted as described in **Supplemental Figure S4**. *BD-BTSL2 was occasionally auto-activating the system, and spotted additionally on higher 3AT concentrations to better distinguish interaction and auto-activation.
B: Schematic representations of full-length ILR3 and truncated versions, as well as bHLH104-C and truncated versions tested in A. Full-length bHLH104 not tested in A, shown to easily relate the bHLH104 fragments. Heatmap summarizes results of A.

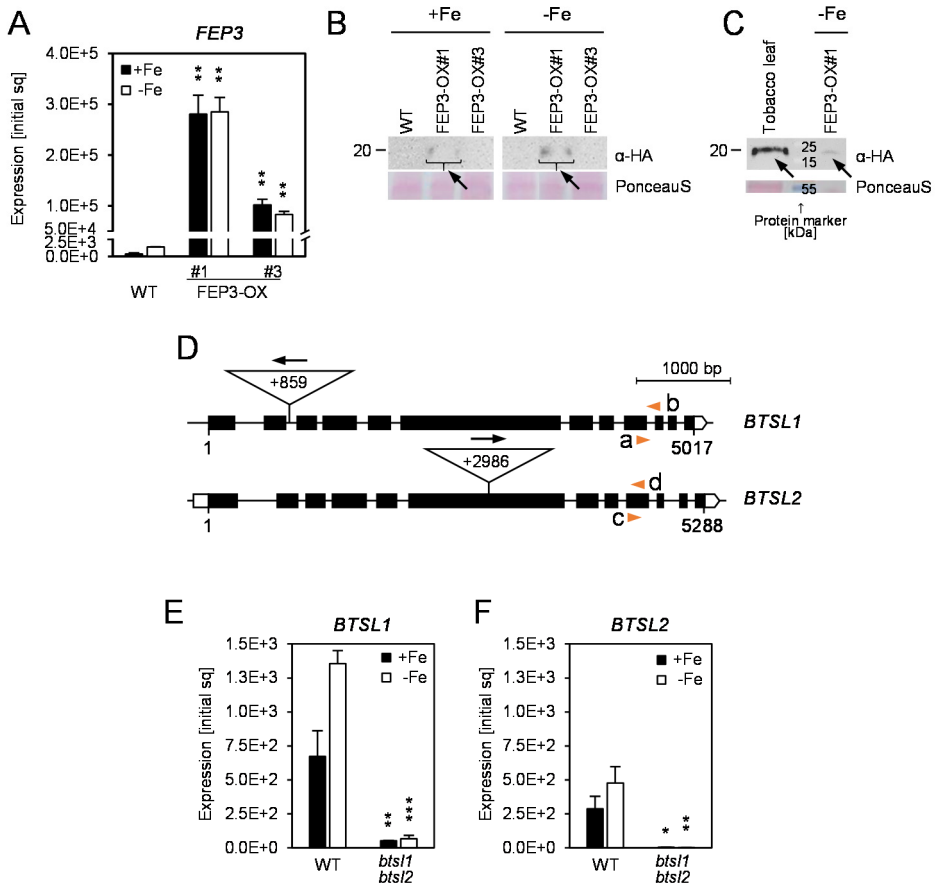

Figure S10. Validation of FEP3-OX and *btsl1 btsl2* mutant lines.

A: *FEP3* gene expression (RT-qPCR) in seedlings of WT and two FEP3-OX lines (#1, #3, WT background) generated in this study. Plants were grown in the 6 d system with sufficient (+Fe, black bars) or deficient (-Fe, white bars) Fe supply.

B, C: Anti-HA immunodetection of HA_3-FEP3 fusion protein (indicated by arrows) in seedlings of FEP3-OX (#1, #3). Seedlings were grown as in A. Tobacco leaf transiently transformed with the HA_3-FEP3 construct served as positive control. WT served as negative control. Loading control: PonceauS staining of the membrane. Molecular weight of the protein (in kDa) is indicated. Because bands in (B) are hardly recognizable (protein accumulated in SDS gel pocket corners), a second membrane with positive control is shown (C).

D: Schematic representation of *BTSL1* and *BTSL2* genes and mutant alleles of the *btsl1 btsl2* line. Black boxes indicate exons, white boxes indicate 5' and 3' untranslated regions. Positions of T-DNA insertions (triangles) and primers used for RT-qPCR (orange arrowheads; a, b, c, d) are indicated. Black arrows indicate orientation of left border primers used for genotyping (see **Supplemental Table S1**).

E, F: *BTSL1* (E) and *BTSL2* (F) gene expression (RT-qPCR) in WT and *btsl1 btsl2* mutant roots. Plants were grown in the 14+3 d system with +Fe or -Fe supply.

A, E, F: Expression [initial sq]=Absolute normalized expression [initial starting quantity]. Data are represented as mean and SD. Asterisks indicate statistically significant differences to the WT of the same growth condition (n=3) (Student's T-Test, **p*<0.05, ***p*<0.01, ****p*<0.001).

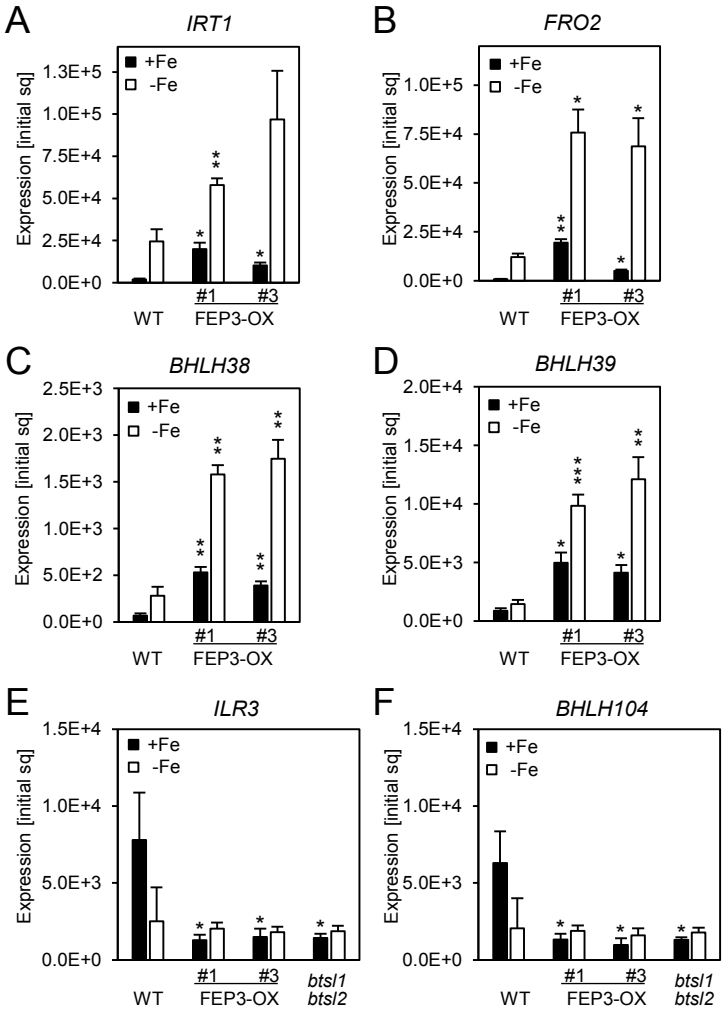

Figure S11. Regulation of selected Fe deficiency response genes in whole seedlings of FEP3-OX and *btsl1-btls2*.
A-D: Expression analysis (RT-qPCR) of Fe deficiency response genes in seedlings of two FEP3-OX lines (#1, #3) in comparison to WT. A: IRT1, B: FRO2, C: BHLH38, D: BHLH39.
E, F: Expression analysis of ILR3 (E) and BHLH104 (F) in seedlings of FEP-OX (#1, #3) and *btsl1 btsl2* mutant lines.
A-F: Plants were grown in the 6 d system with sufficient (+Fe, black bars) or deficient (-Fe, white bars) Fe supply. Expression [initial sq]=Absolute normalized expression [initial starting quantity]. Data are represented as mean and SD. Asterisks indicate statistically significant differences to the WT of the same growth condition (n=3) (Student's T-Test, *p<0.05, **p<0.01, ***p<0.001). Data corresponds to **Figure 5**.

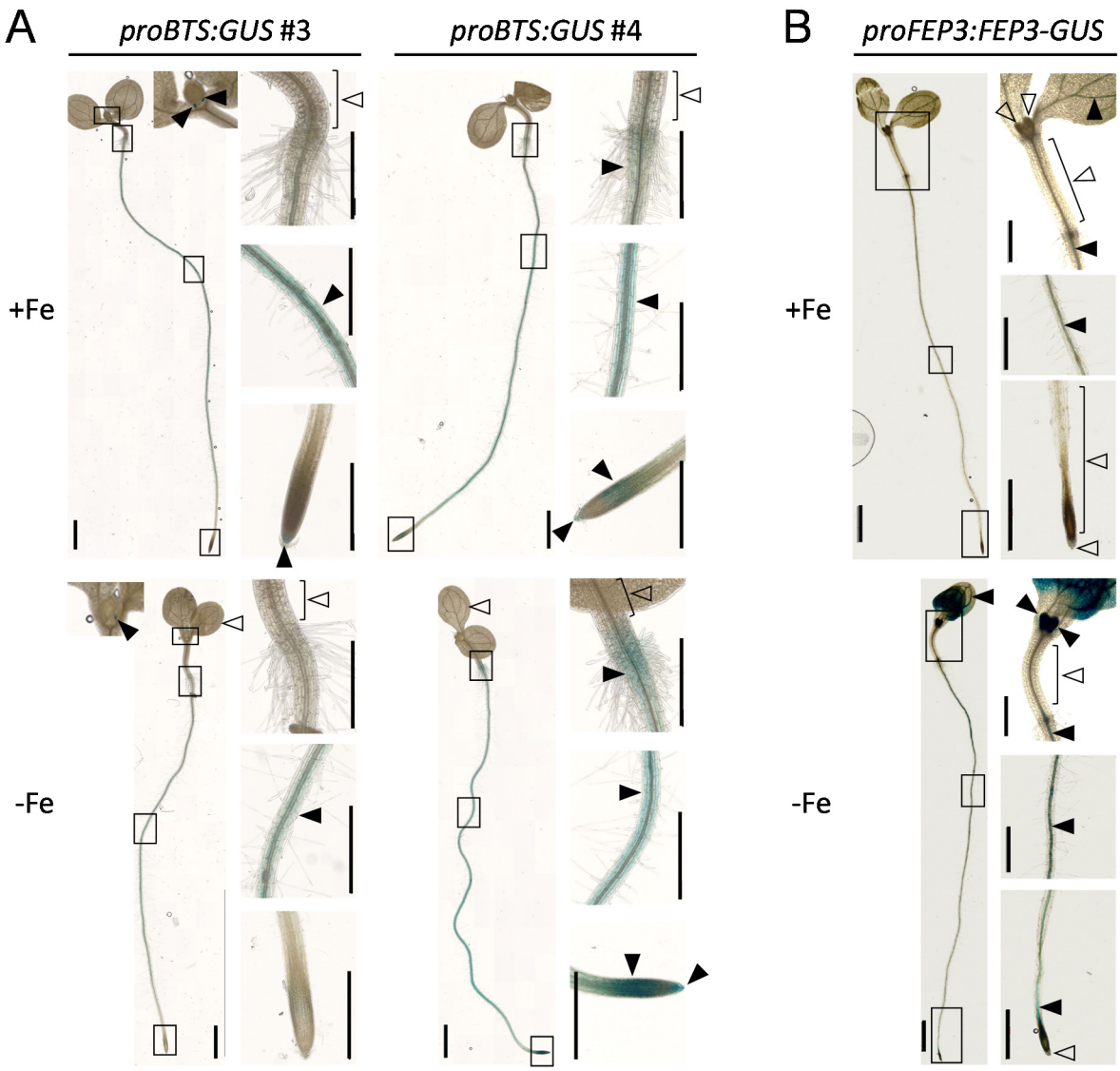

Figure S12. *ProBTS* activity in two additional Arabidopsis lines, and FEP3-GUS protein localization in Arabidopsis seedlings.
A: *BTS*-promoter-driven GUS reporter activity in two additional transgenic Arabidopsis lines expressing *proBTS:GUS* in WT background (correspond to **Figure 6F, L**). Plants were grown in the 6 d system under sufficient (+Fe, **top**) and deficient (-Fe, **bottom**) Fe supply. Reporter gene expression was visualized by a chemical reaction (GUS) resulting in blue staining of the respective tissues. Plants were imaged with brightfield microscopy. Rectangles in whole-seedling images indicate positions of the enlarged images. Filled arrowheads indicate selected areas of GUS staining, non-filled arrowheads indicate selected non-stained areas. Vascular tissue is indicated by the arrowhead pointing directly at it, non-vascular tissue is indicated by the arrowhead pointing more to an outside area. Scale bars of whole seedling images: 1 mm; of magnifications: 0.5 mm.
B: GUS activity indicating FEP3-GUS fusion protein localization. Transgenic Arabidopsis plants expressing *proFEP3:FEP3-GUS* in WT background were grown and imaged as described in A. Images are presented as described in A.

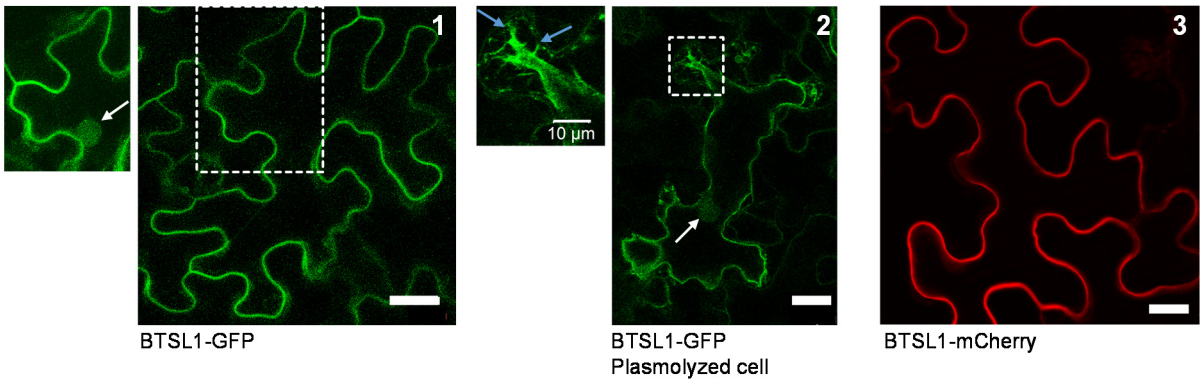

Figure S13. Peripheral localization of BTSL1 in tobacco leaf epidermis cells (additional images).
Images correspond to **Figure 7A (1)** and show localization of BTSL1 with a C-terminal GFP **(1, 2)** and mCherry **(3)** fusions. Magnification of 1 shows a different layer of the Z stack to better show the nucleus. To show that BTSL1-GFP localizes to the plasma membrane **(1)**, cells were plasmolyzed (blue arrows indicate Hechtian strands) **(2)**. Arrows indicate nuclei. (1, 2) were imaged by laser-scanning confocal fluorescence microscopy. (3) was imaged with a fluorescence microscope and an ApoTome for enhanced resolution. Scale bars: 20 µm.

Supplemental Table 1. Primers used in this study.
fw = forward, rev = reverse, s = stop, ns = no stop, d = delta a.k.a. deletion, -C = C-term, -CC = 25 C-terminal aa, -N = N-term, (att)B1/B2/B3/B4 = Gateway B attachment sites for BP reaction.

Primer name	Sequence 5' → 3'	Purpose	Origin
Amplification of full-length CDS or deletion constructs for Y2H, BiFC, (co-) localization and OX lines			
BTSL1_B1 fw	GGGGACAAGTTTGTACAAAAAAGCAGGCTTCATGGGAGGCGGAAATCTTC	cloning of BTSL1, BTSL1-N, BTSL1-dRH, BTSL1-6G (attB1)	This study
BTSL1s_B2 rev	GGGGACCACTTTGTACAAGAAAGCTGGGTCCTAAAGGAGCCTTGAGTTGTAG	cloning of BTSL1, BTSL1-C, BTSL1-C.4, BTSL1-dRH, BTSL1-6G (attB2)	This study
BTSL1ns_B2 rev	GGGGACCACTTTGTACAAGAAAGCTGGGTCAAGGAGCCTTGAGTTGTAGGA	cloning of BTSL1, BTSL1-C, no stop codon (attB2)	This study
BTSL1-Ns_B2 rev	GGGGACCACTTTGTACAAGAAAGCTGGGTCCTAAGGAGGCTGATTCATAATACCTG	cloning of BTSL1-N (attB2)	This study
BTSL1-C_B1 fw	GGGGACAAGTTTGTACAAAAAAGCAGGCTTCATGCCTAATTACAAGGTTGAAGTTGGC	cloning of BTSL1-C, BTSL1-C.1, BTSL1-C.2 (attB1)	This study
BTSL1_B3 fw	GGGGACAACTTTGTATAATAAAGTTGTAATGGGAGGCGGAAATCTTC	cloning of BTSL1 (attB3)	This study
BTSL1s_B4 rev	GGGGACAACTTTGTATAGAAAAGTTGGGTGCTAAAGGAGCCTTGAGTTGTAG	cloning of BTSL1-C (attB4)	This study
BTSL1-C.1s_B2 rev	GGGGACCACTTTGTACAAGAAAGCTGGGTCCTAGTTGCAGTAAGGACAGTGATAA	cloning of BTSL1-C.1 (attB2)	This study
BTSL1-C.2s_B2 rev	GGGGACCACTTTGTACAAGAAAGCTGGGTCCTAGCACTTTTCCCTGCAAACAT	cloning of BTSL1-C.2 (attB2)	This study
BTSL1-C.3_B1 fw	GGGGACAAGTTTGTACAAAAAAGCAGGCTTCATGGAAGAAGCTGATCACTCGGT	cloning of BTSL1-C.3 (attB1)	This study
BTSL1-C.3s_B2 rev	GGGGACCACTTTGTACAAGAAAGCTGGGTCCTAATCAGGCATCTTCTCTTCTGC	cloning of BTSL1-C.3 (attB2)	This study
BTSL1-C.4_B1 fw	GGGGACAAGTTTGTACAAAAAAGCAGGCTTCATGTCACGTACCTTAGTAGAGC	cloning of BTSL1-C.4 (attB1)	This study
BTSL1_dRH rev	CTTTTCCCTGCAAACTGACATACAAGCATTGCAT	cloning of BTSL1-dRH for overlap extension PCR (N-term part)	This study
BTSL1_dRH fw	AATGCTTGTATGTCAGTTTGCAGGGAAAAGTG	Cloning of BTSL1-dRH for overlap extension PCR (C-term part)	This study
BTSL1_dRH-G rev	GCAAACGCCTCCGCCTCCGCCTCCTGACATACAAGCATTGCAT	cloning of BTSL1-6G for overlap extension PCR (C-term part)	This study
BTSL1_dRH-G fw	ATGTCAGGAGGCGGAGGCGGAGGCGTTTGCAGGGAAAAGTG	Cloning of BTSL1-6G for overlap extension PCR (C-term part)	This study
BTSL1_dMC fw	AAATGCAATGCTTGTTTAGAAGATAATTGTCCGATTTGCC	Cloning of BTSL1-dMC for overlap extension	This study
BTSL1_dMC rev	ACAATTATCTTCTAAACAAGCATTGCATTTCATGC	Cloning of BTSL1-dMC for overlap extension	This study
BTSL2_B1 fw	GGGGACAAGTTTGTACAAAAAAGCAGGCTTCATGGGAGTCGGAGATCCT	cloning of BTSL2 (attB1)	This study
BTSL2s_B2 rev	GGGGACCACTTTGTACAAGAAAGCTGGGTCCTAGAAAAGTCTGGTGTTGTAGG	cloning of BTSL2 , BTSL2-C (attB2)	This study
BTSL2-C_B3 fw	GGGGACAACTTTGTATAATAAAGTTGTAATGGGAGTCGGAGATCCT	cloning of BTSL2-C (attB3)	This study
BTS_B1 fw	GGGGACAAGTTTGTACAAAAAAGCAGGCTTCATGGCGACGCCGTTACCA	cloning of BTS (attB1)	This study
BTSs_B2 rev	GGGGACCACTTTGTACAAGAAAGCTGGGTCTCAGGATGAGGTTGAGCAGT	cloning of BTS (attB2)	This study
BTSs_B4 rev	GGGGACAACTTTGTATAGAAAAGTTGGGTGTCAGGATGAGGTTGAGCAGT	cloning of BTS (attB4)	This study
FEP3_B1 fw	GGGGACAAGTTTGTACAAAAAAGCAGGCTTCATGATGTCTTTTGTCGCAAAC	cloning of FEP3, FEP3-N, FEP3-d7 (attB1)	This study

FEP3s_B2 rev	GGGGACCACTTTGTACAAGAAAGCTGGGTCTCACGCAGCAGGAGCATA	cloning of FEP3, FEP3-C (attB2)	This study
FEP3ns_B2 rev	GGGGACCACTTTGTACAAGAAAGCTGGGTCCGCAGCAGGAGCATAATC	cloning of FEP3, proFEP3-FEP3, no stop codon (attB2)	This study
FEP3-Ns_B2 rev	GGGGACCACTTTGTACAAGAAAGCTGGGTCTCATACCACATCTTCAACATACACG	cloning of FEP3-N (attB2)	This study
FEP3-C_B1 fw	GGGGACAAGTTTGTACAAAAAAGCAGGCTTCATGGATAGTTCTCGAGTGGCATATAG	cloning of FEP3-C (attB1)	This study
FEP3-d7s_B2 rev	GGGGACCACTTTGTACAAGAAAGCTGGGTCTCATCAGCCACTGTCATCGTC	cloning of FEP3-d7 (attB2)	This study
ILR3_B1 fw	GGGGACAAGTTTGTACAAAAAAGCAGGCTTCATGGTGTCACCCGAAAACG	cloning of ILR3, ILR3-d25 (attB1)	This study
ILR3s_B2 rev	GGGGACCACTTTGTACAAGAAAGCTGGGTCTTAAGCAACAGGAGGACGAAG	cloning of ILR3 (attB2)	This study
ILR3ns_B2 rev	GGGGACCACTTTGTACAAGAAAGCTGGGTCAGCAACAGGAGGACGAAG	cloning of ILR3, no stop codon (attB2)	This study
ILR3_B3 fw	GGGGACAACTTTGTATAATAAAGTTGTAATGGTGTCACCCGAAAACG	cloning of ILR3 (attB3)	This study
ILR3s_B4 rev	GGGGACAACTTTGTATAGAAAAGTTGGGTGTTAAGCAACAGGAGGACGAAG	cloning of ILR3 (attB4)	This study
ILR3-d25s_B2 rev	GGGGACCACTTTGTACAAGAAAGCTGGGTCTTATCCTGGGTAACTGATGAT	cloning of ILR3-d25 (attB2)	This study
ILR3-CC_B1 fw	GGGGACAAGTTTGTACAAAAAAGCAGGCTTCATGGTTGCCATGTGG	cloning of ILR3-CC (attB1)	This study
bHLH104_B1 fw	GGGGACAAGTTTGTACAAAAAAGCAGGCTTCATGTATCCTTCTCTCGACGA	cloning of bHLH104 (attB1)	This study
bHLH104s_B2 rev	GGGGACCACTTTGTACAAGAAAGCTGGGTCTTAAGCAGCAGGAGGCCTG	cloning of bHLH104, bHLH104-C, bHLH104-CC (attB2)	This study
bHLH104-C_B1 fw	GGGGACAAGTTTGTACAAAAAAGCAGGCTTCATGGCTCT	cloning of bHLH104-C, bHLH104-C-d25 (attB1)	This study
bHLH104-d25s_B2 rev	GGGGACCACTTTGTACAAGAAAGCTGGGTCTTAGTAACCGTAACTTGGATAAAC	cloning of bHLH104-C-d25 (attB2)	This study
bHLH104-CC_B1 fw	GGGGACAAGTTTGTACAAAAAAGCAGGCTTCATGATGCCAATGTGGC	cloning of bHLH104-CC (attB1)	This study
PYE_B1 fw	GGGGACAAGTTTGTACAAAAAAGCAGGCTTCATGGTATCGAAAACTCCTTC	cloning of PYE (attB1)	This study
PYEs_B2 rev	GGGGACCACTTTGTACAAGAAAGCTGGGTCTCATTCACTGGCTTTCAGCC	cloning of PYE (attB2)	This study
PYEns B2 rev	GGGGACCACTTTGTACAAGAAAGCTGGGTCTTCACTGGCTTTCAGCC	cloning of PYE, no stop codon (attB2)	This study
PYE_B3 fw	GGGGACAACTTTGTATAATAAAGTTGTAATGGTATCGAAAACTCCTTC	cloning of PYE (attB3)	This study
PYEs_B4 rev	GGGGACAACTTTGTATAGAAAAGTTGGGTGTCATTCACTGGCTTTCAGCC	cloning of PYE (attB4)	This study
FIT_B1 fw	GGGGACAAGTTTGTACAAAAAAGCAGGCTTCATGGAAGGAAGAGTCAACG	cloning of FIT (attB1)	This study
FITs_B2 rev	GGGGACCACTTTGTACAAGAAAGCTGGGTCTCAAGTAAATGACTTGATG	cloning of FIT, FIT-C (attB2)	This study
FIT-C_B1 rev	GGGGACAAGTTTGTACAAAAAAGCAGGCTTAACTCAACCTTTTCGCGGTATC	cloning of FIT-C (attB1)	(Gratz et al., 2019)
FIT_B3 fw	GGGGACAACTTTGTATAATAAAGTTGTAATGGAAGGAAGAGTCAACG	cloning of FIT (attB3)	This study
bHLH38_B1 fw	GGGGACAAGTTTGTACAAAAAAGCAGGCTTCATGTGTGCATTAGTCCCTTCATTT	cloning of bHLH38 (attB1)	This study

bHLH38_B2 rev	GGGGACCACTTTGTACAAGAAAGCTGGGTCCTAGTTAAACGAGTTTTCACATT	cloning of bHLH38 (attB2)	This study
bHLH39_B1 fw	GGGGACAAGTTTGTACAAAAAAGCAGGCTTCATGTGTGCATTAGTACCTC	cloning of bHLH39 (attB1)	This study
bHLH39_B2 rev	GGGGACCACTTTGTACAAGAAAGCTGGGTCTCATATATATGAGTTTCCAC	cloning of bHLH39 (attB2)	This study
bHLH100_B1 fw	GGGGACAAGTTTGTACAAAAAAGCAGGCTTCATGTGTGCACTTGTCCCTCCATT	cloning of bHLH100 (attB1)	This study
bHLH100_B2 rev	GGGGACCACTTTGTACAAGAAAGCTGGGTCTCATGTAAACGAGTGTCCACATT	cloning of bHLH100 (attB2)	This study
bHLH101_B1 fw	GGGGACAAGTTTGTACAAAAAAGCAGGCTTCATGGAGTATCCATGGCTGCAGTC	cloning of bHLH101 (attB1)	This study
bHLH101_B2 rev	GGGGACCACTTTGTACAAGAAAGCTGGGTCTTATGATTGGCGTAATCCCAAGA	cloning of bHLH101 (attB2)	This study
MYB72_B1 fw	GGGGACAAGTTTGTACAAAAAAGCAGGCTTCATGGGGAAAGGAAGAGCAC	cloning of MYB72 (attB1)	This study
MYB72_B2 rev	GGGGACCACTTTGTACAAGAAAGCTGGGTCTCATAGACATACTTCTCCGA	cloning of MYB72 (attB2)	This study
DGAT3_B1 fw	GGGGACAAGTTTGTACAAAAAAGCAGGCTTCATGGAGAAGGAGAAGAAGGC	cloning of DGAT3 (attB1)	This study
DGAT3s_B2 rev	GGGGACCACTTTGTACAAGAAAGCTGGGTCTCAATATGAGACAGAACCGAGT	cloning of DGAT3 (attB2)	This study
DUF506_B1 fw	GGGGACAAGTTTGTACAAAAAAGCAGGCTTCATGGTAGAGATAGGAGGACGA	cloning of DUF506 (attB1)	This study
DUF506s_B2 rev	GGGGACCACTTTGTACAAGAAAGCTGGGTCCTAAAATATTTGCAACCCCACTT	cloning of DUF506 (attB2)	This study
GRF11_B1 fw	GGGGACAAGTTTGTACAAAAAAGCAGGCTTCATGGAGAACGAGAGAGCG	cloning of GRF11 (attB1)	This study
GRF11s_B2 rev	GGGGACCACTTTGTACAAGAAAGCTGGGTCTTAGATTTTGTTTACCTCATCTTG	cloning of GRF11 (attB2)	This study
JAL12_B1 fw	GGGGACAAGTTTGTACAAAAAAGCAGGCTTCATGTCTCAAGATTCGAATGC	cloning of JAL12 (attB1)	This study
JAL12s_B2 rev	GGGGACCACTTTGTACAAGAAAGCTGGGTCTCACCAGCTTGTGTGTATG	cloning of JAL12 (attB2)	This study
KELCH_B1 fw	GGGGACAAGTTTGTACAAAAAAGCAGGCTTCATGGCAGCGACTCCAATG	cloning of KELCH (attB1)	This study
KELCHs_B2 rev	GGGGACCACTTTGTACAAGAAAGCTGGGTCTCACTTGAGTAGAGTGTTGG	cloning of KELCH (attB2)	This study
NAS2_B1 fw	GGGGACAAGTTTGTACAAAAAAGCAGGCTTCATGGCTTGCGAAAACAACCT	cloning of NAS2 (attB1)	This study
NAS2s_B2 rev	GGGGACCACTTTGTACAAGAAAGCTGGGTCTTACTCGATGGCACTATACTCCT	cloning of NAS2 (attB2)	This study
NAS4_B1 fw	GGGGACAAGTTTGTACAAAAAAGCAGGCTTCATGGGTTATTGCCAAGACGA	cloning of NAS4 (attB1)	This study
NAS4s_B2 rev	GGGGACCACTTTGTACAAGAAAGCTGGGTCCTAGGTAAGTTGTTCTTCATTAGCA	cloning of NAS4 (attB2)	This study
ORG1_B1 fw	GGGGACAAGTTTGTACAAAAAAGCAGGCTTCATGGCACTTTGTGGTGTTTG	cloning of ORG1 (attB1)	This study
ORG1s_B2 rev	GGGGACCACTTTGTACAAGAAAGCTGGGTCCTACATAGACTTATGGTCCAAGC	cloning of ORG1 (attB2)	This study
PRS2_B1 fw	GGGGACAAGTTTGTACAAAAAAGCAGGCTTCATGGCGTCGTTGGCTCT	cloning of PRS2 (attB1)	This study
PRS2s_B2 rev	GGGGACCACTTTGTACAAGAAAGCTGGGTCTCAAAGGAAAATACTACTAACGGAG	cloning of PRS2 (attB2)	This study

S8H_B1 fw	GGGGACAAGTTTGTACAAAAAAGCAGGCTTCATGGGTATCAATTTCGAGGAC	cloning of S8H (attB1)	This study
S8Hs_B2 rev	GGGGACCACTTTGTACAAGAAAGCTGGGTCTCACTCGGCACGTGC	cloning of S8H (attB2)	This study
SDI1_B1 fw	GGGGACAAGTTTGTACAAAAAAGCAGGCTTCATGGAGAGAAGCTTGAAGAA	cloning of SDI1 (attB1)	This study
SDI1s_B2 rev	GGGGACCACTTTGTACAAGAAAGCTGGGTCCTAGCAAACTAATGTATTTCTAAAAG	cloning of SDI1 (attB2)	This study
UIP1_B1 fw	GGGGACAAGTTTGTACAAAAAAGCAGGCTTCATGGCGACTTCTACCTTCT	cloning of UP1 (attB1)	This study
UIP1s_B2 rev	GGGGACCACTTTGTACAAGAAAGCTGGGTCTCAAGAGAACCAATTAACGAG	cloning of UP1 (attB2)	This study
UIP2_B1 fw	GGGGACAAGTTTGTACAAAAAAGCAGGCTTCATGTATCAAGATCGTCAAGGC	cloning of UP2 (attB1)	This study
UIP2s_B2 rev	GGGGACCACTTTGTACAAGAAAGCTGGGTCTCAGTCATCGGAACCATCA	cloning of UP2 (attB2)	This study
UIP3_B1 fw	GGGGACAAGTTTGTACAAAAAAGCAGGCTTCATGGCGACGTCTGCGA	cloning of UP3 (attB1)	This study
UIP3s_B2 rev	GGGGACCACTTTGTACAAGAAAGCTGGGTCTCATTGACCAGTCTGCACC	cloning of UP3 (attB2)	This study
UIP4_B1 fw	GGGGACAAGTTTGTACAAAAAAGCAGGCTTCATGGCGTATGCAAAGATCG	cloning of UP4 (attB1)	This study
UIP4s_B2 rev	GGGGACCACTTTGTACAAGAAAGCTGGGTCTCAATTTCCCACAAGCCAAC	cloning of UP4 (attB2)	This study
Amplification of promoter regions for GUS lines			
proBTSL1_-880_B1 fw	GGGGACAAGTTTGTACAAAAAAGCAGGCTTCAGTATTGATTTTGTGAGCCCAATT	cloning of BTSL1 promoter (attB1)	This study
proBTSL1_-880_B2 rev	GGGGACCACTTTGTACAAGAAAGCTGGGTCCCACCGCAACAACAATAACG	cloning of BTSL1 promoter (attB2)	This study
proBTS_-2994_B1 fw	GGGGACAAGTTTGTACAAAAAAGCAGGCTTCATGAGATGAAATGTCTTATCTTTAT	cloning of BTS promoter (attB1)	This study
proBTS_-2994_B2 rev	GGGGACCACTTTGTACAAGAAAGCTGGGTCTTCCCCCAAAGCTTATCTCCGTTTT	cloning of BTS promoter (attB2)	This study
proPYE_-1120_B1 fw	GGGGACAAGTTTGTACAAAAAAGCAGGCTTCACCGCAAAACTATATATAGTATTT	cloning of PYE promoter (attB1)	This study
proPYE_-1120_B2 rev	GGGGACCACTTTGTACAAGAAAGCTGGGTCCTTTGCTTTTATTACAGAACAAGA	cloning of PYE promoter (attB2)	This study
proFEP3_-1614_B1 fw	GGGGACAAGTTTGTACAAAAAAGCAGGCTTCGGCACAAAGAAATCAGACCAAT	cloning of FEP3 promoter (attB1)	This study
proFEP3_-1614_B2rev	GGGGACCACTTTGTACAAGAAAGCTGGGTCTGATATTTTTTGTTGGATATGAATGAAAGT	cloning of FEP3 promoter (attB2)	This study
TAIL PCR and genotyping			
S1_AL2_LB	ATGCTCTTACGTTGTTGTCGGG	TAIL, binds in T-DNA LB of pAlligator2	
S2_AL2_LB	ACCACTCATCATAGCTCCGC	TAIL, binds in T-DNA LB of pAlligator2	
S3_AL2_LB	TTCAGTACATTAAAAACGTCCGC	TAIL, binds in T-DNA LB of pAlligator2, genotyping of FEP3-OX lines	
AD1	NGTCGASWGANAWGAA	TAIL	AD2 in (Liu et al., 1995)
AD2	TGWGNAGSANCASAG	TAIL	AD1 in (Liu and Whittier, 1995)
AD3	AGWGNAGWANCAWAGG	TAIL	AD2 in (Liu and Whittier, 1995)
AD4	STTGNTASTNCTNTGC	TAIL	AD2 in (Tsugeki et al., 1996)

AD5	NTCGASTWTSGWGTT	TAIL	AD1 in (Liu et al., 1995)
AD6	WGTGNAGWANCANAGA	TAIL	AD3 in (Liu et al., 1995)
LBb1.3	ATTTTGCCGATTTCGGAAC	*btsl1 btsl2* DM genotyping	Salk Institute Genomic Analysis Laboratory
FEP3-OX1_chr5 fw	GCAAACCAAGCTTCCATGC	FEP3-OX#1 genotyping	This study
FEP3-OX1_chr5 rev	CTCGCCTCCAATACCTCCTT	FEP3-OX#1 genotyping	This study
FEP3-OX3_chr1 fw	CGAATGTACTTCGCTGACTTT	FEP3-OX#3 genotyping	This study
FEP3-OX3_chr1 rev	TGTTGTTCTAAATTTTGGGATCTT	FEP3-OX#3 genotyping	This study
btsl1-1_LP	TGCTTGGCATAATCCTTCTTG	*btsl1* allele genotyping	(Rodríguez-Celma et al., 2017)
btsl1-1_RP	GAACTCTCTTGCTTCCTGAAGC	*btsl1* allele genotyping	(Rodríguez-Celma et al., 2017)
btsl2-2_LP	TCGGTTATTCAGGCAAAACAC	*btsl2* allele genotyping	(Rodríguez-Celma et al., 2017)
btsl2-2_RP	CCCTTTGTACTCATCAGCAGC	*btsl2* allele genotyping	(Rodríguez-Celma et al., 2017)
RT-qPCR			
FEP3_stn fw	GGCCATCAAGAGATTTGACC	*FEP3* RT-qPCR mass standard	This study
FEP3_stn rev	TGGAAACCATGTTTGTTCATCT	*FEP3* RT-qPCR mass standard	This study
FEP3_qPCR fw	TGCTTCCACCGTGTATGTTG	*FEP3* RT-qPCR	This study
FEP3_qPCR rev	CAGGAGCATAATCATAGCCACTG	*FEP3* RT-qPCR	This study
BTSL1_stn fw	TCCCTGGATCCTCAGAAGAA	*BTSL1* RT-qPCR mass standard	This study
BTSL1_stn rev	CGGCTGGTTCTACAATGATG	*BTSL1* RT-qPCR mass standard	This study
BTSL1_qPCR fw	CTCCCCAGTGAAGGCTCTTC	*BTSL1* RT-qPCR	This study
BTSL1_qPCR rev	GACCTGCATATCTCCAAGCGA	*BTSL1* RT-qPCR	This study
BTSL2_stn fw	ATGAGCCGTTGGATTGCTAC	*BTSL2* RT-qPCR mass standard	This study
BTSL2_stn rev	CAAAATCAAATGCTTCCAAAAA	*BTSL2* RT-qPCR mass standard	This study
BTSL2_qPCR fw	GCTTGTATGTCGCGACTCAT	*BTSL2* RT-qPCR	This study
BTSL2_qPCR rev	AGAGCCTTCACCGGAGAATT	*BTSL2* RT-qPCR	This study
BTS_stn fw	AACTTGGATGTTCCCCGTCT	*BTS* RT-qPCR mass standard	This study
BTS_stn rev	ATCAACGGGCTTCTTCACAT	*BTS* RT-qPCR mass standard	This study
BTS_qPCR fw	CGGGGAAGGACTAGGAATCG	*BTS* RT-qPCR	This study
BTS_qPCR rev	CAGCAGATGGGGCAATTTGT	*BTS* RT-qPCR	This study
STD-BHLH038-5'	GGAGATAACCTAAATAACGGC	*BHLH38* RT-qPCR mass standard	(Naranjo Arcos, 2017)
STD-BHLH038-3'	GGTCCAGATCAGTGTTAGATTCA	*BHLH38* RT-qPCR mass standard	(Naranjo Arcos, 2017)
RT 5'bHLH38	AGCAGCAACCAAAGGCG	*BHLH38* RT-qPCR	(Wang et al., 2007)
RT 3'bHLH38	CCACTTGAAGATGCAAAGTGTAG	*BHLH38* RT-qPCR	(Wang et al., 2007)
STD-BHLH039-5'	AACCAAAGCAGCTTCCAAG	BHLH39 RT-qPCR mass standard	(Naranjo Arcos, 2017)
STD-BHLH039-3'	CGAAGAGAAAAAGGACGACA	BHLH39 RT-qPCR mass standard	(Naranjo Arcos, 2017)
bHLH039-RT 5'	GACGGTTTCTCGAAGCTTG	BHLH39 RT-qPCR	(Wang et al., 2007)
RT 3'bHLH39	GGTGGCTGCTTAACGTAACAT	BHLH39 RT-qPCR	(Wang et al., 2007)
STD-FIT-5'(MN)	AAGACATGACCAAAAATGTGTGT	*FIT* RT-qPCR mass standard	(Naranjo Arcos, 2017)
STD-FIT-3'(MN)	TGCATCTCCAACAATGGATGC	*FIT* RT-qPCR mass standard	(Naranjo Arcos, 2017)
FIT F (g166-187)	CCCTGTTTCATAGACGAGAACC	*FIT* RT-qPCR	(Naranjo Arcos, 2017)
RT-FIT-3'(MN)	ATCCTTCATACGCCCTCTCC	*FIT* RT-qPCR	(Bauer, 2016)
AtIRT1-temp-5'(898)	TAGCCATTGACTCCATGGC	*IRT1* RT-qPCR mass standard	(Klatte, 2008)

AtIRT1-temp-3'(1910)	AGAAAACTATGAATCGTGGGG	*IRT1* RT-qPCR mass standard	(Klatte, 2008)
AtIRT1-c-5'new	AAGCTTTGATCACGGTTGG	*IRT1* RT-qPCR	(Wang et al., 2007)
AtIRT1-c-3' (1622)	TTAGGTCCCATGAACTCCG	*IRT1* RT-qPCR	(Wang et al., 2007)
AtFRO2-temp-5'(3110)	CCATGCTCGATCTTGTCTTG	*FRO2* RT-qPCR mass standard	(Bauer, 2016)
AtFRO2-temp-3'(4105)	ATTCCGGAACTTTTGAAAGG	*FRO2* RT-qPCR mass standard	(Bauer, 2016)
FRO2-c5-RT5'	CTTGGTCATCTCCGTGAGC	*FRO2* RT-qPCR	(Wang et al., 2007)
FRO2-c3-RT3'	AAGATGTTGGAGATGGACGG	*FRO2* RT-qPCR	(Wang et al., 2007)
PYE_stn fw	ACCGAAAAGGATCAACAAGG	*PYE* RT-qPCR mass standard	This study
PYE _stn rev	CCATCAAGGCCATAACTTCC	*PYE* RT-qPCR mass standard	This study
PYE _qPCR fw	GTTCCCAGGACTTCCCATTT	*PYE* RT-qPCR	This study
PYE _qPCR rev	GTGTCTGGGGATCAGGTTGT	*PYE* RT-qPCR	This study
FRO3_stn fw	AATCAGATCGACCACCTTGC	*FRO3* RT-qPCR mass standard	This study
FRO3_stn rev	TTCTTTTGGTGAGAAGATTTTGG	*FRO3* RT-qPCR mass standard	This study
FRO3_qPCR fw	ATCGACCACCTTGCTGTTTC	*FRO3* RT-qPCR	This study
FRO3_qPCR rev	TTATCCCACTGCCTCCACTC	*FRO3* RT-qPCR	This study
NAS4_stn fw	CACTCTCTTCAAGCAGCTCGT	*NAS4* RT-qPCR mass standard	This study
NAS4_stn rev	CTGTAGCAAAAACAGCCAACA	*NAS4* RT-qPCR mass standard	This study
AtNAS4-RT810-5'	TGTAATCTCAAGGAAGCTAGGTG	*NAS4* RT-qPCR	(Klatte et al., 2009)
AtNAS4-RT947-3'	GCGAACTCCTCGATAATGC	*NAS4* RT-qPCR	(Schuler, 2011)
ILR3_stn fw	TGATGGCTCGGCTGGAAAC	*ILR3* RT-qPCR mass standard	This study
ILR3_stn rev	CTAAGAAAGCCGAGAAAGAGAGGAG	*ILR3* RT-qPCR mass standard	This study
ILR3_qPCR fw	GCATGTAGAGAGAAGCAGCGAC	*ILR3* RT-qPCR	This study
ILR3_qPCR rev	TGCGGACAGCATCAACCAAG	*ILR3* RT-qPCR	This study
bHLH104_stn fw	GAATTTGCAGCAGGAGCCAG	*BHLH104* RT-qPCR mass standard	This study
bHLH104_stn rev	GCCAAACGGAAGAATCCTAAACC	*BHLH104* RT-qPCR mass standard	This study
bHLH104_qPCR fw	GGTTGAGGAGGGAGAAGCTAAATG	*BHLH104* RT-qPCR	This study
bHLH104_qPCR rev	ACGGATTGCATCATCGAGTATAGC	*BHLH104* RT-qPCR	This study
STD-EF1Balpha2-5'	GCTGCTAAGAAGGACACCAAG	*EF1Balpha* (genomic) RT-qPCR mass standard	(Bauer, 2016)
STD-EF1Balpha2-3'	TGTTCTGTCCCTACTGGATCC	*EF1Balpha* (genomic) RT-qPCR mass standard	(Bauer, 2016)
EFc-5'	TATGGGATCAAGAAACTCACAAT	*EF1Balpha* RT-qPCR	(Bauer, 2016)
EFc-3'	CTGGATGTACTCGTTGTTAGGC	*EF1Balpha* RT-qPCR	(Wang et al., 2007)
AtEF-gen-5' (2522)	TCCGAACAATACCAGAACTAC	*EF1Balpha* (genomic) RT-qPCR	(Mai et al., 2016)
AtEF-gen-3' (2726)	CCGGGACATATGGAGGTAAG	*EF1Balpha* (genomic) RT-qPCR	(Wang et al., 2007)

Author contributions to Manuscript 1

Daniela M. Lichtblau

Designed, performed and analyzed the following experiments: Y2H screen (Supplemental Figure S3), targeted Y2H assays (Supplemental Figure S4A, S5), targeted Y2H assay for BTSL1/2 M-C deletions (Figure 3E/F, BTSL2 ongoing), further targeted Y2H assays (data not shown), BiFC assays (Figure 2C (1)), further BiFC assays (investigation of the interaction between BTSLs respectively BTSL-C and their potential interaction partners for which negative BiFC data is not presented, validation of other protein-protein interaction from the Y2H screen, data not included), subcellular protein localization and co-localization analyses (Figure 7A (1-6); 7B (2,3), GUS assays (Figure 4A, B, D, F, G, H, J, L); Supplemental Figure S12A). Prepared stable transgenic lines *proBTS:GUS*, *proPYE:GUS*. Prepared stable transgenic lines which are not yet part of the manuscript: PYE-OX, BHLH104-OX, ILR3-OX. Supervised experiments. Contributed to writing of the first version of the manuscript, reviewed/edited the manuscript. Revised the original manuscript and completed it with new data and the outlook. Prepared Figure 3E and partially F, Figure 6C, I, F, L, M, N, and O. Figure 7A 4, 5, 6, 9; 7B 3, 4. Adapted Figure 1.

Birte Schwarz

Designed, performed and analyzed the following experiments: Y2H screen (Supplemental Figure S2), targeted Y2H assay assays (Figures 2B; 3A; 4A; Supplemental Figures S4B-D), subcellular protein localization analyses (Supplemental Figure S13 (1, 2)), co-expression network construction (Supplemental Figure S1A), multiple sequence alignments (Supplemental Figures S6; S7; S8). Prepared stable transgenic lines FEP-OX, *proFEP3:GUS*, *proBTSL1:GUS.* Supervised experiments. Prepared figures and tables, wrote the first version of the manuscript, reviewed/edited the manuscript.

Christopher Endres

Performed and analyzed the following experiments: targeted Y2H assays (Figure 3D; Supplemental Figures S4B; S9A), RT-qPCRs, immunoblots, seed Fe content measurements, chlorophyll content measurements, root length measurements, remaining subcellular localization and co-localization analyses, remaining GUS assays. Helped with writing of the methods part.

Christin Sieberg

Performed and analyzed the remaining BiFC and co-localization experiments.

Petra Bauer

Conceived and supervised the study, acquired funding, reviewed/edited the manuscript.

8 Manuscript 2

Analysis of the small POPEYE-interacting protein OLIVIA reveals functions in the iron deficiency responses of *Arabidopsis thaliana*

Analysis of the small POPEYE-interacting protein OLIVIA reveals functions in the iron deficiency responses of *Arabidopsis thaliana*

Daniela M. Lichtblau[1], Birte Schwarz[1], Ksenia Trofimov[1], Petra Bauer[1,2*]

[1]Institute of Botany, Heinrich Heine University, Düsseldorf 40225, Germany

[2]Cluster of Excellence on Plant Science (CEPLAS), Heinrich Heine University, Düsseldorf 40225, Germany

***Corresponding author:** Petra Bauer, petra.bauer@hhu.de

Author contributions: D.M.L. performed the experiments and analyzed the data, K.T. performed FRET experiments, D.M.L. and P.B. designed the experiments, D.M.L and P.B. conceived the project, D.M.L. wrote the manuscript, D.M.L, B.S. and P.B. reviewed/ edited the article, P.B. acquired funding, P.B. agrees to serve as the author responsible for contact and ensures communication.

One sentence summary: The novel protein OLIVIA interacts with POPEYE and modulates its function, leading to transcriptional changes within the Fe deficiency response.

Highlights:

- OLIVIA, a highly conserved small protein that is involved in Fe homeostasis was identified
- OLIVIA interacts with the bHLH TF POPEYE in Y2H and *in planta,* based on BiFC and FRET experiments
- A unique conserved motif from OLIVIA is necessary for the protein interaction with POPEYE
- OLIVIA over-expressing plants show partially altered gene expression of POPEYE targets

Key words: Arabidopsis, Fe deficiency, Fe homeostasis, POPEYE, novel protein OLIVIA, protein interaction, regulation

Abbreviations:

bHLH	Basic helix-loop-helix
BiFC	Bimolecular fluorescence complementation
FRET	Förster Resonance Energy Transfer After Photobleaching
GFP	Green fluorescence protein
GUS	ß-Glucuronidase
mCherry	Second generation mRFP derivate
mRFP	Monomeric red fluorescence protein
OLV	OLIVIA
Ox	Over-expression
PYE	POPEYE
RT-qPCR	Reverse transcription quantitative PCR
SD	Standard deviation
TF	Transcription factor
WT	Wild type
Y2H	Yeast two-hybrid
YFP	Yellow fluorescence protein

Abstract

Iron (Fe) is a crucial micronutrient needed in many metabolic processes throughout the life of plants. To be able to adapt to changing environmental conditions, Fe uptake and homeostasis have to be carefully controlled. Consequently, under Fe deficiency a complex regulatory cascade involving many transcription factors (TFs) and other types of regulatory proteins is activated. Not only transcriptional regulation is important to maintain Fe homeostasis, protein-protein interactions among key players are also essential. In Arabidopsis the Fe deficiency induced bHLH TF POPEYE (PYE) is a key regulator of Fe homeostasis and Fe distribution. PYE transcriptionally regulates the expression of genes involved in Fe translocation from roots to shoots such as *NICOTIANAMINE SYNTHASE4* (*NAS4*), *FERRIC-REDUCTION OXIDASE3* (*FRO3*), and the *ZINC-INDUCED FACILITATOR1* (*ZIF1*). A targeted yeast two-hybrid Y2H assay uncovered a protein-protein interaction between PYE and a previously unknown small protein which we named OLIVIA (OLV). In this study OLV and the role of its interaction with PYE within the Fe deficiency response was characterized. Multiple sequence alignment analysis revealed a single conserved motif at the C-term of OLV. By using different OLV- deletion constructs, we show that this conserved motif is necessary for protein interaction with PYE. Transgenic *OLV* over-expressing (OLVox) lines exhibited partially altered gene expression of PYE targets such as *NAS4* and *FRO3* compared to wild type. In total, our results suggest that OLV, through its protein-protein interaction, enhances PYE function in Fe homeostasis.

Introduction

Iron (Fe) is an essential microelement crucial for growth and development in all living organisms. It is a cofactor in many redox reactions and serves multiple functions in fundamental metabolic processes such as photosynthesis and cell respiration (Guerinot and Yi, 1994; Hentze et al., 2004). Despite the fact that Fe is the fourth most abundant element in the continental crust, most of it is present in the form of poorly soluble Fe^{3+} oxides (Wedepohl, 1995; Grotz and Guerinot, 2006). Being sessile, plants had to develop different strategies for Fe uptake to cope with local low Fe bioavailability. Nongraminaceous monocots and dicots such as Arabidopsis (*Arabidopsis thaliana*) take up Fe via a reduction-based mechanism called Strategy I. Protons (H+) are extruded from roots to lower the local pH and solubilize Fe from the soil, while Fe chelating coumarins are released simultaneously. Fe^{3+} is reduced to Fe^{2+} at the plasma membrane and taken up into the roots (Marschner et al., 1986; Brumbarova et al., 2015; Tsai and Schmidt, 2017). Graminaceous monocots including many crops like maize or rice perform a chelation-based strategy called Strategy II. The latter is based on the excretion of phytosiderophores (PS), from the mugineic acid family to chelate Fe and the resulting Fe^{3+}-PS complexes are taken up into the root (Marschner et al., 1986; Nozoye et al., 2011). Fe is not only of fundamental necessity, but can, at the same time, be toxic in higher concentrations. Over-accumulation of Fe can lead to drastic cell damage, necrosis, or cell death due to the formation of reactive oxygen species (ROS) (Brumbarova et al., 2015; Le et al., 2019).

To ensure optimal Fe supply, sufficient, but not toxic, the Fe uptake and homeostasis in Arabidopsis is controlled by a complex network of partially co-expressed proteins with regulatory function, including several transcription factors (TFs). Under Fe deficiency a regulatory cascade consisting of mostly basic helix-loop-helix (bHLH) TFs responsible for Fe uptake and homeostasis is activated (Ivanov et al., 2012; Gao et al., 2019). The bHLH FER-LIKE IRON DEFICIENCY INDUCED TRANSCRIPTION FACTOR (FIT) controls central genes in the Fe acquisition (Colangelo and Guerinot, 2004; Bauer et al., 2007; Mai et al., 2016). Among them, FIT up-regulates gene expression of the *FERRIC-REDUCTION OXIDASE2* (*FRO2*) which is responsible for the reduction of Fe^{3+} to Fe^{2+} and the *IRON REGULATED TRANSPORTER* (*IRT1*) that imports Fe^{2+} (Robinson et al., 1999; Vert et al., 2002; Jakoby et al., 2004). FIT activity strongly relies on its protein interactions with bHLH TFs from subgroup Ib (bHLH38/39/100/101) (Yuan et al., 2008; Wang et al., 2013).

Besides Fe acquisition, storage, remobilization and the intracellular distribution of Fe are central to adapt to changing Fe availability. The bHLH TF POPEYE (PYE), belonging to subgroup IVb, is crucial for maintaining Fe homeostasis. Under Fe deficiency *PYE* is highly expressed in the pericycle, but PYE protein can also be found in the nuclei of multiple cell types throughout the root under these conditions. *pye-1* loss-of-function mutants display shorter root growth and leaf chlorosis along with decreased chlorophyll content under Fe deprivation, indicating that PYE acts in a positive manner. PYE

interacts with its PYE-LIKE homologues of subgroup IVc (bHLH104/105/115) (Long et al., 2010; Zhang et al., 2015) and functions in maintaining Fe homeostasis by directly repressing the transcriptional expression of the Fe distribution genes *NICOTIANAMINE SYNTHASE4* (*NAS4*), *FRO3* and *ZINC-INDUCED FACILITATOR1* (*ZIF1*) (Long et al., 2010). When Fe availability changes, the intracellular distribution and mobilization of Fe between roots and shoots is essential (Zhang et al., 2019). NAS4 is involved in the catalyzation of the metal chelator nicotianamine (NA), which serves in the phloem-based transportation of Fe to sink organs in form of NA-Fe complexes (Klatte et al., 2009; Schuler et al., 2012). Mitochondria are a major Fe sink to ensure the functioning of the respiratory chain and the Fe-sulfur cluster assembly. *FRO3* encodes an Fe reductase which seems to reduce Fe^{3+} in the mitochondrial membrane where it can be taken up by mitochondrial Fe transporters (MITs) (Jain and Connolly, 2013). The vacuole plays a dominant role in Fe storage and detoxification. The transporter ZIF1, located in the vacuolar-membrane, is involved in Zn homeostasis. Additionally it imports NA into the vacuole, thus transporting NA-Fe or NA-Zn into the vacuole which influences Fe availability (Haydon et al., 2012). PYE has an orthologue in rice, namely OsIRO3. As *PYE* in Arabidopsis, *OsIRO3* encodes a transcriptional repressor of *NAS* genes. However, OsIRO3 over-expressing lines are more sensitive to Fe deficiency, implying a negative regulatory function of OsIRO3 in rice (Zheng et al., 2010). It remains unclear how exactly PYE or OsIRO3 influence the Fe deficiency response.

In addition, *pye-1* loss-of-function mutants display a higher expression of the *OLIGOPEPTIDE TRANSPORTER3* (*OPT3*), a phloem specific Fe transporter essential for systemic Fe signaling and redistribution, as well as of the *FERRIC REDUCTASE DEFECTIVE 3* (*FRD3*), involved in Fe movement within the xylem (Long et al., 2010; Zhai et al., 2014). Transcriptional changes in the *pye-1* mutant suggest that there is increased inter- and intracellular Fe movement under sufficient or deficient Fe conditions if PYE is abolished and its target genes are no longer repressed (Long et al., 2010).

PYE is transcriptionally regulated by bHLH TFs of subgroup IVc (bHLH34/104/105/115) which induce *PYE* expression under Fe deficiency. They additionally activate the expression of subgroup *bHLH IB* TFs. The PYE-LIKE TFs have redundant function and act synergistically as homo- or heterodimers to activate the Fe deficiency response (Zhang et al., 2015; Li et al., 2016; Liang et al., 2017). Furthermore, they form heterodimers with UPSTREAM REGULATOR OF IRT1 (URI) in order to activate several Fe deficiency-induced genes such as subgroup *Ib BHLHs* or *PYE* itself (Gao et al., 2019; Kim et al., 2019).

Another recent study investigated the impact of the PYE interaction with the TF IAA-LEUCINE RESISTANT3 (ILR3/bHLH105), which can act as a transcriptional activator or repressor, depending on its interacting partners. Heterodimerisation with PYE leads to repression of the Fe storage proteins *FERRITIN 1/4/3* (*FER*), the *VACUOLAR IRON-TRANSPORTER-LIKE2* (*VTL2*) and the protein *At-NEET*, that transfers [Fe-S] cluster to acceptor proteins. In contrast, heterodimerisation with bHLH34/104/115 mediates increasing expression of *PYE* and subgroup *Ib BHLH* TFs (Zhang et al., 2015; Liang et al., 2017;

Tissot et al., 2019). Furthermore, the PYE-ILR3 heterodimer is involved in regulatory processes controlling the response to wounding pathogens, showing that they mediate regulatory crosstalk between Fe and wounding responses (Samira et al., 2018).

E3 ubiquitin ligases act upstream of PYE-interacting proteins of subgroup IVc (Kobayashi et al., 2013; Selote, 2015; Hindt et al., 2017). The Fe deficiency induced E3 Ligase BRUTUS (BTS) targets subgroup IVc bHLH TFs for 26S proteasomal degradation, controlling their protein level. This results in a lower expression of subgroup Ib bHLH TFs and their downstream targets involved in Fe uptake and homeostasis (Selote et al., 2015).

Small proteins and peptides can have multiple functions in regulatory stress response such as Fe deficiency. They are defined as polypeptides with usually less than 100 amino acids (aa) (Hsu and Benfey, 2018). Peptides are often mobile and can act in nutrient related signaling (Takahashi and Shinozaki, 2019). In regards to Fe deficiency, FE UPTAKE-INDUCING PEPTIDEs (FEPs or IRONMAN (IMA)) are suggested to be phloem-located peptides that promote the Fe uptake. Peptides often harbour a highly conserved consensus motif important for their function (Grillet et al., 2018; Hirayama et al., 2018). In addition to their function in signaling processes, peptides can be involved in the regulation of protein activity through protein-protein interactions (Staudt and Wenkel, 2011). Protein-protein interactions generally play a central role within the regulation of Fe uptake and homeostasis. Recently, a targeted yeast two-hybrid screen (Y2H) was performed to identify novel protein-protein interactions that might be involved in the Fe deficiency response (Lichtblau and Schwarz et al., 2020). This screen revealed an interaction between the TF PYE and a small protein of previously unknown function, which we named OLIVIA (OLV/ At1g73120). OLV is a root-expressed protein that belongs to the FIT target genes (Schwarz and Bauer, 2020), which are generally believed to function in Fe acquisition, while PYE is FIT independent and functions in the regulation of Fe distribution processes (**Supplemental. Figure S1A**). PYE and OLV are induced in response to Fe deficiency within the same root zones. This study aims to characterize OLV and the role of its interaction with PYE within the Fe deficiency response. Different protein deletion constructs of OLV were used in Y2H and Bimolecular Fluorescence Complementation (BiFC) to examine which part of OLV is required for protein-protein interaction with PYE. It could be shown that OLV over-expressing plants exhibit partially altered gene expression of PYE target genes, such as *NAS4* or *ZIF1*. We therefore propose that the interaction of PYE and OLV enhances PYE function.

Results

PYE interacts with OLV in yeast and *in planta*

Protein-protein interactions are crucial to regulate Fe uptake and homeostasis in plants. Fe deficiency-responsive genes are in many cases transcriptionally co-expressed. Because co-expression

is often a good indicator for protein-protein interactions it can be used as a starting point to search for novel interactors. A targeted Y2H interaction screen performed by (Lichtblau and Schwarz et al., 2020) revealed several (14 in total) novel interactions. Among them was a protein-protein interaction between the TF PYE and the small protein OLV (109 aa) with previously unknown function. OLV is a FIT target gene which is upregulated under Fe deficiency in roots (**Supplemental Figure S1B**). Here we explore OLV and the protein interaction with PYE in more detail. To validate their interaction, PYE and OLV were co-transformed into yeast and reciprocally tested in a targeted Y2H assay that re-conformed the results of the Y2H screen (**Figure 1A**). Compared to the Y2H interaction screen the targeted Y2H assay allows more quantitative conclusion about the interaction strength, because yeast serial dilutions were analyzed.

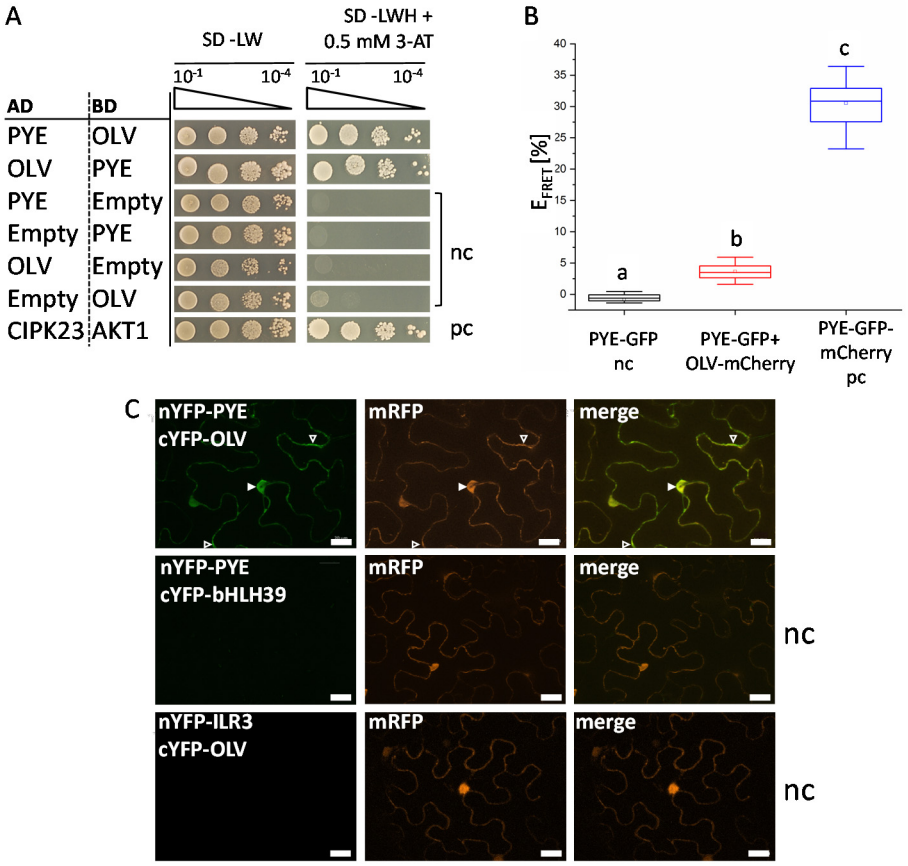

Figure 1: PYE interacts with OLV in yeast and *in planta.*
(A) Reciprocal targeted Y2H assay between OLV and PYE. Proteins were fused to the GAL4 DNA binding domain (BD) and the GAL4 activation domain (AD), and vice versa. Yeast co-transformed with AD and BD plasmid combinations were spotted in 10-fold dilution series (A_{600} = 10^{-1} -10^{-4}) on SD-LW (co-transformation control) and SD-LWH + 0.5 mM 3-AT (selection for protein interaction) plates. Negative controls (nc): empty AD with BD protein and AD protein with empty BD. Positive control (pc): CIPK23 and cAKT1 (Xu et al., 2006). **(B)** FRET-APB measurements in transiently transformed tobacco leaf epidermis cells shown. Box plots show FRET-APB to measure the strength of the interaction. FRET-APB measurements were conducted in the nucleus in which PYE fused to GFP and OLV fused to mCherry served as the FRET pair for the protein interaction study. PYE-GFP was used as donor-only negative control (nc). PYE-GFP-mCherry was used as positive control (nc) for intra-molecular FRET. An increased FRET efficiency (E_{FRET}) of the FRET pair compared to the negative control is an indication for protein interaction. Different letters indicate statistically significant differences (one-way ANOVA and Tukey´s post-hoc test, $p<0.05$), n = 10 nuclei. **(C)** BiFC experiment in transiently transformed tobacco leaf epidermis cells. (1) Interaction between nYFP-PYE and cYFP-OLV. (*legend continued on next page*)

Related non-interacting proteins were selected as negative controls: (2) nYFP-PYE + cYFP-bHLH39, (3) nYFP-ILR3 + cYFP-OLV. mRFP was used as transformation control. YFP signal indicates a protein interaction. Full and empty arrowheads indicate nuclear and cytoplasmic YFP signals. mRFP and YFP signals were imaged with a fluorescence microscope using an ApoTome. Scale bars: 20 µm. nc =negative control, pc = positive control.

Next, we wanted to verify this interaction *in planta* by using Förster resonance energy transfer-acceptor photo bleaching (FRET-APB) and BiFC. FRET-APB analysis was performed in plant nuclei where FRET was measured for the FRET Pair PYE-GFP and OLV-mCherry with a FRET efficiency of 3.5%. The FRET efficiency was significantly higher than the negative control (PYE-GFP only) and significantly lower than the positive control (PYE-GFP-mCherry) (**Figure 1B**), confirming an interaction of PYE and OLV. FRET-APB is a very sensitive method to analyze protein-interactions *in planta*. False positive protein-interactions usually do not occur (Cui et al., 2019). FRET efficiency can be measured in specific compartments of single cells like for example the nuclei or cytoplasm. Furthermore, the interaction strength can be determined using FRET. The interaction was additionally verified using BiFC (Grefen and Blatt, 2012) where a YFP signal could be obtained for PYE and OLV. As negative controls we used either PYE or OLV together with a protein that is structurally similar to the respective interacting partner (**Figure 1C**). BiFC showed that PYE and OLV interact in the nucleus and cytoplasm. BiFC experiments are relatively simple to perform and because the protein interaction can be visualized, it provides first hints about the localization of a protein-interaction (Miller et al., 2015). In summary, the protein-protein interaction of PYE and OLV could be verified by three independent methods in yeast and *in planta.* Since not much is known about OLV, we were interested in whether OLV has orthologues in other species and if parts of the protein are more conserved then others.

Multiple sequence analysis revealed a single conserved motif in OLV and orthologues in various organisms

OLV is a short protein with unknown function. To characterize it, we first wondered whether OLV is a unique protein of Arabidopsis or if orthologues can be found in other angiosperms. A BLAST search revealed that Arabidopsis has no other OVL homologue, but orthologues of OLV can be found throughout the entire angiosperm plant kingdom, from basal angiosperms to monocots and eudicots. Thus, orthologues are present in evolutionary younger and evolutionary older plants. Interestingly, a multiple sequence alignment showed that independent of the size and total percentage of aa identity, all OLV orthologues exhibited a conserved motif in the C-terminus (aa 71-87), which we named TGIYY motif due to its composition of aa (WVPHEG**TGIYY**PKGQEK, **Figure 2 A/B/C, Supplemental Figure S2**). This motif does not resemble any known protein domain (according to e.g Uniprot (www.uniprot.org) or InterPro-EMBL-EBI (www.ebi.ac.uk)). Rice exhibits an OLV orthologue that is less similar to the Arabidopsis OLV than other grass species. However, it also contains the TGIYY motif (**Supplemental Figure S2B**).

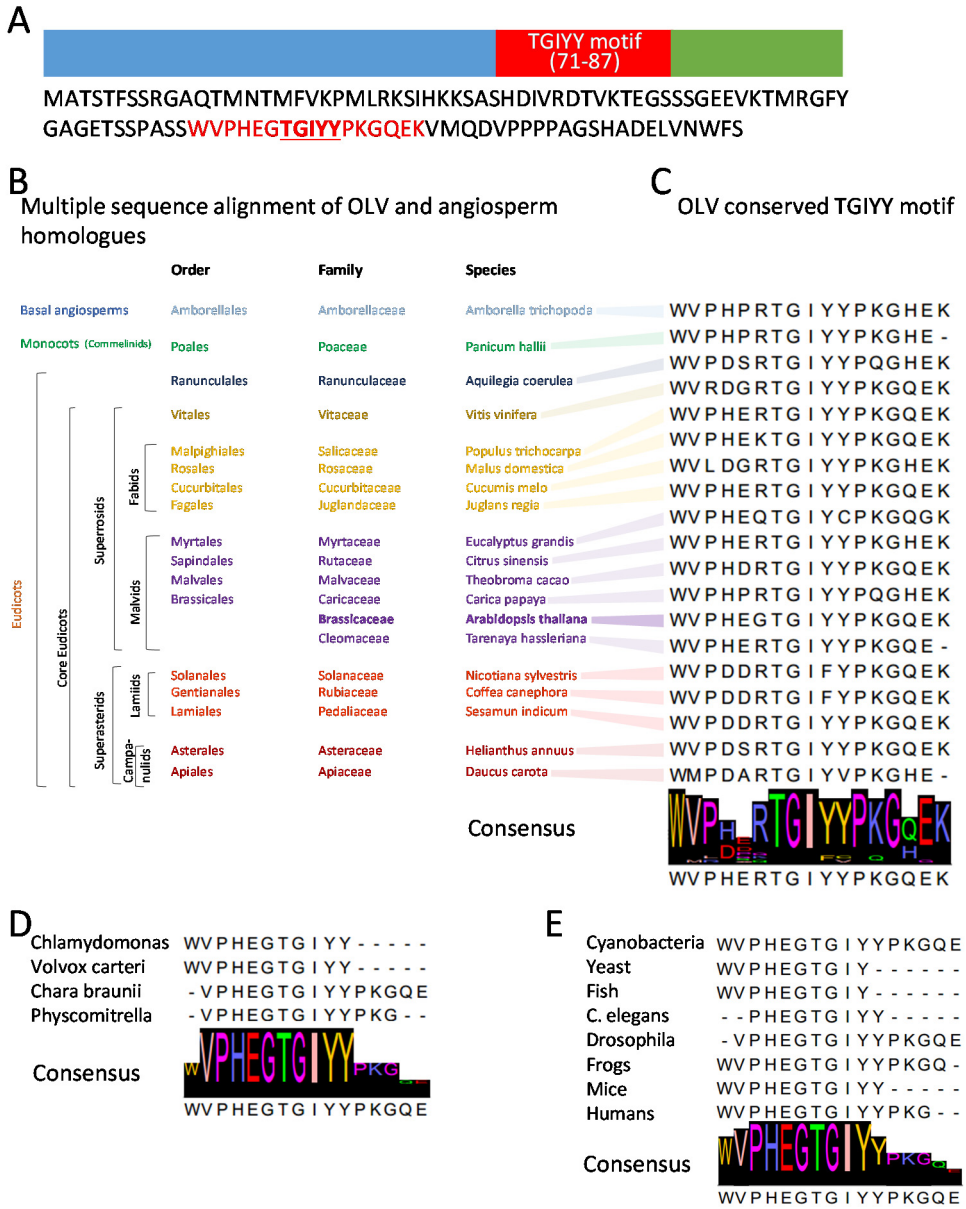

Figure 2: Multiple sequence alignment of OLV and its conserved TGIYY motif revealed orthologues throughout plants and many other species.
(A) Schematic representation of full length OLV which includes the conserved TGIYY motif (marked in red). Its aa sequence is shown underneath. **(B)** Multiple sequence alignment revealed OLV orthologues throughout the entire angiosperm kingdom. The orthologue with the highest maximum score of each order is stated. **(C)** Multiple sequence alignment depicting the TGIYY motif from selected angiosperms (refer to B). **(D)** TGIYY multiple sequence alignment of selected lower plants. **(E)** TGIYY multiple sequence alignment of non-plant organisms.

We also retraced the evolutional origin of OLVs TGIYY motif in lower plants. Small proteins containing a TGIYY (-like) motif, are already present in the unicellular Chlamydomonas and multicellular Volvox green algae. Both exhibit only little cell differentiation. Later emerged plants like Chara braunii or the moos Physcomitrella are conserved in the presence of TGIYY, even though some aa marking the beginning of OLVs conserved motif are lacking (**Figure 4D**). The conserved motif even exists in non-plant species like cyanobacteria, yeast, Drosophila, fish, frogs, mice and humans (examples are represented in **Figure 4E**). Unlike Arabidopsis, some species have more than one

orthologue of OLV (for example: *Vitis vinifera, Populus trichocarpa, Eucalyptus grandis, Sesanum indicum, Daucus carota, Chlamydomonas reinhardtii,* yeast*, Drosphila melanogaster, Homo sapiens*). Regions of conserved aa occur throughout the OLV protein sequence. However, strongest conservation can be seen in the TGIYY motif (**Supplemental Figure S2**). In non-plant species OLV orthologues could often only be found when the TGIYY motif alone was used in the BLAST search. In such cases the resulting orthologues were much bigger than 109 aa of OLV (the size varied from less than hundred to several hundred aa). In summary, orthologues of OLV and particularly the TGIYY motif were found in many different species, indicating a high level of conservation and that OLV might have a general and important function within all organism. As previously mentioned, the TGIYY motif does not resemble any known protein domain. To assess the motif function, we next tested whether it mediates protein-protein interactions.

TGIYY is required for interaction with PYE

To investigate whether the C-term with the conserved TGIYY motif of OLV is responsible for its interaction with PYE and if the TGIYY motif is needed, different protein deletion constructs of OLV were generated (**Figure 3A**). First, the OLV protein was divided into two parts of equal length (OLV-N and OLV-C). In addition, OLV-ΔTGIYY lacking the TGIYY motif and OLV-TGIYY possessing the TGIYY motif alone were analyzed for their ability to interact with PYE. OLV-FL (the entire protein sequence) and OLV-C with the TGIYY motif were able to interact with PYE in yeast and tobacco. In contrast, OLV-N was not sufficient to interact with PYE (**Figure 3B/C**). Interestingly OLV-ΔTGIYY also lost its interaction ability with PYE (**Figure 3B/C**), while OLV-TGIYY did interact with PYE (**Figure 3C**). This indicates that the conserved TGIYY motif is required for protein-protein interaction with PYE. As an interesting side effect, it could be observed that OLV-C showed self-activation activity in Y2H when grown on -LWH + 2 mM 3-AT, which was not the case on -LWH plates supplemented with 15 mM 3-AT, pointing out an important function of OLVs C-term (**Figure 3B**).

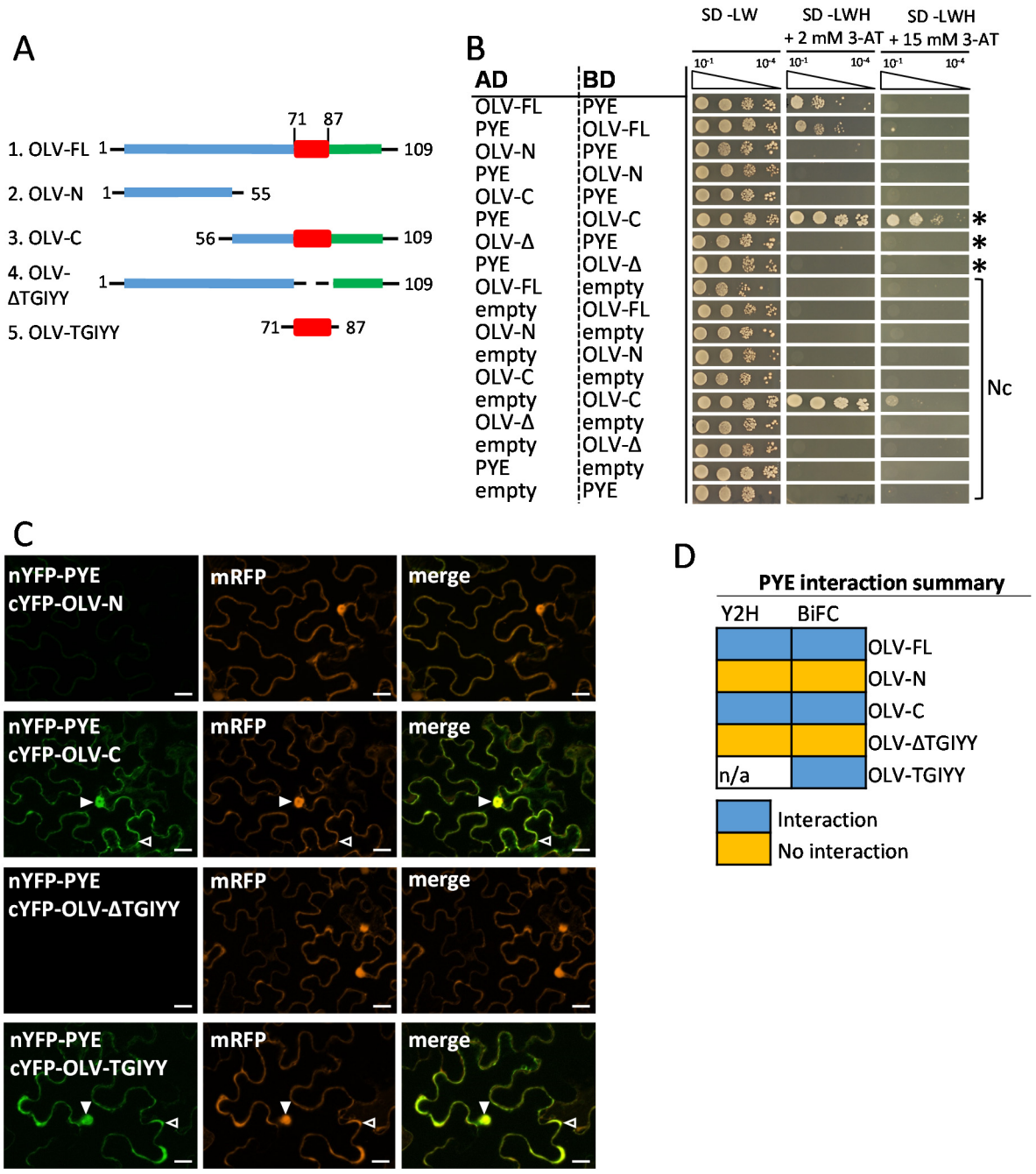

Figure 3: OLV interacts with PYE via the TGIYY motif.
(A) Schematic depiction of OLV-FL and truncations: OLV N-term (aa 1-55), OLV C-term (aa 56-109), OLVΔ (aa 1-70 and 88-109) and OLV-conserved motif (aa 71 to 87). The conserved motif is indicated in red. **(B)** Reciprocal targeted Y2H assay between OLV-FL and OLV truncations with PYE. Yeast co-transformed with AD and BD combinations were spotted on SD-LW, SD-LWH + 2 mM 3-AT and SD-LWH + 15 mM 3-AT plates as described in Figure 1. Negative controls: empty AD with BD protein and AD protein with empty BD. Asterix highlight key results. **(C)** BiFC experiment of OLV truncations with PYE in transiently transformed tobacco leaf epidermis cells. mRFP was used as transformation control. YFP signals indicate a protein interaction. mRFP and YFP signals were imaged with a fluorescence microscope using an ApoTome. Scale bars: 20 µm.Full and empty arrowheads indicate nuclear and cytoplasmic YFP signals. **(D)** Summary protein interactions with Y2H and BiFC.

Having confirmed PYEs and OLVs protein-protein interaction, the subsequent question was in which cell compartment and in what part of the roots both are co-localized and co-expressed.

PYE and OLV co-localize in the nucleus and their promotor is active in similar root zones

Using BiFC, YFP signals indicating a protein interaction for PYE and OLV was detected in the nucleus and cytoplasm. BiFC is usually not a suitable method to determine the exact localization of an interaction because over-abundance of the proteins might lead to the formation of unspecific BiFC protein complexes (Cui et al., 2019). Therefore, protein localization and co-localization studies were performed to examine in which cell compartments PYE and OLV are localized when expressed alone or together, respectively. Single localization experiments of GFP- or mCherry- tagged PYE in *Nicotiana benthamiana* leaves showed, that PYE-mCherry/ PYE-GFP mainly localizes to the nucleus while only low amounts are detected in the cytoplasm (**Figure 4A, Supplemental Figure S5A**). OLV-GFP/ OLV-mCherry on the other hand localizes to the nucleus as well as the cytoplasm (**Figure 4B, Supplemental Figure S5B**). This raises the question if co-expression of both will change their subcellular localization. When PYE-GFP and OLV-mCherry (or PYE-mCherry and OLV-GFP) are co-infiltrated into tobacco leaves they co-localize inside the nucleus (**Figure 4C, Supplemental Figure S5C**). Their subcellular localization was not affected, when both were co-expressed. Co-localization studies suggest that their protein interaction occurs mainly in the nucleus, where both are co-localized.

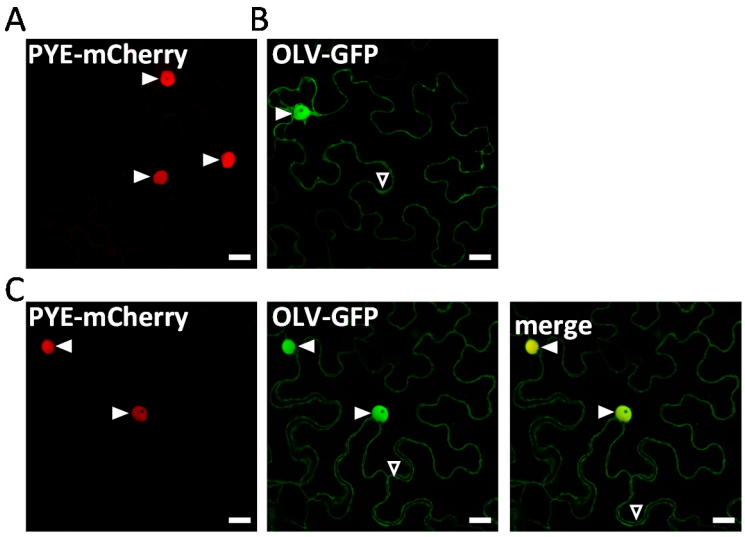

Figure 4: Subcellular localization and co-localization of PYE and OLV.
(A) Subcellular localization of PYE C-terminally tagged to mCherry and **(B)** OLV C-terminally tagged to GFP, in tobacco leaf epidermis cells. **(C)** Co-localization of PYE-mCherry and OLV-GFP. mCherry and GFP signals were imaged with a fluorescence microscope using ApoTome or with a laser scanning confocal microscope. Scale bars: 20 µM. Full and empty arrowheads indicate nuclear and cytoplasmic GFP and mCherry signals.

Next, we wanted to investigate whether or not OLV and PYE are expressed in similar root zones. The promotor activities of both were assayed by using Arabidopsis lines that stably express the GUS (ß-glucuronidase) reporter gene driven by the *OLV* or *PYE* promotors. The lines were grown for six days under +Fe or –Fe and analyzed for promotor-GUS activity (**Figure 5, Supplemental Figure S4**).

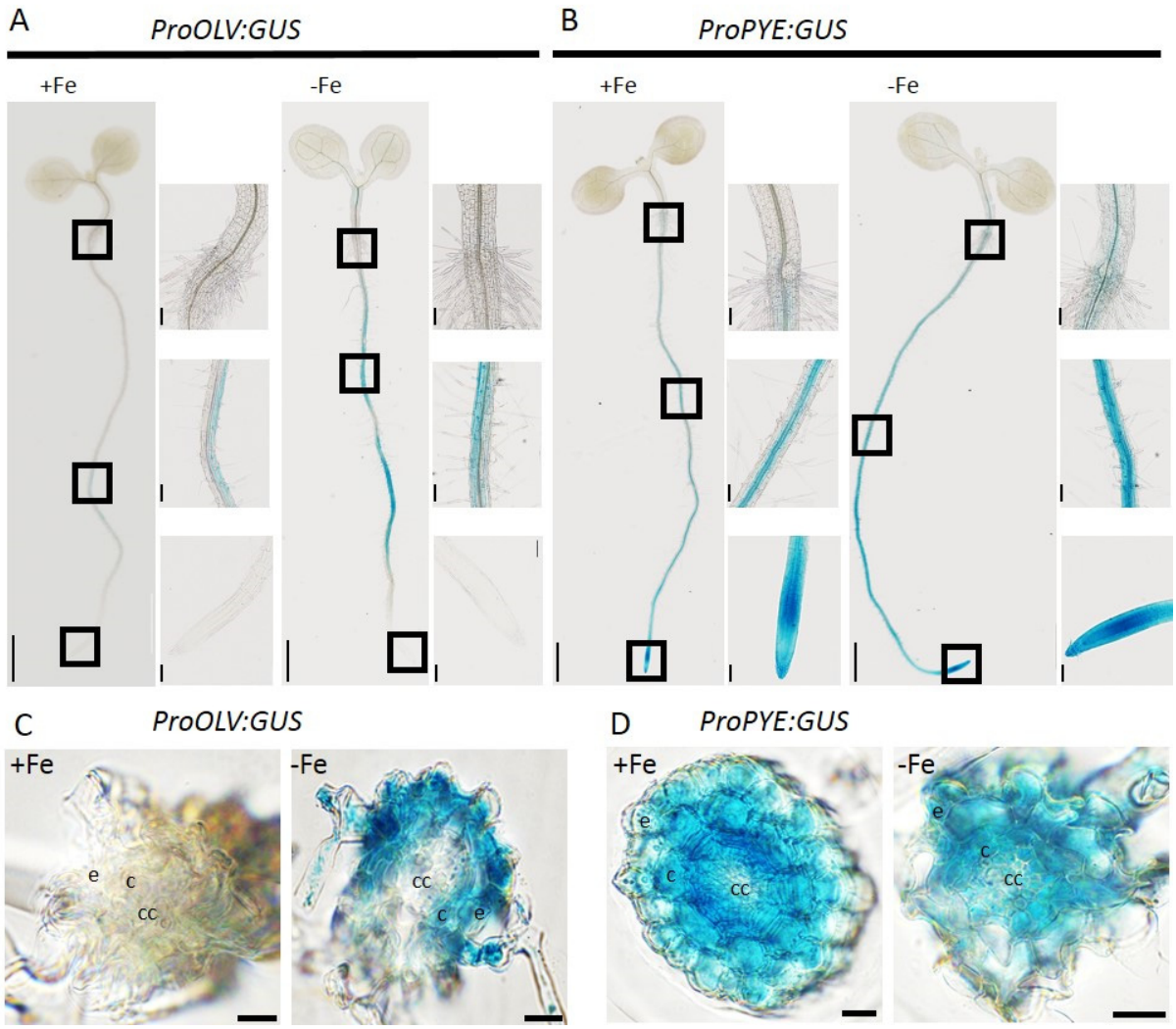

Figure 5: *OLV* and *PYE* are partially expressed in the same root zones.
OLV and *PYE* promotor-driven GUS reporter activity in Arabidopsis seedlings. Transgenic plants carrying either **(A)** pro*OLV*:GUS or **(B)** pro*PYE*:GUS in WT background were grown in the 6 d system under sufficient (+Fe) or deficient (-Fe) Fe supply and analyzed for blue GUS staining. Rectangles in whole-seedling images (left side) indicate the area of enlarged images: root tip, root differentiation zone and transition from root to hypocotyl. Scale bar whole seedling images: 1 mm, close ups: 0.1 mm. **(C)** and **(D)** cross sections of the root differentiation zone from plants imaged in (A) and (B). Abbreviations; cc: central cylinder, c: cortex, e: epidermis. Images were taken with brightfield microscopy using the stitching function of the ZEN 2 BLUE Edition software (ZEISS) for whole seedling images.

In *proOLV* lines, promotor-GUS activity was detected mainly in the cortex and epidermis of different root zones. While no *proOLV* activity occurred in the root tip and elongation zone. *proOLV* activity appeared patchy along the differentiation zone and especially in the early differentiation zone (**Figure 5A, C and Supplemental Figure S4A**). In some plants *proOLV* activity appeared in the hypocotyl. *proOLV* lines grown under -Fe showed stronger GUS activity compared to plants grown under +Fe, implying an induction of *OLV* expression under -Fe conditions. *ProPYE* expression has been reported in (Long et al., 2010) where strongest *PYE* expression was detected in the pericycle of the maturation zone. Our data indicates promotor-GUS activity of *proPYE* lines along the whole root, in the root tip and in the elongation zone as well as root differentiation zone. GUS activity did not only occur in the

pericycle, but also in the cortex and epidermis of roots. *proPYE* was not active in the cotyledons, but in the hypocotyl. *PYE* and *OLV* are both expressed in the root differentiation zone. Their expression pattern shows overlapping regions in the cortex and epidermis of GUS stained cells.

In summary, *PYE* and *OLV* share overlapping regions of expression in Arabidopsis roots. On the subcellular level they co-localize within the nucleus, where their interaction takes place.

Because OLV is localized in the cytoplasm as well as the nucleus we wanted to know whether OLV protein deletions exhibit different localization patterns than OLV-FL (**Supplemental Figure S6**). Therefore, we expressed OLV-FL, OLV-N, OLV-C and OLV-ΔTGIYY fused to an N-terminal YFP tag and found that, all OLV truncations exhibit similar localization patterns as OLV-FL. This indicates that the loss of the interaction ability of OLV-N and OLV-Δ with PYE is not caused by any changes in protein localization.

OLV has a positive effect on PYE function

To further address the role of OLV in the Fe deficiency response and to assess a possible impact on PYE function three independent HA-tagged *OLV* over-expressing lines were generated (OLVox1, OLVox2, OLVox3, **Supplemental Figure S7**). Additionally, an *olv* loss-of-function mutant line is currently constructed in our lab using CRISPR/Cas9. To determine the effects of OLV on the Fe deficiency response, we compared *OLV* over-expression plants to wild type (WT). First, their over-expression under Fe-sufficient (+Fe) and Fe-deficient (-Fe) growth conditions was confirmed by reverse transcription quantitative PCR (RT-qPCR). OLVox1 and OLVox2 over-accumulate *OLV* transcripts compared to WT in 6 d old seedlings (**Figure 6A**) and in roots of plants grown for 14 d on +Fe and transferred to either +Fe or –Fe for another 3 d (referred to as 14 + 3 d growth system) compared to WT (**Supplemental Figure S8A**). Additionally, 3xHA-OLV protein (14.85 kDa) was detected in total protein extracts of 10 d old seedlings of all three lines independent of the Fe supply, confirming the presence of a HA-tagged OLV protein (**Supplemental Figure S7B**).

OLVox plants displayed no visible phenotype, such as leaf chlorosis or reduced growth, and grew like WT under both Fe conditions. The primary root length of 6 d old seedlings grown on either +Fe or -Fe was measured. As expected roots of Fe deficient plants were longer compared to plants grown under Fe sufficiency. This was the case for WT and all OLVox lines without any noteworthy differences between WT and OLVox (**Supplemental Figure S7C**).

Next, gene expression analysis was performed in two independent experiments using different growth systems and two or three *OLV* over-expression lines (whole seedlings of the 6 d system (**Figure 6**) and roots of the 14+3 d system (**Supplemental Figure S8**). *OLV* over-expression of all lines was similar under + and -Fe, meaning the over-expression is independent of Fe availability. The first aim was to find out whether OLV has an impact on *PYE* expression. *PYE* transcript levels were equal in OLVox

compared to WT in 6 d old seedlings or 14 + 3 d roots (**Figure 6B, Supplemental Figure S8B**). PYE is a TF acting in the Fe deficiency response of Arabidopsis. OLV as an interaction partner of PYE might have an impact on gene-expression of PYE targets. Previous studies have identified several PYE targets, among them *NAS4*, *FRO3* and *ZIF1*, that are directly repressed by PYE. Furthermore, several Fe homeostasis genes, such as for example *OPT3*, *FRD3* or *NRAMP4*, are differentially expressed in *pye-1* mutants, indicating a direct or indirect regulation via PYE. The metal ion transport facilitator *OPT3* for instance is up-regulated in *pye-1* (Long et al., 2010). Because hypothesized, that the interaction between PYE and OLV might affect the expression of PYE targets, their expression level was consequently determined in OLVox lines. The expression level of PYE target genes had at least a tendency to be lower in two OLVox lines (**Figure 6C-F, Supplemental Figure S8C-F)**: for NAS4 expression a significant decrease was detected under +Fe compared to WT in 6 d old seedlings (**Figure 6C**). The expression level of *FRO3* was significantly decreased in OLVox1 and 2 under +Fe as well as in OLVox2 under -Fe, in OLVox1 *FRO3* was tended to be decreased under -Fe compared to WT in 6 d old seedlings (**Figure 6D**). Using the 14 +3 d system only OLVox1 and OLVox3 exhibited a significant decreased in *FRO3* expression (**Supplemental Figure S8D**). *ZIF1* expression was significantly decreased in OLVox lines under -Fe in the 6 d system (**Figure 6E**). Likewise, *OPT3* was slightly downregulated in 6 d old seedlings (**Figure 6F**). Interestingly, the PYE target genes seem to be more affected in the 6 d growth system. Overall our data suggest that over-expression of OLV leads to an enhanced function of PYE and increased repression of its target genes.

Because PYE is involved in Fe distribution, we were additionally interested in whether the expression of the Fe storage protein *FER1* is altered in OLVox lines, but this was not found to be the case (**Supplemental Figure S8G**). Besides *PYE*, the transcription levels of *PYE* homologues and *BTS* were determined. They act upstream of PYE within the Fe deficiency response and no altered gene expression in OLVox was observed (**Supplemental Figure S8H, I, J**). Finally, the expression levels of genes involved in Fe uptake were analyzed. As expected, no differences in gene expression levels of *BHLH39, FIT*, *IRT1* and *FRO2* were found in OLVox lines compared to WT (**Figure 6G, H, I, Supplemental Figure S8K, L, M, N**).

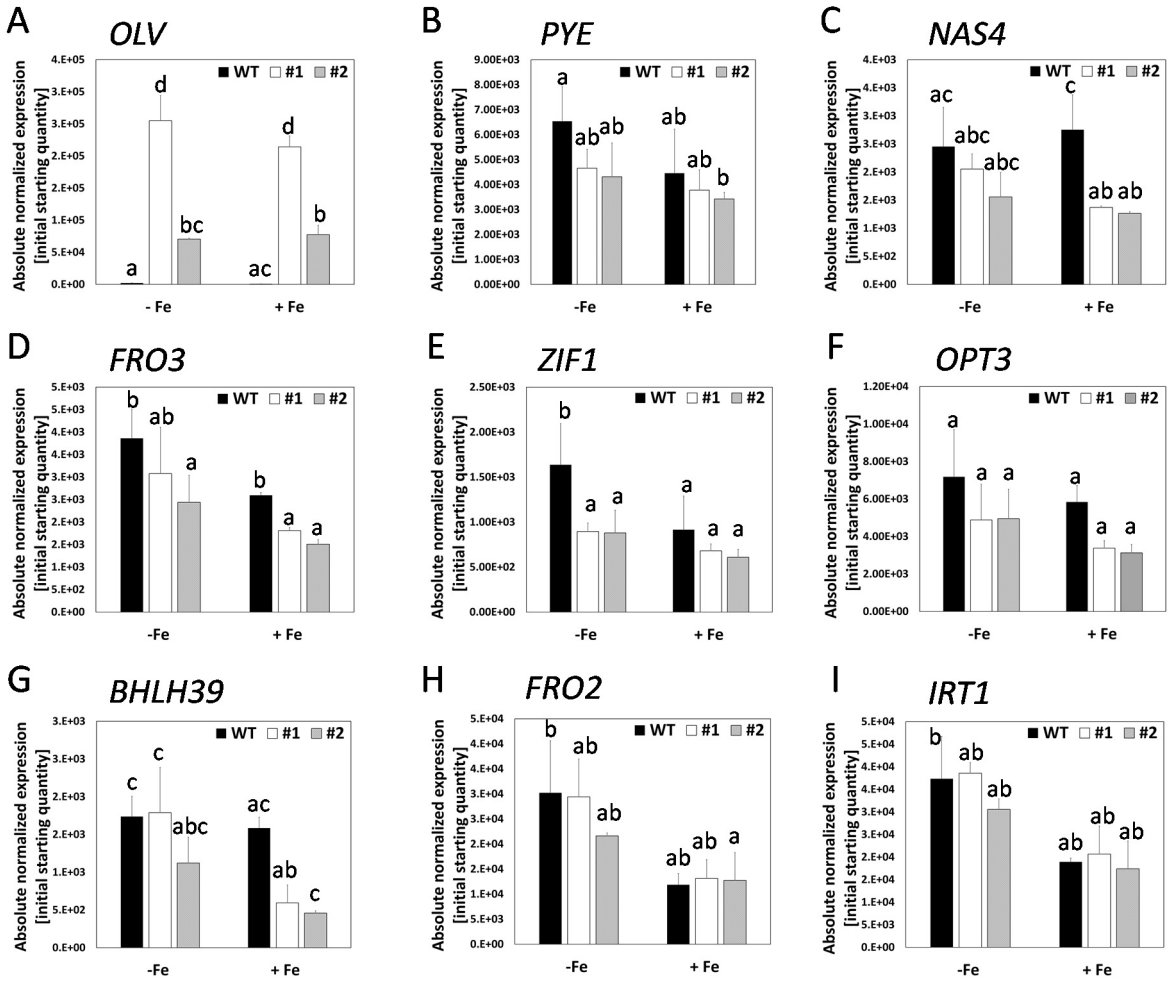

Figure 6: OLV enhances the repression of PYE downstream targets but not Fe uptake genes in 6 d old seedlings. **(A-J)** Gene expression analysis (RT-qPCR) in Arabidopsis roots of two independent OLVox lines (#1, #2). Plants were grown in the 6 d system with sufficient (+Fe) or deficient (-Fe) Fe supply. **(A)** *OLV*, **(B)** *PYE,* **(C)** *NAS4*, **(D)** *FRO3*, **(E)** *ZIF1*, **(F)** *OPT3*, **(G)** *FER1*, **(H)** *BHLH39*, **(I)** *FRO2*, **(J)** *IRT1*, (n=3). The data is depicted as mean and SD. Different letters indicate statistically significant differences (one-way ANOVA and Tukey´s post-hoc test, p<0.05).

In summary, out data show that over-expression of OLV has an effect on the expression of PYE targets, while other Fe homeostasis and the Fe uptake genes remain unaffected. This indicates that OLV has a positive effect on PYE function at the protein level, because PYE expression is not upregulated. As previously mentioned OLV belongs to the FIT-dependent genes, but might be involved in Fe homeostasis processes via its interaction with PYE, suggesting that FIT-dependent genes might possess other functions than just Fe uptake. **Figure 7** sums up the gene expression data of all tested genes under all growth condition in any OLVox line leading to the conclusion that OLVox lines display an increased repression of PYE target genes.

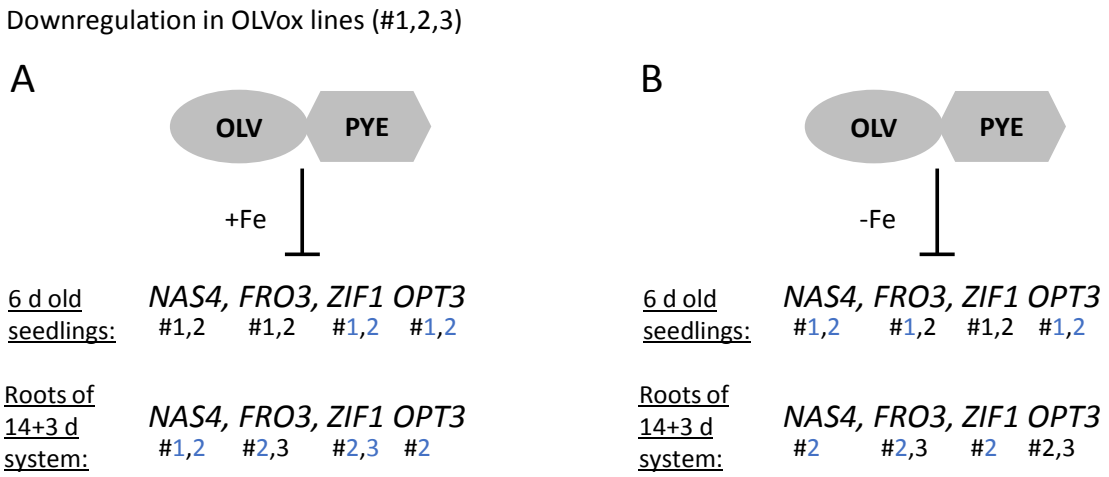

Figure 7: Summary: OLVox lines display increased repression of PYE target genes.
We hypothesize that over-expression of OLV has an impact on the repressive function of PYE on its target genes. Over-expression of OLV leads to a downregulation of PYE target genes *NAS4*, *FRO3*, *ZIF1* and *OPT3* in 6 d old seedlings and roots of plants grown in the 14 + 3 d system under both Fe conditions. Black writing indicates a significant downregulation compared to WT, blue writing indicates at least the tendency for downregulation compared to WT. OLVox lines that did not differ in their gene expression of a specific gene compared to WT are not mentioned in the figure.

Discussion

To ensure an optimal Fe uptake and distribution within the plant body, Fe uptake and homeostasis have to be rigorously controlled by various TFs and other regulatory proteins. In Arabidopsis one major TF, named PYE, was found to be involved in regulating Fe translocation processes (Long et al., 2010). Through different methods in yeast and *in planta,* we were able to verify the previously unknown Fe deficiency responsive protein OLV as a novel interaction partner of PYE. In this study the focus is on the characterization of OLV in general as well as the characterization of its impact on PYE due to its protein-protein interaction.

Like PYE, OLV is a conserved protein in many species

Multiple sequence alignment analysis of OLV revealed the existence of orthologues throughout the entire angiosperm kingdom. Like OLV, all its orthologues are rather small proteins (mostly between 95 and 120 aa) of yet unknown function, that comprise a highly conserved TGIYY motif in their C-terminus. Interestingly, OLV orthologues do not only exist in mono- and dicots but also outside the plant kingdom, for example in cyanobacteria or even in mammals. As in plants, the function of these orthologues is unknown. Therefore, no direct conclusions can be drawn regarding the role of OLV.

Due to OLVs conservation in many different species it can be assumed that these proteins might perform similar functions in a conserved process, in this case a possible function is very likely related to the regulation of Fe deficiency responses. Like OLV, most small proteins are evolutionarily

conserved and if they act in signaling cascades, it is suggested that they play a similar role among land plants (Takahashi et al., 2019). The small peptides FEPs were recently identified to positively regulate the Fe deficiency response. Arabidopsis has eight *FEP* genes that similar to OLV harbor a conserved motif in their C-terminus responsible for their function, while the N-terminus of FEPs is variable (Grillet et al., 2018; Hirayama et al., 2018). It seems to be a common mechanism for small proteins to harbor a variable region combined with a highly conserved region which includes a conserved motif needed to perform their function.

Many peptides are conserved across species and some possess lineage-specific functions (Takahashi et al., 2019). Because OLV interacts with PYE, a protein with existing orthologues in several different species (for example in cyanobacteria, Chlamydomonas, Physcomitrella, rice and even humans), it is very likely that OLV´s function is not lineage-specific and that the interaction of OLV with PYE is also conserved in species with orthologues for OLV and PYE. When Fe uptake and distribution are concerned, several genes are conserved both in plants using Strategy I (e.g Arabidopsis) as well as Strategy II (e.g. rice) to acquire Fe. Among them AtPYE/OsIRO3, which seem to repress the same cluster of Fe homeostasis genes in Arabidopsis and rice (Long et al., 2010; Zheng et al., 2010). A direct comparison of PYE and IRO3, however, is not possible, because OsIRO3 function was investigated on an over-expression line, while PYE function was examined on a loss-of-function line. Even though loss-of PYE leads to a severe Fe deficient phenotype and probable PYE targets are known, the exact mechanism through which PYE is involved in Fe deficiency responses is unclear. To confirm whether PYE and IRO3 act in a similar way to regulate Fe homeostasis, it is of significant interest to analyze the respective corresponding lines (loss-of-function of OsIRO3 and a PYE over-expression line). Interestingly, an OLV orthologue also exists in rice which shows the closest similarity in the TGIYY motif. This again indicates, that not only PYE and OLV are conserved, but so is their interaction and they take over similar functions in different plant species.

PYE and OLV are just an example, showing that many proteins and their functions in the Fe deficiency response are highly conserved. Overall, it can be concluded that both strategy I and strategy II Fe uptake mechanisms share several similarities and homologues with analogues functions. It might be questionable whether there actually is a strict separation between strategy I and II Fe uptake and to what degree they transition into one another.

PYE and OLV interact within the nucleus of cells from different root zones to fulfill their function

The interaction between PYE and OLV was previously discovered by Lichtblau and Schwarz et al. 2020, in a targeted Y2H screen. In this study the Y2H data could be confirmed. Next, we were able to validate this protein interaction by using two different *in planta* methods (FRET, BiFC). BiFC results can visualize protein interactions and give a first indication of the subcellular localization of the interacting

protein complex (Kudla and Bock, 2016). BiFC data from this study suggests, that OLV and PYE mostly interact within the nucleus, but also in the cytoplasm, the latter, however, could only partially be confirmed through co-localization studies. Previous BiFC experiments using PYE with its interaction partners BTS and members of subgroup IVc bHLH TFs, revealed interactions of PYE that occurred only in the nucleus (Selote, 2015; Zhang et al., 2015). Thus, it is possible, that despite of the BiFC results, PYE interacts with OLV mainly in the nucleus.

The subcellular localization of BiFC signals does not always reflect the actual localization pattern of interacting proteins. More information about single and co-localization of both proteins is necessary to validate localization of a protein interaction (Miller et al., 2015). PYE was predominantly detected in the nucleus and only very little PYE was visible in the cytoplasm. OLV on the other hand was detectable both in the nucleus and cytoplasm, indicating that in contrast to our BiFC data both might interact mainly in the nucleus. PYE, as a TF, represses its target genes in the nucleus. Thus, we hypothesize that OLV might have a direct effect on PYE target gene expression through TF binding in the nucleus. Heterodimerization of OLV and PYE could enhance or inhibit the ability of PYE to bind its target gene promotors, thereby regulating PYE´s function (see "OLV positively influences PYE function"). Small proteins and peptides can have regulatory function by regulating biological processes via direct peptide-TF interactions (Vanyushin et al., 2017).

Some small proteins are able to affect the localization of their interaction partners. A recent study analyzing Fe deficiency responsive proteins reported, that the localization of the TF bHLH39 depends on the presence of FIT. While in the absence of FIT bHLH39 mainly localizes to the cytoplasm, it undergoes a change in localization to the nucleus when FIT is present (Trofimov et al., 2019). Therefore, we asked whether OLV might also influence the localization pattern of PYE. However, co-expression of both proteins in tobacco didn't change the localization pattern of either PYE or OLV, indicating that their interaction has no regulatory effect on protein localization. Furthermore, it could be shown, that *PYE* and *OLV* are expressed within the same root zones under Fe deficiency. While only *proPYE* was active in the root tip, *proPYE* and *proOLV* showed overlapping regions of activity under Fe deficiency throughout the root differentiation zone, where OLV might affect PYE and thus, Fe distribution towards the shoots. Consequently, both are active under the same environmental conditions, in the same tissue and the same subcellular localization, suggesting a common function in the Fe deficiency response.

The protein interaction of PYE and OLV is dependent on OLVs TGIYY motif

The TGIYY motif was of special interest, because its conservation in many species implies a universal function in many different organisms. This motif was not described before and does not resemble any feature of already known motifs. To discover its function, first Y2H and BiFC experiments were performed that showed that the TGIYY motif is needed for the protein-protein interaction with

PYE. While the N-terminus of OLV lacking the TGIYY motif and OLV-ΔTGIYY were not able to interact with PYE, TGIYY was sufficient for the interaction. The TGIYY motif is the most conserved part of all OLV orthologues. Thus, it can assumed to be a novel conserved protein-interaction motif. Having identified the TGIYY motif of OLV as the possible site of interaction with PYE, we next wanted to analyze if the TGIYY motif has an effect on protein localization of OLV. The lack of TGIYY could result in a subcellular localization pattern in which OLV and PYE are physically not able to interact because they do not localize together. Our data show, that all truncated OLV versions used in this study have a similar localization pattern as OLV-FL, proving, that the TGIYY motif has no effect on the localization of OLV.

Many such conserved protein interaction motifs are known. For example, the bHLH TF family in plants represents the common HLH motif, responsible for protein-protein interactions with other bHLH TFs (Heim et al., 2003). PYE as a bHLH TF interacts with other bHLH TFs of subgroup IVc to regulate the Fe deficiency response of Arabidopsis (Long et al., 2010; Zhang et al., 2015; Tissot et al., 2019). It is generally assumed, that proteins sharing a common motif often function in similar processes, as is the case for bHLH TFs that interact with various protein partners to regulate multiple cellular processes (Pireyre and Burow, 2015). This could mean, that several TGIYY motif-containing proteins act in the Fe deficiency response of different plants and, potentially, even other higher organisms. OLV and orthologues do not contain a HLH motif. Therefore, it would be interesting to analyze which part of PYE OLV interacts with and whether PYE´s HLH domain plays a role in this interaction. Multiple sequence alignment comparison of PYE and its homologue TFs of subgroup IVc (bHLH34/ 104/ ILR3/ 114) shows that especially their bHLH domain is quite similar, while the C-terminal region of PYE located behind the bHLH domain is unique among these proteins (**Supplemental Figure S3**). Because only PYE is able to interact with OLV the interaction is most likely independent from the HLH motif. Moreover, only PYE harbors an ethylene-responsive element-binding factor-associated amphiphilic repression (EAR) motif (consensus sequence of DLNxxP) in its C-terminal part. EAR motifs are commonly known as transcriptional repression motifs in plants (Tissot et al., 2019). Some EAR motif containing proteins interact with other proteins via their EAR motif, which can influence the transcriptional activity. Whether this is also the case for PYE and OLV will be examined in a future study.

OLV positively influences PYE function

OLV is an interesting novel actor in the Fe deficiency response. OLV over-expressing plants have no visible change in phenotype compared to WT. They are neither chlorotic, nor do they perform better under Fe deficiency compared to WT. It is generally known, that protein-protein interactions, can regulate the activity of TFs, among other things. In this process, dimerization can positively or negatively affect the DNA binding ability, along with the activation or repression capacity

(Schwechheimer and Bevan, 1998). Because PYE targets such as *NAS4*, *FRO3* or *ZIF1* are lower expressed in OLVox plants, we hypothesize that OLV has an enhancing effect on PYE repressive function. Interestingly, the effect was stronger when using the 6 d growth system compared to the 14 + 3 d growth system. This might be explained by the fact, that various genes are expressed at different points in time and during different growth periods, which influences the results in the two growth systems. As expected, there is no effect on the expression of other bHLH TFs from subgroup IVc, BTS or the Fe uptake genes. We assume that OLV does not influence the Fe uptake machinery, but instead the Fe distribution processes, mainly via its interaction with PYE.

In their entirety, our data indicate that PYE transcript levels are not affected in OLVox lines, but PYE target genes are more strongly repressed. It can be concluded, that alterations of PYE activity on PYE target gene repression must be due to changes in protein activity. This means that PYE is either more active when more OLV protein is present or that PYE protein is more stable when interacting with OLV. This hypothesis will be tested in the lab in future experiments.

A similar regulation is already known from FIT, one of the most important TFs regulating the Fe uptake machinery. FIT interacts with ETHYLENE INSENSITIVE3 and ETHYLENE INSENSITIVE3LIKE (EIN3/EIL1) TFs. Their interaction leads to a reduction of the proteasomal degradation of FIT and is required for normal FIT abundance along with the expression of FIT targets under Fe deficiency. Transcript levels of FIT targets *IRT1* and *FRO2* were reduced to 40 % in the *ein3 eil1* mutant compared to WT levels. The interaction is not directly involved in the induction of FIT target genes, but rather maintains high FIT protein levels under Fe deficiency. Additionally, the authors claim that the interaction does not involve FIT´s bHLH domain. (Lingam et al., 2011). This example shows that bHLH proteins do not only interact with other proteins via their bHLH domain. As previously mentioned, it will be important to dissect PYE and perform protein-protein interaction studies of PYE deletions to identify the interaction site for OLV.

Hypothetical role of the PYE-OLV interaction within the Fe deficiency response regulation

Fe uptake, distribution as well as redistribution are crucial for plant survival under limited Fe access. Therefore, a complex regulatory cascade is activated under Fe deficiency. BTS, BTSL1 and 2 are negative regulators of the Fe deficiency response and act at the top of the cascade by negatively regulating bHLH TFs of subgroup IVc. IVc bHLH TFs in turn activate the expression of Ib bHLH TFs, which, as heterodimers with FIT, are needed for the induction of Fe uptake genes. They additionally activate *PYE* expression, thus leading to the repression of a set of genes involved in Fe translocation. The novel player OLV has no impact on the Fe uptake machinery, but is rather involved in influencing the Fe distribution. Within the Fe deficiency response cascade, we hypothesize that OLV, through its interaction with PYE, is jointly responsible for the repression of PYE target genes.

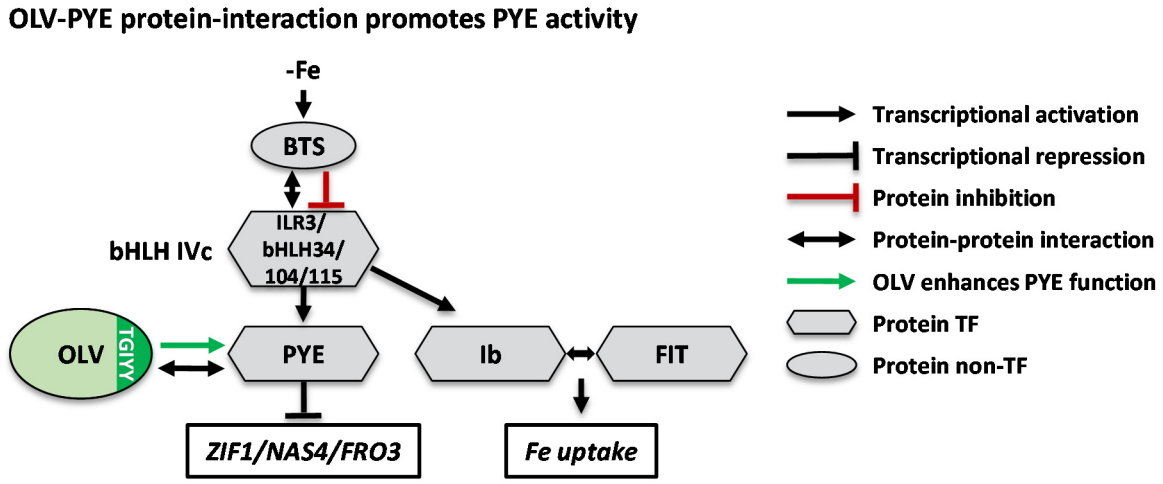

Figure 7: OLV is a new player in the current model of the Fe deficiency response regulation in Arabidopsis roots.
The model displays the present knowledge, based on available literature and incorporates OLV as a new component. OLV´s function was determined by the analysis of OLVox plants. Under Fe deficiency the E3 ligase BTS is induced. BTS interact with IVc bHLH TFs and target them for proteasomal degradation, controlling their activity on the protein level (Selote, 2015; Hindt et al., 2017). bHLH TFs of subgroup IVc act as positive regulators. They activate the expression of subgroup Ib TFs, which then form heterodimers with FIT to activate the Fe uptake machinery. On the other hand, they also activate *PYE* expression (Yuan et al., 2008; Zhang et al., 2015; Li et al., 2016; Liang et al., 2017). PYE is responsible for the direct repression of *ZIF1*, *NAS4* and *FRO3*, all of which are involved in Fe translocation processes (Long et al., 2010). We could show that OLV interacts with PYE via its conserved TGIYY motif. When OLV is over-expressed, PYE target genes are more strongly repressed compared to WT. Therefore, OLV influences PYE on protein level and enhances its protein stability or activity.

In contrast to PYE, OLV belongs to the FIT co-expression cluster that is predominantly comprised of Fe uptake genes. The interaction between the FIT-dependent OLV and the FIT-independent PYE, which in turn belongs to the Fe homeostasis network consisting of genes mainly involved in Fe distribution and relocation, might act as a regulatory connection between Fe uptake and Fe distribution processes. In conclusion we deduce that OLV does not regulate localization or expression of PYE. However, it participates in regulating its transcriptional function.

Outlook and future perspectives

Our data have so far shown, that in OLV we detected a new player in the Fe deficiency response. OLV is highly conserved among monocots and dicots, which implies evolutionary significance. We found a novel motif, named TGIYY that is likely important for protein interactions. Additionally, our data suggest, that OLV enhances PYE function as transcriptional repressor. Several questions remain open and can be explored to assess the detailed function of OLV. So will it be interesting to analyze, whether more PYE protein is available in OLVox plants or if it is the same amount as in WT. Because, if OLVox plants have more PYE protein, it could mean that OLV prevents PYE degradation. If OLVox plants exhibit a similar amount of PYE protein as WT, it would suggest that the interaction with OLV rather leads to enhanced binding of PYE to its target promotors. To address this

question, a PYE-specific antibody will be used to compare the amount of PYE in OLVox and WT plants. Additionally, a plant line that is originated from crossing of OLVox with an Arabidopsis line carrying PYE-GFP will be analyzed. We are currently creating a transgenic Arabidopsis line over-expressing an OLV protein version that lacks the TGIYY motif (OLV-ΔTGIYY). According to our results OLV seems to interact with PYE via its TGIYY motif, a transgenic OLV-ΔTGIYYox line should thus behave like WT. Furthermore, we are constructing an *olv* CRISPR/Cas9 mutant line (Hahn et al., 2017), which might have a physiological phenotype under changing Fe availability. *OLV* is induced under Fe deficiency, therefore one can expect a possible phenotype of the mutant to be stronger under -Fe. This line will also be used to verify the qPCR-based phenotype of OLVox plants. If OLV indeed enhances PYE function, *olv* loss-of-function should lead to a weaker repression of PYE target genes. OLV is up-regulated under excess zinc conditions (van de Mortel et al., 2006). Therefore, phenotypical analysis using different growth conditions, such as excess zinc or other metals, might reveal a phenotype of OLVox or *olv* mutant lines. A transgenic PYE over-expression line is already constructed and under investigation. Besides single over-expression and mutant lines, different plant crossings will be performed to create new transgenic lines. For instance, a transgenic line which over-expresses PYE and at the same time lacks *olv* will be used to determine whether OLV influences PYE protein stability.

PYE is not only interacting with OLV, but also with various other proteins, therefore it might be possible, that OLV influences these other protein-protein interactions of PYE. To address this question, PYE and one of its interactors (e.g. ILR3) could be used in combination with an OLV-over-expressing construct in tobacco leaves to study the ability of PYE and ILR3 to interact in the presence of OLV. At this, only the interactions on part of OLV protein-interaction site have been examined. It would also be of interest to find out which part of PYE OLV interacts with. Experiments to identify the region of PYE that interacts with OLV are currently ongoing. In its entirety, this study already revealed a lot of new information about the conserved protein OLV and the role of its interaction with PYE. Namely that both co-localize in the nucleus of root cells, where their interaction occurs to influence the Fe homeostasis. However, it also exposed new opportunities for future research.

Materials and Methods

Plant Material

The Arabidopsis ecotype Col-0 (Columbia-0) was used as wild type (WT) and background for all transgenic lines constructed in this study. To generate triple HA-tagged over-expression lines, full-length coding sequence (CDS) of PYE and OLV were amplified from cDNA of Fe deficient Arabidopsis WT roots with primer pairs OLV_B1 fw & OLVs_B2 rev, carrying B1 and B2 attachment sites (**Supplemental Table S1**), and then transferred via Gateway cloning into pDONR207 (Invitrogen) according to the manual (BP reaction, Thermo Fisher Scientific). After sequencing, the respective CDS

was shuttled into the plant binary destination vector pAlligator2, via Gateway LR reaction (Thermo Fisher, Scientific). pAlligator2 allows ectopic over-expression of genes N-terminally tagged with a triple HA under the control of a double CaMV 35S promotor (Bensmihen et al., 2004) (**Supplemental Figure S7A**). Final constructs were sequenced and subsequently transformed into Agrobacteria (*Rhizobium radiobacter*) strain GV3101 (pMP90) (Koncz and Schell, 1986). The Agrobacterium mediated floral dip method (Clough and Bent, 1998) was applied to generate stable transgenic Arabidopsis lines. In short, the inflorescences of six to seven weeks old Arabidopsis WT plants were dipped into a suspension of Agrobacteria (OD_{600}= 2.0) in 5% sucrose (w/v), with 0.05% (v/v) Silwet Gold (Spiess-Urania) for 20-30 s. Transformed seeds were selected based on seed specific GFP expression and confirmed by genotyping PCR of leaf gDNA using the 35S fw primer combined with a gene specific reverse primer (**Supplemental Table S1**). Homozygous T3 plants were used for further analysis. To generate pro*OLV:GUS* the promotor sequence of *OLV* (988 bp upstream of start codon) was amplified from Arabidopsis WT leaf gDNA with primer pair proOLV_-988_B1 fw/proOLV_B2 rev (**Supplemental Table S1**), transferred into pDONR207 (Invitrogen) via Gateway BP reaction (Thermo Fisher, Scientific) and then sequenced. To generate the final vector, the promotor sequence was shuttled into the Gateway binary destination vector pGWB3 (Nakagawa et al., 2007) (kindly provided by Dr. Andreas Weber, HHU Düsseldorf, Germany) via LR reaction (Thermo Fisher, Scientific), followed by sequencing. Stable Arabidopsis lines were constructed as described above. The pro*PYE:GUS* line was previously described by (Lichtblau and Schwarz et. al, 2020). Tobacco (*Nicotiana benthamiana*) plants were used for transient subcellular localization and protein interaction studies.

Plant Growth Conditions

Arabidopsis seeds were surface-sterilized and stratified for at least two days as described by (Lingam et al., 2011). Propagation and seed production was performed on soil in a climate chamber under long day conditions (16 h light, 8 h dark, 21°C). Three different growth systems were used for phenotypic, physiological, and histochemical analyses. For all growth systems Arabidopsis seedlings were grown on upright sterile plates containing modified half-strength Hoagland medium [1.5 mM $Ca(NO_3)_2$, 1.25 mM KNO_3, 0.75 mM $MgSO_4$, 0.5 mM KH_2PO_4, 50 µM KCL, 50 µM H_3BO_3, 10 µM $MnSO_4$, 2 µM $ZnSO_4$, 1.5 µM $CuSO_4$, 0.075 µM $(NH_4)_6MO_7O_{24}$, 1% (w/v) sucrose, pH 5.8, containing 1.4% plant agar (Duchefa)] and supplemented with either sufficient Fe (50 µM FeNaEDTA, +Fe) or Fe deficient (0 µM FeNaEDTA). After stratification, the plates were transferred into plant growth chambers (CLF Plant Climatics) with long day conditions for either six or ten days with +Fe or -Fe (6 d system: whole seedlings were harvested for phenotypical analysis or mRNA isolation, 10 d system: whole seedlings were harvested for protein analysis). Plants grown in the 14 + 3 d system, were grown under +Fe for 14 days and subsequently transferred on +Fe or -Fe for another three days. Roots and shoots were

harvested separately for mRNA or protein analysis. Tobacco plants were grown on soil for three to four weeks in a greenhouse facility under long day conditions. After tobacco leaf infiltration the plants were kept at room temperature under long day light conditions in the lab for two to three days until localization and protein interaction studies were performed.

Construction of OLV truncated versions

pDONR207:OLV (see plant material) was used as a template to generate different OLV truncated versions. For OLV-N (aa 1 to 55), the primer pair OLV_B1 fw/OLV +165 bp _B2 rev was used, and for OLV-C (aa 56 to 109) the primer pair OLV + 165 bp_B1 fw/OLV_B2 rev. To amplify the conserved motif (OLV-TGIYY, aa 71 to 87) the primer pair OLV + 210 bp_B2 fw/OLV + 261 bp_B2 rev was used. Deletion of TGIYY (OLV-ΔTGIYY, aa 1-70 and 88-109) was generated by overlap-extension PCR. Two partially overlapping parts of OLV were amplified with the primer pair OLV_B1 fw/OLVΔ rev and OLVΔ fw/OLV_B2 rev (**Supplemental Table S1**). Both amplicons served as template in a second PCR to amplify OLVΔ with the underlined outer primers. All primers (except OLVΔ rev and OLVΔ fw) carry B1 and B2 Gateway attachment sites. Subsequently all amplicons were transferred into pDONR207 (Invitrogen), sequenced, and further shuttled into Y2H destination vectors pACT2-GW and pGBKT7-GW, as well as into pH7WGY2 for protein localization studies (Karimi et al., 2005).

Targeted Yeast Two-Hybrid (Y2H) Assay

To study protein-protein interactions full-length OLV and truncated versions of OLV were tested with PYE in a targeted Y2H assay. All constructs were N-terminally fused to the GAL4-AD (vector: pACT2-GW), which acts as prey within the Y2H system. To generate the bait, all constructs were N-terminally fused to the GAL4-BD (vector: pGBKT7-GW) (kindly provided by Dr. Yves Jacob, Institut Pasteur, Paris, France). Full-length PYE was pairwise tested against OLV-FL (full length) and three truncated OLV versions (OLV-N, OLV-C, OLV-Δ) in both reciprocal combinations. The CDS of PYE and OLV-FL were amplified from cDNA of Fe deficient Arabidopsis WT roots with primer pairs carrying B1 and B2 attachment sites (**Supplemental Table S1**) and transferred via Gateway cloning into pDONR207 (Invitrogen) according to the manual (BP reaction, Thermo Fisher Scientific). pDONR207 constructs were sequenced, the respective CDS shuttled into the destination vectors pACT2-GW/pGBKT7-GW via Gateway LR reaction (Thermo Fisher, Scientific) followed by additional sequencing. Bait and prey constructs were co-transformed into the yeast strain AH109 via the lithium acetate (LiAc)/SS carrier DNA/PEG method based on (Gietz and Schiestl, 2007). Briefly, a 50 ml AH109-YPDA culture was grown up to OD_{600} = 0.5 and then made competent by the addition of 100 mM LiAc. 50 µl competent yeast cells were mixed with 33.3 % (w/v) PEG 4000, 0.1 M LiAc, 50 µg denatured Calf Thymus DNA (Invitrogen), 0.5-0.7 µg AD-plasmid, 0.5-0.7 µg BD-plasmid and sterile water to a final volume of 360 µl for each transformation event. Heat shock treatment was performed at 42°C for 20 min. Yeast cells

were cultivated on minimal synthetic defined (SD) media (Clontech), lacking Leu (selection for pACT2-GW) and Trp (selection for pGBKT7-GW) for 2-3 days at 30°C, to select for positive double transformants. As negative controls, bait or prey were combined with empty BD or AD plasmids and used in Y2H assays. As positive control the combination of pGBT9.BS:CIPK23 and pGAD.GH:cAKT1 was used (Xu et al., 2006). To test for protein interactions, overnight liquid cultures of transformed AH109 were adjusted to OD_{600}=1, and ten-fold serial dilutions down to 10^{-4} in sterile water were prepared. 10 µl of each suspension were spotted on SD agar plates lacking Leu, Trp and His and supplemented with 0.5 mM/15 mM 3-amino-1,2,4-triazole (SD-LWH + 3AT, suppression of background growth, detection of interaction). In parallel 10 µl of the same serial dilutions were spotted on SD agar plates lacking Leu and Trp (growth and double transformation control). Plates were cultivated at 30°C for 7 d. Growth was documented by photographing the plates every second day. Final pictures were taken on day 7.

Subcellular (co-) localization

Subcellular protein localization studies, were performed to analyse the localization of proteins. Therefore, fluorophore tagged proteins were transiently expressed in tobacco leaf epidermis cells. For N-terminal fusions the entry clones pDONR207:PYE, pDONR207:OLV (see Plant Material), pDONR207:OLV-N, pDONR207:OLV-C and pDONR207:OLV-ΔTGIYY (see Construction of OLV truncated versions) were used for subcloning PYE and OLV via Gateway LR reaction (Gateway, Thermofisher, Scientific) into the destination vector pH7WGY2 (N-terminal YFP) (Karimi et al., 2005). Final constructs were sequenced. For C-terminal fusions the CDS of PYE and OLV were amplified from cDNA of Fe deficient Arabidopsis WT roots with primer pairs PYE_B1 fw/PYEns_B2 rev and OLV_B1 fw/OLVns_B2 rev carrying B1 and B2 attachment sites without stop codon (**Supplemental Table S1**) and transferred via Gateway cloning into pDONR207 (Invitrogen) according to the manual (Gateway, BP reaction, Thermo Fisher Scientific). After sequencing, the respective CDS was shuttled into the destination vectors pMDC83 (C-terminal GFP fusion) (Curtis and Grossniklaus, 2003), as well as into the ß-estradiol-inducible pABind-GFP/pABind-mCherry (C-terminal GFP and mCherry fusions) (Bleckmann et al., 2010), via Gateway LR reaction (Thermo Fisher, Scientific). Constructs were sequenced and transformed into Agrobacteria strain GV3101 (pMP90). For tobacco leaf infiltration, an overnight culture of Agrobacteria, carrying one of the constructs, was centrifuged and the pellet re-suspended in infiltration solution (2 mM NaH_2PO_4, 0.5 % (w/v) glucose, 50 mM MES, 100 µM acetosyringone (in DMSO), pH 5.6), according to (Hötzer et al., 2012). The suspension was adjusted to OD_{600}=0.4 and infiltrated with a 1 ml syringe into the abaxial side of two tobacco leaves on two different plants. For co-localization experiments using GFP- and mCherry-tagged proteins, both Agrobacteria suspensions were mixed 1:1 to obtain a final OD_{600}=0.4 for each. Transformed tobacco plants were kept in the lab for 48 to 72 h at RT under long day conditions (16 h light, 8 h dark). To induce the expression of pABind

constructs, infiltrated tobacco leaves were sprayed abaxially with 20 µM ß-estradiol (in DMSO, supplemented with 0.1 % (w/v) Tween20) 24 h post-infiltration. To analyze transgene expression and protein localization, 0.5 cm leaf discs were punched out 20 h after induction and imaged using an Axio Imager M2 with ApoTome (Zeiss) or laser-scanning confocal microscopy (LSM 780, Zeiss). GFP and YFP were imaged at an excitation wavelength of 488 nm and emission wavelength of 500 to 530 nm. mCherry was imaged at an excitation wavelength of 563 nm and emission wavelength of 560 to 615 nm. Localization and co-localization experiments were performed in three independent experiments with two infiltrated leaves of two different plants.

Bimolecular Fluorescence Complementation (BiFC)

To verify PYE interactions with OLV *in planta* the BiFC 2in1 vector system was applied (Grefen and Blatt, 2012). The CDS of PYE and OLV-FL was amplified from pDONR207 constructs (see "Plant Material"), CDS of OLV truncated versions (OLV-N, OLV-C, OLV-TGIYY and OLV-ΔTGIYY) was amplified from cDNA of Fe deficient Arabidopsis WT roots using primer pairs carrying B3, B2 and primer pairs carrying B1, B4 attachment sites (**Supplemental Table S1**). Via BP reaction (Gateway, Thermo Fisher) all amplicons carrying B3, B2 attachment sites were transferred into pDONR221-P3P2 (Invitrogen, for nYFP fusion) and amplicons carrying B1, B4 attachment sites into pDONR221-P1P4 (Invitrogen, for cYFP fusion). Constructs were sequenced. OLV-FL or one of the truncated OLV versions were shuttled simultaneously with PYE into the destination vector pBiFC-2in1-NN (Grefen and Blatt, 2012) (N-terminal nYFP and cYFP fusions) via multisite LR reaction (Gateway, Thermo Fisher). Hereby pBiFC-2in1-NN:OLV-FL-PYE and pBiFC-2in1-NN:PYE-OLV-FL (additionally all truncated OLV versions were cloned into pBiFC-2in1-NN combined with PYE as described for OLV-FL) were created and sequenced. An internal mRFP, served as transformation control. As negative controls for PYE and OLV proteins that do not interact with either partners were selected. For PYE ILR3 was used as negative control. As negative control of OLV bHLH39 was chosen. Therefore, pBiFC-2in1-NN:PYE-bHLH39, pBiFC-2in1-NN:bHLH39-PYE, pBiFC-2in1-NN:OLV-ILR3 and pBiFC-2in1-NN:ILR3-OLV were cloned as described above. All constructs were transformed into Agrobacteria strain GV3101 (pMP90) and used for tobacco leaf infiltration as described in "Subcellular (co-) localization". After 48 to 72 h, cells which were mRFP positive were analysed for YFP signals using the Axio Imager M2 (Zeiss) with ApoTome. mRFP was imaged at an excitation wavelength of 563 nm and emission wavelength of 560 to 615 nm, YFP was imaged at an excitation wavelength of 488 nm and emission wavelength of 500 to 530 nm. Three independent BiFC experiments were performed, using two leaves for each construct. The pBiFC-2in1-NN vector was kindly provided by Dr. Christopher Grefen, Tübingen, Germany.

Förster Resonance Energy Transfer After Photo Bleaching assay (FRET-APB) between PYE and OLV

To investigate protein-protein interaction between PYE and OLV via FRET-APB, the full-length CDS of PYE and OLV were cloned into pABind-GFP, pABind-mCherry and pABind-GFP-mCherry (pABindFRET) (Bleckmann et al., 2010) as described above. For FRET-APB experiments, tobacco leaves were infiltrated with Agrobacteria carrying pABind-GFP:PYE and pABind-mCherry:OLV, or vice versa, to determine the strength of the protein-interaction ability. GFP-tagged proteins with donor only (pABind-GFP:PYE or OLV) served as negative control, the corresponding protein fused to a double tag of GFP-mCherry (pABindFRET:PYE or OLV) as positive control. To induce gene expression, infiltrated tobacco leaves were sprayed with 20 µM ß-estradiol 24 h after infiltration. The experiment was performed 20 h after ß-estradiol treatment.

FRET-APB measurements were taken with a laser-scanning confocal microscope (LSM 780, Zeiss) and controlled by the ZEN2 Black Edition software (Zeiss). For both fluorophores the fluorescence intensity was determined in the nucleus, with 20 frames of a 128 x 128 pixel format with a pixel dwell time of 2.55 µs. mCherry was photobleached after the 5^{th} frame, using 100 % laser power at 561 nm and 80 iterations. The FRET efficiency (FRET E) was calculated in percent of the relative GFP intensity increase after mCherry acceptor photobleaching (Gratz et al., 2019). Two independent experiments analyzing at least 10 nuclei with equal expression of both fluorophores were performed.

Multiple Sequence Alignment of OLV homologues

A BLAST search of Arabidopsis OLV-FL aa as well as the TGIYY motif sequence was performed in every order of the angiosperms, selected lower plants and other non-plant organisms (Cole and Hilger, 2016) using NCBI blastp. The protein sequence of the hit with the highest maximum score of each order was re-blasted in another BLAST analysis against the Arabidopsis TAIR10 protein sequence collection, applying TAIR BLAST 2.2.8 for validation. Multiple sequence alignments of all members with highest maximum score of each order were performed using the Clustal Omega algorithm (Sievers et al., 2011) and visualized with Jalview 2.10.4 (Waterhouse et al., 2009).

Histochemical ß-glucuronidase (GUS) Assay

Pro*PYE:GUS* transgenic plants have previously been reported in (Lichtblau and Schwarz et al. 2020). Pro*OLV:GUS* lines have been generated as described above. Two independent pro*OLV:GUS* and pro*PYE:GUS* lines were chosen and propagated to T2 or T3 for further analysis. Plants were grown in the 6 d system on +Fe and -Fe, in two biological replicates, and assayed for histochemical GUS activity. Four to six seedlings of each line were incubated in 1 ml GUS staining solution containing [50 mM Na_2HPO_4, 50 mM NaH_2PO_4 pH 7.2, 2 mM $K_4[Fe(CN)_6]Fe^{2+}$, 2 mM $K_3[Fe(CN)_6]Fe^{3+}$, 0.2 % Triton-X, 2 mM 5-bromo-4-chloro-3-indoyl-b-D-glucuronic acid (X-Gluc)] (Jefferson et al., 1987) for 15 min to four hours at 37°C in the dark, until blue staining was observed. Afterwards leaf chlorophyll was removed

by incubation in 70% EtOH for 24 h (EtOH was exchanged every few hours). Whole seedlings were imaged with the Axio Imager M2 (Zeiss, 10x objective magnification). Single images were assembled by using the stitching function of the ZEN 2 BLUE Edition (Zeiss).

Root Length Measurement

Plants were grown on Hoagland agar plates (see "Plant Growth Conditions") for 6 d on +Fe and -Fe. Seedlings were imaged on day 6. Primary root length of individual seedlings was measured as previously described in (Ivanov et al., 2014) using the JMicroVision software (Version 1.2.7, http://www.jmicrovision.com). Root length was measured in two independently grown sets of plants with 45 to 60 plants for each line (WT and OLVox) and condition.

Gene Expression Analysis by RT-qPCR

Gene expression analysis was performed as described previously (Abdallah and Bauer, 2016). In brief, total RNA was either extracted from whole seedlings grown in the 6 d system (n= 60-70 plants per replicate) or from roots/shoots of plants grown in the 14 + 3 d system (n=20-25 roots/shoots per replicate), using the peqGOLD Plant RNA KIT (PeqLab). Reverse transcription using oligo(dt) primer and the RevertAid first-strand cDNA synthesis kit (Thermo Fisher, Scientific) was performed to obtain cDNA. RT-qPCR was carried out on the SFX96 Touch™ Real Time Detection System (Bio-Rad) with the iTag™ Universal SYBR® Green Supermix (Bio-Rad) according to the manual. The Bio-Rad SFX Manager™ software (version 3.1) was applied to process the data. Absolute gene expression values were calculated by gene specific mass standard curve analysis. Data was normalized to the Arabidopsis elongation factor EF1Bα. All primer pairs for this study are listed in **Supplemental table S1**. The experiment was performed with at least three biological and two technical replicates.

Statistical Analysis

For statistical analysis a one-way analysis of variance (ANOVA) and a Tukey´s post-hoc test, which allow the comparison of more than two groups, were performed. Null hypothesis was rejected for p-values smaller than 0.05. Different letters indicate significant differences ($p<0.05$).

Immunoblot Analysis

Total proteins were extracted from ground plant material of either whole Arabidopsis seedlings grown in the 10 d system (Arabidopsis seedlings: n=40) or from tobacco leaves. Protein extraction, SDS-PAGE and immunodetection was performed as previously described in (Le et al., 2016). In summary, frozen plant material was homogenized using the Precellys 24 (Peqlab Life Science, VWR) and proteins were extracted with 2x SDG buffer (62 mM Tris-HCL pH 8.6, 2.5 % (w/v) SDS, 2 % (w/v) dithiothreitol, 10 % (w/v) glycerol, 0.002 % (w/v) bromphenol blue). Samples containing equal amounts of protein were separated on 12 % (w/v) SDS polyacrylamide gels via electrophoresis, followed by the

protein transfer to a Protran nitrocellulose membrane (GE Healthcare). To control for equal loading of whole protein, proteins on the membrane were stained using PonceauS (0.2 % (w/v) PonceauS, 3 % (w/v) trichloroacetic acid, 3 % (w/v) sulfosalicylic acid). To detect HA-tagged PYE or OLV protein the membranes were blocked in 5 % (v/w) milk solution (Roth) in 1x TBST (20 mM Tris-HCL pH 7.4, 180 mM NaCl, 0.1 mM (w/v) Tween20) for 30 min to avoid nonspecific antibody binding. Afterwards, the membranes were incubated with anti-HA-peroxidase high-affinity monoclonal rat antibody (clone 3F10; Roche) 1:1000 diluted in 2.5 % (w/v) milk-TBST solution, followed by three times washing in 1x TBST for 15 min each. To detect chemiluminescence signals of HA-tagged proteins the FluorChem Q System for quantitative western blot imaging (ProteinSimple) was applied and images were processed by the AlphaView® software (version 3.4.0.0, ProteinSimple).

Accession Numbers

Sequence data of PYE, OLV, AKT1 and CIPK23 can be found in the TAIR library with the following accession numbers: AKT1 (AT2G26650), BHLH39 (AT3G56980), BHLH104 (AT4G14410), BTS (AT3G18290), CIPK23 (AT1G30270), FER1 (AT5G01600), FIT (AT2G28160), FRO2 (AT1G01580), FRO3 (AT1G23020), ILR3 (AT5G54680), IRT1 (AT4G19690), NAS4 (AT1G56430), PYE (AT3G47640), OLV (AT1G73120), OPT3 (AT4G16370), ZIF1 (AT5G13740).

Supplemental Material

Figure S1. PYE and OLV belong to Fe deficiency co-expression networks in Arabidopsis roots.

Figure S2: OLV-FL protein sequence alignments reveal a highly conserved region in the C-terminus of OLV and its orthologues.

Figure S3: Multiple sequence alignment of PYE and IVc bHLH TFs identified similar and non similar areas.

Figure S4: Pro*OLV* and pro*PYE* are partially active in the same root zones of additional transgenic Arabidopsis lines.

Figure S5: Subcellular localization and co-localization of PYE and OLV

Figure S6: OLV truncations exhibit a similar subcellular localization pattern as OLV-FL.

Figure S7: OLVox lines possess HA-tagged OLV protein and are overall not different in root length compared to WT.

Figure S8: OLVox has a positive effect on PYE function.

Acknowledgements

We thank Gintaute Matthäi and Elke Wieneke for technical support. We acknowledge Rumen Ivanov, Tzvetina Brumbarova and Inga Mohr for advice with the microscope. We are thankful to them and Hans-Jörg Mai for discussions of the project. We thank Christopher Endres for technical help with *A. thaliana* root cross sections and Florian Hahn for guidance of CRISPR/Cas9 cloning. D.L and B.S are members of the international graduate school iGRAD-Plant, Düsseldorf.

Literature Cited

Abdallah HB, Bauer P (2016) Quantitative reverse transcription-qPCR-based gene expression analysis in plants. *In* Plant Signal Transduction. Springer, pp 9-24

Bauer P, Ling HQ, Guerinot ML (2007) FIT, the FER-LIKE IRON DEFICIENCY INDUCED TRANSCRIPTION FACTOR in Arabidopsis. Plant Physiol Biochem **45:** 260-261

Bensmihen S, To A, Lambert G, Kroj T, Giraudat J, Parcy F (2004) Analysis of an activated ABI5 allele using a new selection method for transgenic Arabidopsis seeds. FEBS letters **561:** 127-131

Bleckmann A, Weidtkamp-Peters S, Seidel CA, Simon R (2010) Stem cell signaling in Arabidopsis requires CRN to localize CLV2 to the plasma membrane. Plant physiology **152:** 166-176

Brumbarova T, Bauer P, Ivanov R (2015) Molecular mechanisms governing Arabidopsis iron uptake. Trends in Plant Science **20:** 124-133

Clough SJ, Bent AF (1998) Floral dip: a simplified method for Agrobacterium-mediated transformation of Arabidopsis thaliana. The plant journal **16:** 735-743

Colangelo EP, Guerinot ML (2004) The essential basic helix-loop-helix protein FIT1 is required for the iron deficiency response. The Plant Cell **16:** 3400-3412

Cole TC, Hilger HH (2016) Angiosperm phylogeny poster–flowering plant systematics.

Cui Y, Zhang X, Yu M, Zhu Y, Xing J, Lin J (2019) Techniques for detecting protein-protein interactions in living cells: principles, limitations, and recent progress. Science China Life Sciences **62:** 619-632

Curtis MD, Grossniklaus U (2003) A gateway cloning vector set for high-throughput functional analysis of genes in planta. Plant physiology **133:** 462-469

Gao F, Robe K, Bettembourg M, Navarro N, Rofidal V, Santoni V, Gaymard F, Vignols F, Roschzttardtz H, Izquierdo E (2019) The Transcription Factor bHLH121 Interacts with bHLH105 (ILR3) and its Closest Homologs to Regulate Iron Homeostasis in Arabidopsis. The Plant Cell

Gao F, Robe K, Gaymard F, Izquierdo E, Dubos C (2019) The transcriptional control of iron homeostasis in plants: a tale of bHLH transcription factors? Frontiers in plant science **10:** 6

Gietz RD, Schiestl RH (2007) High-efficiency yeast transformation using the LiAc/SS carrier DNA/PEG method. Nature protocols **2:** 31

Gratz R, Brumbarova T, Ivanov R, Trofimov K, Tünnermann L, Ochoa-Fernandez R, Blomeier T, Meiser J, Weidtkamp-Peters S, Zurbriggen M (2019) Phospho-mutant activity assays provide evidence for alternative phospho-regulation pathways of the transcription factor FIT. New Phytologist

Grefen C, Blatt MR (2012) A 2in1 cloning system enables ratiometric bimolecular fluorescence complementation (rBiFC). Biotechniques **53:** 311-314

Grillet L, Lan P, Li W, Mokkapati G, Schmidt W (2018) IRON MAN is a ubiquitous family of peptides that control iron transport in plants. Nature plants **4:** 953

Grotz N, Guerinot ML (2006) Molecular aspects of Cu, Fe and Zn homeostasis in plants. Biochimica et Biophysica Acta (BBA)-Molecular Cell Research **1763:** 595-608

Guerinot ML, Yi Y (1994) Iron: nutritious, noxious, and not readily available. Plant Physiology **104:** 815

Hahn F, Eisenhut M, Mantegazza O, Weber A (2017) Generation of Targeted Knockout Mutants in Arabidopsis thaliana Using CRISPR/Cas9. Bio-Protocol **7**

Haydon MJ, Kawachi M, Wirtz M, Hillmer S, Hell R, Kramer U (2012) Vacuolar nicotianamine has critical and distinct roles under iron deficiency and for zinc sequestration in Arabidopsis. Plant Cell **24:** 724-737

Heim MA, Jakoby M, Werber M, Martin C, Weisshaar B, Bailey PC (2003) The basic helix–loop–helix transcription factor family in plants: a genome-wide study of protein structure and functional diversity. Molecular biology and evolution **20:** 735-747

Hentze MW, Muckenthaler MU, Andrews NC (2004) Balancing acts: molecular control of mammalian iron metabolism. cell **117:** 285-297

Hindt MN, Akmakjian GZ, Pivarski KL, Punshon T, Baxter I, Salt DE, Guerinot ML (2017) BRUTUS and its paralogs, BTS LIKE1 and BTS LIKE2, encode important negative regulators of the iron deficiency response in Arabidopsis thaliana. Metallomics **9:** 876-890

Hirayama T, Lei GJ, Yamaji N, Nakagawa N, Ma JF (2018) The putative peptide gene FEP1 regulates iron deficiency response in Arabidopsis. Plant and Cell Physiology **59:** 1739-1752

Hötzer B, Ivanov R, Brumbarova T, Bauer P, Jung G (2012) Visualization of Cu2+ uptake and release in plant cells by fluorescence lifetime imaging microscopy. The FEBS journal **279:** 410-419

Hsu PY, Benfey PN (2018) Small but mighty: functional peptides encoded by small ORFs in plants. Proteomics **18:** 1700038

Ivanov R, Brumbarova T, Bauer P (2012) Fitting into the harsh reality: regulation of iron-deficiency responses in dicotyledonous plants. Mol Plant **5:** 27-42

Ivanov R, Brumbarova T, Blum A, Jantke A-M, Fink-Straube C, Bauer P (2014) SORTING NEXIN1 is required for modulating the trafficking and stability of the Arabidopsis IRON-REGULATED TRANSPORTER1. The Plant Cell **26:** 1294-1307

Jain A, Connolly EL (2013) Mitochondrial iron transport and homeostasis in plants. Frontiers in plant science **4:** 348

Jakoby M, Wang HY, Reidt W, Weisshaar B, Bauer P (2004) FRU (BHLH029) is required for induction of iron mobilization genes in Arabidopsis thaliana. FEBS Lett **577:** 528-534

Jefferson RA, Kavanagh TA, Bevan MW (1987) GUS fusions: beta-glucuronidase as a sensitive and versatile gene fusion marker in higher plants. The EMBO journal **6:** 3901-3907

Karimi M, De Meyer B, Hilson P (2005) Modular cloning in plant cells. Trends in plant science **10:** 103-105

Kim SA, LaCroix IS, Gerber SA, Guerinot ML (2019) The iron deficiency response in Arabidopsis thaliana requires the phosphorylated transcription factor URI. Proceedings of the National Academy of Sciences

Klatte M, Schuler M, Wirtz M, Fink-Straube C, Hell R, Bauer P (2009) The analysis of Arabidopsis nicotianamine synthase mutants reveals functions for nicotianamine in seed iron loading and iron deficiency responses. Plant Physiology **150:** 257-271

Kobayashi T, Nagasaka S, Senoura T, Itai RN, Nakanishi H, Nishizawa NK (2013) Iron-binding haemerythrin RING ubiquitin ligases regulate plant iron responses and accumulation. Nature Communications **4:** 2792

Koncz C, Schell J (1986) The promoter of T L-DNA gene 5 controls the tissue-specific expression of chimaeric genes carried by a novel type of Agrobacterium binary vector. Molecular and General Genetics MGG **204:** 383-396

Kudla J, Bock R (2016) Lighting the way to protein-protein interactions: recommendations on best practices for bimolecular fluorescence complementation analyses. The Plant Cell **28:** 1002-1008

Le CT, Brumbarova T, Ivanov R, Stoof C, Weber E, Mohrbacher J, Fink-Straube C, Bauer P (2016) ZINC FINGER OF ARABIDOPSIS THALIANA12 (ZAT12) Interacts with FER-LIKE IRON DEFICIENCY-INDUCED TRANSCRIPTION FACTOR (FIT) Linking Iron Deficiency and Oxidative Stress Responses. Plant Physiol **170:** 540-557

Le CTT, Brumbarova T, Bauer P (2019) The Interplay of ROS and Iron Signaling in Plants. *In* Redox Homeostasis in Plants. Springer, pp 43-66

Li X, Zhang H, Ai Q, Liang G, Yu D (2016) Two bHLH transcription factors, bHLH34 and bHLH104, regulate iron homeostasis in Arabidopsis thaliana. Plant Physiology **170:** 2478-2493

Liang G, Zhang H, Li X, Ai Q, Yu D (2017) bHLH transcription factor bHLH115 regulates iron homeostasis in Arabidopsis thaliana. Journal of experimental botany **68:** 1743-1755

Lichtblau D, Schwarz B, Endres C, Sieberg C, Bauer P (2020) E3 ligases BTSL1 and BTSL2 interact with small protein FEP3 and bHLH transcription factors regulating iron deficiency responses in Arabidopsis roots – *in preparation*.

Lingam S, Mohrbacher J, Brumbarova T, Potuschak T, Fink-Straube C, Blondet E, Genschik P, Bauer P (2011) Interaction between the bHLH transcription factor FIT and ETHYLENE INSENSITIVE3/ETHYLENE INSENSITIVE3-LIKE1 reveals molecular linkage between the regulation of iron acquisition and ethylene signaling in Arabidopsis. Plant Cell **23:** 1815-1829

Long TA, Tsukagoshi H, Busch W, Lahner B, Salt DE, Benfey PN (2010) The bHLH transcription factor POPEYE regulates response to iron deficiency in Arabidopsis roots. Plant Cell **22:** 2219-2236

Long TA, Tsukagoshi H, Busch W, Lahner B, Salt DE, Benfey PN (2010) The bHLH transcription factor POPEYE regulates response to iron deficiency in Arabidopsis roots. The Plant Cell **22:** 2219-2236

Mai H-J, Pateyron S, Bauer P (2016) Iron homeostasis in Arabidopsis thaliana: transcriptomic analyses reveal novel FIT-regulated genes, iron deficiency marker genes and functional gene networks. BMC plant biology **16:** 211

Marschner H, Römheld V, Kissel M (1986) Different strategies in higher plants in mobilization and uptake of iron. Journal of plant nutrition **9:** 695-713

Miller KE, Kim Y, Huh W-K, Park H-O (2015) Bimolecular fluorescence complementation (BiFC) analysis: advances and recent applications for genome-wide interaction studies. Journal of molecular biology **427:** 2039-2055

Nakagawa T, Kurose T, Hino T, Tanaka K, Kawamukai M, Niwa Y, Toyooka K, Matsuoka K, Jinbo T, Kimura T (2007) Development of series of gateway binary vectors, pGWBs, for realizing efficient construction of fusion genes for plant transformation. Journal of bioscience and bioengineering **104:** 34-41

Nozoye T, Nagasaka S, Kobayashi T, Takahashi M, Sato Y, Sato Y, Uozumi N, Nakanishi H, Nishizawa NK (2011) Phytosiderophore efflux transporters are crucial for iron acquisition in graminaceous plants. Journal of Biological Chemistry **286:** 5446-5454

Obayashi T, Aoki Y, Tadaka S, Kagaya Y, Kinoshita K (2018) ATTED-II in 2018: a plant coexpression database based on investigation of the statistical property of the mutual rank index. Plant and Cell Physiology **59:** e3-e3

Pireyre M, Burow M (2015) Regulation of MYB and bHLH transcription factors: a glance at the protein level. Molecular Plant **8:** 378-388

Robinson NJ, Procter CM, Connolly EL, Guerinot ML (1999) A ferric-chelate reductase for iron uptake from soils. Nature **397:** 694

Samira R, Li B, Kliebenstein D, Li C, Davis E, Gillikin JW, Long TA (2018) The bHLH transcription factor ILR3 modulates multiple stress responses in Arabidopsis. Plant molecular biology **97:** 297-309

Schuler M, Rellán-Álvarez R, Fink-Straube C, Abadía J, Bauer P (2012) Nicotianamine functions in the phloem-based transport of iron to sink organs, in pollen development and pollen tube growth in Arabidopsis. The Plant Cell **24:** 2380-2400

Schwarz B, Bauer P (2020) FIT, a regulatory hub for iron deficiency and stress signaling in roots, and FIT-dependent and-independent gene signatures. Journal of Experimental Botany

Schwechheimer C, Bevan M (1998) The regulation of transcription factor activity in plants. Trends in plant science **3:** 378-383

Selote (2015) Iron Binding E3 Ligase Mediates Iron response in Plants by targeting basic helix loop helix transcription factors Plant Physiology

Sievers F, Wilm A, Dineen D, Gibson TJ, Karplus K, Li W, Lopez R, McWilliam H, Remmert M, Söding J (2011) Fast, scalable generation of high-quality protein multiple sequence alignments using Clustal Omega. Molecular systems biology **7**

Staudt AC, Wenkel S (2011) Regulation of protein function by 'microProteins'. EMBO reports **12:** 35-42

Takahashi F, Hanada K, Kondo T, Shinozaki K (2019) Hormone-like peptides and small coding genes in plant stress signaling and development. Current opinion in plant biology **51:** 88-95

Takahashi F, Shinozaki K (2019) Long-distance signaling in plant stress response. Current opinion in plant biology **47:** 106-111

Tissot N, Robe K, Gao F, Grant-Grant S, Boucherez J, Bellegarde F, Maghiaoui A, Marcelin R, Izquierdo E, Benhamed M, Martin A, Vignols F, Roschzttardtz H, Gaymard F, Briat JF, Dubos C (2019) Transcriptional integration of the responses to iron availability in Arabidopsis by the bHLH factor ILR3. New Phytol

Trofimov K, Ivanov R, Eutebach M, Acaroglu B, Mohr I, Bauer P, Brumbarova T (2019) Mobility and localization of the iron deficiency-induced transcription factor bHLH039 change in the presence of FIT. Plant Direct **3:** e00190

Tsai HH, Schmidt W (2017) Mobilization of iron by plant-borne coumarins. Trends in plant science **22:** 538-548

van de Mortel JE, Villanueva LA, Schat H, Kwekkeboom J, Coughlan S, Moerland PD, van Themaat EVL, Koornneef M, Aarts MG (2006) Large expression differences in genes for iron and zinc homeostasis, stress response, and lignin biosynthesis distinguish roots of Arabidopsis thaliana and the related metal hyperaccumulator Thlaspi caerulescens. Plant physiology **142:** 1127-1147

Vanyushin B, Ashapkin V, Aleksandrushkina N (2017) Regulatory peptides in plants. Biochemistry (Moscow) **82:** 89-94

Vert G, Grotz N, Dedaldechamp F, Gaymard F, Guerinot ML, Briat JF, Curie C (2002) IRT1, an Arabidopsis transporter essential for iron uptake from the soil and for plant growth. Plant Cell **14:** 1223-1233

Wang N, Cui Y, Liu Y, Fan H, Du J, Huang Z, Yuan Y, Wu H, Ling H-Q (2013) Requirement and functional redundancy of Ib subgroup bHLH proteins for iron deficiency responses and uptake in Arabidopsis thaliana. Molecular plant **6:** 503-513

Waterhouse AM, Procter JB, Martin DM, Clamp M, Barton GJ (2009) Jalview Version 2—a multiple sequence alignment editor and analysis workbench. Bioinformatics **25:** 1189-1191

Wedepohl KH (1995) The composition of the continental crust. Geochimica et cosmochimica Acta **59:** 1217-1232

Xu J, Li H-D, Chen L-Q, Wang Y, Liu L-L, He L, Wu W-H (2006) A protein kinase, interacting with two calcineurin B-like proteins, regulates K+ transporter AKT1 in Arabidopsis. Cell **125:** 1347-1360

Yuan Y, Wu H, Wang N, Li J, Zhao W, Du J, Wang D, Ling H-Q (2008) FIT interacts with AtbHLH38 and AtbHLH39 in regulating iron uptake gene expression for iron homeostasis in Arabidopsis. Cell research **18:** 385

Zhai Z, Gayomba SR, Jung H-i, Vimalakumari NK, Piñeros M, Craft E, Rutzke MA, Danku J, Lahner B, Punshon T (2014) OPT3 is a phloem-specific iron transporter that is essential for systemic iron signaling and redistribution of iron and cadmium in Arabidopsis. The Plant Cell **26:** 2249-2264

Zhang J, Liu B, Li M, Feng D, Jin H, Wang P, Liu J, Xiong F, Wang J, Wang H-B (2015) The bHLH transcription factor bHLH104 interacts with IAA-LEUCINE RESISTANT3 and modulates iron homeostasis in Arabidopsis. The Plant Cell **27:** 787-805

Zhang X, Zhang D, Sun W, Wang T (2019) The Adaptive Mechanism of Plants to Iron Deficiency via Iron Uptake, Transport, and Homeostasis. International journal of molecular sciences **20:** 2424

Zheng L, Ying Y, Wang L, Wang F, Whelan J, Shou H (2010) Identification of a novel iron regulated basic helix-loop-helix protein involved in Fe homeostasis in Oryza sativa. BMC plant biology **10:** 166

Supplemental Figures and Tables

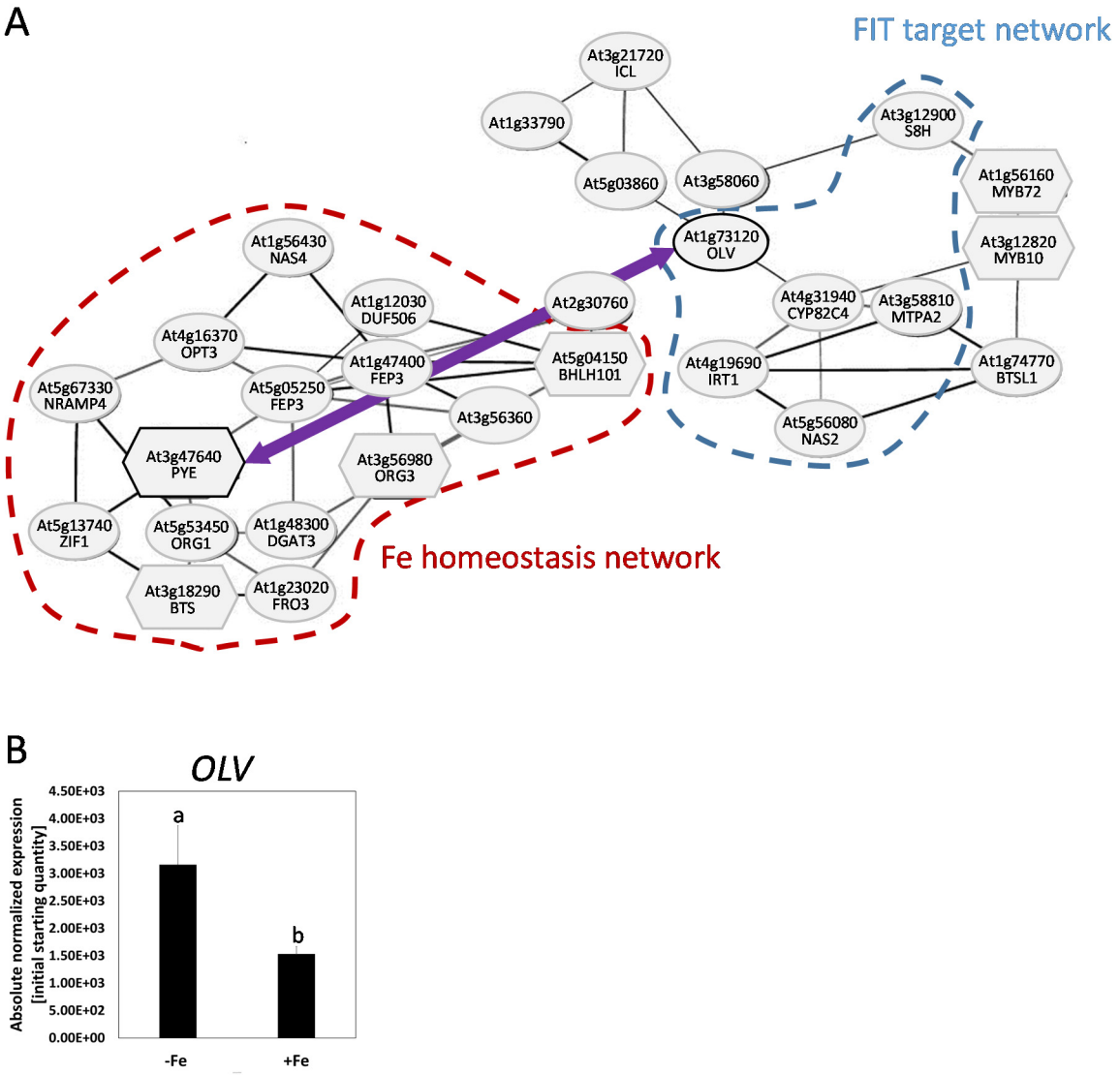

Figure S1. PYE and OLV belong to Fe deficiency co-expression networks in Arabidopsis roots.
A) Co-expressed Fe deficiency-responsive genes are shown. OLV belongs to the FIT target network (surrounded by a blue dashed line) containing FIT-dependent genes. PYE belongs to the Fe homeostasis network (surrounded by a red dashed line) including FIT-independent genes (Schwarz and Bauer, 2020). The ATTED-II tool (Ver. 9.2) was used to generate the network (Obayashi et al., 2018) based on PYE and OLV as input genes. The purple arrow links the two interacting proteins PYE and OLV. **(B)** *OLV* gene expression analysis (RT-qPCR) in Arabidopsis WT roots. Three independent replicates of plants grown in the 14 + 3 d system with sufficient (+Fe) or deficient (-Fe) supply for the last three days. The data is depicted as mean and SD. Different letters indicate statistically significant differences (one-way ANOVA and Tukey´s post-hoc test, $p<0.05$).

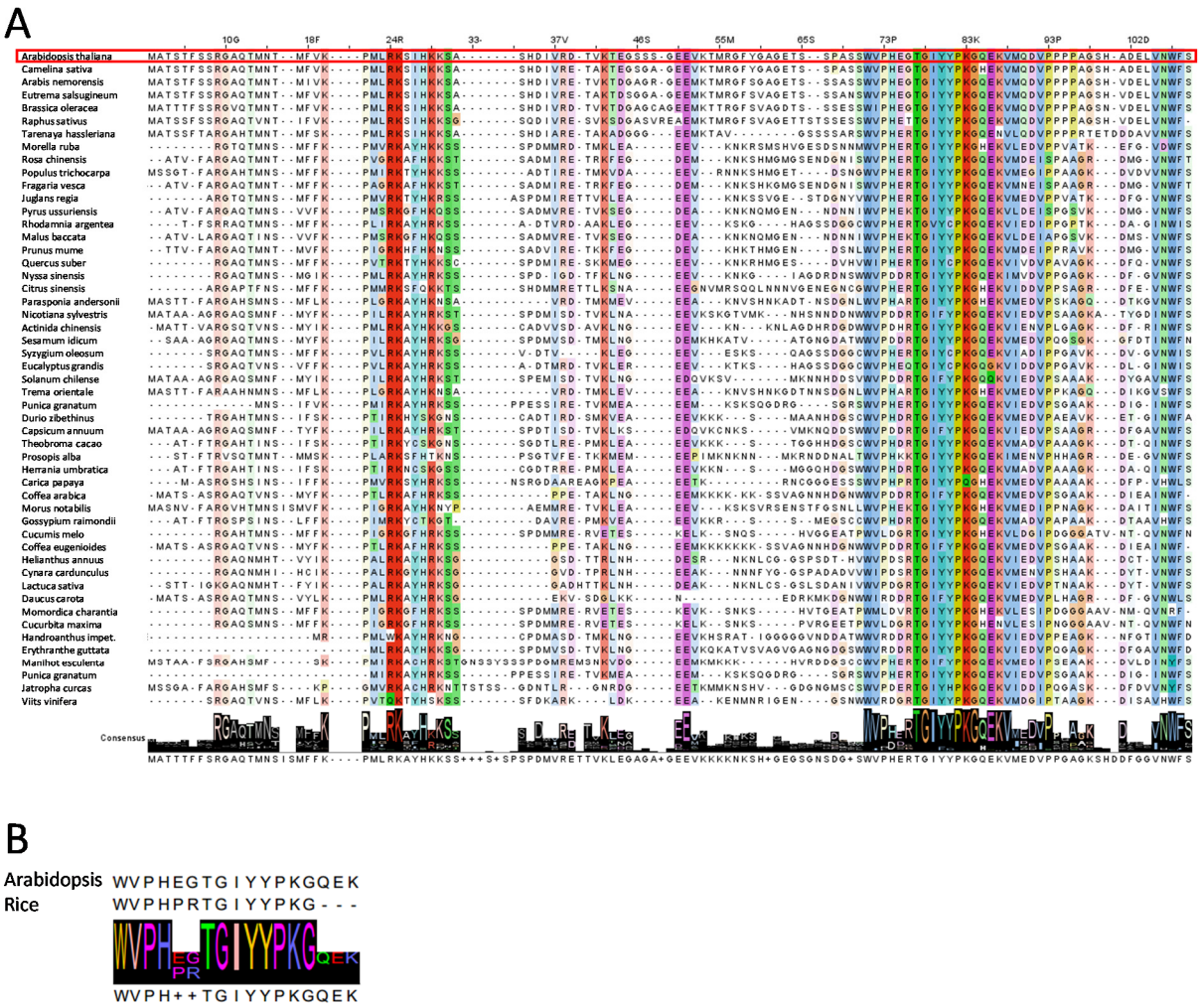

Figure S2: OLV-FL protein sequence alignments reveal a highly conserved region in the C-terminus of OLV and its orthologues.

(A) Multiple sequence alignment of OLV full length protein sequence revealed existence orthologues throughout the entire angiosperm kingdom. The orthologue with the highest maximum score of each order is shown. Corresponds to Figure 2. **(B)** Sequence alignment of the TGIYY motif from OLV and the highest BLAST hit of rice species.

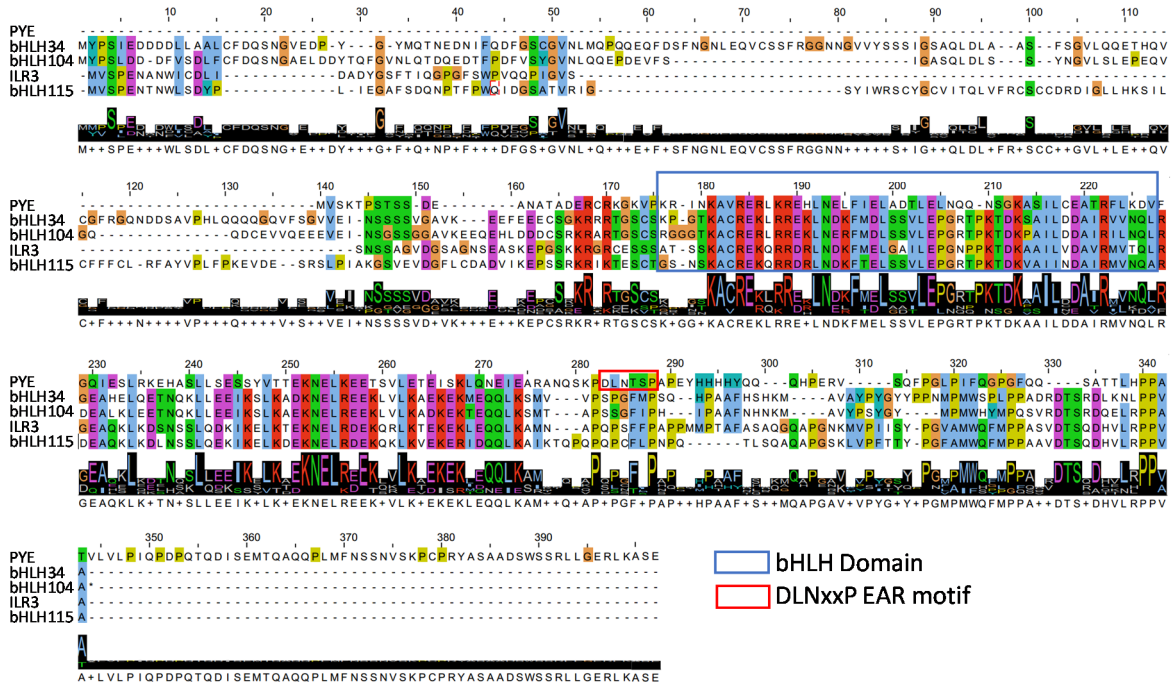

Figure S3: Multiple sequence alignment of PYE and IVc bHLH TFs identified similar and non similar areas.
Multiple sequence alignment of full length PYE, bHLH34, bHLH104, ILR3 and bHL115 protein sequence. The bHLH domain and the EAR motif are indicated in blue/ red, the annotation is based on UniProt (www.uniprot.org).

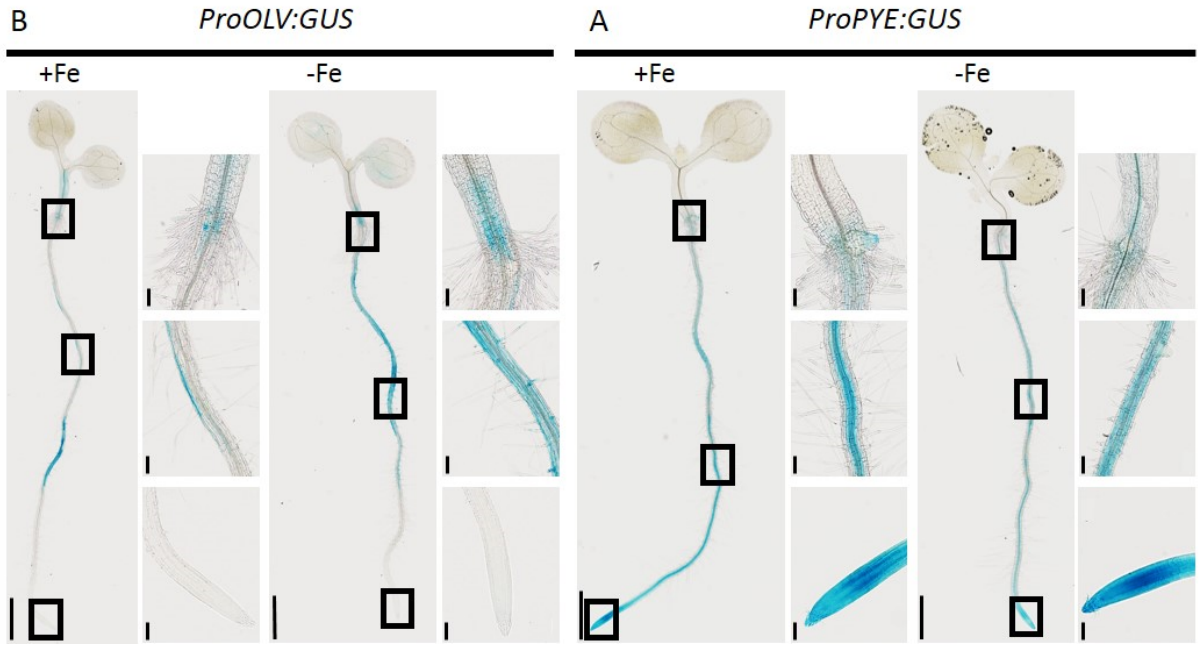

Figure S4: Pro*OLV* and pro*PYE* are partially active in the same root zones of additional transgenic Arabidopsis lines.
OLV and PYE promotor-driven GUS reporter activity in Arabidopsis seedlings. Transgenic plants carrying either **(A)** pro*OLV:GUS* or **(B)** pro*PYE:GUS* in WT background were grown in the 6 d system under sufficient (+Fe) or deficient (-Fe) Fe supply and analyzed for blue GUS staining, to indicate reporter gene activity. Rectangles in whole-seedling images (left side) mark the area of enlarged images: root tip, root differentiation zone and transition from root to hypocotyl. Scale bar whole seedling images: 1 mm, close ups: 0.5 mm. Images were taken with brightfield microscopy using the stitching function of the ZEN 2 BLUE Edition software (ZEISS) for whole seedling images.

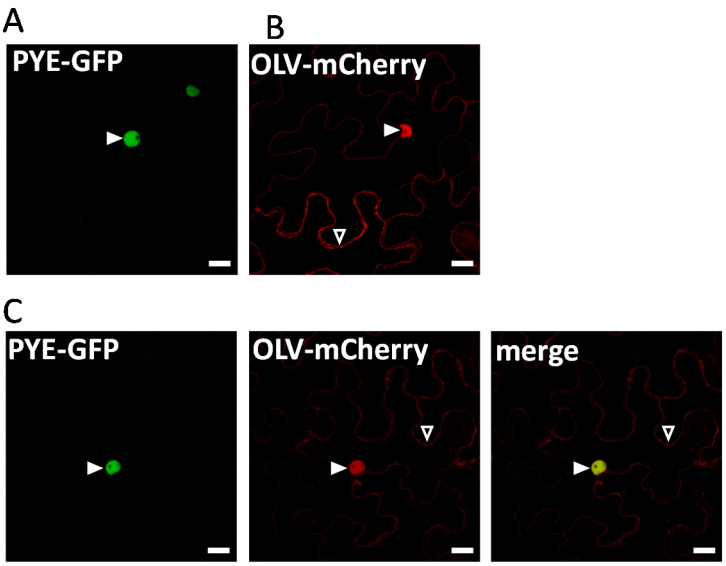

Figure S5: Subcellular localization and co-localization of PYE and OLV.
Subcellular localization of **(A)** PYE-GFP and **(B)** OLV-mCherry, in tobacco leaf epidermis cells. **(C)** Co-localization of PYE-GFP and OLV-mCherry. Refer to Figure 4. GFP and mCherry signals were imaged with a fluorescence microscope using ApoTome or with a laser scanning confocal microscope. Scale bars: 20 µM.

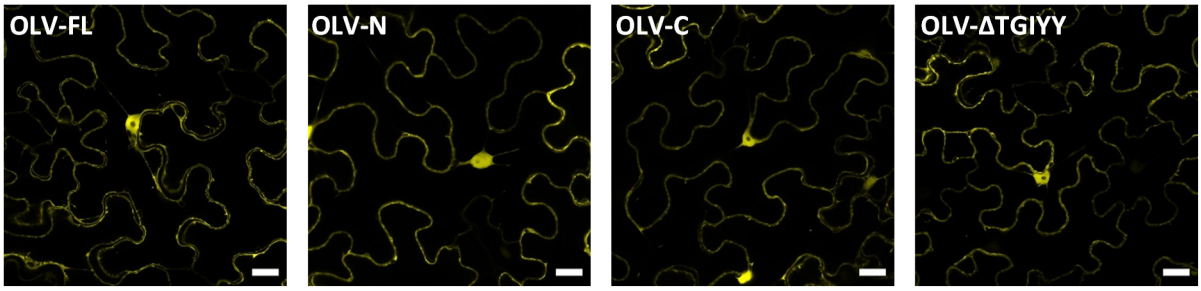

Figure S6: OLV truncations exhibit a similar subcellular localization pattern as OLV-FL.
Subcellular localization of OLV-FL and different truncations in tobacco leaf epidermis cells. Proteins were N-terminally tagged to YFP. YFP signals were imaged with a fluorescence microscope using ApoTome. Scale bar: 20 µm.

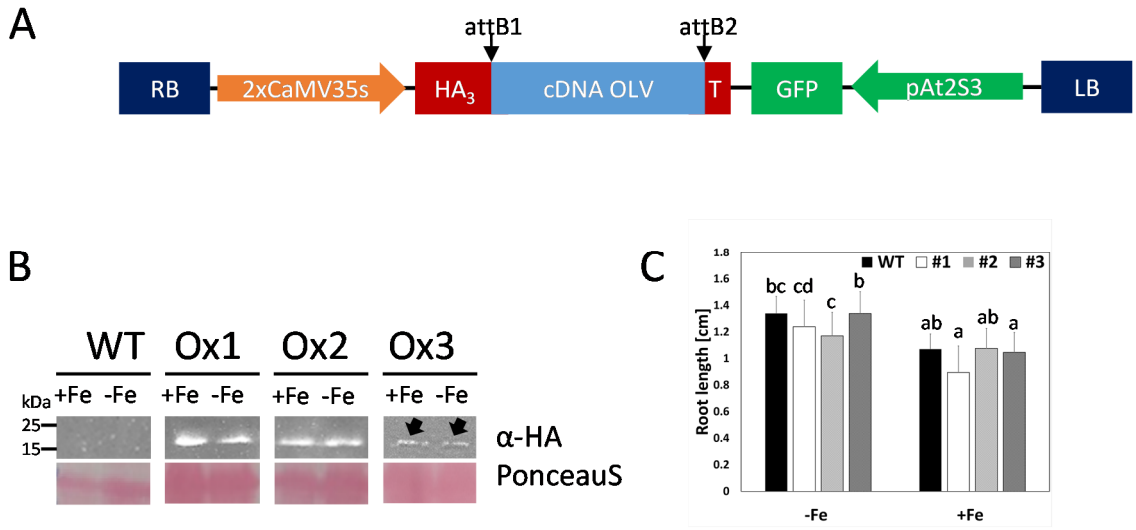

Figure S7: OLVox lines possess HA-tagged OLV protein and are overall not different in root length compared to WT.

(A) pAlligator2 cloning cassette containing a 2xCaMV35S-promotor in front of the 3xHA-tagged OLV/ PYE cDNA. The gene constructs are under the control of a 2xCaMV25S-promotor. Seed specific GFP expression driven by pAT2S3 is used for the selection of positive transgenic seeds. **(B)** Anti-HA immunodetection of HA_3-OLV protein in three independent lines (#1, #2, #3, for line 3 indicated by black arrows). Protein extract of whole seedlings, grown for 10 d under + Fe or -Fe was loaded. WT served as negative control. PonceauS staining of the membrane is used as loading control. Expected molecular weight of HA_3-OLV: 14.85 kDa. **(C)** Root length of WT and OLVox (#1, #2, #3) seedlings grown in the 6 d system with -Fe or +Fe supply (n>60).

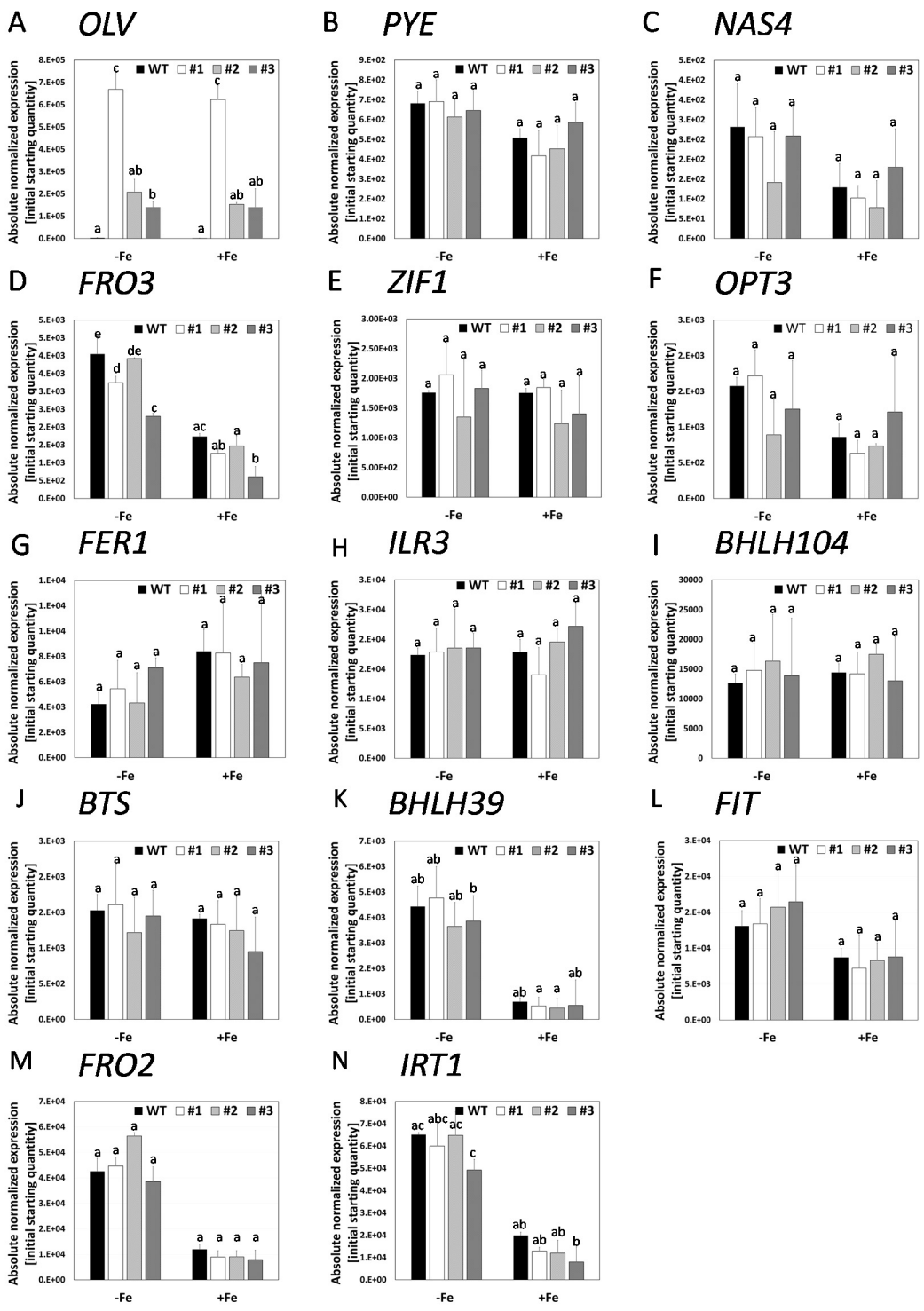

Figure S8: OLVox has a positive effect on PYE function.
(A-L) Gene expression analysis (RT-qPCR) in Arabidopsis roots of three independent OLVox lines (#1, #2, #3). Plants were grown in the 14 + 3 d system with sufficient (+Fe) or deficient (-Fe) Fe supply for the last three days. **(A)** *OLV,* **(B)** *PYE*, **(C)** *NAS4*, **(D)** *FRO3*, **(E)** *ZIF1*, **(F)** *OPT3,* **(G)** *FER1*, **(H)** *ILR3*, **(I)** *BHLH104*, **(J)** *BTS*, **(K)** *BHLH39*, **(L)** *FIT*, **(M)** *FRO2* and **(N)** *IRT1* (n=3). The data is depicted as mean and SD. Different letters indicate statistically significant differences (one-way ANOVA and Tukey´s post-hoc test, p<0.05).

Supplemental Table S1: Primers used in this study.

Fw = forward, rev = reverse, s = stop codon, ns = no stop codon, FL = full length, Δ = delta conserved motif, B1/B2/B3/B4 = (attb) gateway attachment sites

Primer Name	Sequence 5´ → 3´	Application	Origin
Amplification of full-length or truncated CDS for Y2H, (co-) localization, BiFC, FRET and OX/ mutant lines			
OLV_B1 fw	GGGGACAAGTTTGTACAAAAAAGCAG GCTTCATGGCGACTTCTACCTTCT	cloning of OLV-FL, OLV_1-55, 7320Δ	Lichtblau and Schwarz et al. 2020
OLVs_B2 rev	GGGGACCACTTTGTACAAGAAAGCTGG GTTCAAGAGAACCAATTAACGAG	cloning of OLV-FL, OLV_55-109, OLVΔ	Lichtblau and Schwarz et al. 2020
OLVns_B2 rev	GGGGACCACTTTGTACAAGAAAGCTGG GTCAGAGAACCAATTAACGAG	cloning of OLV-FL, OLV_55-109, OLVΔ	This study
OLV_B3 fw	GGGGACAACTTTGTATAATAAAGTTGT AATGGCGACTTCTACCTTCTC	cloning of OLV-FL, OLV_1-55	This study
OLVs_B4 rev	GGGGACAACTTTGTATAGAAAAGTTGG GTGTCAAGAGAACCAATTAACGA	cloning of OLV-FL, OLV_55-109	This study
OLVns_B4 rev	GGGGACAACTTTGTATAGAAAAGTTGG GTGAGAGAACCAATTAACGA	cloning of OLV-FL, OLV_55-109	This study
OLV+165s_B2 rev	GGGGACCACTTTGTACAAGAAAGCTGG GTCTCACATCGTCTTCACCTCCT	cloning of OLV_1-55	This study
OLV+165s_B4 rev	GGGGACAACTTTGTATAGAAAAGTTGG GTGTCACATCGTCTTCACCTCCT	cloning of OLV_1-55	This study
OLV+165_B1 fw	GGGGACAAGTTTGTACAAAAAAGCAG GCTTCATGAGAGGCTTCTACGGCGCCG G	cloning of OLV_55-109	This study
OLV+165_B3 fw	GGGGACAACTTTGTATAATAAAGTTGT AATGAGAGGCTTCTACGGCGCCGG	cloning of OLV_55-109	This study
OLV+210_B1 fw	GGGGACAAGTTTGTACAAAAAAGCAG GCTTCATGTGGGTGCCACATGAAGGT	cloning of OLV motif	This study
OLV+264s_B2 rev	GGGGACCACTTTGTACAAGAAAGCTGG GTCTCATTTCTCTTGTCCCTTTGGATA	cloning of OLV motif	This study
OLV+210_B3 fw	GGGGACAACTTTGTATAATAAAGTTGT AATGTGGGTGCCACATGAAGGT	cloning of OLV motif	This study
OLV+264s_B4 rev	GGGGACAACTTTGTATAGAAAAGTTGG GTGTCATTTCTCTTGTCCCTTTGGATA	cloning of OLV motif	This study
OLVΔ fw	CGTCGTCGCCGGCGAGTAGTGTGATGC AAGATGTGCCTCC	cloning of OLVΔ	This study
OLVΔ rev	GGAGGCACATCTTGCATCACACTACTC GCCGGCGACGACG	cloning of OLVΔ	This study
OLV sgRNA_1 fw	ATTGCATGATATAGTGAGGGATA	cloning of *olv*	This study
OLV sgRNA_1 rev	AAACTATCCCTCACTATATCATG	cloning of olv	This study
OLV sgRNA_2 fw	ATTGTGAATTGATTTCCTAAGCAT	cloning of *olv*	This study
OLV sgRNA_2 rev	AAACATGCTTAGGAAATCAATTCA	cloning of *olv*	This study
FH41	AAACGACGGCCAGTGCCAGAATTGGG CCCGACGTCG	cloning of *olv*	Hahn et al. 2017
FH42	TACTGACTCGTCGGGTACCAAGCTATG CATCCAACGCG	cloning of *olv*	Hahn et al. 2017
FH254	GCCCAATTCCAAGCTATGCATCCAACGC G	cloning of *olv*	Hahn et al. 2017
FH255	CATAGCTTGGAATTGGGCCCGACGTCG	cloning of *olv*	Hahn et al. 2017
M13_CRISPR fw	GTAAAACGACGGCCAG	*olv* mutant line	Hahn et al. 2017
M13_CRISPR rev	CAGGAAACAGCTATGAC	*olv* mutant line	Hahn et al. 2017
PYE_B1 fw	GGGGACAAGTTTGTACAAAAAAGCAG GCTTCATGGTATCGAAAACTCCTTC	cloning of PYE	Lichtblau and Schwarz et al. 2019
PYEs_B2 rev	GGGGACCACTTTGTACAAGAAAGCTGG GTCTCATTCACTGGCTTTCAGCC	cloning of PYE	Lichtblau and Schwarz et al. 2020
PYEns_B2rev	GGGGACAAGTTTGTACAAAAAAGCAG GCTTCGAGAAAAGGATTCTAATTTAGG A	cloning of PYE	Lichtblau and Schwarz et al. 2020
PYE_B3 fw	GGGGACAACTTTGTATAATAAAGTTGT AATGGTATCGAAAACTCCTTC	cloning of PYE	Lichtblau and Schwarz et al. 2020
PYEs_B4 rev	GGGGACAACTTTGTATAGAAAAGTTGG GTGTCATTCACTGGCTTTCAGCC	cloning of PYE	Lichtblau and Schwarz et al. 2020
PYEns_B4 rev	GGGGACAACTTTGTATAGAAAAGTTGG GTGTTCACTGGCTTTCAGCC	cloning of PYE	Lichtblau and Schwarz et al. 2020
ILR3_B1 fw	GGGGACAAGTTTGTACAAAAAAGCAG GCTTCATGGTGTCACCCGAAAACG	colony PCR ILR3	Lichtblau and Schwarz et al. 2020

ILR3_B2 rev	GGGGACCACTTTGTACAAGAAAGCTGG GTCTTAAGCAACAGGAGGACGAAG	colony PCR ILR3	Lichtblau and Schwarz et al. 2020
bHLH39_B1 fw	GGGGACAAGTTTGTACAAAAAAGCAG GCTTCATGTGTGCATTAGTACCTC	colony PCR bHLH39	Lichtblau and Schwarz et al. 2020
bHLH39_B2 rev	GGGGACCACTTTGTACAAGAAAGCTGG GTCTCATATATATGAGTTTCCAC	colony PCR bHLH39	Lichtblau and Schwarz et al. 2020
Amplification of promotor sequences for promotor-GUS lines			
proOLV_-988_B1 fw	GGGGACAAGTTTGTACAAAAAAGCAG GCTTCGAGAAAAGGATTCTAATTTAGG A	cloning of OLV promotor	This study
ProOLV_-988_B2 rev	GGGGACCACTTTGTACAAGAAAGCTGG GTCGTAAATCTCTATGGTCTATTG	cloning of OLV promotor	This study
proPYE_-1120_B1 fw	GGGGACAAGTTTGTACAAAAAAGCAG GCTTCACCGCAAAACTATATATAGTATT T	cloning of PYE promotor	Lichtblau and Schwarz et al. 2020
proPYE_-1120_B2 rev	GGGGACCACTTTGTACAAGAAAGCTGG GTCCTTTGCTTTTATTACAGAACAAGA	cloning of PYE promotor	Lichtblau and Schwarz et al. 2020
Genotyping primer			
35S fw	ATCCCACTATCCTTCGCAAGACCC	HA-ox lines	Institute of Botany, HHU Düsseldorf
pGWB3_seq fw	TACACTTTATGCTTCCGGCTC	Gus lines	This study
pGWB3_seq rev	CTTTCCCACCAACGCTGATC	Gus lines	This study
RT-qPCR primer			
OLV_stn fw	GGGCACAAACCATGAACACC	OLV_RT-qPCR mass standard	This study
OLV_stn rev	GAGTCTTCGACGAGATCGAGATG	OLV_RT-qPCR mass standard	This study
OLV_qPCR fw	GGGCACAAACCATGAACACC	OLV_RT-qPCR	This study
OLV_qPCR rev	ACTATATCATGCGAGGCACTCTTC	OLV_RT-qPCR	This study
PYE_stn fw	ACCGAAAAGGATCAACAAGG	PYE_RT-qPCR mass standard	Lichtblau and Schwarz et al. 2020
PYE_stn rev	CCATCAAGGCCATAACTTCC	PYE_RT-qPCR mass standard	Lichtblau and Schwarz et al. 2020
PYE_qPCR fw	GTTCCCAGGACTTCCCATTT	PYE_RT-qPCR	Lichtblau and Schwarz et al. 2020
PYE_qPCR rev	GTGTCTGGGGATCAGGTTGT	PYE_RT-qPCR	Lichtblau and Schwarz et al. 2020
FIT_stn fw	AAGACATGACCAAAAATGTGTGT	FIT_RT-qPCR mass standard	(Naranjo Arcos, 2017)
FIT_stn rev	TGCATCTCCAACAATGGATGC	FIT_RT-qPCR mass standard	(Naranjo Arcos, 2017)
FIT_qPCR fw	CCCTGTTTCATAGACGAGAACC	FIT_RT-qPCR	(Bauer, 2016)
FIT_qPCR rev	ATCCTTCATACGCCCTCTCC	FIT_RT-qPCR	(Bauer, 2016)
bHLH39_stn fw	AACCAAAGCAGCTTCCAAG	bHLH39_RT-qPCR mass standard	(Naranjo Arcos, 2017)
bHLH39_stn rev	CGAAGAGAAAAAGGACGACA	bHLH39_RT-qPCR mass standard	(Naranjo Arcos, 2017)
bHLH39_qPCR fw	GACGGTTTCTCGAAGCTTG	bHLH39_RT-qPCR	(Wang et al., 2007)
bHLH39_qPCR rev	GGTGGCTGCTTAACGTAACAT	bHLH39_RT-qPCR	(Wang et al., 2007)
FRO2_stn fw	CCATGCTCGATCTTGTCTTG	FRO2_RT-qPCR mass standard	(Bauer, 2016)
FRO2_stn rev	ATTCCGGAACTTTTGAAAGG	FRO2_RT-qPCR mass standard	(Bauer, 2016)
FRO2_qPCR fw	CTTGGTCATCTCCGTGAGC	FRO2_RT-qPCR	(Wang et al., 2007)
FRO2_qPCR rev	AAGATGTTGGAGATGGACGG	FRO2_RT-qPCR	(Wang et al., 2007)
IRT1_stn fw	TAGCCATTGACTCCATGGC	IRT1_RT-qPCR mass standard	(Klatte, 2008)
IRT1_stn rev	AGAAAACTATGAATCGTGGGG	IRT1_RT-qPCR mass standard	(Klatte, 2008)
IRT1_qPCR fw	AAGCTTTGATTCACGGTTGG	IRT1_RT-qPCR	(Wang et al., 2007)
IRT1_qPCR rev	TTAGGTCCCATGAACTCCG	IRT1_RT-qPCR	(Wang et al. 2007)
ILR3_stn fw	TGATGGCTCGGCTGGAAAC	ILR3_RT-qPCR mass standard	Lichtblau and Schwarz et al. 2020
ILR3_stn rev	CTAAGAAAGCCGAGAAAGAGAGGAG	ILR3_RT-qPCR mass standard	Lichtblau and Schwarz et al. 2020
ILR3_qPCR fw	GCATGTAGAGAGAAGCAGCGAC	ILR3_RT-qPCR	Lichtblau and Schwarz et al. 2020
ILR3_qPCR rev	TGCGGACAGCATCAACCAAG	ILR3_RT-qPCR	Lichtblau and Schwarz et al. 2020
bHLH104_stn fw	GAATTTGCAGCAGGAGCCAG	bHLH104_RT-qPCR mass standard	Lichtblau and Schwarz et al. 2020
bHLH104_stn rev	GCCAAACGGAAGAATCCTAAACC	bHLH104_RT-qPCR mass standard	Lichtblau and Schwarz et al. 2020
bHLH104_qPCR fw	GGTTGAGGAGGGAGAAGCTAAATG	bHLH104_RT-qPCR	Lichtblau and Schwarz et al. 2020

bHLH104_qPCR rev	ACGGATTGCATCATCGAGTATAGC	bHLH104_RT-qPCR	Lichtblau and Schwarz et al. 2020
BTS_stn fw	AACTTGGATGTTCCCCGTCT	BTS_RT-qPCR mass standard	Lichtblau and Schwarz et al. 2020
BTS_stn rev	ATCAACGGGCTTCTTCACT	BTS_RT-qPCR mass standard	Lichtblau and Schwarz et al. 2020
BTS_qPCR fw	CGGGGAAGGACTAGGAATCG	BTS_RT-qPCR	Lichtblau and Schwarz et al. 2020
BTS_qPCR rev	CAGCAGATGGGGCAATTTGT	BTS_RT-qPCR	Lichtblau and Schwarz et al. 2019
Fer1_stn fw	GCGGCTCAACACTATCCTCT	Fer1_RT-qPCR mass standard	(Schuler, 2011)
Fer1_stn rev	ACAGAGCCAACTCCATTGCT	Fer1_RT-qPCR mass standard	(Schuler, 2011)
Fer1_qPCR fw	ACGCACTCTCGTCTTTCACC	Fer1_RT-qPCR	(Schuler, 2011)
Fer1_qPCR rev	GAAAGGCTGGAACACGACTC	Fer1_RT-qPCR	(Schuler, 2011)
NAS4_stn fw	CACTCTCTTCAAGCAGCTCGT	NAS4_RT-qPCR mass standard	Lichtblau and Schwarz et al. 2020
NAS4_stn rev	CTGTAGCAAAAACAGCCAACA	FAS4_RT-qPCR mass standard	Lichtblau and Schwarz et al. 2020
AtNAS4-RT810-5´	TGTAATCTCAAGGAAGCTAGGTG	NAS4_RT-qPCR	Klatte et al., 2009
AtNAS4-RT947-3´	GCGAACTCCTCGATAATGC	NAS4_RT-qPCR	Institute of Botany, HHU Düsseldorf
FRO3_stn fw	AATCAGATCGACCACCTTGC	FRO3_RT-qPCR mass standard	Lichtblau and Schwarz et al. 2020
FRO3_stn rev	TTCTTTTGGTGAGAAGATTTTGG	FRO3_RT-qPCR mass standard	Lichtblau and Schwarz et al. 2020
FRO3_qPCR fw	ATCGACCACCTTGCTGTTTC	FRO3_RT-qPCR	Lichtblau and Schwarz et al. 2020
FRO3_qPCR rev	TTATCCCACTGCCTCCACTC	FRO3_RT-qPCR	Lichtblau and Schwarz et al. 2020
ZIF1_stn fw	AAGGCTTCTCAGTCTCTCTTG	ZIF1_RT-qPCR mass standard	This study
ZIF1_stn rev	TAACGGTTCAAGTAAGTTCCTCTC	ZIF1_RT-qPCR mass standard	This study
ZIF1_qPCR fw	TTGGCTGAGAAACTGCTAGG	ZIF1_RT-qPCR	This study
ZIF1_qPCR rev	CTTAGACTGAGACCTGACAAGC	ZIF1_RT-qPCR	This study
OPT3_stn fw	TCGGTTATATCCTGCCTG	OPT3_RT-qPCR mass standard	This study
OPT3_stn rev	GACAGATGTCTCAATAGCTC	OPT3_RT-qPCR mass standard	This study
OPT3_qPCR fw	TGATAGGACCAAGACGGCTC	OPT3_RT-qPCR	This study
OPT3_qPCR rev	GCAAAGCCGTAGGAGATAACTG	OPT3_RT-qPCR	This study
STD-EF1Balpha2-5´	GCTGCTAAGAAGGACACCAAG	EF1Balpha (genomic) RT-qPCR mass standard	(Bauer, 2016)
STD-EF1Baplha2-3´	TGTTCTGTCCCTACGGATCC	EF1Balpha (genomic) RT-qPCR mass standard	(Bauer 2016)
EFc-5´	TATGGGATCAAGAAACTCACAAT	EF1Balpha RT-qPCR	(Bauer, 2016)
EFc-3´	CTGGATGTACTCGTTGTTAGGC	EF1Balpha RT-qPCR	(Wang et al., 2007)
At-EF-gen-5´	TCCGAACAATACCAGAACTAC	EF1Balpha (genomic) RT-qPCR	(Wang et al. 2007)
At-EF-gen-3´	CCGGGACATATGGAGGTAAG	EF1Balpha (genomic) RT-qPCR	(Wang et al., 2007)

Authors Contribution to Manuscript 2

Daniela M. Lichtblau

Designed the research, performed and analyzed all experiments, except imaging and analysis of FRET samples. Wrote the manuscript, prepared final figures and reviewed/ edited the manuscript.

Birte Schwarz

Together with D.M.L designed and performed the Y2H screen which revealed the protein-interaction of PYE and OLV. Reviewed/ edited the manuscript.

Ksenia Trofimov

Performed the microscopy part of FRET and analyzed FRET data.

Petra Bauer

Conceived and supervised the study, provided funding and reviewed/ edited the manuscript.

9 Concluding remarks

The results presented in this thesis emphasize the importance of protein-protein interactions in regulating Fe deficiency responses. Here, we show that not only TFs but also E3 ligases and especially small proteins are involved in regulating the Fe uptake and distribution.

This study began with a targeted Y2H screen resulting in the discovery of several novel protein-protein interactions that could be clustered into different projects. Another important conclusion was that yeast co-transformation of two genes of interest was better suitable to capture weak protein-protein interactions with Y2H than mating.

The Fe deficiency response is controlled by a complex cascade of partially interacting proteins. The three homologous E3 Ligases BTS, BTSL1 and BTSL2 negatively regulate Fe deficiency responses (Selote, 2015; Hindt et al., 2017; Rodriguez-Celma et al., 2019). Interestingly, these E3 ligases appeared to be in the center of a highly interconnected protein-interaction network created in this study. BTS was already known to interact with bHLH TFs of subgroup IVc, leading to their proteasomal degradation. This work showed that BTSL1 and BTSL2 interact with some of the same set of TFs as BTS. Unlike BTS they also interacted with PYE. Therefore, BTS, BTSL and BTSL2 seem to have partly redundant but also specific functions. That they perform individual functions is supported by the fact that they are expressed in different plant tissues: BTSLs are predominantly expressed in roots, BTS is expressed in roots and shoots (Rodríguez-Celma et al., 2019). The BTSLs might not only be involved in regulating the Fe uptake, but also Fe distribution processes through controlling PYE protein levels. Likely all three BTS(L)s are responsible for posttranslational regulation of bHLH IVc TFs which positively influence the Fe deficiency response. In this way a rapid shut down mechanism prevents excess uptake of Fe and other metals during prolonged Fe shortage. This work identified FEP3 as BTSL interaction partner and possible inhibitor. The small peptide FEP3 was recently determined as a novel player, possibly functioning in Fe long-distance signaling. Overall, the data of this study points out that over-expression of FEP3 phenocopies the *btsl1 btsl2* loss-of-function mutant. Likely, FEP3 inhibits BTSL1/2 protein function through its interaction, possibly by preventing that BTSL1/2 can target subgroup IVc bHLH TFs and PYE for degradation. Thus FEP3 positively influences the Fe deficiency response. FEP3 did not interact with BTS. However, because FEP3 has at least three homologues in Arabidopsis, it is possible that one of them regulates BTS in a similar manner. Overall, it seems that this study discovered a new mechanism in which a small peptide controls E3 ligase function on protein level.

Furthermore, this work introduces OLV as a novel important player indirectly involved in regulating Fe homeostasis. Although, orthologues of OLV exist in various other organisms ranging from lower plants to mammals, a function is not known. OLV interacted with PYE. This interaction depends on the presence of a conserved novel TGIYY motif. Thus, this study possibly identified a new conserved

protein-protein interaction motif. Because PYE likewise possesses orthologues in other organisms, even the OLV-PYE interaction might be conserved across species. When OLV was over-expressed PYE target genes were more repressed. Because OLVox lines had similar transcript levels of *PYE* as the WT it is hypothesized that OLV influences PYE activity on protein level. So far, it is not known whether this happens through PYE protein stabilization or improved binding of PYE to its target promotors. To date, only little is known about PYE function and further investigations are necessary to understand the role of PYE and thus in turn the impact of its interaction with OLV. Interestingly, OLV belong to the FIT-dependent genes while PYE is FIT-independent. This interaction might somehow link the Fe uptake mechanism to Fe distribution.

In both studies relatively small proteins (FEP3 and OLV) play important roles in Fe deficiency response. This again highlights the importance of small proteins in plant nutrient uptake, as it is already known from N acquisition especially under N deprivation. This work provides valuable insights into the mechanism controlling Fe deficiency response. It also opens up a platform for new questions. For example, it needs to be determined whether the BTSLs indeed target their interacting proteins for proteasomal degradation. One could ask what determines an individual target of the BTSLs and why only the BTSLs interact with PYE. Additionally it would be interesting to know what coordinates the localization and function of BTS(L)s and if BTS is regulated in a similar way as the BTSLs. Especially the exact role of PYE is still not clear and available data is inconsistent. Another open question deals with OLV and its potential further functions. If OLV has similar functions in all organisms, this might point towards OLV possessing a universal function in the Fe deficiency response. OLV might also possess other Fe independent functions. Lastly, we focused only on a few new protein-protein interactions here. We found various more interactions in our initial targeted Y2H interaction screen, which provides diverse opportunities for additional studies.

References

Hindt MN, Akmakjian GZ, Pivarski KL, Punshon T, Baxter I, Salt DE, Guerinot ML (2017) BRUTUS and its paralogs, BTS LIKE1 and BTS LIKE2, encode important negative regulators of the iron deficiency response in Arabidopsis thaliana. Metallomics **9:** 876-890

Rodriguez-Celma J, Chou H, Kobayashi T, Long TA, Balk J (2019) Hemerythrin E3 Ubiquitin Ligases as Negative Regulators of Iron Homeostasis in Plants. Front Plant Sci **10:** 98

Rodríguez-Celma J, Connorton JM, Kruse I, Green RT, Franceschetti M, Chen Y-T, Cui Y, Ling H-Q, Yeh K-C, Balk J (2019) Arabidopsis BRUTUS-LIKE E3 ligases negatively regulate iron uptake by targeting transcription factor FIT for recycling. Proceedings of the National Academy of Sciences**:** 201907971

Selote D, Samira R, Matthiadis A, Gillikin JW, Long TA (2015) Iron Binding E3 Ligase Mediates Iron response in Plants by targeting basic helix loop helix transcription factors Plant Physiology